



Development of new lightweight green composites reinforced with nonwoven structures of flax fibres

Heura Ventura Casellas

ADVERTIMENT La consulta d'aquesta tesi queda condicionada a l'acceptació de les següents condicions d'ús: La difusió d'aquesta tesi per mitjà del repositori institucional UPCommons (<http://upcommons.upc.edu/tesis>) i el repositori cooperatiu TDX (<http://www.tdx.cat/>) ha estat autoritzada pels titulars dels drets de propietat intel·lectual **únicament per a usos privats** emmarcats en activitats d'investigació i docència. No s'autoritza la seva reproducció amb finalitats de lucre ni la seva difusió i posada a disposició des d'un lloc aliè al servei UPCommons o TDX. No s'autoritza la presentació del seu contingut en una finestra o marc aliè a UPCommons (*framing*). Aquesta reserva de drets afecta tant al resum de presentació de la tesi com als seus continguts. En la utilització o cita de parts de la tesi és obligat indicar el nom de la persona autora.

ADVERTENCIA La consulta de esta tesis queda condicionada a la aceptación de las siguientes condiciones de uso: La difusión de esta tesis por medio del repositorio institucional UPCommons (<http://upcommons.upc.edu/tesis>) y el repositorio cooperativo TDR (<http://www.tdx.cat/?locale-attribute=es>) ha sido autorizada por los titulares de los derechos de propiedad intelectual **únicamente para usos privados enmarcados** en actividades de investigación y docencia. No se autoriza su reproducción con finalidades de lucro ni su difusión y puesta a disposición desde un sitio ajeno al servicio UPCommons No se autoriza la presentación de su contenido en una ventana o marco ajeno a UPCommons (*framing*). Esta reserva de derechos afecta tanto al resumen de presentación de la tesis como a sus contenidos. En la utilización o cita de partes de la tesis es obligado indicar el nombre de la persona autora.

WARNING On having consulted this thesis you're accepting the following use conditions: Spreading this thesis by the institutional repository UPCommons (<http://upcommons.upc.edu/tesis>) and the cooperative repository TDX (<http://www.tdx.cat/?locale-attribute=en>) has been authorized by the titular of the intellectual property rights **only for private uses** placed in investigation and teaching activities. Reproduction with lucrative aims is not authorized neither its spreading nor availability from a site foreign to the UPCommons service. Introducing its content in a window or frame foreign to the UPCommons service is not authorized (*framing*). These rights affect to the presentation summary of the thesis as well as to its contents. In the using or citation of parts of the thesis it's obliged to indicate the name of the author.



2017

Departament de Ciència dels Materials i Enginyeria Metal·lúrgica

Programa de Doctorat en Enginyeria Tèxtil i Parerera



**DEVELOPMENT OF NEW
LIGHTWEIGHT GREEN
COMPOSITES REINFORCED
WITH NONWOVEN
STRUCTURES OF FLAX
FIBRES**

Heura Ventura Casellas



UNIVERSITAT POLITÈCNICA
DE CATALUNYA
BARCELONATECH

Tesis doctoral

**DEVELOPMENT OF NEW LIGHTWEIGHT GREEN
COMPOSITES REINFORCED WITH NONWOVEN
STRUCTURES OF FLAX FIBRES**

Presentada por

Heura Ventura Casellas

para optar al grado de Doctora

por la Universitat Politècnica de Catalunya

Dirigida por:

Prof. Dra. MÒNICA ARDANUY RASO - *Universitat Politècnica de Catalunya*

Co-dirigida por:

Prof. Dr. MIGUEL ÀNGEL RODRÍGUEZ PÉREZ - *Universidad de Valladolid*

Departament de Ciència dels Materials i Enginyeria Metal·lúrgica

Programa de Doctorat en Enginyeria Tèxtil i Parerera

Terrassa, 2017

En memòria del meu pare...

En memoria de mi padre...

In memory of my father...

... JV TdT (1955-2012)

FUNDING

This thesis was possible thanks to the financial assistance of the Ministerio de Educación, Cultura y Deporte (MECD) from the Spanish Government, by means of the FPU grant (reference FPU12/05869) and the complementary mobility grant (reference EST14/00273) with which I was awarded.

Moreover I want to acknowledge the funding support from the research group Tectex of the Universitat Politècnica de Catalunya (UPC) and the CellMat research group of the Universidad de Valladolid (UVa), in the framework of the following research projects:

- BIA2014-59399-R. DESARROLLO DE MATERIALES DE ALTA RESISTENCIA Y DURABILIDAD BASADOS EN MORTEROS DE CEMENTO REFORZADOS CON NO TEJIDOS DE FIBRAS VEGETALES APLICABLES EN FACHADAS VENTILADAS. Ministerio de Economía y Competitividad (MINECO). January 2015 – December 2017. Principal researcher: M. Ardanuy
- BIA2011-26288. DESARROLLO DE COMPUESTOS Y NANOCOMPUESTOS DE ALTAS PRESTACIONES A BASE DE CEMENTOS REFORZADOS CON FIBRAS DE CELULOSA PARA APLICACIONES EN MATERIALES DE CONSTRUCCIÓN MÁS RESPETUOSOS CON EL MEDIO AMBIENTE. Ministerio de Ciencia y Tecnología (MCYT). January 2012 – December 2015. Principal researcher: M. Ardanuy
- MAT2015-69234-R. DESARROLLO Y FABRICACIÓN EN CONTÍNUO DE AISLANTES TÉRMICOS AVANZADOS BASADOS EN POLÍMEROS NANOCELULARES. Ministerio de Economía y Competitividad (MINECO). January 2016 – December 2019. Head researcher in UVa: M.A. Rodríguez Pérez
- MAT2012-34901. DESARROLLO DE PLÁSTICOS SUB-MICROCELULARES Y NANOCELULARES: FABRICACIÓN, ESTRUCTURA, PROPIEDADES Y POTENCIALES APLICACIONES. MINISTERIO DE ECONOMÍA Y COMPETITIVIDAD (MINECO). January 2013 – December 2015. Principal researcher: M.A. Rodríguez Pérez

FINANÇAMENT

Aquesta tesi ha estat possible gràcies al suport econòmic del Ministerio de Educación, Cultura y Deporte (MECD) del Govern Espanyol, a través de la beca FPU (referència FPU12/05869) i al complement de beca per a la mobilitat (referència EST14/00273) que em van ser atorgades.

Més a més vull agrair el finançament rebut pel grup de recerca Tectex de la Universitat Politècnica de Catalunya i el grup de recerca CellMat de la Universidad de Valladolid, mitjançant els següents projectes d'investigació:

- BIA2014-59399-R. DESARROLLO DE MATERIALES DE ALTA RESISTENCIA Y DURABILIDAD BASADOS EN MORTEROS DE CEMENTO REFORZADOS CON NO TEJIDOS DE FIBRAS VEGETALES APLICABLES EN FACHADAS VENTILADAS. Ministerio de Economía y Competitividad (MINECO). Gener 2015 – Diciembre 2017. Investigador principal: M. Ardanuy
- BIA2011-26288. DESARROLLO DE COMPUESTOS Y NANOCOMPUESTOS DE ALTAS PRESTACIONES A BASE DE CEMENTOS REFORZADOS CON FIBRAS DE CELULOSA PARA APLICACIONES EN MATERIALES DE CONSTRUCCIÓN MÁS RESPETUOSOS CON EL MEDIO AMBIENTE. Ministerio de Ciencia y Tecnología (MCYT). Gener 2012 – Diciembre 2015. Investigador principal: M. Ardanuy
- MAT2015-69234-R. DESARROLLO Y FABRICACIÓN EN CONTÍNUO DE AISLANTES TÉRMICOS AVANZADOS BASADOS EN POLÍMEROS NANOCELULARES. Ministerio de Economía y Competitividad (MINECO). Gener 2016 – Diciembre 2019. Investigador responsable a la UVA: M.A. Rodríguez Pérez
- MAT2012-34901. DESARROLLO DE PLÁSTICOS SUB-MICROCELULARES Y NANOCELULARES: FABRICACIÓN, ESTRUCTURA, PROPIEDADES Y POTENCIALES APLICACIONES. MINISTERIO DE ECONOMÍA Y COMPETITIVIDAD (MINECO). Gener 2013 – Diciembre 2015. Investigador principal: M.A. Rodríguez Pérez

FINANCIACIÓN

Esta tesis ha sido posible gracias al apoyo económico del Ministerio de Educación, Cultura y Deporte (MECD) del Gobierno de España, a través de la beca FPU (referencia FPU12/05869) y el complemento de beca para la movilidad (referencia EST14/00273) que me fueron otorgadas.

Además quiero agradecer la financiación recibida por el grupo de investigación Tectex de la Universitat Politècnica de Catalunya y el grupo de investigación CellMat de la Universidad de Valladolid, a través de los siguientes proyectos de investigación:

- BIA2014-59399-R. DESARROLLO DE MATERIALES DE ALTA RESISTENCIA Y DURABILIDAD BASADOS EN MORTEROS DE CEMENTO REFORZADOS CON NO TEJIDOS DE FIBRAS VEGETALES APLICABLES EN FACHADAS VENTILADAS. Ministerio de Economía y Competitividad (MINECO). Enero 2015 – Diciembre 2017. Investigador principal: M. Ardanuy
- BIA2011-26288. DESARROLLO DE COMPUESTOS Y NANOCOMPUESTOS DE ALTAS PRESTACIONES A BASE DE CEMENTOS REFORZADOS CON FIBRAS DE CELULOSA PARA APLICACIONES EN MATERIALES DE CONSTRUCCIÓN MÁS RESPETUOSOS CON EL MEDIO AMBIENTE. Ministerio de Ciencia y Tecnología (MCYT). Enero 2012 – Diciembre 2015. Investigador principal: M. Ardanuy
- MAT2015-69234-R. DESARROLLO Y FABRICACIÓN EN CONTÍNUO DE AISLANTES TÉRMICOS AVANZADOS BASADOS EN POLÍMEROS NANOCELULARES. Ministerio de Economía y Competitividad (MINECO). Enero 2016 – Diciembre 2019. Investigador responsable en la UVA: M.A. Rodríguez Pérez
- MAT2012-34901. DESARROLLO DE PLÁSTICOS SUB-MICROCELULARES Y NANOCELULARES: FABRICACIÓN, ESTRUCTURA, PROPIEDADES Y POTENCIALES APLICACIONES. MINISTERIO DE ECONOMÍA Y COMPETITIVIDAD (MINECO). Enero 2013 – Diciembre 2015. Investigador principal: M.A. Rodríguez Pérez

AGRADECIMIENTOS

En primer lugar, quiero dar las gracias a mis directores.

A Mònica, por creer en mí, por su confianza, por escucharme, comprenderme y guiarme por este largo recorrido, por su tiempo, sus consejos, su apoyo, su paciencia, por abrirme las puertas de su laboratorio y su taller que han sido mi segunda casa... porque sin ella esta tesis no habría sido posible. *Gràcies de tot cor. Saps que dins d'aquest gràcies n'hi ha molts d'agraïments.*

A Miguel Ángel, por abrirme las puertas de su laboratorio, permitirme formar parte de un equipo excelente, por su sabiduría y paciencia, por poner a mi disposición todos los equipos y conocimientos a su alcance, por sus aportaciones, su tiempo, su interés, por sus palabras de apoyo en los momentos de mayor necesidad. *Sin tu ayuda esta tesis no existiría. Cada una de tus palabras me ha animado a seguir en el empeño. Gracias por todo.*

Debo dar también las gracias a la Dra. Diana Cayuela, por facilitar todo el proceso, por su generosidad, por darme acceso a todos los equipos de los que disponía y por su inestimable ayuda en los inicios de esta tesis.

Agradezco al Dr. Salvatore Iannace la oportunidad que me brindó para realizar la provechosa estancia en el Istituto per i Polimeri Compositie Biomateriali (IPCB-CNR, Italia).

Por supuesto, estoy en deuda con el Dr. Luigi Sorrentino, mi supervisor durante dicha estancia, por cálida acogida, por su disponibilidad, su ayuda y dedicación, por poner a mi disposición todos los equipos necesarios, por sus imprescindibles aportaciones, por su empeño... *Luigi, ti ringrazio per tutto l'aiuto che mi hai dato. Se il mio soggiorno a Portici è stato un successo è stato a grazie a te. Grazie mille.*

Agradezco también...

...al Dr. José Antonio Tornero y a Francesc Cano del Insituto INTEXTER (UPC, Terrassa), por su participación en la fabricación y el estudio de los no-tejidos empleados en esta tesis.

...al Prof. Dr. Josep M^a Canal por su confianza y colaboración al facilitar el acceso a los equipamientos del grupo de investigación de Superficies, Productos y Procesos Textiles (SPPT-UPC).

...al Dr. Antonio Navarro del Departamento de Ingeniería Química de la UPC, por su colaboración en la parte de tratamientos de plasma.

...al Dr. Josep Claramunt del Departamento de Ingeniería Agroalimentaria y Biotecnología de la UPC, con quien he tenido el placer de trabajar, por su cercanía y disponibilidad.

Durante la duración de esta tesis he tenido varias “segundas casas”. La primera fue el Departamento de Ingeniería Textil y Papelera. A todos los compañeros, profesores y PAS que compartieron conmigo el día a día durante todo este tiempo les agradezco su compañía, apoyo y preocupación. Y a mis compañeros del Taller de Tisaje, que se convirtieron en parte de mi familia. *Ferran, Dora, Helena: gràcies per les converses, per la companyia, pel vostre recolzament en els mals moments i per estar sempre disposats a donar-me un cop de mà. Gràcies de tot cor.*

Mi segunda casa se trasladó durante un largo período (y posteriores visitas) a Valladolid. Allí pude formar parte de un grupo en el que aprendí mucho más que conocimientos académicos. Gracias a la gente de CellMat, a todos y cada uno de ellos, por recibirme con los brazos abiertos, por su ayuda y por su apoyo. Ha sido un verdadero placer sentirme parte de esta familia. *Gracias a Merce, Edu, Dani, Leandra, Santi, Michele, Alberto III y Paula, por su amistad, complicidad y por aguantarme, que no es poco; a Saúl, Judith, Vicky, Josías, Mikel y Belén por arrancarme siempre una sonrisa; a Javi, Puri, Haritz y Pablo por estar siempre dispuestos a echarme una mano; a Blanca por su dedicación y ayuda, y a Laura por las cálidas bienvenidas y por su ayuda, por supuesto; a Cris y Alberto por sus consejos y enseñanzas; y a Ester, porque ha sido un placer trabajar contigo.*

Mi tercera casa se localizó algo más lejos, a los pies del Vesubio, en Portici (Nápoles). Si puede realizar importantes avances en la tesis durante mi estancia de tres meses fue gracias a todo el equipo del IPCB-CNR. Desde el primer minuto me hicieron sentir como en casa. A todos ellos les agradezco su recibimiento, su complicidad y compañía durante esos meses. *Grazie anche a tutti gli altri colleghi. Livia, Marco, Steffania, Marcella, Enzo, Maria Rosaria, Marika, Fabio, Alessandra, Mario, Fabiana, Loredana, Valentina, Enza, Letizia, Andrea... grazie per avermi fatto sentire parte del gruppo, e grazie per i momenti di pausa per il caffè.*

A mi familia tengo mucho que agradecerle. Siempre. Por su apoyo, comprensión, ayuda, abrazos y palabras de ánimo en los momentos de necesidad. *Laia, Ferran, Arantza, Ona... sou la pinya més important del món per a mi. Passi el que passi, sempre estarem tots junts, units, fent força. Gràcies per estar sempre allà.* A mi abuela, aunque sólo está de cuerpo presente, porque siempre me animó y apoyó, y fue quien me contagió el interés por el mundo del textil a través de la costura. A mi madre, porque sin su apoyo incondicional, sus palabras de calma y sosiego, su

compañía y su comprensión, probablemente me habría hundido en muchos momentos. *Sempre has estat al meu costat, recolzant-me independentment de lo dures que fossin les circumstàncies. No crec que hi hagi ningú al món que m'entengui millor que tu. Gràcies per estar al meu costat i ajudar-me en tot el que ha estat a la teva mà... sempre. Ets un exemple a seguir.*

A mis amigos y compañeros les agradezco su comprensión y su apoyo a lo largo del tiempo y la distancia. *Miki, Maddy, Pilar, María, Xavi, Ana, Xave, Laia, Raül, Marta... por vuestra compañía y apoyo. Cada vez que me habéis mandado fuerza me habéis cargado las pilas. Gracias.* A Sean, por sus siempre bienvenidas correcciones. También debo agradecer el haber llegado hasta aquí a Javier Peña, quien me introdujo en el mundo de los materiales y me hizo soñar con que podía llegar a ser lo que quisiera, incluso doctora. *Fuiste el primero que confió y apostó por mí. Por ello te estaré siempre agradecida.*

Por último diré que cuando apenas había iniciado este camino recibí un duro golpe, por ello esta tesis va dedicada en memoria de mi padre. Él era una persona con una gran conciencia ecológica, y creo que se sentiría orgulloso de este trabajo. *Allà on siguis... gràcies. Sé molt bé que has estat al meu costat tot aquest temps i que m'has donat més d'un cop de mà, movent els fils dels que disposaves. Fins que ens tornem a trobar.*

ABSTRACT (EN)

Composite materials offer good mechanical performance with lower weight than classical materials. These specific properties have encouraged the use of composites in many industry applications such as automotive, construction or sports, among others. Moreover, the progress towards green composites has become an important trend for industry and society, owing to rising awareness about environmental problems. Due to this, there is a great interest around the use of reinforcements and matrices obtained from renewable resources, such as natural fibres and biopolymers, thus leading to the development of new environmentally-friendly and more sustainable composite materials.

A scientific goal of this thesis is the development of increasingly lighter components to achieve even further improved specific properties. The specific strategy chosen here is the enhancement of weight reduction of the matrix by means of foaming processes. The use of fibres of high strength is a key factor for counteracting the loss in the mechanical properties of the matrix, produced as a consequence of the cellular structure obtained after foaming. In this sense, a novel approach is given for the use of flax fibres—of high stiffness and low cost—as reinforcement, since they are used in the form of nonwoven structures.

This PhD thesis focuses on the development of green composites made of polyhydroxyalkanoate (PHA) matrix and with a reinforcement of flax nonwoven fabrics, while considering materials and processes with low ecological impact. The approach considered in this thesis differs from the classical approaches with these materials in its use of foaming techniques to obtain a cellular structure in the matrix. The combination of the properties of both components leads to a biodegradable, stiff and lightweight solution that presents good regularity in the foaming process, which prompts a possible replacement of other less sustainable materials in automotive, construction and other applications.

The use of natural fibres in composites has two main concerns: the fibre/matrix interaction and their sensibility to moisture absorption. Fibre/matrix interaction can be improved by physically and/or chemically modifying the surface of the fibres to enhance their compatibility with the matrix. Moisture absorption can also be altered by treating the fibres. The methods employed for reducing these concerns were green, adding further benefit. Regarding this, wet/dry cycling is an interesting option to increase fibre stability, and plasma treatments to perform surface modifications in fibres—without affecting their bulk properties—with a minimal use of chemicals and no need of water.

The effectiveness of the “green” treatments was evaluated by means of hydrothermal aging and mechanical characterisation on (solid) PHA/flax composites. Wet/dry cycling treatment stabilised the absorption of water and dimensional changes of the flax fibres. Plasma treatments with air, argon or ethylene gases modified the surface roughness and surface chemistry of the fibres, changing their hydrophilicity and improving, in some cases, the fibre/matrix adhesion.

The foaming of the matrix contributes advantageously to the development of lighter solutions, bringing the reduction of polymer required—and hence, its cost—added to the benefit of the biodegradability. The current high price of commercial biopolymers—compared to other commodity polymers—affects the competitiveness of green composites for their use as replacement of conventional materials in some applications. Due to this, the required study of the capabilities to generate cellular structures of the PHA matrix is presented in this thesis. The matrix foamability was evaluated by means of extrusion foaming, considering two main strategies for improving this process: the use of chain extenders and cooling by means of a water quenching.

Finally, the most challenging and novel—as shown by the scarce literature found about the topic—is the achievement of the cellular composites reinforced with the optimized flax fabrics. A gas dissolution batch foaming was used for the production from solid precursors, after considering the limitations imposed by the reinforcement structures and the foamability of the matrix. This breakthrough strategy was evaluated and optimised for such a purpose, leading to cellular composite materials with good specific properties and a reduced density.



Composite material: before foaming (left) and after foaming (right).

Due to the aforementioned, this thesis presents the development of a challenging new approach for lightweight green composites from a multidisciplinary point of view.

RESUM (CAT)

Els materials compostos ofereixen bones prestacions mecàniques amb un menor pes que els materials convencionals. Aquestes propietats específiques han permès estendre el seu ús a sectors com l'automoció, la construcció o el lleure, entre d'altres. A més, l'evolució cap a materials sostenibles s'ha convertit en una important tendència tant per a la indústria com per a la societat degut a la conscienciació sobre els problemes mediambientals. Això ha generat un gran interès pel que fa a l'ús de reforços i matrius provinents de recursos renovables com les fibres naturals i els biopolímers, que ha dut al desenvolupament de nous materials compostos més sostenibles i respectuosos amb el medi ambient.

Una meta científica d'aquesta tesi, és el desenvolupament de components cada cop més lleugers per a aconseguir encara millors propietats específiques. L'estratègia emprada per aquest propòsit, és la de reduir el pes de la matriu mitjançant tècniques d'escumat. L'ús de fibres d'alta resistència esdevé un factor clau per contrarestar la pèrdua de propietats mecàniques de la matriu, derivada de la generació d'una estructura cel·lular per efecte de l'escumat. En aquest sentit, l'ús de fibres de lli (d'alta rigidesa i baix cost) en la forma d'estructures no-teixides suposa un nou enfocament.

Aquesta tesi es centra en el desenvolupament de compòsits sostenibles de matriu de polihidroxialcanoat (PHA) i reforç de teles no-teixides de lli, sempre tenint en compte materials i processos de baix impacte ambiental. L'enfocament d'aquesta tesi, difereix dels enfocaments clàssics emprats en aquest tipus de materials en l'ús de tècniques d'escumat per a obtenir estructures cel·lulars en la matriu polimèrica. La combinació de propietats d'ambdós components duu a l'obtenció de materials biodegradables, rígids i lleugers que presenten bona regularitat en el procés d'escumat, el que planteja una possible solució per al reemplaçament d'altres materials menys sostenibles en automoció, construcció o d'altres aplicacions.

L'ús de fibres naturals en materials compostos presenta dues problemàtiques: la interacció fibra/matriu i la sensibilitat vers l'absorció d'humitat. La interacció fibra/matriu pot millorar-se modificant física i/o químicament la superfície de les fibres per a millorar la seva compatibilitat amb la matriu. L'absorció d'humitat també pot alterar-se mitjançant el tractament de les fibres. Això es pot aconseguir amb mètodes sostenibles, el que implica un valor afegit. En aquest sentit, el ciclat sec/humit és una interessant opció per a incrementar l'estabilitat de la fibra, i els tractaments de plasma permeten la modificació de la seva

superfície, sense afectar a les seves propietats generals, amb un ús mínim de productes químics i sense necessitat d'aigua.

L'efectivitat d'aquests tractaments ecològics aplicats al no-teixit s'avalua mitjançant la caracterització mecànica i l'envelliment hidrotèrmic dels compòsits (sòlids) de PHA/lli. L'estabilitat de les fibres vers l'absorció d'aigua i els canvis dimensionals s'aconsegueix mitjançant el tractament de ciclat sec/humit, i els tractaments de plasma amb aire, argó i etilè permeten la modificació de la rugositat i la química superficials, modificant-ne l'hidrofilia i millorant, en alguns casos, la interacció fibra/matriu.

L'escumat de la matriu afavoreix el desenvolupament de materials més lleugers, amb el benefici de la biodegradabilitat i de la reducció de la quantitat de polímer necessari i, per tant, del cost. L'alt preu que tenen actualment els biopolímers comercials, comparat amb els polímers convencionals, afecta a la competitivitat d'aquests compostos sostenibles com a substituïts dels materials clàssics en algunes aplicacions. Per tant, en aquesta tesi es presenta la avaluació necessària de les capacitats de la matriu de PHA per a generar estructures cel·lulars. L'escumabilitat de la matriu s'avalua en un escumat per extrusió considerant dues estratègies per a millorar-ne el resultat: l'ús d'additius per l'extensió de cadena i un refredament ràpid en aigua.

Finalment, la novetat que presenta un major repte, a jutjar per l'escassa literatura trobada sobre el tema, és la d'aconseguir materials compostos cel·lulars reforçats amb estructures optimitzades de lli. Per a l'esmentada obtenció, s'empra un procés de dissolució de gas per lots a partir de precursors sòlids, tenint en compte les limitacions imposades tant per l'estructura de reforç com per l'escumabilitat de la matriu. Aquesta estratègia novedosa s'avalua i optimitza per a tal propòsit, aconseguint l'obtenció de materials compostos cel·lulars amb una reducció de densitat i bones propietats específiques.

Per tot això, aquesta tesi presenta el desenvolupament d'un nou i desafiant mètode per a l'obtenció de compòsits sostenibles i lleugers, tot des d'un punt de vista multidisciplinari.

RESUMEN (ES)

Los materiales compuestos ofrecen buenas prestaciones mecánicas con un menor peso que los materiales convencionales. Dichas propiedades específicas han permitido extender su uso en sectores como la automoción, la construcción o el ocio, entre otros. Además, la evolución hacia materiales sostenibles se ha convertido en una importante tendencia tanto para la industria como para la sociedad, debido a la concienciación sobre los problemas ambientales. Ello ha generado un gran interés en lo que concierne al uso de refuerzos y matrices provenientes de recursos renovables como las fibras naturales y los biopolímeros, que ha llevado al desarrollo de nuevos materiales compuestos más sostenibles y respetuosos con el medio ambiente.

Una meta científica de esta tesis, es el desarrollo de componentes cada vez más ligeros para conseguir aún mejores propiedades específicas. La estrategia considerada para dicho propósito, es la de reducir el peso de la matriz mediante técnicas de espumado. El uso de fibras de alta resistencia es un factor clave para contrarrestar la pérdida de propiedades mecánicas de la matriz, derivada de la formación de la estructura celular por efecto del espumado. En ese sentido, el uso de fibras de lino (de alta rigidez y bajo coste) en la forma de estructuras no-tejidas supone un enfoque novedoso.

Esta tesis se centra en el desarrollo de compuestos sostenibles de matriz de polihidroxialcanoato (PHA) y refuerzo de telas no-tejidas de lino, siempre considerando materiales y procesos de bajo impacto ambiental. El enfoque de esta tesis, difiere de los enfoques clásicos empleados para este tipo de materiales en el uso de técnicas de espumado para obtener estructuras celulares en la matriz polimérica. La combinación de propiedades de ambos componentes lleva a la obtención de materiales biodegradables, rígidos y ligeros que presentan buena regularidad en el proceso de espumado, lo que plantea una posible solución para el reemplazo de otros materiales menos sostenibles en automoción, construcción u otras aplicaciones.

El uso de fibras naturales en materiales compuestos presenta dos problemáticas: la interacción fibra/matriz y la sensibilidad frente a la absorción de humedad. La interacción fibra/matriz puede mejorarse modificando, física y/o químicamente, la superficie de las fibras para mejorar su compatibilidad con la matriz. La absorción de humedad también puede alterarse mediante el tratamiento de las fibras. Esto puede conseguirse con métodos sostenibles, lo que resulta un valor añadido. En ese sentido, el ciclado seco/húmedo es una interesante opción para incrementar la estabilidad de la fibra, y los tratamientos de plasma

permiten la modificación de la superficie de las fibras, sin afectar sus propiedades generales, con un mínimo uso de productos químicos y sin necesidad de agua.

La efectividad de estos tratamientos ecológicos aplicados al no-tejido se evalúa mediante caracterización mecánica y envejecimiento hidrotérmico en los compuestos (sólidos) de PHA/lino. La estabilidad de las fibras frente a la absorción de agua y los cambios dimensionales se consigue mediante el tratamiento de ciclado seco/húmedo; y los tratamientos de plasma con aire, argón y etileno permiten la modificación de la rugosidad y química superficiales, modificando su hidrofilia y mejorando, en algunos casos, la interacción fibra/matriz.

El espumado de la matriz favorece el desarrollo de materiales más ligeros, con el beneficio de la biodegradabilidad y de la reducción de la cantidad de polímero necesario y, por tanto, del coste. El alto precio que tienen actualmente biopolímeros comerciales, comparado con los polímeros convencionales, afecta a la competitividad de dichos compuestos sostenibles para su empleo en el reemplazo de materiales clásicos en algunas aplicaciones. Por tanto, en esta tesis se presenta la evaluación necesaria de las capacidades de la matriz de PHA para generar estructuras celulares. La espumabilidad de la matriz se evalúa durante un espumado por extrusión considerando dos estrategias para su mejora: el uso de aditivos para la extensión de cadenas y un enfriamiento rápido en agua.

Finalmente, la novedad que presenta un mayor reto, a juzgar por la escasa literatura hallada sobre el tema, es el de conseguir materiales compuestos celulares reforzados con estructuras optimizadas de lino. Para dicha obtención, y consideradas las limitaciones impuestas tanto por las estructuras de refuerzo como por la espumabilidad de la matriz, se emplea un proceso de disolución de gas por lotes a partir de precursores sólidos. Esta estrategia novedosa se evalúa y optimiza para tal propósito, permitiendo la obtención de materiales compuestos celulares con una reducción de densidad y buenas propiedades específicas.

Por todo esto, esta tesis presenta el desarrollo de un nuevo método para la obtención de compuestos sostenibles y ligeros, todo ello desde un punto de vista multidisciplinar.

CONTENTS

INTRODUCTION

i.	Motivation and scope of the thesis.....	33
ii.	Objectives	40
iii.	Framework of the thesis	41
iv.	Structure of the thesis	42
v.	Scientific production.....	45
v.1.	Publications in journals.....	45
v.1.1.	Derived from this thesis.....	45
v.1.2.	Related with the research line.....	45
v.2.	Communications.....	46
v.3.	Patents	47
	References.....	48

CHAPTER I. STATE OF THE ART

I.1.	Biocomposites.....	53
I.1.1.	Fibre reinforcements in composite materials	55
I.1.1.1.	Nonwoven production.....	56
I.2.	Natural fibres as reinforcement in biocomposites.....	59
I.2.1.	Chemical composition and properties of cellulosic fibres	59
I.2.2.	Bast fibres	62
I.2.2.1.	Flax	63
I.3.	Biopolymers as matrix in biocomposites.....	68
I.3.1.	Biopolymers classification	68
I.3.2.	Bio-based biodegradable polymers: PHAs	69
I.3.2.1.	PHA production.....	70
I.3.2.2.	PHA types	72
I.3.2.3.	Characteristics of PHAs	75
I.4.	Critical factors for biocomposite production	79
I.4.1.	Fibre and matrix selection	79
I.4.2.	Fibre/matrix interaction	80
I.4.3.	Fibre content and porosity	81
I.4.4.	Fibre orientation and dispersion	82

I.4.5.	Composite manufacturing process.....	83
I.4.5.1.	Processing conditions.....	84
I.4.6.	Durability and degradation.....	84
I.4.7.	Treatment of cellulosic fibres.....	85
I.4.7.1.	Plasma treatment.....	86
I.4.7.2.	Wet/dry cycling.....	89
I.5.	Cellular materials.....	90
I.5.1.	Fundamentals of foaming.....	92
I.5.2.	Critical factors for foaming.....	95
I.5.2.1.	Polymer matrix characteristics.....	95
I.5.2.2.	Blowing agents for polymeric foams.....	96
I.5.2.3.	Other additives and fillers for polymeric foams.....	97
I.5.2.4.	Foaming method and processing conditions.....	98
I.5.3.	Characteristics of cellular materials.....	101
I.5.3.1.	Cellular structure.....	101
I.5.3.2.	Mechanical properties and deformation mechanisms.....	102
I.6.	Cellular composites.....	106
	References.....	112

CHAPTER II. MATERIALS AND METHODS

II.1.	Materials.....	123
II.1.1.	Flax.....	123
II.1.2.	PHA matrix.....	124
II.1.3.	Blowing agents.....	124
II.1.4.	Chain extender.....	125
II.1.5.	Products for flax treatment.....	125
II.2.	Production techniques.....	126
II.2.1.	Nonwoven production.....	126
II.2.2.	Surface treatments.....	127
II.2.2.1.	Wet/dry cycling.....	127
II.2.2.2.	Plasma treatments.....	128
II.2.3.	Melt compounding.....	130
II.2.4.	Composite production.....	131
II.2.5.	Foaming techniques.....	133
II.2.5.1.	Extrusion foaming.....	133

II.2.5.2. Pressure quench batch foaming	134
II.2.6. Summary of the composite techniques	135
II.3. Characterisation methods	137
II.3.1. Composition and microstructural characterisation	137
II.3.1.1. Fibre content determination.....	137
II.3.1.2. Density and open cell content.....	137
II.3.1.3. SEM.....	138
II.3.2. Mechanical characterisation techniques	139
II.3.2.1. Tensile testing.....	139
II.3.2.2. Macro-mechanical modelling methods	140
II.3.2.3. Compression testing.....	144
II.3.2.4. DMA.....	144
II.3.2.5. Charpy impact tests	146
II.3.3. Thermal characterisation techniques	146
II.3.3.1. DSC	146
II.3.3.2. TGA.....	147
II.3.4. Techniques related with water absorption properties	147
II.3.4.1. Moisture content	147
II.3.4.2. Water retention.....	147
II.3.4.3. Contact angle.....	148
II.3.4.4. Hydrothermal testing.....	148
II.3.4.5. Kinetics of the water absorption.....	149
II.3.5. Other techniques	149
II.3.5.1. DRX	149
II.3.5.2. Rheometry	150
II.3.5.3. XPS.....	150
II.3.6. Summary of the characterisation methods.....	150
References.....	152

CHAPTER III. TREATMENT OF FLAX-NONWOVEN FABRICS

Abstract.....	159
III.1. Introduction	161
III.2. Experimental section	163
III.2.1. Materials.....	163
III.2.2. Nonwoven preparation	163

III.2.3. Nonwoven treatment	163
III.2.3.1. Wet/dry cycling treatment	163
III.2.3.2. Plasma treatments	163
III.2.4. Characterization of the NW fibres	165
III.2.4.1. Surface characterization.....	165
III.2.4.2. Wetting properties.....	165
III.2.4.3. Thermal stability.....	166
III.2.4.4. Fibre crystallinity	166
III.2.4.5. Mechanical properties	166
III.3. Results and discussion	167
III.3.1. Surface characterization.....	167
III.3.1.1. SEM analysis.....	167
III.3.1.2. XPS Analysis	170
III.3.2. Wetting Properties.....	176
III.3.2.1. Water Retention Values.....	176
III.3.2.2. Moisture Regain	176
III.3.2.3. Contact Angles	177
III.3.3. Thermal Stability.....	178
III.3.4. Fibre crystallinity	180
III.3.5. Mechanical properties.....	181
III.3.6. Considerations for Reinforcement Applications	183
III.4. Conclusions.....	184
References	185

CHAPTER IV. MECHANICAL PERFORMANCE AND AGING OF PHB/FLAX FABRIC COMPOSITES

Abstract.....	193
IV.1. Introduction.....	195
IV.2. Experimental section	197
IV.2.1. Materials	197
IV.2.2. Sample preparation.....	197
IV.2.2.1. Production and treatment of the reinforcements	197
IV.2.2.2. Composite fabrication.....	197
IV.2.3. Hydrothermal aging.....	198
IV.2.3.1. Kinetics of the water absorption.....	198

IV.2.4. Characterization of the composites.....	199
IV.2.4.1. Tensile test.....	199
IV.2.4.2. Thermal characterisation.....	199
IV.2.4.3. Morphologic characterisation.....	199
IV.3. Results and discussion.....	200
IV.3.1. Water uptake and kinetics of water absorption.....	200
IV.3.2. Analysis of the mechanical performance.....	203
IV.3.2.1. Macromechanical modelling.....	203
IV.3.2.2. Mechanical behaviour of the unaged samples.....	205
IV.3.2.3. Effects of the aging on the composites' mechanical properties.....	206
IV.3.3. Thermal characterisation.....	207
IV.3.4. Aging effect on the aging on the morphology of the composites.....	209
IV.4. Conclusions.....	211
References.....	212

CHAPTER V. EVALUATION OF THE FOAMABILITY OF THE PHB MATRIX

Abstract.....	221
V.1. Introduction.....	223
V.2. Experimental section.....	225
V.2.1. Materials.....	225
V.2.2. Sample preparation.....	225
V.2.3. Characterization methods.....	226
V.2.3.1. Rheological characterisation.....	226
V.2.3.2. Density.....	227
V.2.3.3. Open cell content.....	227
V.2.3.4. Characterisation of the cellular structure.....	227
V.2.3.5. Differential scanning calorimetry.....	227
V.2.3.6. Compression tests.....	228
V.2.3.7. Tensile tests.....	228
V.2.3.8. Charpy impact tests.....	228
V.3. Results and discussion.....	229
V.3.1. Rheological characterization.....	229
V.3.2. Density.....	229
V.3.3. Cellular morphology.....	230
V.3.4. Thermal behaviour analysis.....	234

V.3.4.1.	Crystallinity degree	234
V.3.4.2.	Melting and crystallisation temperatures.....	236
V.3.5.	Mechanical properties	237
V.3.5.1.	Compression testing results	237
V.3.5.2.	Tensile testing results	240
V.3.5.3.	Impact testing results	241
V.4.	Conclusions	242
	References.....	243

CHAPTER VI. CELLULAR PHB/FLAX COMPOSITES

SECTION 1: PRODUCTION

Abstract.....	251
VI.1.1. Introduction	253
VI.1.2. Experimental section	256
VI.1.2.1. Preparation of the solid composite precursors.....	256
VI.1.2.1.1. Production of the reinforcement fabrics	256
VI.1.2.1.2. CE addition to the matrix.....	257
VI.1.2.1.3. Solid composite precursors' fabrication.....	257
VI.1.2.2. Preparation of the foamed composites.....	257
VI.1.2.3. Samples characterisation	259
VI.1.2.3.1. Rheology of the solid precursors	259
VI.1.2.3.2. Density.....	259
VI.1.2.3.3. Cell size and cell density	259
VI.1.3. Results and discussion.....	260
VI.1.3.1. Preliminary tests.....	260
VI.1.3.2. Influence of the presence of fibre	262
VI.1.3.3. Influence of the processing conditions in the CellFRC properties	264
VI.1.3.3.1. Density.....	264
VI.1.3.3.2. Cellular structure.....	265
VI.1.4. Conclusions	269
References.....	270

SECTION 2: CHARACTERISATION

Abstract.....	275
VI.2.1. Introduction	277

VI.2.2. Experimental section.....	279
VI.2.2.1. Materials	279
VI.2.2.1.1. Matrix	279
VI.2.2.1.2. Reinforcement	279
VI.2.2.1.3. Blowing agent	280
VI.2.2.2. Production of the cellular fabric-reinforced composites.....	280
VI.2.2.2.1. Precursor preparation	280
VI.2.2.2.2. Pressure quench batch foaming.....	280
VI.2.2.3. Design of experiments	281
VI.2.2.4. Samples characterisation.....	281
VI.2.2.4.1. Density.....	281
VI.2.2.4.2. Mechanical characterisation.....	282
VI.2.2.4.3. DSC analysis	285
VI.2.3. Results and discussion.....	286
VI.2.3.1. Mechanical behaviour at room temperature (DMA results).....	286
VI.2.3.2. Dynamic mechanic thermal behaviour of the C-series (DMTA results).....	290
VI.2.3.3. DSC results.....	293
VI.2.3.4. Fibre reinforcing effect	295
VI.2.4. Conclusions	296
References.....	298
Conclusions and Future Work	303
List of Figures.....	309
List of Tables	315
General Bibliography.....	317

INTRODUCTION

SECTION CONTENTS

i.	Motivation and scope of the thesis	33
ii.	Objectives	40
iii.	Framework of the thesis	41
iv.	Structure of the thesis	42
v.	Scientific production	45
v.1.	Publications in journals.....	45
v.1.1.	Derived from this thesis.....	45
v.1.2.	Related with the research line.....	45
v.2.	Communications.....	46
v.3.	Patents.....	47
	References	48

i. Motivation and scope of the thesis

Nowadays, problems such as the persistence of plastics, the shortage of landfill space, the depletion of petroleum resources, the emissions during incineration and hazards to living beings are increasing awareness about the necessity for preservation of the environment. The growing environmental consciousness of humankind has motivated the research, development and application of more eco-friendly materials. All this is leading to the rise of bio-based materials that, given their origin in renewable sources, present an environmentally-friendly and sustainable nature.

In the composite materials field, the path towards this more eco-friendly trend has led to the rise of the so-called “biocomposites”. According to Mohanty et al. [1], the term “biocomposites” is a general term that—regarding to composites of polymeric matrix with fibre reinforcement—comprises: a) composites of synthetic matrix and natural fibres; b) composites of bio-based matrix and synthetic fibres; and c) composites of bio-based matrix and natural fibres (Figure 1). This last group, also referred to as “green composites”, has further attracted considerable interest from industry and research, and their applications are increasing in industries such as automotive, construction and packaging, among others [2].

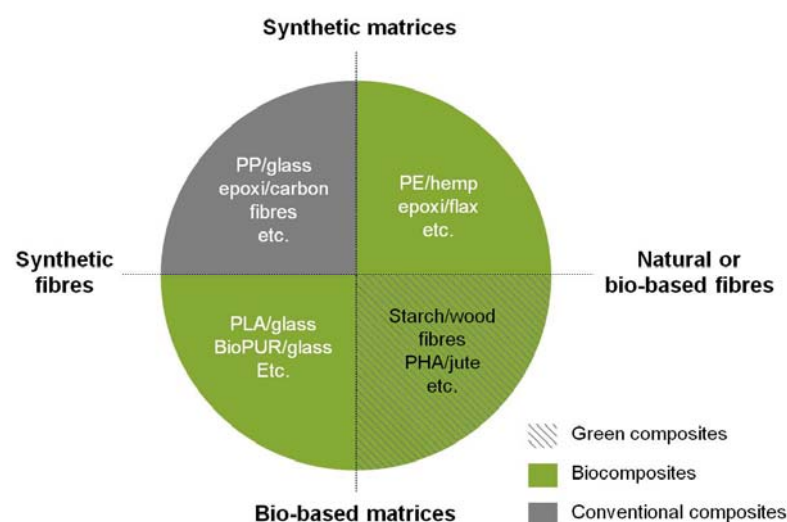


Figure 1. Biocomposites definition.

With regards to matrix materials, bio-based polymers have been proposed in the last few years as an alternative to the largely extended petroleum-based polymers owing to their sustainability, since proceed from renewable resources. It is worth mentioning that bio-based polymers are part of the biopolymers kind. Compared to conventional polymers—which are

petroleum-based and non-biodegradable—biopolymers can be: a) fossil-based but biodegradable; b) bio-based and non-biodegradable; and c) bio-based and biodegradable (Figure 2). It is the last group that are the most promising, since they offer interesting possibilities—such as compostability—for the end-of-life of the goods produced with them. However, the growing interest in environmentally friendly materials is not enough to consider biopolymers as potential candidates to substitute other conventional polymers. In this sense, it is necessary to ensure their competitive price, availability and similar properties to allow any massive replacement of the commodity polymers.

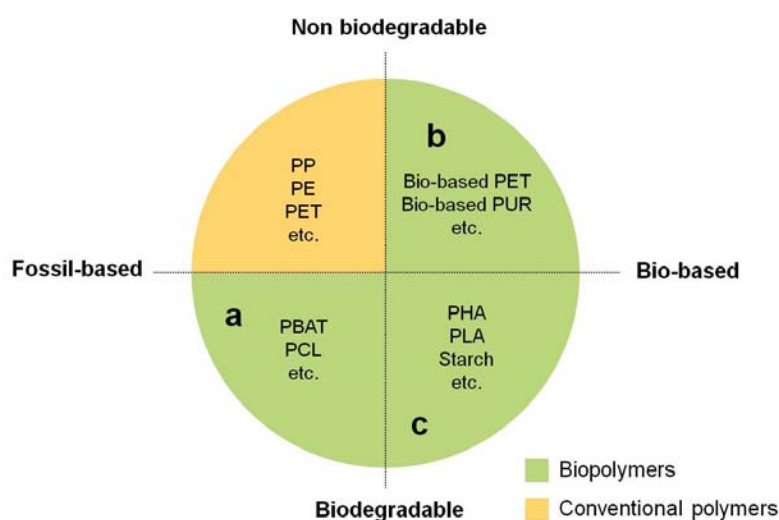
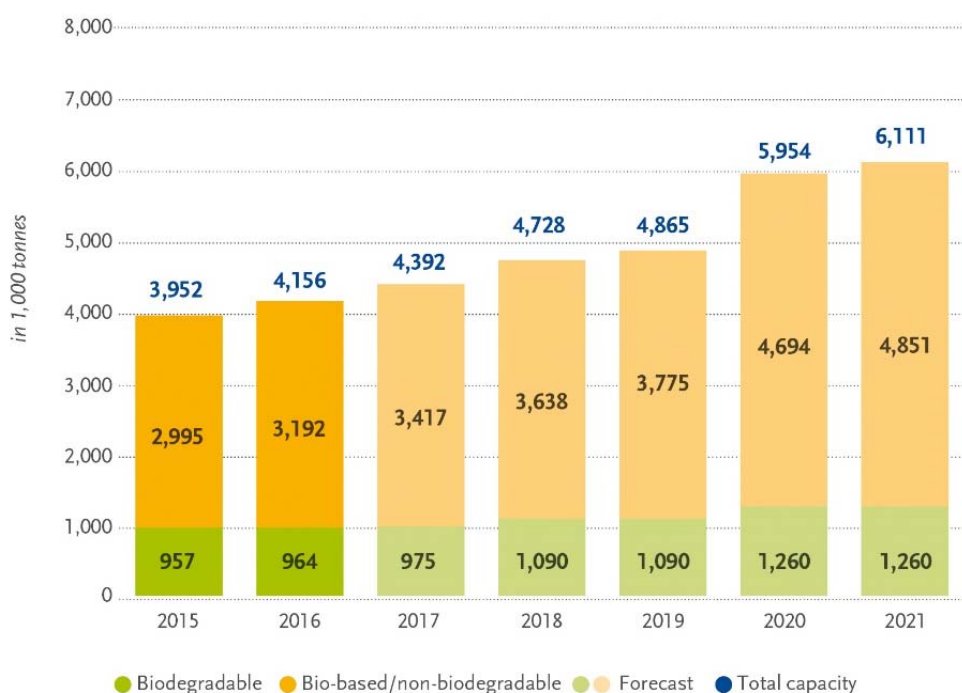


Figure 2. Difference between a conventional polymer and a biopolymer, showing that biopolymers can be: a) fossil-based but biodegradable; b) bio-based and non biodegradable; and c) bio-based and biodegradable. Adapted from [3]

Regarding price and availability, an encouraging increase in the general production capacity of biopolymers—or bioplastics—is observed. In the last decade, this growth has increased each year. In Figure 3, the 2016's forecast for biopolymer production capacities is shown. Although is still very far from the quantities in conventional plastics production, the projections are encouraging. Notably, Europe presents a strong demand for bio-based polymers [4], although the main production is currently in Asia and America (Figure 4). In any case, the factors that favour this increase are the rising price of fossil sources—i.e. oil—, the climate change, and the market acceptance—due to the eco-friendly consciousness—, among others. All these facts have a key effect on the price, which is tending to decrease, and moreover, the continuous advances in research and innovation applied to the extraction, performance and application of biopolymers could speed up this price reduction.



Source: European Bioplastics, nova-Institute (2016).
 More information: www.bio-based.eu/markets and www.european-bioplastics.org/market

Figure 3. “Global production capacities of bioplastics”, from <http://www.european-bioplastics.org>.

Production capacities of biodegradable biopolymers were near 900,000 tonnes in 2016, and 1,200,000 tonnes are expected for 2021. Actually, the higher productions are found for starch blends and polylactic acid (PLA), although the forecast expects a high increase for the polyhydroxyalkanoates (PHAs) production in the next five years.



Source: European Bioplastics, nova-Institute (2016).
 More information: www.bio-based.eu/markets and www.european-bioplastics.org/market

Figure 4. “Global production capacities of bioplastics in 2016 (by region)”, from <http://www.european-bioplastics.org>.

In terms of properties, the main drawbacks of these polymers are, in general terms, hydrophilicity, low thermal stability and lower mechanical properties. To reduce these disadvantages blending with other polymers and reinforcement with fillers or fibres are methods commonly used. This can improve their mechanical and thermal properties, as well as their processability and stability against humidity [5,6].

An interesting area of study are PHAs. They are bio-based polymers produced by bacteria as an energy storage resource when fed in extreme conditions—i.e. excess of carbon and deficiency of other nutrients such as oxygen, nitrogen or phosphorous—. At present, more than 300 species of PHA-producing bacteria are known [7]. These fully biodegradable polyesters are mainly hydrophobic, insoluble in water, largely stable in air, inert, non-toxic and biocompatible [7,8]. Moreover, they can easily degrade to water and carbon dioxide under environmental conditions [9]. PHAs have mechanical properties comparable to those of polypropylene, although they have a much lower elongation at break and are more brittle. Compared to polypropylene, PHAs are more stable to UV degradation but less resistant to solvents [7]. Their properties, biodegradability, and origin in renewable sources, make PHAs interesting for a wide range of applications. Moreover, PHAs are available in the market, and thus is of interest given that the production of the PHAs to be used as matrix in composites is out of the scope of the thesis.

With regard to the reinforcement, the utilisation of natural fibres as reinforcement for polymer matrixes is one possible path towards the development of more eco-friendly composites. Natural plant (cellulosic) fibres—such as flax—present interesting properties: availability, renewability, low-cost, non-toxicity, biodegradability, and other technical characteristics, such as good acoustic and thermal insulation, as well as competitive mechanical behaviour—i.e. high modulus and fair resistance—. Because of this, natural cellulosic fibres have emerged as an alternative reinforcement to conventional carbon and glass fibres and other inorganic fillers [10,11], and are the main candidates for biocomposites development. Therefore, as a result of the research in new applications of natural fibre composites, innovative solutions have appeared on the market, offering alternative products which are more environmentally friendly [12].

In the field of fibre reinforced composites is referred, two main types are commonly considered: those containing short fibres—known as fibre reinforced composites (FRC)—, and those reinforced with long fibres forming structures—known as textile reinforced composites (TRC)—, as summarised in Figure 5.

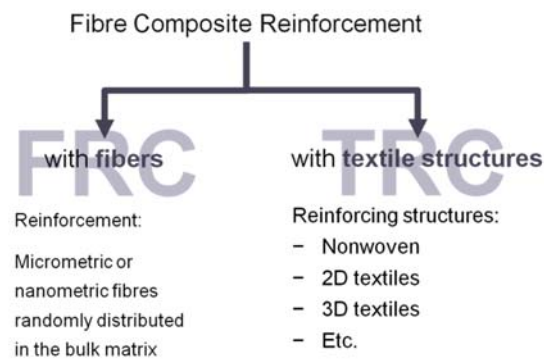


Figure 5. Classification of the fibre reinforced composites.

FRC typically contain micro or nano fibres randomly distributed in the bulk matrix. Reinforcing capabilities strongly depend on the amount and type of fibre, its geometry and its adhesion to the matrix. TRC contain textile structures as reinforcement. The reinforcing capability is here dependant not only in the previously cited fibre parameters but also on the structure, because there is fibre distribution and orientation in the textile. The most common textile structures used for composite reinforcement are nonwoven or fibre mats, weaved 2D or 3D fabrics, knitted fabrics, 2D or 3D braided structures [13,14]. The cheapest textile structures are the nonwoven ones, in which fibres are randomly distributed (although it is possible to have a main direction orientation due to the production process).

Fibres used for TRC need to have adequate length and fineness for their processability by the existent textile technologies, thus pointing to those like the cellulosic fibres traditionally used by textile industry—that have high aspect ratio and low mass—, such as: flax, hemp, ramie, jute or kenaf.

On the other hand, an important parameter to be controlled is the adhesion between the matrix and the fibre. It has a key role in load distribution and hence, in the final mechanical properties of the composite. Therefore, it is important to improve the adhesion to the matrix in order to achieve new environmentally-friendly composites with good mechanical properties. One of the strategies that can be considered is the functionalisation of the fibre surface by chemical or physical methods [15]. This modification must be consistent with the matrix, because different matrices require different fibre surface properties.

In this sense, the plasma technology is an environmentally-friendly and cost-efficient solution for the surface modification of fibres. The advantages of this green process are that the low amount of chemicals used, that no water is required, and the low waste production—residual waste, water, solvents or chemicals—, since the treatment is performed in the gas

state. Moreover, these phenomena take places in the most external layer of the substrate (10-100 nm), thus meaning that only the surface is altered while the bulk of the fibres and their properties are preserved. By varying the process parameters—such as type of gas, power, processing time and pressure, and gas flow—, different effects can be obtained. A large amount of gases—such as air, nitrogen, argon, oxygen or fluorocarbon gases, among others—are used in plasma technologies in textile fabrics to produce several effects, such as: hydrophilicity, hydrophobicity, dyeability and printability performance, or other functional finishing modifications—such anti-bacterial, for instance—, among others [16]. Thus, plasma technologies are focussing the interest of the industrial textile, and can also be a great opportunity for the composites industry.

Nonetheless, the use of bio-based matrices and natural fibres as reinforcement is not the only possible strategy to obtain environmentally-friendly composites, Development of lighter composites with improved specific properties can be another interesting path to obtain more efficient composites. This is related to a more adequate use of the energy, what leads to greener composites too. The obtaining of these lightweight composites can be reached by foaming the polymer used as matrix. Concerning to this, the foaming of some of the thermoplastic biopolymers is still a challenge to be faced, in the sense that only few literature has been published. Polymers such as PLA, starch or PHA present some difficulties to be foamed that encourage the researchers to develop and optimise foaming techniques for these.

In this sense, considering greener methods for foaming, a growing interest is focussed in foaming with gases of low environmental-impact such as carbon dioxide (CO₂). CO₂ is an eco-friendly, non-flammable, not ozone-depleting, chemically inert, non-toxic and low cost blowing agent, which is obtained as a by-product in other production processes, and presents good gas solubility in polymers—with PHAs among them [17]—. It can be used in supercritical state in several foaming techniques such as injection foaming, extrusion foaming or batch foaming. Supercritical state in CO₂ (scCO₂) is achieved in specific conditions—when the temperature is higher than 31.1 °C and the pressure higher than 7.39 MPa—. In the supercritical state, the CO₂ bears both the properties of a liquid and a gas, presenting high diffusivity, low viscosity and high density, and is interesting due to expected effects of melting temperature depression and plasticization. In fact, solubility of scCO₂ in PHAs has been observed to rapidly dissolve with the increase in pressure, and to decrease the melting temperature—at a rate around 1.3 °C/MPa—up to 24 MPa [18].

Therefore, there are some challenging features to be focussed: treatment of the fibres to perform adequate adhesion to the matrix and better stability, foaming of the biopolymeric matrix, optimisation of biocomposites with natural fibres and biopolymer matrix and, as a final goal, the development of lightweight and environmentally-friendly composites using foaming techniques. In this sense, the novelty of this thesis is in the line of achieving foamed composite materials reinforced with textile structures from solid precursors.

ii. Objectives

The milestone of this thesis is the development of new composite materials based on biopolymers and natural cellulosic fibres with high specific properties, lightweight and low cost regarding the eco-efficiency in all stages of the life cycle.

Moreover, are also objectives of this research:

- To acquire knowledge of surface modification of natural cellulosic fibres for increasing adhesion and stability in bio polymeric matrices.
- To acquire knowledge of development of textile structures to optimise processing, fibre orientation, easy handling and final properties of the composite.
- To acquire knowledge about biopolymers and their feasibility to be used as foamed matrices in composite materials.
- To establish proceedings for the lab-scale production of composites with biopolymer as matrix and natural cellulosic fibres or its nonwoven structures as reinforcement.
- To contribute to the general knowledge of structures, morphologies and properties of the elaborated composites.
- To study possible synergic effects in those properties derived from the combination of fibres and textiles structures and the foaming process of a bulk material.
- To identify possible applications for the developed composites, to spread the results by journal papers and conference lectures, and to establish the bases for future work.

iii. Framework of the thesis

This thesis has been possible thanks to the financial assistance of the Ministerio de Educación, Cultura y Deporte (MECD) from the Government of Spain, by means of the FPU grant (reference FPU12/05869) awarded to H. Ventura. The thesis is framed in the Doctoral Program of Textile and Paper Engineering, located in the School of Industrial, Aerospace and Audiovisual Engineering of Terrassa—“Escola Superior d’Enginyeries Industrial, Aeroespacial i Audiovisual de Terrassa” (ESEIAAT)—from the Universitat Politècnica de Catalunya (UPC).

The thesis has been developed mainly between the textile laboratories of the Textile Engineering Division of the Materials Science and Metalurgic Engineering Department—Departament de Ciència dels Materials i Enginyeria Metal·lúrgica (CMEM), Secció Àmbit d’Enginyeria Tèxtil (SAET)—of the UPC, and the Cellular Materials Laboratory (CellMat) of the Condensed Matter Physics Department of the Universidad de Valladolid (UVA). Briefly, the part of the study related to fibres, fabrics, reinforcements and their treatments, as well as part of the characterisation, has been performed in the SAET, while the production of foams and solid composites, as well as samples characterisation has been performed in CellMat. Collaboration of both departments has been key to the proper accomplishment of the research, given that this collaboration has permitted access to complementary facilities and equipments. In this sense, financial support of the Ministerio de Economía, Industria y Competitividad (MINECO) of the Government of Spain, by means of FEDER programs (references BIA2011-26288, BIA2014-59399-R, MAT 2012-34901 and MAT2015-69234-R), and the Junta of Castile and Leon (references VA035U13 and VA011U16) is also gratefully acknowledged.

Besides this, a stay of three-months has been carried out in the Istituto per i Polimeri, Compositi e Biomateriali (IPCB) of the Consiglio Nazionale della Ricerca (CNR) in Portici-Naples (Italy), and hence this thesis fulfils the requirements to be accredited with the International Mention. This stay has been possible thanks to the financial assistance of the mobility complement for the FPU grant (reference EST14/00273) awarded to H. Ventura. The purpose of the stay—the evaluation of the gas dissolution batch foaming for the production of foamed composite samples—has been successfully achieved.

Funding and access to all the facilities and equipment are gratefully acknowledged.

iv. Structure of the thesis

This manuscript is divided in six chapters, which can be summarised as follows:

Chapter I, STATE OF THE ART. In this chapter the background and state of the art are revised. Considering the multidisciplinary of the thesis, the fundamentals of: cellulosic fibres—focussing on flax—, nonwoven fabrics, polyhydroxyalkanoates, main factors that affect composite processing, fabric treatments used in the thesis, cellular materials, and key factors that affect foaming, are covered. A final literature review regarding cellular composites is presented, focussed in cellular green composites, and in cellular composites that contain structured fibres as reinforcement.

Chapter II, MATERIALS AND METHODS. This chapter summarises all the materials, production methods and characterisation methods used in the thesis. The materials—flax fibres, matrix resin, additives, blowing agents and products for treatments—are presented. The production techniques—fabrication and treatment of nonwovens, techniques for composite production and foaming methods used—are described. Given the disparity of the areas covered by the thesis—textiles, foams and composites—, a small basis of some techniques is given, with the aim of ensure the comprehension of the work to many potential readers. Finally, a briefly description of the conditions used in the characterisation techniques is included.

Chapter III, TREATMENT OF FLAX-NONWOVEN FABRICS. Two main treatment paths are investigated to modify the flax fibre nonwoven with the aim of improving the fibre/matrix adhesion in composites. On the one hand, a wet/dry cycling is considered. On the other hand, two sorts of plasma treatment—low pressure and atmospheric pressure—are evaluated. The former is to stabilise the fibres against water absorption, the latter are to modify the chemical groups present in the fibre surface, producing hydrophylicity or hydrphobicity depending on the gases. The plasma conditions required are also studied. The treated NW samples are characterised evaluating mechanical properties, water-related properties and chemical composition of the fibre's surface. Those treatments presenting the most interesting properties for polymer matrix composites reinforcement are selected for Chapter IV.

Chapter IV, MECHANICAL PERFORMANCE AND AGING OF PHB/FLAX FABRIC COMPOSITES.

In this chapter, selected nonwoven fabrics studied in the previous chapter are used to produce composites with the PHB-matrix. The composites are characterised before and after performing a hydrothermal aging. The water absorption kinetics is studied, the composites are mechanically characterised, and macro-mechanical models—both considering and not considering the porosity of the composites—are compared to the experimental data. From this study, the treatments presenting higher fibre/matrix adhesion and higher durability—lower loss of properties after aging—are selected for their use in Chapter VI.

Chapter V, EVALUATION OF THE FOAMABILITY OF THE PHB-MATRIX. Given that a final objective is to produce foamed (cellular) composites, the feasibility of the selected matrix to produce such cellular structures—of certain quality—is evaluated in this chapter. In this sense, two strategies are considered: the use of a chain extender and a fast cooling achieved by water quenching. The extrusion foaming technique is used to that purpose, and the foaming is achieved by means of chemical blowing agents. The cellular structure achieved is characterised, as well as the mechanical properties of the obtained foams.

Chapter VI, CELLULAR PHB/FLAX COMPOSITES. This chapter is divided into two sections. On the first one, the production of the cellular composites is addressed. Since the references about foaming composites with textile structures are scarce, a new approach is proposed: a pressure quench method of gas dissolution of batch foaming. The conditions to achieve low density cellular composites are optimized, and evaluated through the analysis of the cellular structure. On the second section, the effect of the NW, chain extender addition and expansion temperature and pressure in the mechanical properties of the foams are evaluated. Some of the samples are selected to perform in-deep characterisation by means of dynamical mechanical analysis and differential scanning calorimetry.

In Figure 6, the relationship between the chapters and related scientific publications is presented.

Go to next page

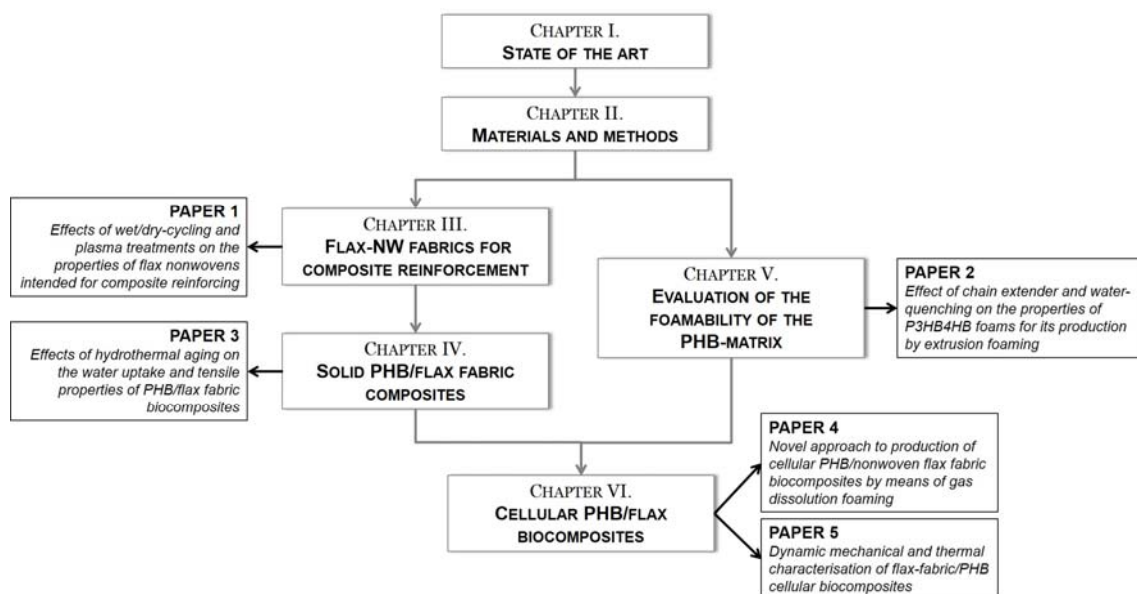


Figure 6. Summary of the chapters and scientific publications in the thesis.

v. Scientific production

v.1. Publications in journals

v.1.1. Derived from this thesis

- *Dynamic mechanical and thermal characterisation of flax-fabric/PHB cellular biocomposites*. Ventura, H.; Sorrentino, L.; Rodríguez-Pérez, M.A.; Ardanuy, M. Preparing the final version of the manuscript.
- *Novel approach to production of cellular PHB/nonwoven flax fabric biocomposites by means of gas dissolutions foaming*. Ventura, H.; Sorrentino, L.; Laguna-Gutiérrez, E.; Rodríguez-Pérez, M.A.; Ardanuy, M. Preparing the final version of the manuscript.
- *Effects of hydrothermal aging on the water uptake and tensile properties of PHB/flax fabric biocomposites*. Ventura, H.; Claramunt, J.; Rodríguez-Pérez, M.A.; Ardanuy, M. Under review (Polymer Degradation and Stability).
- *Effect of chain extender and water-quenching on the properties of poly(3-hydroxybutyrate-co-4-hydroxybutyrate) foams for its production by extrusion foaming*. Ventura, H.; Laguna-Gutiérrez, E.; Rodríguez-Pérez, M.A.; Ardanuy, M. European Polymer Journal. Vol. 85, p. 14-25. Published on 2016-10-01. doi: 10.1016/j.eurpolymj.2016.10.001. Estimated impact factor: 3.485, Q1 (13/85)
- *Effects of wet/dry-cycling and plasma treatments on the properties of flax nonwovens intended for composite reinforcing*. Ventura, H.; Claramunt, J.; Navarro, A.; Rodríguez-Pérez, M.A.; Ardanuy, M. Materials. Vol. 9, num. 2, p. 93:1-93:18. Published (in Open Access) on 2016-02-03. doi: 10.3390/ma9020093. Estimated impact factor: 2.651, Q1 (55/260)
- *Effects of needling parameters on some structural and physico-mechanical properties of needle-punched nonwovens*. Ventura, H.; Ardanuy, M.; Capdevila, F.X.; Cano, F.; Tornero, J.A. Journal of the Textile Institute. Vol. 105, num. 10, p. 1065-1075. Published on 2014-06-26. doi: 10.1080/00405000.2013.874628. Impact factor: 0.770, Q2 (11/22)

v.1.2. Related with the research line

- *Tensile and flexural properties of cement composites reinforced with flax nonwoven fabrics*. Claramunt, J.; Ventura, H.; Fernandez-Carrasco, L.; Ardanuy, M. Materials. Vol. 10, num 215, p. 1-13. Published on 2017-02-22. doi: 10.3390/ma10020215. Estimated impact factor: 2.651, Q1 (55/260)
- *Natural fiber nonwoven reinforced cement composites as sustainable materials for building envelopes*. Claramunt, J.; Fernandez-Carrasco, L.; Ventura, H.; Ardanuy, M. Construction & building materials. Vol. 115, p. 230-239. Published on 2016-04-16. doi: 10.1016/j.conbuil dmat.2016.04.044. Estimated impact factor: 2.265, Q1 (7/58)

- *Effect of water treatment on the fiber-matrix bonding and durability of cellulose fiber cement composites.* Ardanuy, M.; Claramunt, J.; Ventura, H.; Manich, A.M. Journal of biobased materials and bioenergy. Vol. 9, num. 5, p. 486-492. Published on 2015-11-23. Impact factor: 0.653, Q4 (57/70)
- *Characterization and treatments of oil palm frond fibers and its suitability for technical applications.* Ventura, H.; Morón, M.; Ardanuy, M. Journal of natural fibers. Vol. 12, num. 1, p. 84-95. Published on 2014-09-29. doi: 10.1080/15440478.2014.897670. Impact factor: 0.512, Q3 (15/22)

v.2. Communications

- *Treatments of cellulosic fabrics to reduce the water absorption in composite reinforcement.* Ventura, H.; Claramunt, J.; Rodríguez-Pérez, M.A.; Ardanuy, M. GEP 2016, Burgos-Spain, 2016. Proceedings of the XIV Reunión del Grupo Especializado de Polímeros (GEP) de la RSEQ y RSEF, p. 316-317.
- *Extrusion foaming of PHB-copolymer: effect of chain extender and cooling system on the cellular structure and properties.* Ventura, H.; Rodríguez-Pérez, M.A.; Ardanuy, M. Biofoams 2015, Sorrento-Italy, 2015. Proceedings of the 5th International Conference on Biofoams, p. 1-2.
- *The influence fiber treatment on the mechanical properties of biocomposites reinforced with flax nonwovens.* Ventura, H.; Claramunt, J.; Navarro, A.; Rodríguez-Pérez, M.A.; Ardanuy, M. Biopol 2015, San Sebastian-Spain, 2015. Proceedings of the 5th International Conference on Biodegradable and Biobased Polymers, p. 1-5.
- *Cellular structure and mechanical properties of polydihydroxyalkanoate (PHA) based foams.* Ventura, H.; Rodríguez-Pérez, M.A.; Ardanuy, M. Biopol 2015, San Sebastian-Spain, 2015. Proceedings of the 5th International Conference on Biodegradable and Biobased Polymers, p. 1-2.
- *Evaluation of fire behaviour of flax fabrics treated with expandable graphite based coatings.* Ardanuy, M.; Ventura, H.; Claramunt, J.; Haurie, L. 6th ITTC, Izmir-Turkey, 2015. Proceedings of the 6th International Technical Textiles Congress, p. 277-282.
- *The influence of wet/dry treatment on the properties and fibre-matrix bonding of vegetable fibre cement mortar composites.* Ardanuy, M.; Claramunt, J.; Ventura, H.; Fernandez-Carrasco, L.; Manich, A.M. 2nd ICNF, São Miguel de Las Azores-Portugal, 2015. Proceedings of the 2nd International Conference on Natural Fibers, p. 145-146.
- *Effects of drying and rewetting cycles on the water absorption of vegetable fibres for composite reinforcement.* Ardanuy, M.; Claramunt, J.; Perron, H.; Ventura, H.; Manich, A.M. Biobased Materials 2014, Stuttgart-Germany, 2014. Proceedings of the 10th Congress for Biobased Materials, Natural Fibres and WPC. **Best poster award.**

- *Evaluation of the mechanical behavior of natural fiber nonwoven cement composites under flexural loading*. Ardanuy, M.; Claramunt, J.; Ventura, H.; Pares, F.; Fernandez-Carrasco, L. XIII CNM, Barcelona, Spain, 2014. Proceedings of the XIII Congreso Nacional de Materiales.
- *Estructuras no tejidas de fibras naturales como refuerzo para compuestos de cemento de elevada ductilidad*. Claramunt, J.; Ventura, H.; Pares, F.; Ardanuy, M. 10th CNMC, Algeciras-Spain, 2013. Proceedings of the 10º Congreso Nacional de Materiales Compuestos, p. 317-321.
- *Natural fibre nonwovens as reinforcement for cement mortar composites*. Claramunt, J.; Ventura, H.; Pares, F.; Ardanuy, M. 1st ICNF, Guimarães-Portugal, 2013. Proceedings of the 1st International Conference on Natural Fibers, p. 191-192.
- *Cement mortar composites reinforced with nano and micro-scale cellulose fibers*. Ardanuy, M.; Claramunt, J.; Ventura, H. 1st ICNF, Guimarães-Portugal, 2013. Proceedings of the 1st International Conference on Natural Fibers, p. 195-196.
- *Mechanical performance of cement mortar composites reinforced with cellulose fibres*. Claramunt, J.; Ardanuy, M.; Pares, F.; Ventura, H. 9th ICCST, Sorrento-Italy, 2013. Proceedings of the 9th International Conference on Composite Science and Technology, p. 477-484.

v.3. Patents

- *Producto de material compuesto de aglomerante inorgánico y fibras vegetales, y método para su fabricación*. Claramunt, J.; Ardanuy, M.; Fernandez-Carrasco, L.; Ventura, H. Invention patent, Spain, 2014.

References

- [1] Mohanty AK, Misra M, Drzal LT. *Natural Fibers, Biopolymers, and Biocomposites*. CRC Press; 2005. doi:10.1201/9780203508206
- [2] Thomas S, Pothen LA. *Natural Fibre Reinforced Polymer Composites. From Macro to Nanoscale*. Paris: Old City Publishing; 2009.
- [3] European Bioplastics. *Technology/Materials 2013*. <http://en.european-bioplastics.org> (accessed May 27, 2014).
- [4] Carus M. Production capacities for bio-based polymers in Europe: Status and trends towards 2020. *Jec Compos Mag* 2013;20–12.
- [5] Vroman I, Tighzert L. Biodegradable Polymers. *Materials (Basel)* 2009;2:307–44. doi:10.3390/ma2020307
- [6] Luckachan GE, Pillai CKS. Biodegradable Polymers- A Review on Recent Trends and Emerging Perspectives. *J Polym Environ* 2011;19:637–76. doi:10.1007/s10924-011-0317-1
- [7] Laycock B, Halley P, Pratt S, Werker A, Lant P. The chemomechanical properties of microbial polyhydroxyalkanoates. *Prog Polym Sci* 2014;39:397–442. doi:10.1016/j.progpolymsci.2013.06.008
- [8] Reddy CSK, Ghai R, Rashmi, Kalia VC. Polyhydroxyalkanoates: An overview. *Bioresour Technol* 2003;87:137–46. doi:10.1016/S0960-8524(02)00212-2
- [9] Shanks RA, Hodzic A, Wong S. Thermoplastic biopolyester natural fiber composites. *J Appl Polym Sci* 2004;91:2114–21. doi:10.1002/app.13289
- [10] Satyanarayana KG, Arizaga GGC, Wypych F. Biodegradable composites based on lignocellulosic fibers—An overview. *Prog Polym Sci* 2009;34:982–1021. doi:10.1016/j.progpolymsci.2008.12.002
- [11] López-Manchado MA, Arroyo M. Fibras naturales como refuerzos de matrices poliméricas. *Rev plásticos Mod* 2003;594–600.
- [12] Carus M, Scheurer H. *Directory for Innovative Renewable Materials and Bio-based Products*. Nova-Institut GmbH 2011.
- [13] Chou W, Ko F. *Textile structural composites*. vol. 1. Elsevier S. New York: Elsevier Science & Technology Books; 1989.
- [14] Larrodé E. *Materiales Compuestos*. Barcelona: Reverte; 2003.
- [15] Faruk O, Bledzki A, Fink H, Sain M. Biocomposites reinforced with natural fibers: 2000–2010. *Prog Polym Sci* 2012;37:1552–96. doi:10.1016/j.progpolymsci.2012.04.003.
- [16] Zille A, Oliveira FR, Souto AP. Plasma Treatment in Textile Industry. *Plasma Process Polym* 2014;n/a-n/a. doi:10.1002/ppap.201400052
- [17] Wright ZC, Frank CW. Increasing cell homogeneity of semicrystalline, biodegradable polymer foams with a narrow processing window via rapid quenching. *Polym Eng Sci* 2014;54:2877–2886. doi:10.1002/pen.23847
- [18] Takahashi S, Hassler JC, Kiran E. Melting behavior of biodegradable polyesters in carbon dioxide at high pressures. *J Supercrit Fluids* 2012;72:278–87. doi:10.1016/j.supflu.2012.09.009

CHAPTER I

STATE OF THE ART

CHAPTER CONTENTS

I.1.	Biocomposites.....	53
I.1.1.	Fibre reinforcements in composite materials.....	55
I.1.1.1.	Nonwoven production.....	56
I.2.	Natural fibres as reinforcement in biocomposites.....	59
I.2.1.	Chemical composition and properties of cellulosic fibres.....	59
I.2.2.	Plant bast fibres.....	62
I.2.2.1.	Flax.....	63
I.3.	Biopolymers as matrix in biocomposites.....	68
I.3.1.	Biopolymers classification.....	68
I.3.2.	Bio-based biodegradable polymers: PHAs.....	69
I.3.2.1.	PHA production.....	70
I.3.2.2.	PHA types.....	72
I.3.2.3.	Characteristics of PHAs.....	75
I.4.	Critical factors for biocomposite production.....	79
I.4.1.	Fibre and matrix selection.....	79
I.4.2.	Fibre/matrix interaction.....	80
I.4.3.	Fibre content and porosity.....	81
I.4.4.	Fibre orientation and dispersion.....	82
I.4.5.	Composite manufacturing process.....	83
I.4.5.1.	Processing conditions.....	84
I.4.6.	Durability and degradation.....	84
I.4.7.	Treatment of cellulosic fibres.....	85
I.4.7.1.	Plasma treatment.....	86
I.4.7.2.	Wet/dry cycling.....	89
I.5.	Cellular materials.....	90
I.5.1.	Fundamentals of foaming.....	92
I.5.2.	Critical factors for foaming.....	95
I.5.2.1.	Polymer matrix characteristics.....	95
I.5.2.2.	Blowing agents for polymeric foams.....	96
I.5.2.3.	Other additives and fillers for polymeric foams.....	97
I.5.2.4.	Foaming method and processing conditions.....	98
I.5.3.	Characteristics of cellular materials.....	101

I.5.3.1.	Cellular structure	101
I.5.3.2.	Mechanical properties and deformation mechanisms	102
I.6.	Cellular composites	106
References	112

I.1. Biocomposites

Composites can be defined as materials formed by a matrix and a reinforcement in which both components contribute synergistically to the properties. Composites can be found throughout the human history, from the straw reinforced breaks used by antique cultures—Egyptian and Mesopotamian—and the concrete compositions used by Romans, to the modern carbon fibre composites used in the Formula1 vehicles. However, it was in the 20th century—with the emergence of polymers—when the polymer matrix composites were popularized. The shortage of metallic materials during the World War II boosted the use of fibre-reinforced polymers (FRP) on housings and vehicle bodyworks. FRP were popularized on the 1950's, when thermosetting polyester resins reinforced with glass fibres were used in chairs, boats and many other applications of mass consume. In the 1970's, short glass fibres were introduced in thermoplastic polymers—such as polypropylene or polyamides—in injection processes, largely increasing the stiffness and strength of the moulded parts. Continuous research and development of materials and production techniques has made of composites one of the most relevant families of materials at the present time, and are used in many industrial sectors, from sport goods to automotive. Their lightweight and high specific properties have played a key role in that sense.

Conventional composites are produced with thermosetting resins or thermoplastic petrochemical-based polymers, which have problems concerning to their final disposal or their recyclability, and concerning to the depletion of resources, among others. In the last decades, concepts such as sustainability, eco-efficiency, eco-design, carbon footprint, etc. have gained relevance for both the research and the industry. These have slowly proved to deserve this attention due to both environmental and economic benefits. Thus, added to the increasing environmental problems and the growing eco-friendly consciousness, has prompted research and industry towards the search of the so-called biocomposite materials.

This general term “biocomposites” comprises [1]:

- Composites of synthetic matrix and natural fibres.
- Composites of bio-based matrix and synthetic fibres.
- Composites of bio-based matrix and natural fibres or “green composites”.

Regarding the applications of biocomposites, they have extended to multiple sectors—being synthetic polymers reinforced with natural fibres the most common—and are constantly growing, especially in automotive and aerospace industries [2]. In this sense,

numerous examples of commercial interior car components can be found—such as door interiors (Figure I.1), roof linings, instrument panels, dashboard consoles, seat backs, trims, or internal engine covers, among others [3–5]—and also in exterior parts, such as commercial exterior underfloor panelling [3] or in the bodywork of some electrical concept vehicles, for instance. The aircraft industry is using natural fibre reinforced composites for interior panelling [3]. In construction, biocomposites are being used for non-structural applications in door and window frames, roof structures, floors and wall insulation [3,5], and the use of natural fibres for cement reinforcement is being assessed [6]. In the sport and leisure industries, the use of biocomposites in surfboards, snowboards and fishing rods, and of hybrid biocomposites—which contain other fibres like carbon fibres—in tennis rackets and bicycle frames is also reported [3,7].



Figure I.1. Interior carpeting of a car door made on PE/hemp fibres biocomposite*.

On the other hand, the group of green composites is gaining the attention of the research community, owing to a lower environmental impact because of their renewable origin and, in most cases, their biodegradability. Recyclability of composites of thermoplastic matrices present some drawbacks, since natural fibres suffer from thermal degradation during the reprocessing. Therefore, when recycling is not an appropriate option, the fact that the whole material—matrix and reinforcement—can biodegrade, helps to face the problem of end-of-life disposal of the final good/product. These biodegradable composites are the sort of biocomposites under the scope of the thesis, and hence, the possible candidates for such a material are further reviewed.

* (Modified). Original by Christian Gahle, nova-Institut GmbH - Work by Christian Gahle, nova-Institut GmbH, CC BY-SA 3.0, <https://commons.wikimedia.org/w/index.php?curid=4423801>

I.1.1. Fibre reinforcements in composite materials

Fibres can be added to the composites in the form of randomly dispersed fibres or forming textile structures. According to this, two main sort of composites are defined depending on the form of the fibre reinforcement:

- *Fibre reinforced composites* (FRC) with non-entangled fibres.
- *Textile reinforced composites* (TRC), reinforced with fibres forming structures (fabrics).

FRC typically contain micro or nano fibres randomly distributed in the bulk matrix. Reinforcing capabilities strongly depend on the amount and type of fibre, its geometry and its adhesion to the matrix.

TRC contain textile structures as reinforcement. The reinforcing capability is here dependant not only in the aforementioned fibre parameters, but also on the structure because of the fibre distribution and orientation in the textile.

The textile structures used for composite reinforcement can be woven 2D or 3D fabrics (Figure I.2a), nonwoven or fibre mats (Figure I.2b), knitted, multiaxial and non-crimp fabrics (Figure I.2c), and 2D or 3D braided structures, among others [8,9].

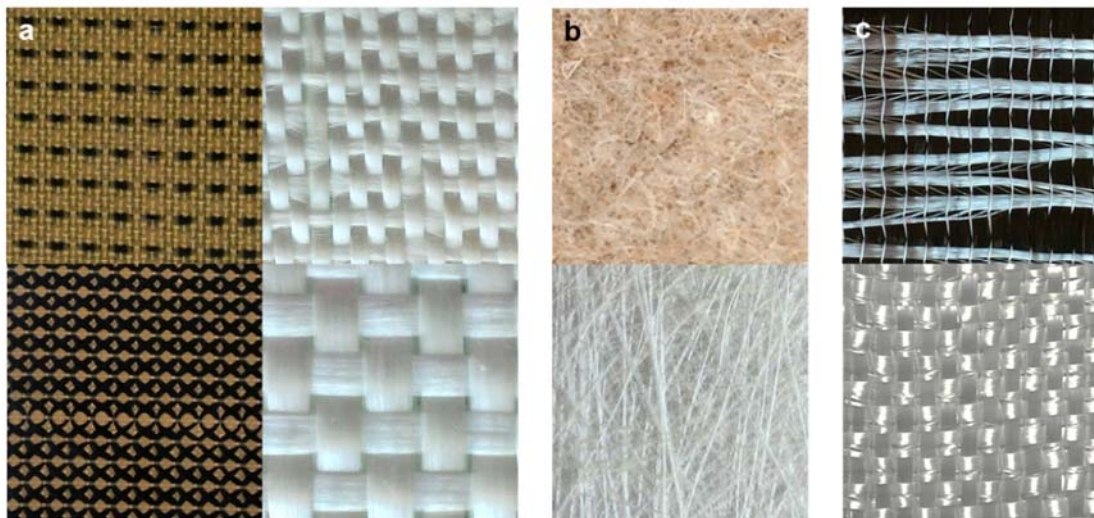


Figure I.2. Typical structures of fibre reinforcements: a) woven fabrics with several structures; b) nonwoven fabrics (mats); c) non-crimp fabrics.

Fibres used for TRC requires an adequate length and fineness for being processed by textile technologies. This requirement is fulfilled by some of the most common natural fibres such as flax, jute or sisal. Woven 2D fabrics and fibre mats—2D nonwoven structures—are the most relevant types of TRC reinforcement, being the production of nonwovens the

cheapest technology. Although in nonwoven structures fibres are randomly distributed, it is possible to have certain degree of orientation in a main direction due to the production process.

I.1.1.1. Nonwoven production

The fabrication process of nonwovens (NW) consists in general in three steps: web formation, web bonding and finishing (Figure I.3).

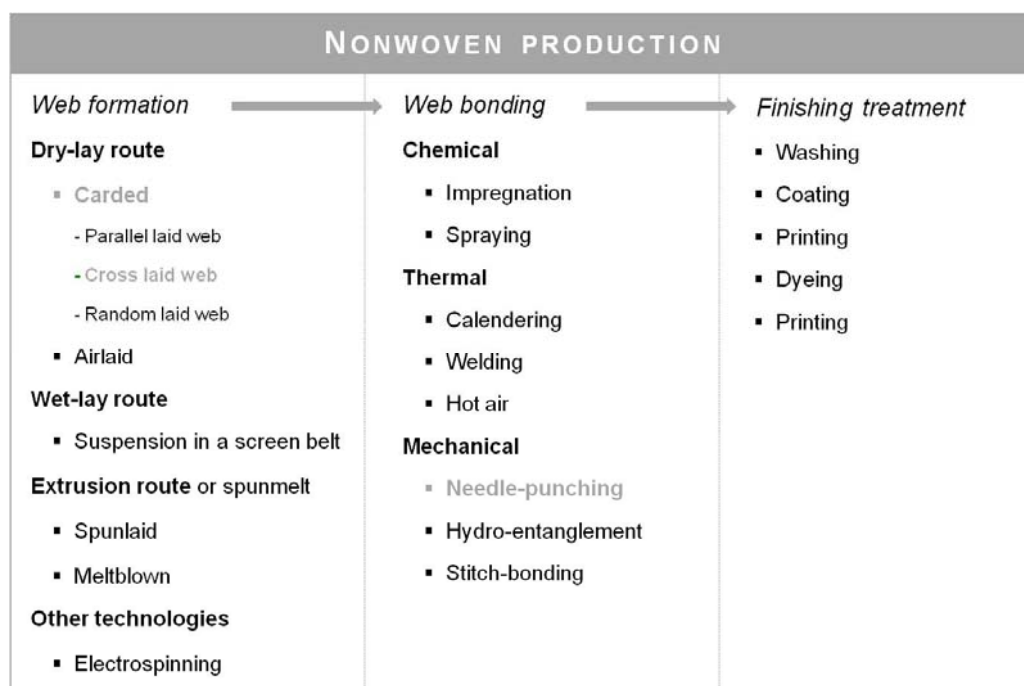


Figure I.3. Scheme for nonwoven production methods.

The first step consists in the preparation of a web of random fibres. From all the techniques available, the dry-lay route, which consists of a carding process followed by cross-lapping, is the one used in this thesis. The second step consists in the bonding of the web. This bonding in NWs of natural fibres is mainly achieved by mechanical entanglement. Since needle-punching bonding has been used in this thesis, this technique is further analysed. The third step is the application of finishing treatments.

Carding and Needle-punching process

The carding process (Figure I.4) has the aim to disentangle the tufts into single fibres, in order to mix them and to form a homogeneous web with uniform weight per unit area. To that purpose, the tufts are fed in the card, where a series of toothed rolls interact in order to

produce the separation of the fibres. Then, this thin web is layered from side to side onto a lower conveyor, perpendicular to the in-feed web, in the cross-lapping process to obtain a batt.

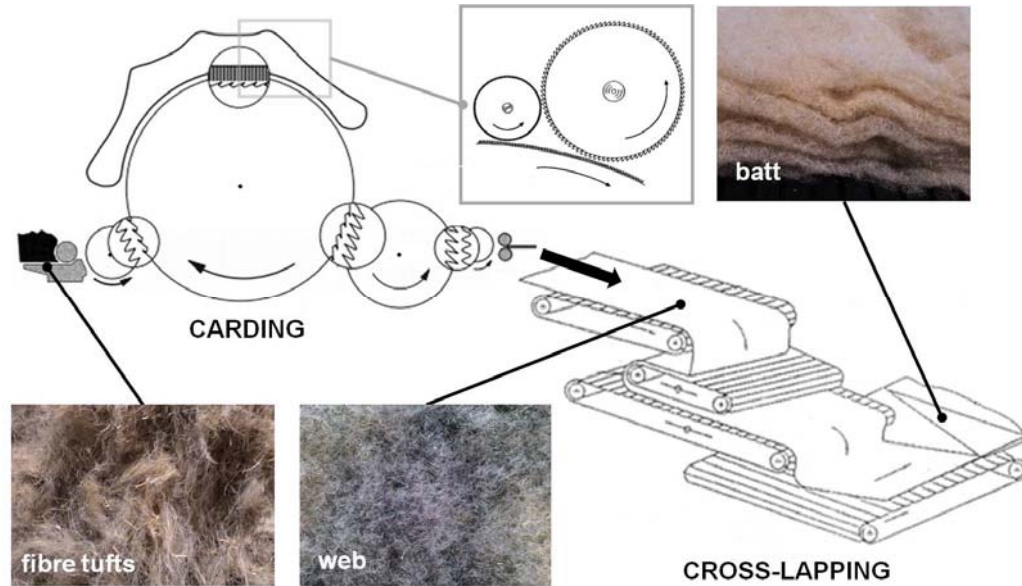


Figure I.4. Carding process showing the evolution of fibres during the process.

Regarding the web bonding or consolidation, needle-punching is a clean, high-speed and low cost manufacturing method for NW, in which fibres are mechanically entangled to produce a fabric. The entanglement is achieved by the action of barbed needles that produce partial fibre reorientation (Figure I.5). These needles, placed in the boards of the needle-loom, oscillate vertically trespassing the batt, which is retained between two perforated plates during its advance. As the batt moves along the loom, more fibres are progressively reoriented and entangled by the needle barbs, friction between fibres increase, and a consolidated fabric structure is formed.

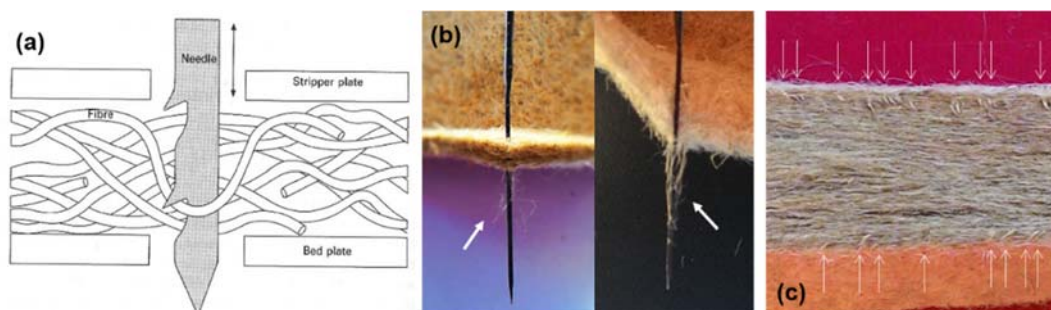


Figure I.5. Needle-punching principle: (a) scheme of the action of a barbed needle, from [10]; (b) fibre entanglement in the needle's barbs; (c) image showing fibre reorientation until the penetration depth of the needle in a thick NW structure.

Influence of the processing parameters

The final characteristics of the product obtained are highly influenced by some of the needle-punching parameters such as the needle arrangement in the needle-board, the direction, penetration depth and density of needling, or the needle characteristics, among others [11–13].

Processing parameters can be adjusted to define final characteristics of the NW [14]:

- The drawing ratio—between the delivery and feeding speeds at which the batt enters and exits the needle-loom—is related to some deformation, decreasing the mass per unit area
- The maximum needling penetration determines the fibre entanglement, thus decreasing the thickness, weight and permeability of the NW but rising its mechanical resistance.
- The bed-gap—distance between the two plates in the needle-loom—is related to the thickness and compactness of the fibres in the NW.
- The stroke frequency—number of needling cycles produced per minute—is related with the entanglement degree.

I.2. Natural fibres as reinforcement in biocomposites

Natural fibres can be sorted depending on their origin into *mineral*, such as basalt or asbestos; *animal*, such as silk or wool; and *vegetal*—also known as plant fibres—. The use of vegetable fibres as reinforcements in composite materials [15] has emerged as an alternative reinforcement to the conventional carbon and glass fibres or other inorganic fillers [16,17]. In general terms, vegetable fibres present: large availability; low cost; non-hazardous nature, safer/better working conditions; biodegradability—for a more sustainable end-of-life, although they can also be incinerated for energy recovery—; CO₂ neutrality; low density—and hence, good specific properties—; well-balanced stiffness, toughness and strength; good thermal and acoustic insulation; friendly processing—reduced wearing on tools—; and an easily tuneable surface, which can be modified to reach more hydrophilicity or hydrophobicity [6,18,19]. Moreover, can be found in a wide variety of morphologies [6], such as long fibres, staple, pulp, strands, tufts, technical fibres, etc. However, they present some disadvantages such as swelling due to moisture absorption, lower durability, poor fire resistance, limited processing temperature, and variable quality—this last owing to intrinsic variability in diameter and length, surface roughness and chemical compositions that depends on many factors, from the crop variety or harvesting time to the weather conditions, among others [4,20]—. Nonetheless, some treatments can be used to modify and improve most of these drawbacks [19].

I.2.1. Chemical composition and properties of cellulosic fibres

Vegetable fibres—or cellulosic or lignocellulosic fibres—are composed of cellulose, lignin and hemicellulose as major components, and of other minor components such as pectin, waxes or inorganic compounds, among others (Table I.1). In fact, plant fibres can be themselves considered as composite materials, consisting of (cellulose) microfibrils embedded into an amorphous matrix of lignin and hemicellulose [21]. The combination of these components, which present variable contents depending in multiple factors, is responsible of the properties of cellulosic fibres and of their aforementioned variability.

Cellulose is the main component of plant fibres, a strictly linear—unbranched [22]—polymer formed by $\beta(1\rightarrow4)$ linked D-glucose repeating units (Figure I.6). Cellulose chains form both random amorphous pockets and well packed crystalline regions [23,24]. It presents high tensile strength and large stability in normal environments [19], and as the main structural component, cellulose content influences the strength and stiffness of the fibre.

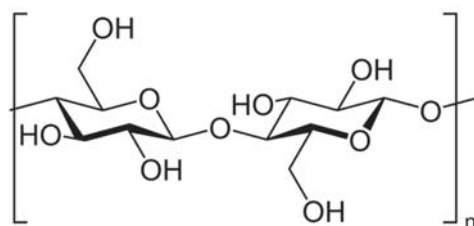


Figure I.6. Cellulose.

Hemicellulose is amorphous polymer consisting of random short highly branched chains, which forms some cross-linking with the cellulose molecules, resulting in a higher structural integrity [20]. It presents poor strength and poor thermal stability, and a high sensitivity to water—is the most hydrophilic component [4]—. Due to that, hemicellulose plays a key role in moisture absorption and biological and thermal degradation of vegetable fibres.

Lignin is a long-chain and high molecular weight substance [25] that presents aromatic structures and is resistant to the attack of microorganisms and anaerobic processes [19]. It is hydrophobic [26], has a high contribution to the char formation [4] and confers to the fibre its resistance against UV degradation.

Lignin and hemicellulose do not contribute too much to the fibre tensile strength, but due to their branched and cross-linked nature act as a “natural cement”, providing some degree of structural integrity and rigidity to the walls to harnessing the cellulose strength, while conferring flexibility [19,27].

Table I.1. Chemical composition of selected natural fibres. Data from [19].

Fibre	Cellulose (wt.%)	Hemicellulose (wt.%)	Lignin (wt.%)	Pectin (wt.%)
Flax	60-81	14-18.6	2-3	1.8-2.3
Jute	51-72	12-20.4	5-13	0.2
Sisal	43-88	10-13	4-12	0.8-2
Kenaf	36	21	18	2
Hemp	70-78	17.9-22	3.7-5	0.9
Ramie	68.6-76	13.1-15	0.6-1	1.9-2
Cotton	82.7-92	2-5.7	0.5-1	5.7
Coir	43	0.3	45	4.0
Banana	60-65	6-19	5-10	3-5
Wood fibres	45-50	23	27	-

In Figure I.7, the influence of the chemical components in some of the properties of cellulosic fibres is schematised.

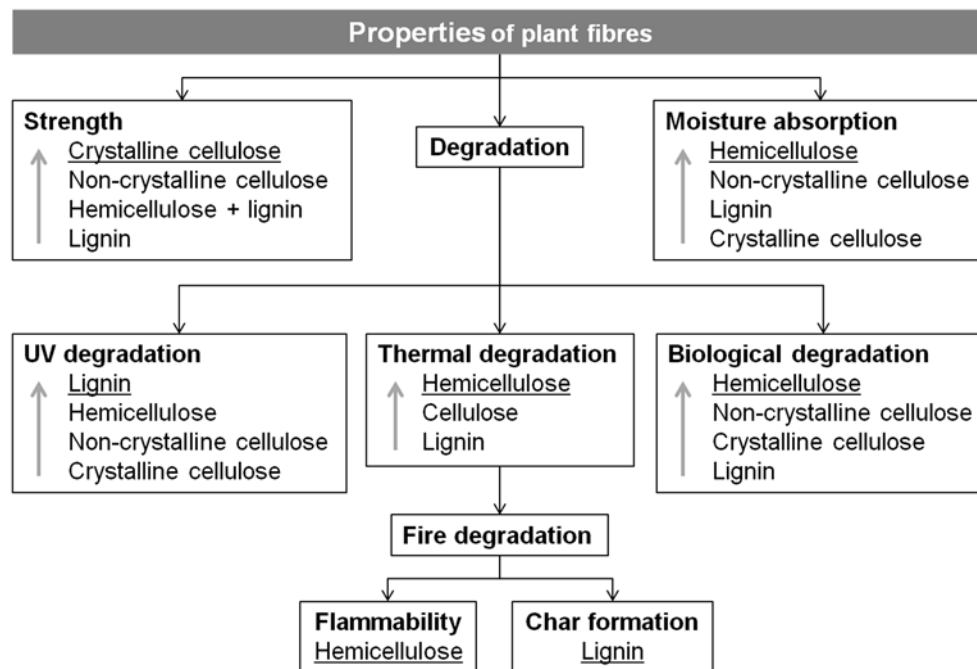


Figure I.7. Influence of the constituents on some of the properties of the plant fibres [26,28].

In Table I.2, the properties of the most common cellulosic fibres are presented.

Table I.2. Properties of selected cellulosic fibres. Data from [19].

Fibre	Density (g/cm ³)	Diameter (µm)	Elongation at break (%)	Tensile strength (MPa)	Young Modulus (GPa)
Flax	1.4-1.5	40-620	2.7-3.2	343-1035	27-80
Jute	1.3-1.5	30-140	1.4-3.1	187-773	3-55
Sisal	1.3-1.5	100-300	2.0-2.9	507-855	9-28
Kenaf	1.22-1.4	40-90	3.7-6.9	2.95-930	22-53
Hemp	1.4-1.5	16-50	1.3-4.7	580-1110	3-90
Ramie	1.5	40-60	3.6-3.8	400-938	44-128
Cotton	1.5-1.6	16-21	2-10	287-597	5.5-12.6
Coir	1.25-1.5	11-450	15-47	106-270	3-6
Banana	1.3-1.35	50-280	3-10	529-914	7.7-32

I.2.2. Bast fibres

Vegetable fibres can be classified in one of the six botanical basic types [29–31]. However, the most common classification is the division into non-wood fibres and wood fibres [19]. Non-wood fibres, in their turn, can be classified according to the part of the plant where they are originated as:

- *Bast fibres*: such as flax, hemp, jute, kenaf or ramie
- *Leaf fibres*: such as abaca, sisal, henequen or pineapple
- *Seed/fruit fibres*: such as cotton or coir
- *Straw*: such as corn, wheat or rice
- *Grass fibres*: bagasse, esparto, bamboo or switch grass

Among all these fibres, bast fibres like jute, flax, ramie, and sisal are the most widely used for polymer composites [21] when high performance is needed [24].

Bast fibres, which contain around 60–75% of cellulose, are found in fibre bundles in the inner of the stem of the plant—providing structural strength and stability—and present high aspect ratio and low mass. In Figure I.8, the section of a flax stem is shown, where the bundles of bast fibres can be observed just under the stem bark. At the macroscopic level, the stem is composed, from the outside to inside, of bark—epidermis and cortex—, phloem—made up of about 30 bundles of fibres [32]—, xylem—xylem and protoxylem—and a central void (pith).

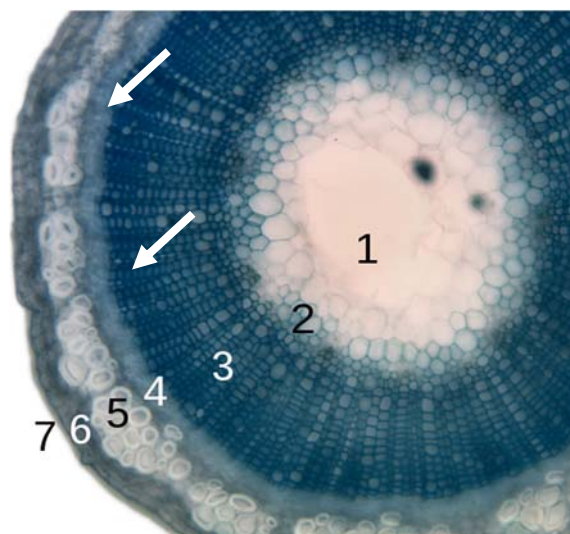


Figure I.8. Stem cross-section—of a flax plant—showing: (1) pith; (2) protoxylem; (3) xylem; (4) phloem; (5) bast tissue; (6) cortex; and (7) epidermis. Arrows mark the bast fibre bundles.

In Figure I.9, the stem configuration is presented, showing the hierarchical structure of the bast fibres.

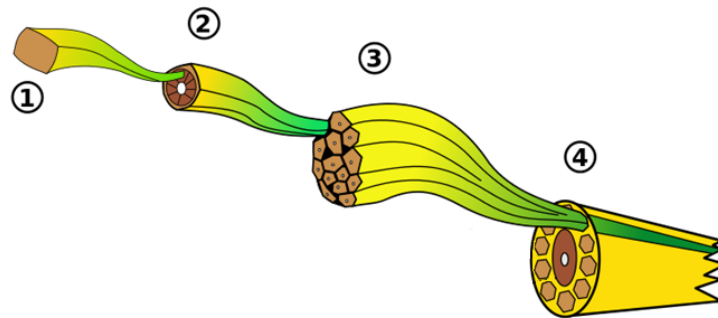


Figure I.9. Diagram of a stem configuration: (1) microfibril; (2) elementary fibre; (3) bast fibre bundle; (4) stem.

Each bundle contains around 10-40 fibres elementary fibres linked together mainly by pectin [32] (Figure I.9-3). At the microscopic scale, elementary fibres (Figure I.9-2) are composed of concentric layers, which are, in their turn, composed of parallel microfibrils (Figure I.9-1), organised in helices with S or Z orientation [24], forming a determined angle of the microfibrils with respect to the fibres axis: the microfibrillar angle. This angle strongly influences the axial tensile properties of the fibre [24], and good ductility is often observed in fibres that present a spiral orientation of these microfibrils [32]. At the nano-scale, microfibrils are constituted of cellulose chains in a crystalline configuration embedded in an amorphous matrix, mainly made of pectins and hemicelluloses [32].

I.2.2.1. Flax

Flax is one of the fibres most widely used since ancient times—flax textiles dated back on 5000 BC have been reported in Egyptian burials, for instance—[33]. Despite long flax fibres have been traditionally used to produce high quality textiles, the use of flax fibres—specially lower fibre grades—in the composites industry is growing, owing to its good mechanical properties, low price and availability. In this sense, its high cellulose content and high crystallinity leads to high strength, stiffness, and ease to wrinkle.

Flax structure

As a cellulosic fibre, flax presents a complex hierarchical structure, shown in (Figure I.9 and Figure I.10). Flax fibres are, typically, long (elementary) fibres of polygonal hollow section, with smooth surface and nodes—also called dislocations—(Figure I.11), thick walls

and the central and well-defined lumen. Elementary fibres are grouped in bundles: entire or partial bundles are also denominated “technical fibres”.

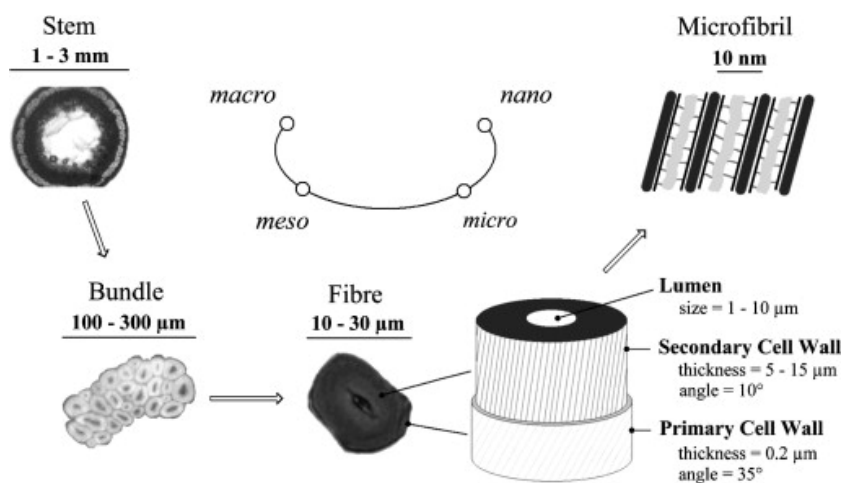


Figure I.10. Flax structure from stem to cellulose crystals, from [32].

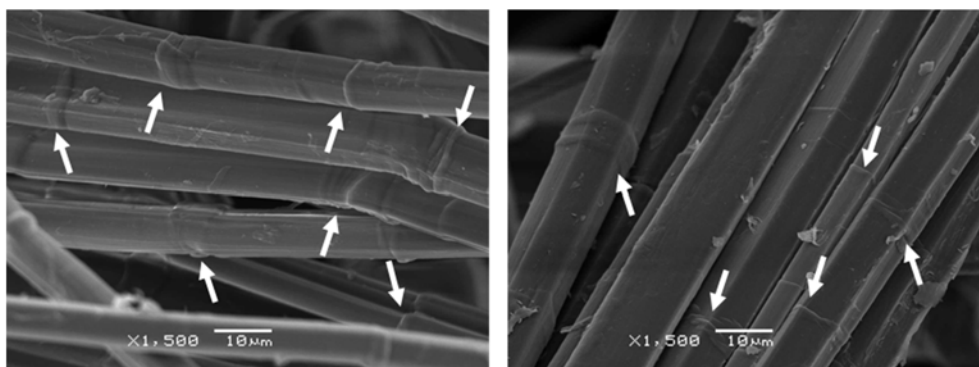


Figure I.11. SEM images of flax bundles showing several fibres. Arrows mark the nodes.

As aforementioned, elementary fibres are composed of concentric cell walls or layers surrounding a central open channel (lumen), and each layer—made of microfibrils—presents diverse chemical composition and structure. For flax, the outer thin layer, primary cell wall that acts as a coat, is around 0.2 μm thick and the microfibrillar angle—respect the fibre axis—is of 35°.

The inner layer, secondary cell wall, has a thickness around 5-15 μm, and represents the bulk of the fibre. As reviewed by [24], the secondary cell wall consists of three layers. The S1 layer controls fibre stability in compression by limiting the lateral cell expansion. The S2 layer is much relevant according to its relative size compared to S1 and S3, and due to that plays a major role in the definition of the fibre properties. It contains, mainly, amorphous hemicelluloses and cellulose oriented at 10°. Since the microfibrillar angle of the secondary

cell wall is minimum, the tensile strength of flax is high. Finally, the S3 layer is found nearer the fibre lumen, and contributes to the fibre stability by supporting the hydrostatic pressure.

Extraction of flax fibres

Flax plants are pulled out of the ground to harnessing the maximum length [34], since flax plants can present lengths up to 90 cm [33]—. After harvesting, a rippling process helps to separate the seeds and flower heads. [34]. Since flax fibre bundles are located just under the “bark”—in the phloem—, surrounded by a pectin layer than binds them to the bast tissue [34], a degumming process is required. Degumming methods are retting, chemical methods or physical methods, performed by means of chemicals—such as sulphuric acid or sodium hydroxide for instance—, or by ultrasound oscillation, steam explosion, osmosis degumming, or electron radiation, among others [35]. However, retting processes seem to be the most common.

Briefly, retting is a biochemical process that leads to rotting, and hence to the fibre separation from the woody core, by the complex action of enzymes, and plays a key role in the fibre quality. It can take place under aerobic or anaerobic conditions, and there are two main methods: water retting and dew-retting. In the dew-retting, the flax straw is spread in the ground, under the action of the sun and weather, for several weeks. During this period the turning over of the straw and the moisture are essential. The latter is due to the necessary proliferation of fungus and bacteria, which provide the enzymes that destroy the pectin layer. Therefore, if not provided by the weather, moisture has to be artificially supplied. Dew-retting is commonly used in Europe since is considered of lower cost and less polluting than water retting. This latter is because in water retting the flax straw is immersed in running water for several days—in rivers or tanks—, and hence some odours or polluted water can be generated. Further drying is required in both cases.

After retting, a scutching process is performed. Scutching consists in a mechanically beating of the retted stems, with the aim of eliminating the bark and the xylem—woody stem parts, also called shives—while producing a roughly separation of the bundles. Then, hackling process, which consists of combing the bundles to separate and align them—in order to achieve finer technical fibres—can be performed. Further chemical treatments can be considered after the extraction to improve fibre separation [32].

Because of pricing reasons, flax fibres generally used for mat reinforcements are either green decorticated fibres or dew-retted and scutched fibres [34]. Decortication is a faster and

cheaper method, which consists in a direct extraction of the fibres by tearing off raw (green) straw, mechanically removing the fibres [35]. However, the quality of fibres is lower and often further treatments are required. Moreover, green decorticated fibres present the disadvantage of being sensitive to water [34].

Properties of flax fibres

As aforementioned, flax presents biodegradability, low cost—around ~0.4-1.1€/kg in 2014, according to [20]—, low density—1.4-1.54 g/cm³—, moisture absorption—of ~7% [18]—, and good thermal and acoustical insulation, among other properties. However, flax fibres are of a great interest for composite reinforcement owing to their mechanical properties. In general terms, flax presents high stiffness—27-80 GPa—and good strength—345-1830 MPa—[3]. When considering the specific properties, flax fibres have an outstanding performance, equal or higher than those for glass fibres, for instance [18,20]. Also the elongation of the flax fibres is very low—1.2-3.2% [3]—, what is interesting for the obtaining of rigid composites and for ensuring a good stress transfer.

The flax properties are strongly influenced by multiple conditions and, due to that, present unavoidable variability, as pointed by the wide range of values observed in the previous data.

On the one hand, as reviewed in [20,33], the mechanical performance of the flax fibres is affected by:

- The plant species, crop cultivation, fibre location in plant and weather conditions, due to their influence in the plant growth.
- The cell wall thickness, coarseness, microfibril angle, porosity and size and shape of lumen, determined by the harvesting stage.
- The fibre extraction methods—decortication process, type of retting or conditions for fibre bundle separation.
- The transportation and storage conditions, as well as the age of fibres.

On the other hand, some variability responds to measurement conditions such as: sort of fibre—whether it is a technical fibre/bundle or an elementary fibre—, moisture or temperature conditions, fibre diameter and determination of the cross-section, testing speed or clamping distance (gauge length), among others [33,36]. The intrinsic variability of natural fibres also contribute to the scatter of the results, and hence, to large variations in the measured properties. In general terms, flexural and tensile performance of the natural fibres

depends on the environmental conditions [4]. Moisture absorption—and hence, environmental humidity—can affect the mechanical properties of cellulosic fibres. An increasing clamping distance leads to a decrease in the strength values [36]. The stiffness of flax fibres is known to decrease with the increase on the fibre diameter [37].

Moreover, the properties of the flax fibres can be tailored by means of surface treatments. Many treatments can be applied to cellulosic fibres, in general terms, to modify their properties. In this sense, numerous chemical or physical treatments can be applied to modify the hydrophobic/hydrophilic nature of the fibres, surface chemistry, surface roughness, dimensional stability, stiffness, strength or elongation.

I.3. Biopolymers as matrix in biocomposites

The term “biopolymer” comprises a range of materials of a bio-based origin and/or biodegradable nature. All the polymers that fulfil at least one of these two principles are considered biopolymers, thus leading to three main groups:

- *Petrochemical-based biodegradable polymers*: such as polybutylene adipate-co-terephthalate (PBAT) or polycaprolactone (PCL).
- *Bio-based non-biodegradable polymers*: such as bio-based polyethylene (bioPE), bio-based polyethylene terephthalate (bioPET) or bio-based polyamides (bioPA).
- *Bio-based biodegradable polymers*: such as polyhydroxyalkanoates (PHAs), polylactic acid (PLA) or polybutylene succinate (PBS).

Taking into account that the cellulosic fibres are biodegradable, the use of a these fibres combined with a biodegradable matrix leads to a very interesting solution since is possible to obtain completely biodegradable materials.

In general, composite materials are difficult to recycle because of the heterogeneity of their components and the difficulties in matrix/reinforcement separation. Therefore, the production of biodegradable composites simplifies the final disposal of the product at their end of life, since compostability is a more economic and viable option.

I.3.1. Biopolymers classification

As can be seen in Figure I.12, bio-based polymers can be divided into three main categories based on their origin and production:

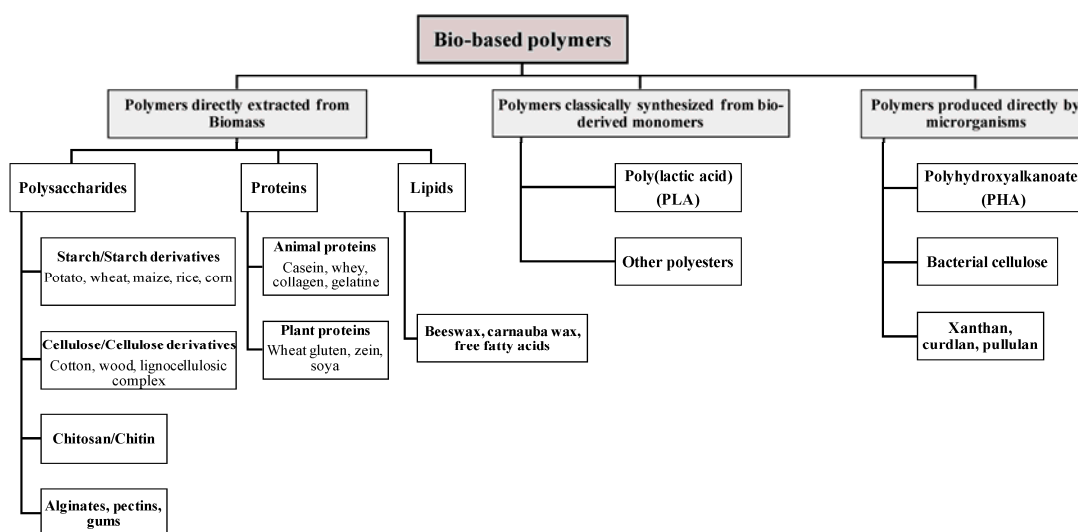


Figure I.12. Schematic overview of bio-based polymers, from [38].

- *Natural*: directly extracted/removed from biomass, such as polysaccharides (starch and cellulose) and proteins (casein and gluten).
- *Synthetic*: produced by classical chemical synthesis using renewable bio-based monomers, such as PLA.
- *Microbial-fermented*: produced by microorganisms or genetically modified bacteria, such as PHAs.

I.3.2. Bio-based biodegradable polymers: PHAs

The properties of some bio-based biodegradable polymers are presented in Table I.3. In the group of thermoplastic matrices, three key polymers for its potential applications can be highlighted: thermoplastic starch (TPS), polylactic acid (PLA) and polyhydroxyalkanoate (PHA).

Table I.3. Properties of some bio-based biodegradable polymers. χ : crystallinity; T_g : glass transition temperature; T_m : melting temperature; E: Young modulus. Data from [28].

Polymer	χ (%)	T_g (°C)	T_m (°C)	E (GPa)	Mass loss (month)
PBS	n.a.	-45 to -10	90-120	0.4-0.6	n.a.
PLLA	~37	60-65	170-180	4.8	12-24
PDLLA	-	55-60	-	1.9	12-16
P3HB	80	5	173-180	0.9-4	n.a.

Polyhydroxyalkanoates or PHAs are bio-based polymers produced by bacteria as an energy storage resource. This carbon source is produced when some sort of bacteria are in extreme feeding conditions—excess of carbon and deficiency of other nutrients such as oxygen, nitrogen or phosphorous—. Nowadays, more than 300 species of PHA-producing bacteria are known [39]. Among the properties of these fully biodegradable polyesters, it is worth to mention that they are biocompatible and can be easily degraded to water and carbon dioxide by numerous microorganisms—such as bacteria, fungi and algae—under environmental conditions [40]. Moreover, they are hydrophobic, insoluble in water, largely stable in air, inert and non-toxic [39,41], and have mechanical properties comparable to those of polypropylene, although they have much lower elongation to break and are more brittle. Compared to polypropylene, PHAs are more stable to UV degradation but less resistant to solvents [39].

Their properties and biodegradability, as well as their origin in a renewable source and their no-dependence on oil, make these polymers interesting for a wide range of applications. The current and potential uses of PHAs have been reviewed for: packaging, film formation, bags, paper-coating, motor oil containers and biomedical uses such as drug delivery, among others [40,41]. However, their high cost—3-5 times higher than commodity polymers—makes them less competitive against other commodity polymers used nowadays in packaging industry, for instance. Therefore, the use of strategies for reducing the amount of biopolymer required for an application are an interesting option to be considered for increasing their competitiveness.

I.3.2.1. PHA production

PHAs are mainly produced in fed-batch processes by means of pure or mixed microbial cultures, although other techniques, such as production in genetically modified plants, are also known and currently being studied [39]. The most common feedstock used to produce PHAs are sugar and starch [42], despite other cheaper sources have been investigated [43].

Often, fermentations are carried out in fed-batch processes consisting in two-stage batch production methods using pure microbial cultures. In the first stage (grown stage), bacteria are introduced into a proper solution in a sterile reactor, and fed in adequate conditions with the aim to reach a maximum cell density. In the second stage (accumulation stage), an essential nutrient—such as oxygen, nitrogen or phosphorous—is limited meanwhile carbon feedstock is supplied. This forces the bacteria to produce PHA accumulation in the form of granules—around 5-10 granules with average size of 0.2-0.5 μm [39]—in the cell cytoplasm as can be observed in Figure I.13.

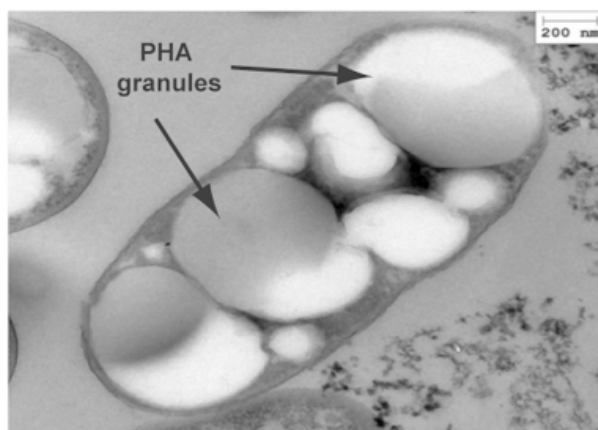


Figure I.13. PHA-producer bacteria accumulating PHA granules, from [44].

The biochemistry of the PHA synthesis influences the properties of the final product [39]. When achieved a maximum accumulation—80-90% of the cell dry mass—, the recovery is performed generally by means of organic solvent extraction [45]. However, recently, researchers of the “Centro de Investigaciones Biológicas de Madrid (CIB-CSIC)”, in Spain, have developed a genetically modified bacteria that would predate the PHA-producer bacteria, extracting the biopolymer contained on them with no degradation of the PHA [44]. This could be relevant if applied to the industrial production of PHAs, since the current extraction processes are rather complex and contaminant.

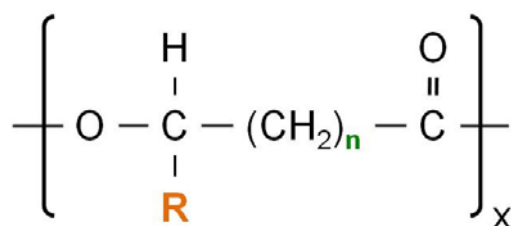
However, mixed cultures contain a diversity of microorganisms, which have the potential to produce large amounts of a wide variety of PHAs meanwhile lowering production costs [39,42]. This is due to the lower requirements in equipment, sterility and control, if compared to those for pure cultures. Moreover, mixed cultures own the capability of adaptability to various feedstock, which can proceed from agricultural or industrial wastes. This means that fermented effluents from food industry, by-products and other wastes can be used as cheap substrates for PHA production [39]—substrates are in major part the responsible of the production costs—. The mixture cultures production capabilities relies on the ecological selection favouring those microorganisms with higher production capacities [39], since PHA accumulation is not induced by nutrient limitation [46]. Therefore, mixed cultures can easily provide a broad range of PHA compositions containing other co-monomers in high contents [39]. Thus, renewable agricultural and biomass feedstock can offer promising alternatives for replacement of classical petroleum-based solutions without competing with food crops [47].

In recent years, the use of transgenic plants has also been investigated since some authors see in this production method the answer to the cost problem. The large scale production of PHAs in transgenic plants could really reduce the cost and make these polymers to be competitive with current synthetic plastics [41,48–50], especially if the polymer is produced as a by-product in agricultural crops [51]. This is because this system relies on sunlight, water, CO₂ and soil nutrients, and not on costly fermentation processes. In fact, for PHA production in plants, the most remarkable part of the cost would rely in the extraction of the polymer from the plant [51]. To the date, PHAs have been obtained from multiple plants such as rice roots [52], tobacco plants, or flax [53]. Other investigations are currently in process, such as PHB and PHBV production from oil palm [50]. The main issue to be developed is the PHA extraction from the plant, as it has not been succeed with cost-effectiveness.

I.3.2.2. PHA types

PHAs are linear polyesters with pendant groups that extend from the polymer backbones. The alkyl pendant groups, which occupy the R configuration in the general structure (Figure I.14), vary from one carbon (C1) to over 14 carbons (C14) in length. Depending on the length of this alkyl groups, PHA can be classified into:

- Short chain length PHAs (scl-PHA): up to C5
- Medium chain length PHAs (mcl-PHA): from C6 to C14
- Long chain length PHAs (lcl-PHA): more than C14.



x = 100-30000

n = 1	R = methyl	poly(3-hydroxybutyrate)	P3HB
	R = ethyl	poly(3-hydroxyvalerate)	P3HV
	R = propyl	poly(3-hydroxyhexanoate)	P3HHx
	R = pentyl	poly(3-hydroxyoctanoate)	P3HO
n = 2	R = H	poly(4-hydroxybutyrate)	P4HB
n = 3	R = H	poly(5-hydroxyvalerate)	P5HV

Figure I.14. General structure of PHAs and examples. Adapted from [54].

Despite some authors consider the three groups for classification [51], others only consider scl-PHAs and mcl-PHAs [39]. In general terms, scl-PHAs have closer properties to conventional polymers, meanwhile mcl-PHAs are more similar to elastomers.

There are near 150 different types of PHAs according to the composition, thus leading to a wide range of properties and functionalities [42]. However, only a few PHAs—comprising homopolymers and copolymers—are produced in large quantities, mainly [42,55]:

- poly(3-hydroxybutyrate) P3HB
- poly(3-hydroxybutyrate-*co*-3-hydroxyvalerate) PHBV
- poly(3-hydroxybutyrate-*co*-4-hydroxybutyrate) P3HB4HB
- poly(3-hydroxybutyrate-*co*-3hydroxyhexanoate) PHBHHx

Poly(3-hydroxybutyrate)

Poly(3-hydroxybutyrate)—P3HB or, sometimes, just PHB—is a scl-PHA and the most common member of the PHAs' family. P3HB homopolymer presents: T_g below the room temperature (~ 5 °C), a crystallinity around 50-80%, stiffness of around 2.9 GPa, strength of around 37 MPa and an elongation at break of $\sim 4\%$, with a relatively low impact strength compared with commodity polymers due to its high crystallinity. Moreover, is relatively hydrophobic and biodegradable, since can be reduced to water and carbon dioxide by degradation in environmental conditions [39,56]. PHB presents some difficulties for its melt processing because its degradation temperature—thermal degradation starts around 185-195 °C—is just above its melting temperature— T_m 173-180 °C—. Some grades of PHB present similar mechanical properties than polypropylene, and offer good resistance to moisture and barrier properties against aroma [56].

PHB-based copolymers

In order to improve the processability of P3HB, and to reduce its brittleness and thermal instability, a wide variety of PHB-based copolymers have been developed, as well as the use of additives, plasticisers and blends. The addition, in HB based copolymers, of a fraction of scl-PHA monomers, such as 3-hydroxyvalerate (3HV) or 4-hydroxybutyrate (4HB), or mcl-PHA monomers such as hydroxyhexanoate (HHx) or hydroxyoctanoate (HO), leads to higher flexibilities and toughness [51]. PHA copolymers present, typically, a random sequence of the monomers, which also vary in proportion [57]. The properties of some PHAs, including copolymers with different molar contents of co-monomer, are presented in Table I.4.

Table I.4. Properties of some PHAs. Data from [42,58].

Polymer	T_m (°C)	E (GPa)	σ (MPa)	ϵ (%)
P3HB	175–180	3.5–4	40	3–8
P(3HB-co-3HV) (3 mol% HV)	170	2.9	38	n.a.
P(3HB-co-3HV) (20 mol% HV)	145	1.2	32	50–100
P(3HB-co-4HB) (10 mol% 4HB)	160	n.a.	24	242
P(3HB-co-4HB) (16 mol% 4HB)	152	n.a.	26	444

In general, the properties of the PHA copolymers depend on the sort of co-monomer and its proportion: the higher the co-monomer molar content, the lower the Young modulus and the strength, and the higher the flexibility and elongation. However, it has to be taken into account that the processing and testing conditions can also influence the values of those properties.

PHBV: Poly(3-hydroxybutyrate-co-3-hydroxyvalerate)

PHBV is produced in pure cultures when propionic acid is added as co-substrate— together with glucose—[55], leading to the incorporation of HV units to the HB backbone during fermentation [59]. The inclusion of HV increases toughness and processability of the resultant PHA [60], owing to a lower crystallinity. Hence, PHBV presents lower melting point, decreased stiffness and brittleness, improved flexibility and elongation at break and similar or even higher increased tensile strength if compared to P3HB [39,61]. The improved properties are attributed to dislocations, crystal strain and crystallites produced due to the insertion of the 3HV unit into the P3HB crystalline lattice [39].

P3HB4HB: Poly(3-hydroxybutyrate-co-4-hydroxybutyrate)

P3HB4HB is produced using glucose and 1,4-butanediol—one of the 4HB-generating carbon sources—as substrates for pure cultures [55,59,62]. Depending on the molar fraction of 4HB monomer content, it presents a wide range of properties and melting points, ranging from highly crystalline plastic to elastic rubber [63]. This is because P3HB4HB—a scl-PHA—at low 4HB contents is semi-crystalline, presenting inherent structure defects, slow crystallization rate, formation of large-size spherulites and secondary crystallization [64]. However, increasing the 4HB content leads to crystallinity decrease—for high 4HB molar contents, P3HB4HB can be considered as an amorphous rubber [65]—, to melting temperature decrease and to rise of elongation at break.

PHBHHx: Poly(3-hydroxybutyrate-co-3-hydroxyhexanoate)

PHBHHx require the use of fatty acids as substrate in pure cultures [55]. PHBHHX are random copolymers consisting of 3HB and 3HHx monomers, and given that HHx is a mcl-PHA, the mechanical properties and processability of PHBHHx have been shown to improve over PHB and PHBV [66]. In this sense, copolymers of mcl-PHA typically present low crystallinity values (20–40%) and high elongation at break (300–450%) [45]. According to [55], PHBHHx is also non-toxic, presents piezoelectric properties, and its degradation

products do not produce immuno-stimulation; all thus promoting the regeneration of damaged tissues and the bone growing and hence, is a good implant biomaterial option.

I.3.2.3. Characteristics of PHAs

Crystal structures in PHA

As reviewed by Laycock et al. [39], the PHA granules present, *in vivo*, a core of amorphous polyester that the theories attribute to physical-kinetic limitations on the one hand, or to plasticizer effect of the water present in the granule on the other. Anyhow, once released from the granule structure, the crystallinity develops to define the physical, chemical, mechanical and rheological characteristics presented by PHAs.

In general terms, PHAs crystallization is complex and slow, thus meaning that the polymer suffers an evolution on its crystallinity even after being processed and while being below its melting temperature [67]. According to the literature [39,67], crystals on PHAs attain basically two forms: α -form and β -form crystals shown in Figure I.15

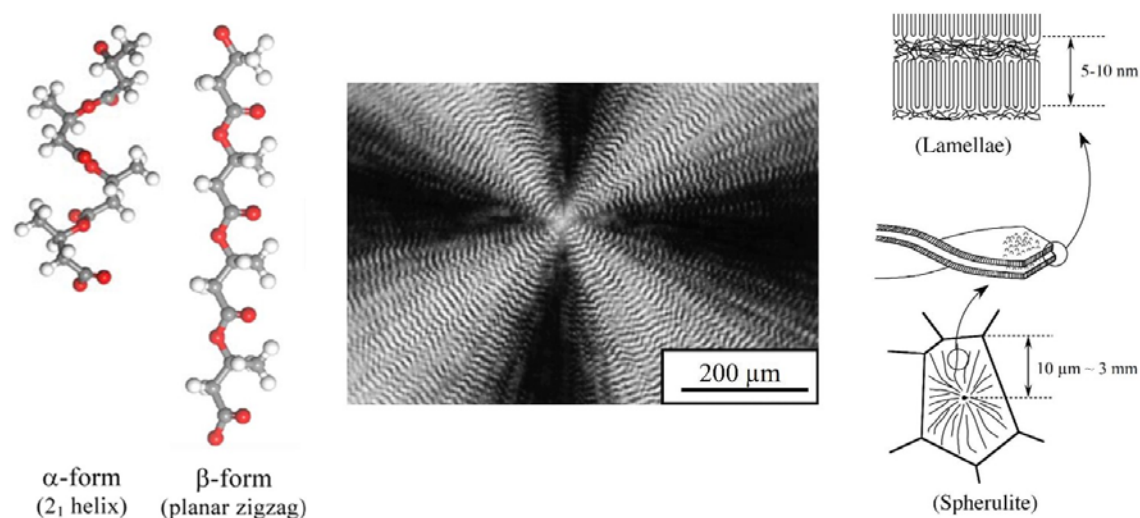


Figure I.15. Molecular conformations of α and β forms, from [68] (left); banded texture of a P3HB spherulite crystallised at 85 °C from melt, from [69] (centre); and schematic representation of spherulites and lamellar aggregates, from [69] (right).

The crystalline α -form is the most common, generally found in P3HB under the typical conditions from melt, cold or solution state. According to the literature, corresponds to an orthorhombic lattice structure, which presents a 2_1 helix molecular conformation. Lamellar crystals—with thicknesses around 4-10 nm, depending on the crystallization temperature—grow in multiple radial directions, forming spherulites. Moreover, due to the twisting of the

lamellar crystals, spherulites typically present a banded texture which depends on the crystallisation temperature and molecular weight [69], as shown in Figure I.15. It is worthy to mention that crystallisation—in P3HB—is slow when cooled from the melt [70], and secondary crystallization of the amorphous phase can take place during storage at room temperature, thus leading to a higher brittleness of the polymer [56].

The crystalline β -form of the P3HB is strain-induced. It is obtained after deformation processes in PHAs—such as under drawing in fibres or in uniaxially stretched films, for instance—and is metastable, what means that can be annealed to an α -form at temperatures around 130 °C [39]. The β -form corresponds, in this case, to an imperfect orthorhombic system with planar zigzag conformation, generated from the chains of the amorphous regions between the lamellar crystals, since it does not requires previous alignment from the α -form lamellae. The drawing or stretching leads to a strong extension of the tie molecules found between the lamellar crystals—see Figure I.16—, thus reaching high mechanical properties [39].

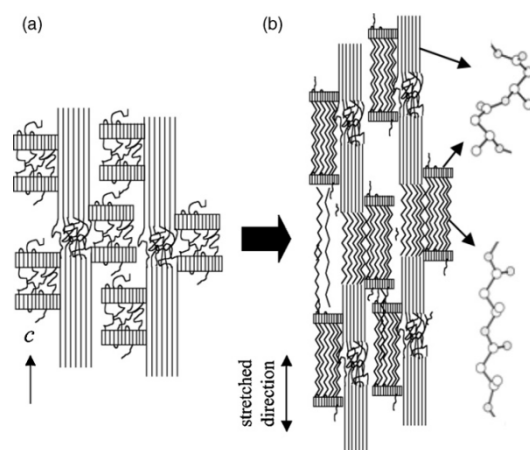


Figure I.16. Schematic representation of the β -crystals formation in a P3HB, from [71].

Different mechanisms have been proposed for explaining the β -crystalline formation in other PHAs under other processing conditions [39,71]. In fact, the crystal characteristics and associated properties may change depending on the copolymer and the co-monomer content, due to co-crystallisation processes that would lead to lower crystallinity and lower melting temperatures.

Anyhow, drawing and stretching techniques and annealing treatments have been proposed as interesting procedures for increasing the stiffness, tensile strength and elongation at break for PHAs, since long term properties are achieved and the secondary crystallisation seems to be suppressed [39].

Processability and degradation in PHAs

It is known that the thermal steps required processing the polymer, even the pelletisation step, slightly degrade the polymer, thus leading to a significant decrease of the molecular weight and so viscosity [72]. In general terms, PHAs suffer from thermal degradation and also hydrolytic degradation at high temperatures [73], and due to that, it has been reported that the P3HB suffers from considerably molecular weight loss during pelletisation and transformation processes [74], thus decreasing the molecular weight. Therefore, it is suggested minimizing the processing temperatures and residence times to reach feasible values of degradation of the polymer [70]. Also reversed temperature profiles are recommended for PHA processing in melt extrusion [39].

The use of plasticizers in PHAs lowers the glass transition and melting temperatures, and hence, lower processing temperatures are required, thus avoiding the thermal degradation. Moreover, plasticizers improve the toughness of the polymer and the elongation at break by decreasing crystallinity and weakening some bonds, what ease their processability [60]. In the literature, many plasticizers have been reported to be used in PHAs such as tri(ethylene glycol)bis(2-ethylhexanoate) TEGB; poly(ethylene glycol) and tributyl citrate; epoxy soyate, triethyl citrate, dodecanol or lauric acid, among others [56,60,61,75].

Biodegradability of PHAs

Biodegradation in a polymer can be defined as the deterioration and a decrease of the molecular mass under the enzymatic action of microorganisms—in aerobic or anaerobic conditions—; although other chemical reactions—like photodegradation, oxidation and hydrolysis—can also aid the process. Due to biodegradation, the polymer is transformed into carbon dioxide, water, methane— when performed in anaerobic conditions—, inorganic compounds and/or biomass. Biodegradation time will depend on several factors such as: microbial activity of the environment, exposed surface area, moisture, temperature, pH, molecular weight, nature of the monomer and crystallinity, among others [41].

PHAs are biodegradable when exposed to soil, compost or marine sediment—in which the required microorganisms are present—what is a remarkable strength against other petrochemical-based commodity polymers. In this sense, the 85% of PHAs can degrade in seven weeks under the appropriate conditions [41], although a wider rate of 3 to 9 months is also given in the literature [51]. This highly biodegradable behaviour is due to the large amount of microorganisms that are capable to produce PHB depolymerase. This enzyme

hydrolyze the ester bonds, breaking down the polymer into monomers and oligomers that can be easily degraded to water and carbon dioxide by the microorganisms [42].

I.4. Critical factors for biocomposite production

The production of biocomposites using cellulosic fibres and thermoplastic polymers presents some critical factors. As reviewed by Pickering et al. [3], fibre and matrix selection, interfacial strength, fibre dispersion and orientation, porosity and manufacturing processes have a great influence in the mechanical properties obtained. These critical factors, among others, are here briefly reviewed.

I.4.1. Fibre and matrix selection

Multiple variables can be considered for the fibre selection, despite the probably most relevant are: availability, cost, mechanical properties, length and quality. Given their influence in the fibre's properties, chemical composition, harvesting time, extraction methods, treatment, or growing and storage conditions are relevant parameters to be taken into account in the fibre selection. In this sense, differences around 15-20% in fibre strength due to optimal harvesting time or manual extraction methods have been reported in the literature, as reviewed in [3]. For optimal mechanical performance, fibres with high cellulose contents and microfibrils aligned in multiple directions are preferred, as is the case of bast fibres [3]. Also low moisture absorption and high lignin content—for better long term resistance and better thermal stability—are preferred [24]. However, geographical location often plays the major role in fibre selection for composites application, since the fibre availability depends on the climate conditions for growing. A favourable climate makes of flax a common crop in Europe and due to that, flax is the most widely used natural fibre for composite reinforcement in this region.

Regarding the matrix selection, also multiple considerations are required. From a technical point of view, the polymer selected has to fulfil the mechanical and other functional requirements for the application, as well as being suitable for the production process defined. In this sense, the matrix selection is limited by the processing temperature, which has to be low to avoid degradation of the natural fibres—that are thermally unstable above ~180 °C—[3]. The matrix requires performing an optimal stress transfer in order to achieve a biocomposite with good mechanical performance. A good compatibility between the fibre and the matrix is key challenge to achieve. As further reviewed, there are possibilities for matrix modification or fibre treatment that can enhance this interaction if required. Other factors to be taken into account in the matrix selection lie in the fact that it provides

protection to the fibres, since acts as a barrier against adverse environments—such as to moisture absorption or abrasion—[3], and hence, barrier properties are desirable for some applications. From the point of view of sustainability, other factors such as recyclability, origin on renewable resources or biodegradability are extra benefits, which can offer a smarter solution when considering the overall life cycle of the material. This is where biopolymers find their market niche.

1.4.2. Fibre/matrix interaction

When the fibres and matrix selected present a weak interface, the stress-transfer is affected, leading to a poor reinforcement effect of the fibres that can, in extreme cases, even worsen the performance of the bare matrix due to the introduction of small defects that act as stress concentrators. Considering the higher stiffness and strength of the natural fibres when compared to biopolymers, a good fibre/matrix interaction is often revealed by an increase in strength and in toughness, while the stiffness is often increased regardless the fibre wettability—although the increase is greater if the adhesion is optimised—. However, a too strong interface can also enable crack propagation, thus impoverishing the mechanical properties of the composite [3]. Nowadays there are numerous possibilities for increasing such a compatibility between the fibre and the matrix.

Concerning the fibre modification, there are many treatments of physical, chemical or enzymatic nature that can be applied in order to adapt the fibre surface for an enhancement of the strength of the composite. In this sense, the treatment must be in accordance to the matrix of the composite—to improve the wettability—, and in most cases the optimization of the treatment conditions is required. On the one hand, physical surface modification of fibres bases its effectiveness in the mechanical interlocking, produced by a high fibre roughness that increases the shear strength in the fibre/matrix interface [3]. Some examples of physical treatments are the plasma technologies that will be discussed later.

On the other hand, chemical treatments are based in the generation of bonds between chemical groups of the fibre's and the matrix's surfaces. The increase in the interfacial strength depends, in this case, in the sort and density of the bonds generated [3]. This chemical bonding can be produced by coupling agents bridging the fibre/matrix interface, by grafted groups on the fibre surface, or by activation of surface groups, for example. Among the chemical treatments, are common the use of alkaline treatments—such as mercerization, which consists of a treatment with NaOH—, acetylation, silane treatment, or use of maleated

coupling agents, among others [4,22,24,30]. Enzymatic treatments can be cost-effective and environmentally-friendly solutions to achieve good quality fibres, which have shown to improve composite properties due to removal of adverse fibre components and increase of fibre surface area—mainly due to fibrillation—[3,30].

Regarding the matrix modification, a possibility—used in conventional thermoplastic matrices such as PP—is the addition of coupling agents such as maleic anhydride [30], that react with the hydroxyl groups increasing the fibre/matrix adhesion. However, the modification of the natural fibres according to the aforementioned techniques is more common.

1.4.3. Fibre content and porosity

The increase in fibre content is generally translated into a rise in the mechanical properties of the composite. A higher amount of fibres will be translated in higher stiffness, and in higher composite strength, whether the fibre/matrix adhesion is optimised, as mentioned before. However, some limitations can be reached, especially in plant fibre composites. On the one hand, the fibre content can be increased up to threshold in which the water uptake and the odour of the composite become relevant side effects [24].

On the other hand, these limitations are related to achieving a balance between fibre content and proper wettability, and hence good stress transfer. In this sense, there is a critical volume fraction—expectedly <10%—from which lower contents of natural fibres produce a negative effect in the composite strength, acting as simple pores/holes in the matrix, but also there is a maximum volume of fibres fraction—around 50-60%—that leads to a poor wetting due to a deficient fibre/matrix ratio [3]. The former is not often observed given that higher fibre contents are normally used; the latter is produced because the amount of matrix cannot cover the all the fibre surface and a large porosity is obtained, thus affecting the stress transfer and hence, the mechanical properties.

Regarding porosity and in addition to the aforementioned, cellulosic fibres present intrinsic porosity due to their lumen—for flax, lumen is the 6.8% of the fibre section [76]—. The porosity has an important effect in lowering the final properties of the composite. Madsen, Lilholt and co-workers have worked in the relationship between fibre contents and porosity—what is of special interest for modelling the mechanical behaviour of the composites—, and have developed correcting factors for the modified rule of mixtures that have shown a better accuracy in the stiffness prediction in natural fibre composites [77–79].

I.4.4. Fibre orientation and dispersion

The orientation of the fibres with respect to the direction in which the load is applied plays a key role, as can be observed in Figure I.17. In this sense, the best mechanical properties are observed for fibres aligned in the direction of the applied load [80]. Despite natural fibres are more difficult to align due to their finite length—unlike the synthetic fibres that are produced in continuous—, there exist methods based in carding systems to achieve reinforcements of natural fibres of aligned fibres, or yarns of spun natural fibres can also be considered, although some twisting is implied—not perfect alignment—.

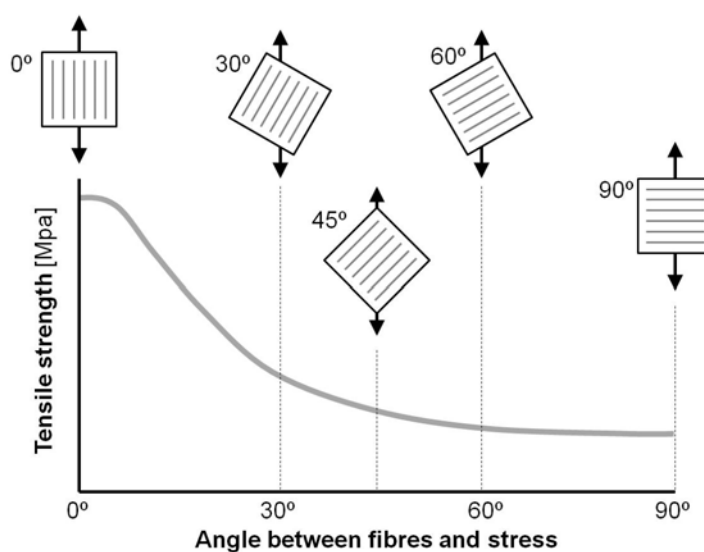


Figure I.17. Effect of fibre orientation on the tensile strength of a composite reinforced with uniaxial fibres, adapted from [80].

However, fibre orientation can be a positive or negative factor depending on the processing technique and final application of the composite. For instance, sandwich structures of uniaxial fibres oriented in multiple directions can be of interest in high performance applications, such as the structure of a bike or the fin of a surfboard. However, having oriented short fibres following the flux direction in a composite part that has been produced by injection moulding can be translated in inhomogeneity on the stress transfer throughout the material, what can lead to a premature fracture.

Regarding the fibre dispersion, it is an extremely important factor, especially in biocomposites with short fibre reinforcement, since a random and good distribution of the fibres has to be achieved to produce an isotropic material, in which the fibres are fully surrounded by the matrix—not agglomerated—to reach a good stress-transfer. The increase

in the length of the fibres ease their trend to agglomerate, thus leading to irregular properties throughout the material. The use of twin-screw instead of single-screw extruders for mixing the fibres and the thermoplastic matrices helps to enhance a good dispersion but causes some damage to the fibres, reducing their length [3]. Therefore, for the reinforcement of thermoplastic biopolymers with long fibres, the use of textile structures is an interesting option to solve or minimize the problems of fibre orientation and dispersion, despite it leads to limitations in what to the manufacturing processes available is concerned.

1.4.5. Composite manufacturing process

The criteria for the selection of the most suitable process to fabricate a composite depends on the target properties, size and shape to achieve, on the reinforcement type, or on the manufacturing costs and production speed, among others [24].

The reinforcement morphology—i.e. length and structure—can also be a critical factor for the composite production. In this sense, the processing technique can determine/limit the good distribution of the fibres throughout the material, the use of textile structures, the maximum content fibre achievable or the maximum length that can be processed. Despite there exist lots of processing techniques, the most used for thermoplastic matrices are injection, extrusion and film-stacking. In injection or extrusion, the process presents high shear rates because of the screw of the machine, as previously mentioned. Thus means that the length of the fibres used in this fabrication method have to be relatively short—otherwise they can be damaged/cut in their pass or even block the screw—, and also that the use of fabric reinforcement is almost impossible. In film-stacking method, several layers of fibre reinforcement and matrix film are heated and compacted under high pressure. Therefore, the structure of the fibres is less limiting, but some difficulties can be found in the good distribution of the fibres, which depends directly on the structure, and in the fibre orientation throughout the thickness of the composite, since the hot-pressing compacts the reinforcing structures reaching 2D layers, mainly.

Regarding the target size, autoclave and open moulding methods are preferred for large composites, while injection and compression moulding for the small ones [24]. Regarding the target shape, some of the manufacturing processes present limitations that impede the production of complex pieces, or sandwich structures, for instance. Therefore, a good balance involving all these issues needs to be set in the design process, in order to reach the desired specifications in the final composite.

I.4.5.1. Processing conditions

Moreover, cellulosic fibres can present symptoms of degradation at relatively low temperatures (~180 °C). As aforementioned, this limits their use in matrices that require high temperature conditions for processing. This is a minor drawback, given that most the thermoplastic biopolymers can be processed at lower temperatures than these at which the cellulosic fibres start to degrade. However, some biopolymers like PHB present a very narrow processing window, and undergo in thermal degradation when exposed to temperatures just above their melting point. Other factors such as viscosity, pressures or shear rates that depend on the processing require an optimisation. Therefore, a critical factor in the final properties of the composite material is the determination and setting of the proper processing conditions for its production.

I.4.6. Durability and degradation

The structure of cellulosic fibres and their hydrophilic nature—favoured by the chemical composition—is responsible of their sensibility to moisture and water absorption. Therefore, biocomposites, typically, tend to absorb water when exposed to humid environments or when immersed in water. In this sense, the water transport is associated to diffusion throughout the matrix, to cracks, pores or other imperfection in the matrix, and to capillarity along the fibre and or the fibre/matrix interface [26]. Anyhow, once the water absorption reaches the fibres causes their swelling, thus inducing cracks in the surrounding matrix—matrix damaging—and debonding of the fibres—weakening of the fibre/matrix adhesion—, among other effects [26,81]. In Figure I.18, a scheme of the effect of water in the fibre/matrix interface is presented. The fibre debonding is translated into an ineffective stress-transfer, and hence, to the impoverishment of the mechanical properties of the biocomposites—sometimes referred to as aging—. Therefore, the moisture absorption of the cellulosic fibres is an important drawback for biocomposites, since affects their durability. In this sense, given that the water uptake is related to the fibre content, the use of large amounts of cellulosic fibres can have a potential negative effect in the long term properties due to higher degradation by water/moisture absorption [3]. Due to that, several fibre treatments that can be used to reduce the hydroxyl groups—and hence the hydrophilicity of the cellulosic fibres—can be found in the literature, causing an increase in the mechanical behaviour and a higher dimensional stability, too [81].

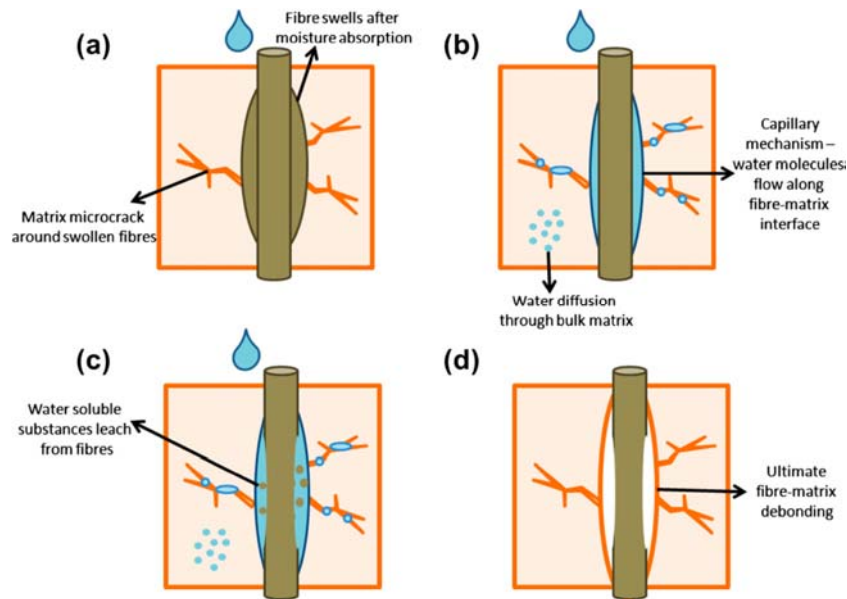


Figure I.18. Effect of water on fibre/matrix interface, from [26].

On the other hand, the moisture absorption increases the potential microbial attack that is related with the biodegradation of the biocomposites, thus being a benefit for those applications in which such an effect is desired.

I.4.7. Treatment of cellulosic fibres

As aforementioned, cellulosic fibres present two main drawbacks for their use in polymer matrix composites: the fibre/matrix compatibility and the moisture absorption [82]. In this sense, numerous studies focussing on treatments to overcome these difficulties have been published.

As previously mentioned, the fibre/matrix adhesion governs the stress transfer and hence, the mechanical performance of the composite. Therefore, it is a key parameter in composites production. This compatibility depends on the nature of both the matrix and reinforcement. Cellulosic fibres—which present a hydrophilic nature—present poor adhesion with most of the matrices commonly used—mainly hydrophobic—. The improvement of wettability can be addressed by chemical or physical methods [30] or modify the matrix or the fibre surface, such as: alkaline treatment, silane treatment, acetylation of natural fibres, benzylation treatment, acrylation and acrylonitrile grafting, maleated coupling agents, isocyanate treatment, or plasma treatments, among others. Anyhow, this modification must be consistent with the matrix, because different matrices require different fibre surface properties.

In general, PHAs present better adhesion to natural fibres than polyolefins due to the presence of polar groups that can interact with the hydroxyl groups of cellulose [61,83]. However, fibre treatment can enhance this favourable adhesion between the PHA matrix and the flax fibres.

On the other hand, the moisture sensibility of the natural fibres can have dramatic results in composites, in the sense that water absorption can produce the aging of the material. Concerning this, some fibre treatments reduce the hydrophilicity of the fibres can also be an interesting option to increase the durability of the biocomposites produced.

Given the marked environmentally friendly character of the composites focussed in this thesis—the green composites—, an interesting option is the use of eco-friendly methods to perform the aforementioned enhancements. In this sense, enzymatic and plasma treatments applied for the fibre modification are, generally, qualified as “green” techniques [84].

I.4.7.1. Plasma treatment

Plasma is the fourth state of matter: an ionized gas of overall zero charge density (Figure I.19). Plasma can be considered as a gaseous mixture of electrons (negative charge) and positively charged ions, and can be created by subjecting a gas to a strong electromagnetic field.

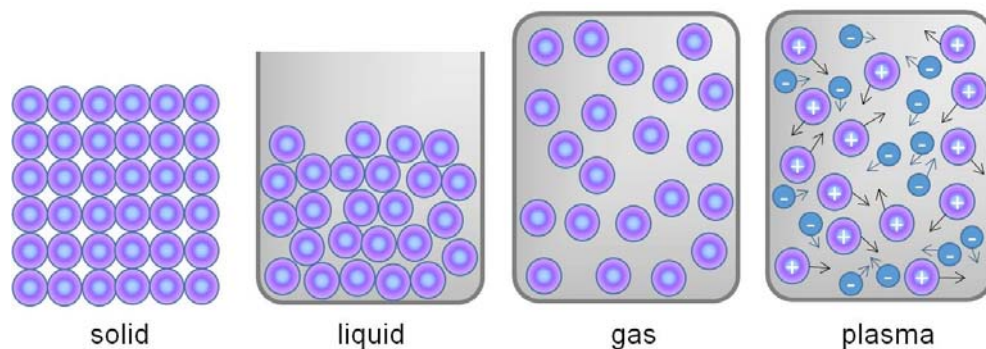


Figure I.19. States of matter.

Plasma technology is an environmentally-friendly and cost-efficient solution for surface-modification of fibres. The advantages of this green process are that a low amount of chemical products are used, no water is required, and the waste production—residual waste, water, solvents or chemicals—is very low, since the treatment is performed in the gas state. By varying the process parameters—such as type of gas, power, processing time and pressure, and gas flow—, different effects can be obtained. A large amount of gases—such

as air, nitrogen, argon, oxygen or fluorocarbon gases, among others—are used in plasma technologies in textile fabrics to produce several effects, such as: hydrophilicity, hydrophobicity, dyeability and printability performance, or other functional finishing modifications—such anti-bacterial, for instance—, among others [85].

Each combination of gas, target substrate and processing parameters generates a unique plasma medium, which comprises a mix of ions, electrons, neutrons, photons, free radicals, meta-stable excited species and molecular and polymeric fragments [86]. Thus generates a complex system which enables a large variety of surface modifications such as: surface activation, since reactive sites can be created by bond breaking; grafting of functional groups; etching—removal of material from the surface—; cleaning of surface contaminants; and deposition of coatings, such as plasma-polymerized coatings.

Moreover, these phenomena take place in the most external layer of the substrate (10–100 nm), while the inner material remains unaltered. This is another advantage, since is possible to obtain different wettability behaviours in the natural fibres without decreasing their bulk mechanical properties. Otherwise, other methods for fibre modification, such as the NaOH treatment for cleaning and hydrophilicity increase, can undergo in serious detriment of the mechanical resistance of cellulosic fibres.

As reviewed in [84], the plasma can lead to two main sort of interactions with the surface according to the gas used. On the one hand, it can produce chain scission on the surface—thus leading to the surface etching (Figure I.20), cleaning or activation aforementioned—, what is achieved with non-polymerizing gases such as helium, oxygen, air, argon or nitrogen. On the other hand, the use of polymerising gases leads to plasma induced polymerization or grafting, which is achieved with gases and precursors like fluorocarbons, hydrocarbons or silicon containing monomers.

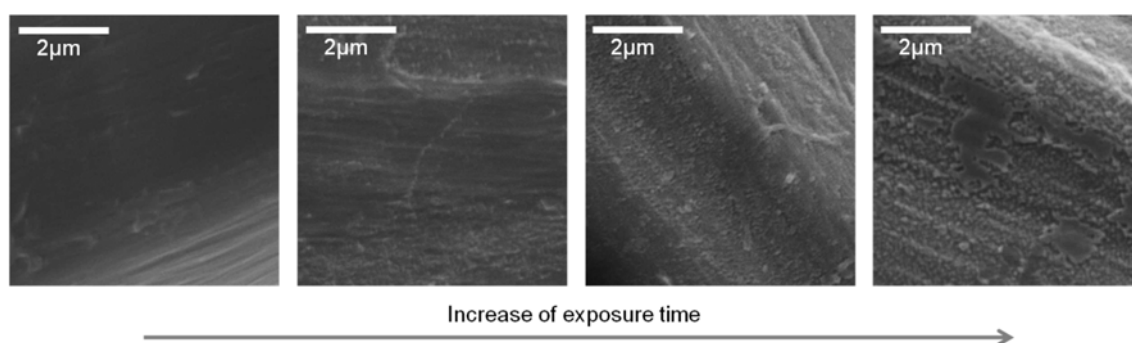


Figure I.20. Surface etching in flax produced due to increasing exposure time to argon plasma.

In industry and research, plasma reactors are used to that purpose, where the power supply can be generated by low-frequency (50-450 kHz), radio-frequency (13.56 or 27.12 MHz) or microwave (915 MHz or 2.45 GHz) sources. Plasma techniques are classified into hot/thermal plasma and cold/non-thermal plasma [87]. Moreover, cold plasma techniques are divided into two groups: low pressure plasma and atmospheric plasma technologies, and the latter is further classified into corona discharge, dielectric barrier discharge (DBD) and atmospheric pressure glow discharge. Both kinds of techniques have been used for textile treating in the literature.

On the one hand, the low pressure plasma is a type of cold plasma produced in a vacuum chamber under a pressure around 10^{-2} - 10^{-3} MPa. The treatment gas is supplied into the chamber under vacuum, and ionised between two electrodes with the help of a high frequency generator. This plasma technique offers high control and reproducibility, although the vacuum required implies the drawback of a batch production. With the use of gases of diverse nature, the hydrophobic/hydrophilic behaviour of the fibre surface can be tailored.

In the corona discharge plasma the plasma gas is produced at atmospheric pressure by means of low-frequency generator, and due to the lack of void conditions can be used in continuous processes, thus pointing to a better cost-effectiveness. In general terms, the corona treatments include the use of oxygen-containing species, and produce both an increase in roughness and an activation of the surface—due to an expected increase of carboxyl and hydroxyl groups—.

Plasma techniques have already been used for the treatment of natural fibres to be used in composite reinforcement. Yuan et al. studied in [88] the plasma treatment in wood fibres to improve the performance of their composites with PP. They treated wood fibres in pulp form with low pressure plasma of air and argon gas, observing an improvement on the tensile modulus of the composites, and an increase in tensile strength for composites with treated fibres, especially for the air-plasma ones—20% higher—. Moreover, they reported an increase on the surface roughness of the fibres, higher O/C ratios—thus pointing to oxidation of the fibre surface—and higher presence of $-C=O$ and $O-C=O$ functionalities, all this leading to the improvement of the adhesion.

Bozaci et al. in [89] used a glow discharge plasma with air and argon gas under atmospheric pressure to treat a flax fabric. They observed changes in the surface chemical composition, higher O/C ratio, presence of plasma-generated functionalities—such as $-C=O$, $O-C-O$ and $O-C=O$ —and an increase on roughness, all this expected to

contribute to a better adhesion of the matrix and hence, to contribute to the increase of the composite performance. The increase of the plasma power—100, 200 and 300W—lead to higher roughness, although the appearance of cracks in the surface was also observed, attributed to the etching effect of the treatment. However, despite they observed a loss on the fabric strength—up to a ~12%—, the pull-out tests revealed an increase in the interfacial shear strength between the unsaturated polyester resin and treated fabrics—for all powers—, and between HDPE and fabrics treated at 300W.

1.4.7.2. Wet/dry cycling

The wet/dry cycling is a treatment in which water—without chemical products—is used to clean waxes and pectins in the cellulosic fibres, thus leading to a modification of some of the properties of the flax fibres. Drying and rewetting cycles cause shrinkage of the natural fibres, attributed to the formation of hydrogen bonds in cellulose [90], and also a reduction of the pore size [91].

One of the most relevant modifications is the water uptake behaviour. After performing 4-5 cycles of rewetting and forced drying, the fibres loss surface waxes and other hydrophobic products, and hence the fibres present more hydrophilic behaviour. However, the total amount of moisture retained by the samples is reduced. Thus could be attributed to the partial loss of hemicellulose content during the cycling. Such a loss is translated in a reduction of the moisture absorption, but also into a higher thermal resistance. In this sense, Claramunt et al. [92] used a wet/dry cycling known as hornification—commonly used in the paper industry—in kraft pulp and cotton linter. The hornification treatment consisted of 4 cycles of drying at 60 °C, rewetting by soaking overnight and further disintegration of the wet pulp. They observed a reduction in the water retention values. Moreover, the cement mortar composites produced with the treated fibres, revealed a higher durability, despite it did not prevent the partial loss of the mechanical reinforcement.

I.5. Cellular materials

Cellular materials are composed by two phases, a continuous solid phase—often named as matrix—and other gaseous phase, which can be either continuous or discontinuous [93]. Cellular materials can be ceramic, metallic or polymeric depending on the nature of the matrix. The interest of this thesis is focussed on polymeric cellular materials. It is worthy to mention that “cellular material” is a general term, while the term “foam” refers, strictly, to cellular materials produced from a liquid or melt state [93]—both terms are used in this thesis—.

Under the point of view of ecology and sustainability, cellular materials present an interesting advantage, which is the material and weight reduction. In this sense, the use of bio-based matrices and natural fibres as reinforcement is not the only possible strategy to obtain environmentally-friendly composites. Development of lighter solutions by means of the use of cellular materials can be another interesting path to obtain composites with improved specific properties and higher efficiency—related to a more adequate use of the energy and resources—, what leads to “greener” solutions.

Classification

Cellular materials can be classified depending on the continuity of the gaseous phase into open cell or closed cell foams (Figure I.21).

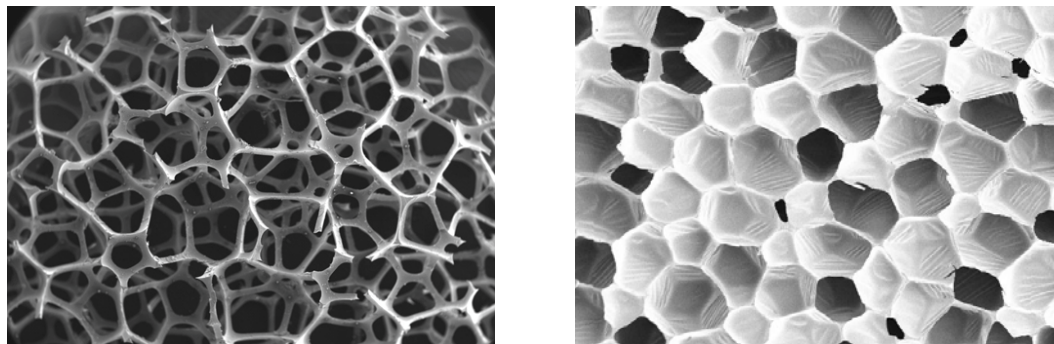


Figure I.21. Open cell foam (left), from <http://www.qmed.com/mpmn/medtechpulse/developing-fully-open-cell-silicones-implantable-devices>; and closed cell foam (right).

In open cell foams, the structure is formed by interconnected cells, and hence the gas phase can flow through the material. In closed cell foams, the gas forms a discontinuous phase since it is retained in the cells. However, often the cellular materials present a mixture between these two, showing both closed and open cells in a certain fraction.

One of the important parameters considered when working with cellular materials is the relative density (ρ_{rel}). ρ_{rel} is the ratio between the density of the foam and the density of the solid phase and, therefore is a parameter that gives an idea of the expansion or void content of the foam—since expansion can be calculated as $1/\rho_{rel}$, and porosity or void content as $1-\rho_{rel}$ —. According to their ρ_{rel} , cellular solids can be classified into:

- high density cellular materials: $\rho_{rel} \geq 0.7$
- medium density cellular materials: $0.2 < \rho_{rel} < 0.7$
- low density cellular materials: $\rho_{rel} \leq 0.2$

Despite polymeric cellular materials are often in the desirable range of low density, the cellular materials obtained in this thesis are mainly of medium density.

General properties of cellular materials

Properties of cellular materials are often in ranges that the solid or dense materials cannot cover, as shown in Figure I.22. As previously mentioned, the low density is one of the strengths of cellular materials for those applications this is a desirable property. Regarding the mechanical behaviour, cellular materials present lower values than the solid materials, since the weight reduction is achieved in expense of the mechanical resistance.

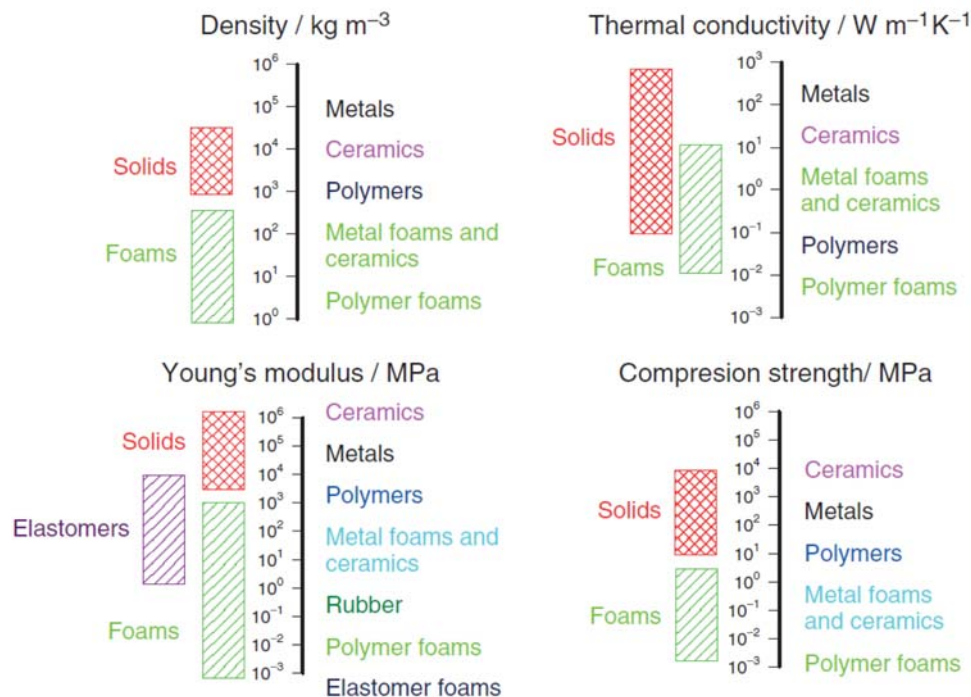


Figure I.22. Comparative properties of dense and foamed materials, from [93].

Applications of polymeric cellular materials

Polymeric cellular materials present several interesting properties useful for a wide range of applications. Therefore, polymeric cellular materials are used in buoyancy applications and cores of sandwich panels due to their low density; thermal insulation—in buildings, for instance—because of their low thermal conductivity; in acoustic insulation and protective applications because of their energy-absorbing properties; or in cushioning due to their stiffness, strength and compressive strain properties, among others.

I.5.1. Fundamentals of foaming

Typically, polymeric foams are obtained in a process in which gas bubbles nucleate and growth in the polymeric matrix, although some exceptions can be found [94]. This process can be summarised in several stages:

- First, a homogeneous and completely miscible phase of matrix/blowing agent is formed. Therefore, the gas is dissolved in the matrix forming a single phase—often in a melt or liquid state, despite solid state foaming is also possible—. This is typically achieved at high pressures and/or high temperatures.
- A sudden change in the thermodynamic equilibrium leads to the evolution of this gas. Since the solubility is reduced because of a reduction of the pressure or temperature, the gas starts small and dispersed bubbles (cell nucleation).
- The bubbles (cells) tend to increase in size (cell growth), thus reducing the progressively the density of the material, since it expands its volume. This stage depends in many factors concerning the conditions, the polymers properties and the gas (blowing agent) content, mainly.
- Further growth leads to lower densities, but once the cells approach to each other some kind of distortion is achieved. The cells, initially spherical, tend to adopt a polyhedral shape, forming the cellular structure. Due to viscous and surface tension effects, the melt/liquid flows towards the edges of the polyhedron.
- If the growing stage is not limited, and hence the flow towards the edges is not stopped, a rupture of the cell walls can be achieved, leading to the obtaining of open cell foams. Moreover, other degenerative processes of the cellular structure can take place such as drainage, cell coarsening, cell coalescence or final collapse.

- Finally, the morphology of the cellular structure stabilized by solidification of the polymer matrix (cooling) or by cross-linking, mainly.

The scheme of this process is presented in Figure I.23.

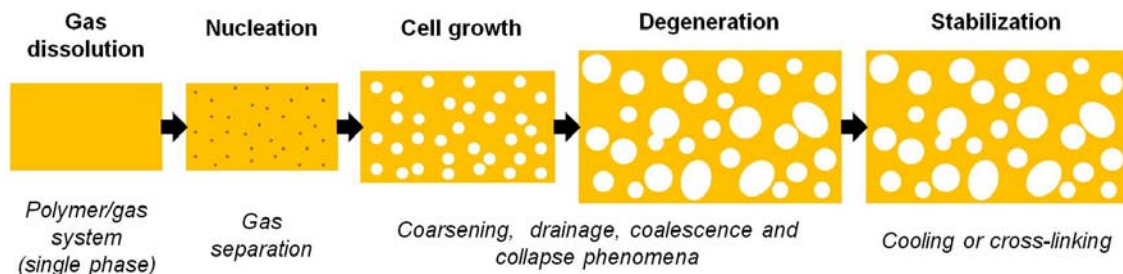


Figure I.23. Scheme regarding the cellular structure evolution of the foaming process.

Nucleation

Nucleation takes place when a thermodynamic instability of the polymer/gas system is reached by a pressure drop or a temperature increase. The system becomes supersaturated, the solubility of the gas decreases and hence, the gas molecules tend to diffuse into clusters, forming spherical nuclei. There are two kind of nucleation mechanisms: homogeneous or heterogeneous nucleation. On the one hand, in the classical homogeneous nucleation theory, nuclei formation in the liquid/viscous bulk is produced due to the aforementioned thermodynamic instability, and depends on the concentration of gas molecules, the activation energy to form the nuclei, the surface free energy in the polymer/bubble interface and, of course, on the temperature and the pressure drop. On the other hand, the heterogeneous nucleation requires another solid phase—such as impurities, fillers or other particles—since the lower surface energy of the interface between the polymer and these solid particles promotes the creation of the nuclei [95]. Therefore, the particles act as nucleation sites and can help to control the final cellular structure. The heterogeneous nucleation depends on the density of this nucleating agents, the activation energy, the surface free energy, the contact angle at the polymer/nucleating agent interface, the temperature and the pressure drop, mainly.

Cell growth and degeneration mechanisms

The cell growth is produced because of the diffusion of the gas molecules from the polymer melt—considering the polymer in a liquid/melt/viscous state—to the nucleated cell, thus progressively reducing the gas molecules concentration in the polymer melt surrounding the cell. Due to that, the cell growth rate depends on the bubble radius, both the

internal and external pressures affecting the bubble, the surface tension and the matrix viscosity, being the latter a key parameter in the cell growth process—the lower the viscosity, the faster the cell growth—. However, a variation of the viscosity is desirable, lower at the beginning for an easy promotion of the cell nucleation, and increasing meanwhile the foaming is produced in order to withstand the deformation, thus avoiding the excessive degeneration of the cell structure and cell ruptures [95].

The advance in the cell growth and hence, the expansion, leads to the obtaining of a cellular structure in which the cells are separated by thin walls. This evolution requires to be stabilized by means of cooling or cross-linking; otherwise, the cellular structure can evolve up to its degeneration. The cell degeneration is mainly explained by three mechanisms, which are briefly described [95]:

- Coarsening consists in the gas diffusion from the smaller to the larger cells, thus increasing the size of the latter and dissolving the former.
- Coalescence is produced due to the rupture of the cell wall between two growing neighbour cells, what leads to their combination and the obtaining of a larger cell.
- Drainage is related to the reduction of the wall thickness due to capillary forces that transports the polymer from the walls to the edges, especially for very low viscosities. Due to drainage, coarsening and coalescence mechanisms are favoured.

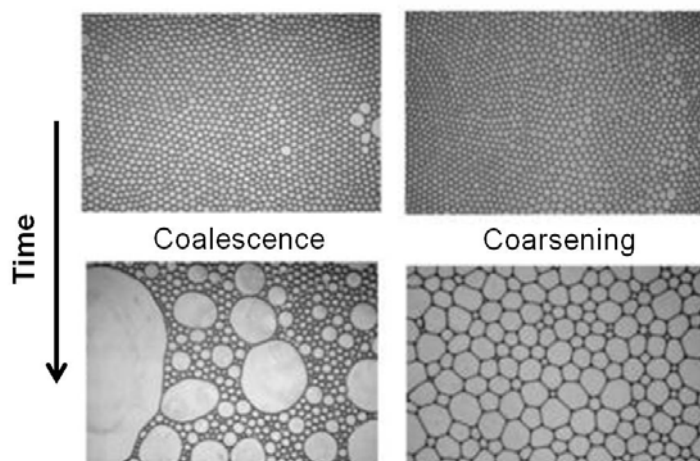


Figure I.24. Effects of coalescence and coarsening, adapted from: <https://www.equipes.lps.u-psud.fr/sil/spip.php?rubrique31>.

Finally, in the same way that the gas tends to diffuse from cell to cell, it can also tend to diffuse to the atmosphere, escaping from the polymer matrix, thus reducing the amount of gas available for expansion. Therefore, if the stabilization is not achieved, the cells tend to

collapse causing a contraction of the foam. The skin formation present in most polymeric foams is a consequence of the diffusion rate of gas out of the foam. In general terms, the stabilization in thermoplastic materials is achieved by cooling the polymer (solidification).

1.5.2. Critical factors for foaming

There is a close relationship between the foaming processes, the structure and the properties of the foams, since these three concepts are connected and feedback. The structure of the foam depends on the processing technique used, and in its turn, the properties of the foam strongly depend on their structure. Therefore, is interesting to briefly revise few of the factors that affect foaming in order to give a closer understanding of the foams behaviour.

1.5.2.1. Polymer matrix characteristics

The characteristics of the polymer to be foamed play a key role in the conditions of the foaming process and the correspondent results, especially those properties related with their rheological behaviour.

Focussing in thermoplastic polymeric matrices, those polymers that present very short and linear molecules often present a higher difficulty to be foamed, owing to lower melt strength and low viscosity—thus related with the rheological properties—. For these materials, the improvement of their properties can be reached using additives that produce chain extension and/or ramification, generating some cross-linking by additives or other methods such as irradiation, for example. On the contrary, polymers presenting ramifications and/or high molecular weights are expected to present better foamability owing to a probably higher viscosity.

Crystallinity

Also the crystalline nature of the polymer is relevant for some foaming processes—such as for the solid state foaming—, since the gas diffusion is affected by whether the polymer is amorphous or semicrystalline. In general terms, the gas diffusion is relatively easy through the amorphous areas, meanwhile crystals typically act as gas barriers. Thus means that for amorphous polymers, the gas diffusion is relatively easy, and the increase in temperature over the glass transition temperature (T_g)—to reach the rubbery state—is enough to greatly enhance this diffusion. However, for semicrystalline polymers, the increase of the

temperature over the T_g can be not enough to promote the gas diffusion—depending on the crystallinity degree—. In this case, reaching temperatures higher than the melting point is necessary to ensure a proper gas diffusion.

Rheological properties

Moreover, for achieving the cell growth, a certain viscosity and melt strength are required [95]. These properties, related with the rheological behaviour of the polymer, are important because the matrix has to withstand the deformation at which is subjected during the cell growth. In fact, ideally the matrix should increase the behaviour during the foaming process, showing very low viscosities at the beginning to promote a fast nucleation of numerous cells, but then increase to avoid excessive cell degeneration, rupture and collapse. The polymers that show strain hardening during the cell growth are optimal for foaming.

Degradation of the polymer is another factor to be taken into account, since it induces lowering of the molecular weight, shortening the polymeric chains and hence, reduces their viscosity, which affects their foamability.

In this sense, the PHAs that are used in this thesis are known to have high crystallinity, low viscosity [39], low melt strength and suffer from thermal degradation—what lowers their molecular weight during processing—, and hence, achieving their foaming is a challenge to be succeed.

1.5.2.2. Blowing agents for polymeric foams

In the production cellular materials, the gaseous phase is introduced and dispersed throughout the solid phase in the foaming process by means of a blowing agent. Blowing agents can be chemical or physical.

Chemical Blowing Agents (CBAs)

CBAs are chemical additives that generate the gas phase as a by-product of their thermal decomposition reaction, which will require different temperature ranges and temperature exposure times depending on the nature of the CBA. Therefore, CBAs cover a wide range of processing conditions for foaming most of the thermoplastic polymers. CBAs can be, in their turn, exothermic—such as azodicarbonamides, one of the most common CBAs used— or endothermic depending on their nature.

Regarding the endothermic CBAs, eco-friendly solutions—typically based in sodium bicarbonate and citric acid—can be found. The thermal decomposition of such a product generates CO₂ gas but also water, which is a drawback for the foaming of some biopolymers that present sensibility to hydrolytic degradation such as PHAs [73]. However, some additives can be added to counteract this effect, and the lack of complex equipments or conditions makes of the use of CBAs in continuous processes an interesting alternative to achieve low-cost foams in a simple way.

Moreover, for CBAs in masterbatch form, the nature of the carrier polymer used has to be taken into account since must be compatible with the polymer matrix, owing that, despite in very low amounts, it will end in the cell walls.

Physical Blowing Agents (PBAs)

Physical blowing agents (PBA) are gases which can be directly dissolved into the polymer, such as CO₂, N₂, or aliphatic hydrocarbons [94]. Concerning to this, the interest on the use of gases in supercritical state for foaming has grown in the last years. Nitrogen (N₂) and carbon dioxide (CO₂) are the most commonly used gases for foaming in supercritical state, both in continuous and discontinuous processes —such as extrusion foaming and batch foaming, respectively—.

Furthermore, foaming with CO₂ is considered as a green foaming method, given the low environmental-impact of this gas. In this sense, CO₂ is an eco-friendly, non-flammable, not ozone-depleting, chemically inert, non-toxic and low cost blowing agent, which is obtained as a by-product in other production processes, and presents good gas solubility in polymers—with PHAs among them—. Its supercritical state (scCO₂) is achieved under specific temperature and pressure conditions: temperature higher than 31.1 °C and pressure higher than 7.39 MPa.

In the supercritical state, the CO₂ bears both the properties of a liquid and a gas, presenting high diffusivity, low viscosity and high density, and is interesting due to expected effects of melting temperature depression and plasticization. In fact, solubility of scCO₂ in PHAs has been observed to rapidly dissolve with the increase in pressure, and to decrease the melting temperature—at a rate around 1.3 °C/MPa—up to 24 MPa [96]. The lowering of the melting temperature, for instance, what finally influences the foaming process

1.5.2.3. Other additives and fillers for polymeric foams

Regarding additives, there are a lot of possible additives to solve many concerns in foaming. Plasticizers can help to the processing of some biopolymers to enhance chain mobility and reduce the brittleness and excessive stiffness. The plasticizer to be used depends on the polymer matrix, and also the required amount has to be optimized for such a purpose. As aforementioned, chain extender additives can enhance the foamability of those matrices presenting low molecular weight. These products can generate a reattachment of the broken chains—produced during processing—to the backbone, producing ramification and/or chain extension [97], what increases the viscosity and hence, improves the foamability [98].

Addition of fillers is other technique used to control the foaming owing to their role as nucleating agents. A wide range of micro and nanoparticles are used to that purpose—from the simple talc particles to the advanced nanoclays or carbon nanotubes, among others—. The addition of wood particles to biopolymers in foaming has been deal by many research studies [99]. However, fillers can also have other effects to be taken into account—depending on the filler used—, such as increase of crystallinity, the increase of gas barrier properties, the stress-concentration effect, the increase in conductivity, etc.

Due to all that, there are many possibilities in the tailoring of properties of polymeric foams that open a wide range of possible studies.

1.5.2.4. Foaming method and processing conditions

There exist numerous processing techniques to produce foams. Regarding the foaming of thermoplastic materials, the most relevant are probably those based in extrusion and injection foaming—with both CBA, PBA and supercritical PBA—and batch techniques—including the compression moulding and gas dissolution foaming—. In this thesis, extrusion foaming and gas dissolution foaming have been used to produce foams. Due to that, the fundamentals of these techniques are here briefly revised.

Extrusion foaming

Extrusion foaming is a continuous production technique of relative simplicity, high productivity and low production cost, what makes of this technique a useful tool for both production and investigation purposes. Both CBAs and PBAs can be used in extrusion foaming, although CBAs can be added in any conventional extruder to foam a polymer matrix, while the use of PBAs requires of specialised extrusion equipments to allow the introduction of the gas at higher pressure.

Anyhow, the first step of the extrusion foaming is the melting of the matrix. This is achieved by both the action of the screw, which applies pressure and shear to the polymer pellets, and the temperature. When CBAs are used, are often fed at the same time than the matrix to ensure a proper thermal decomposition during the residence time at the extruder. Then, the mixing takes place—again due to the shear action of the screw and temperature—, where the matrix melt is mixed and homogenised. At this point, fillers and additives—often fed with the pellets—and the blowing agent reach a proper homogeneous distribution. When using PBAs, the gas is added at this point. The final goal of mixing is the achievement of a single-phase polymer/gas system.

Once the gas is dissolved in the melt, a sudden pressure drop is reached, reducing the solubility of the dissolved gas into the melt, what undergoes into nucleation of gas bubbles. Further growth of the nucleated cells takes place at the exit of the die—what is essential to achieve an optimum foaming operation [94]—, thus causing the instantaneous polymer expansion. The growth rate of the bubbles is fast at the beginning and then decreases with the polymer cooling—as the viscosity decreases—. To prevent the collapse of the structure, a fast stabilization has to be reached. Nonetheless, extrusion foaming typically reaches high expansion ratios, and due to that, high shock absorption, insulation, and noise reduction characteristics can be achieved [100].

The processing conditions play a critical role in the final foam morphology and therefore, in the properties of the same [94]. The temperature control is a key parameter in extrusion foaming, since is related with the viscosity of the melt. Heat and shear applied to the melt influence the decomposition of the blowing agent and the melt viscosity. The foam density tends to decrease with increasing extrusion temperature, although at certain point it begins to rise because of cell rupture and collapse caused by the too low melt viscosity. The volumetric flow rate has also been found to decrease the density due to better mixing and reduced viscosity. The screw speed has to be optimized to achieve good foaming. Moreover, also the pressure drop rate influences the cellular structure achieved.

Gas dissolution foaming

The gas dissolution foaming is a batch technique (discontinuous) that uses physical blowing agents—often CO₂ gas—to produce cellular polymers. The technique can be described in two main steps, as schematized in Figure I.25.

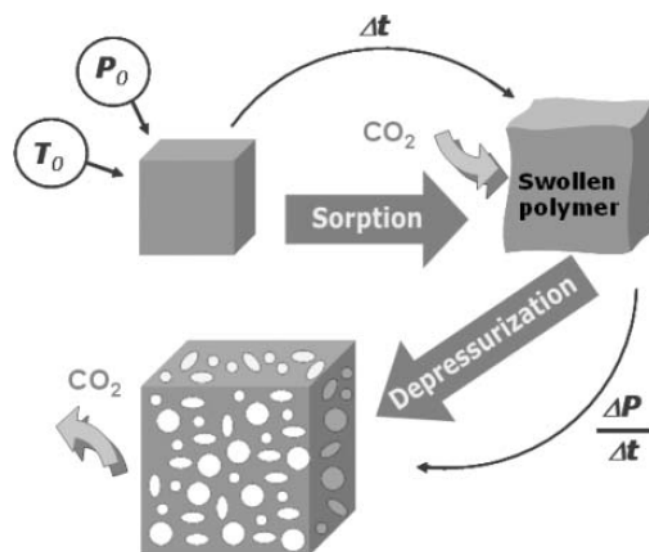


Figure I.25. Schematic representation of the CO₂-foaming process, from [101].

The first step consists on the saturation of the polymer with the gas. The temperature at which the saturation is performed depends on the nature of the polymer—amorphous or semicrystalline—. The pressure, instead, is high, and often this technique is applied with gases in supercritical state. This supercritical state tends to lower the melting and glass transition temperature due to plasticization effects, what benefits the diffusion and hence, the saturation of the gas. Due to this, the polymer matrix swells and the viscosity of the polymer decreases, allowing to process the material at lower temperatures [101].

The type of polymer, the applied pressure and temperature determine to a large extent the amount of gas that can be dissolved in the polymer [101]. Since the amount of gas dissolved is directly proportional to pressure and inversely proportional to temperature [100], saturation is preferably produced at low temperature. However, for semicrystalline polymers such as PHAs the reduction of the solubility is outbalanced by the increase in the diffusivity due to the crystal melting, and hence the use of high temperatures is justified. The result of the saturation step is the formation of a single-phase polymer/gas solution.

Once reached the saturation, a pressure drop induces a shift in the thermodynamic equilibrium, leading to an oversaturation of the gas in the polymer, what does not necessarily lead to nucleation and cell growth, since it will depend in the temperature at which the saturation is performed owing to the impossibility of foaming if the polymer is in a too rigid (glassy) state [101]. For instance, amorphous polymers can be saturated at a low temperature, extracted from the high-pressure vessel and then expanded by increasing the temperature over the T_g in an oil-bath, for instance—temperature soak method—.

Therefore, the second step consists in the gas separation, which is forced to produce the expansion. This is achieved due to a thermodynamic instability that leads to the evolution of the dissolved gas—or phase separation—, promoting the cell nucleation and grow. This thermodynamic instability can be induced by a temperature increase—temperature soak method—or by a quick pressure release—pressure quench method—. The cell growth stops when the polymeric matrix returns to a glassy state—for amorphous polymers—or solidifies by cooling—for semicrystalline polymers—.

The final cell morphology is determined by the amount of gas dissolved during the saturation process, and by the heat applied to the test specimen after the saturation process [100]. Typically, higher gas sorption is translated into a higher nucleation density and lower cell size, and cell growth is influenced by the energy input leading to greater cell size. In Figure I.26, the effects of foaming conditions in the final cellular structure are schematised.

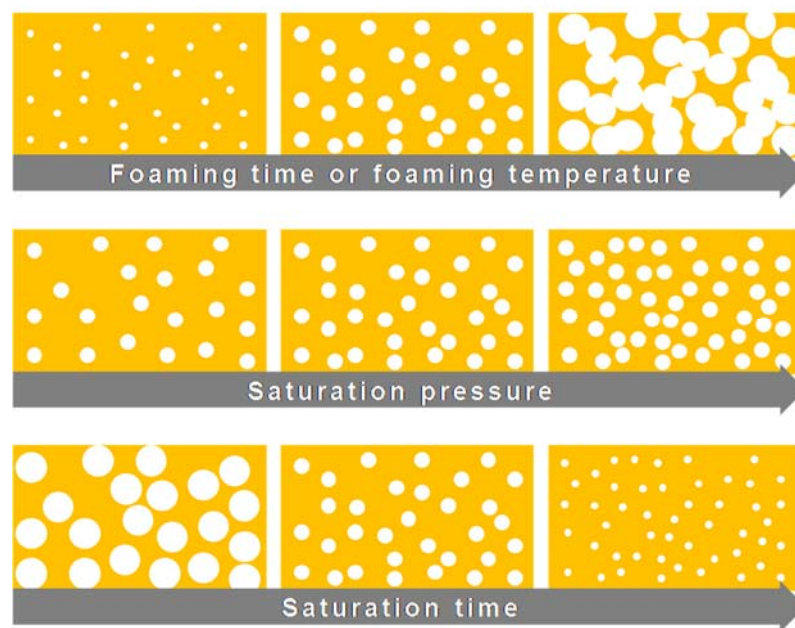


Figure I.26. Effect of batch foaming process variables on cell morphology, adapted from [100].

Jeon et al. reviewed in [100] the microcellular foam processing of biodegradable polymers, reporting numerous examples of PLA foams produced by gas dissolution batch foaming. In this same review, microcellular foams of PHBV were also reported, although those were produced by means of microcellular injection moulding—with PBAs—.

I.5.3. Characteristics of cellular materials

I.5.3.1. Cellular structure

Cellular materials are characterised, besides their relative density and porosity, by their cellular structure: cell size (mean cell diameter) can influence some of the properties of foams—such as the mechanical or thermal insulating properties—; cell shape plays a key role; and the interconnection between the cells is also another relevant parameter.

Regarding the cell shape, the three dimensional structures of cells are often represented as geometrical volumes, using models from very simple—such as cubes or hexagonal prisms—to more complex ones—such as dodecahedra, tetrakaidecahedra or icosahedra—. Therefore, the cells present multiple faces (cell walls) connected by edges (or struts) in which the material presents a higher accumulation, as shown in Figure I.27. Moreover, depending on whether the cells are equiaxed or elongated the macroscopic properties will be isotropic or anisotropic, respectively [102].

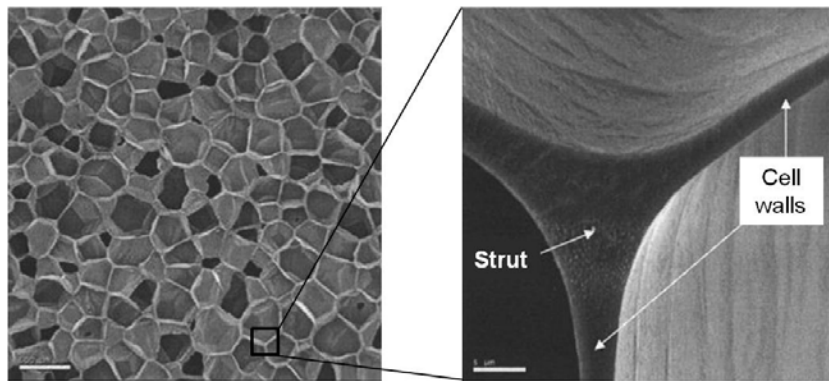


Figure I.27. Three dimensional structure of a cellular material. General overview (left) and detail of a strut (right), adapted from [103].

Regarding the interconnection between cells, foams present open-cell or closed-cell structures, as was previously mentioned. The gas trapped inside the cells in closed-cell structures can have a great influence in thermal insulation properties or in mechanical damping—due to a counteracting effect opposing to the deformation of the cell wall—. Therefore, this is a relevant parameter in the mechanical performance of cellular materials.

I.5.3.2. Mechanical properties and deformation mechanisms

In general terms, the mechanical properties of cellular materials lower, when decreasing the relative density, by following the scaling law.

$$\frac{\text{Foam's property}}{\text{Solid's property}} = C \cdot \left(\frac{\rho_{\text{foam}}}{\rho_{\text{solid}}} \right)^n \quad (\text{I.1})$$

where C is a constant that mainly depends on the polymer matrix [102] and n is the density exponent related to the deformation mechanisms and the cellular structure characteristics. Although the mechanical properties of the foams largely depend on the foam's density, also the properties of the solid material from which the cell walls are made is important. In general terms, rigid polymer foams, such as those obtained in this thesis, are plastic in compression but brittle under tensile loads. The behaviour of foams under tensile and compression modes is briefly described as follows, according to Gibson and Ashby [102].

Behaviour under compression mode

Under uniaxial compression mode, cellular materials present three common regions which consists of a linear elastic region for low stress-deformation values, followed by a long collapse plateau, and a densification region, as shown in Figure I.28.

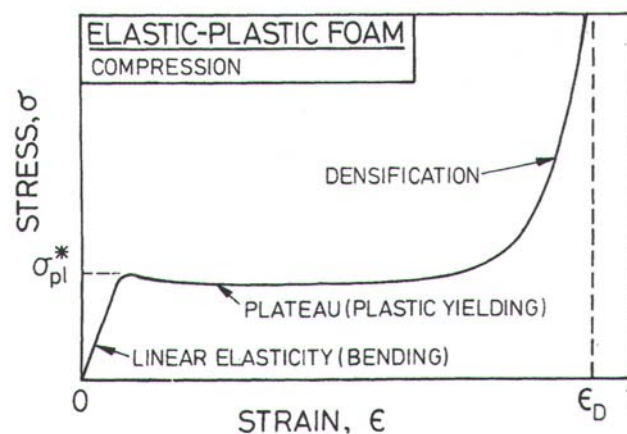


Figure I.28. Schematic compressive stress curves for an elastic-plastic foam, from [102].

In the linear elastic region, the deformation of the foam is almost completely recoverable—the linear elasticity is only truly found at low strains, since the axial load on cell edges leads to buckling at certain critical point—, controlled mainly by bending, and additionally by cell wall stretching for closed-cell foams. In this sense, the deformation mechanisms in compression are, for open-cell foams: bending, axial deformation and fluid flow between cells—forced by the deformation, what generates a force that has to be overcome—; and for closed-cell foams: bending, edge contraction and membrane stretching, and enclosed gas pressure—since the compression of the cellular structure leads to the compression of the gas retained in the cells, which tends to apply a restoring force—. However, in closed-cell foams, the mechanical behaviour is strongly related to the fraction of

mass in the struts, since very thin walls can present a performance equivalent to the one of an open cell.

The plateau region is associated with the collapse of the cells due to a progressive failure of the cellular structure under a more or less constant strength. This, for rigid polymeric foams, can be attributed to the formation of plastic hinges and to brittle crushing. Then, deformation reaches a region in which the cells are collapsed—the cell walls and edges touch—and further strain yields to the compression of the solid itself leading to the increase of the foam's density (densification region). Due to that, the stress shows an abrupt increase.

It is worthy to mention that, as pointed by the scaling-law (Equation (I.1)), density is the main factor in the mechanical properties of foams. Therefore, all this is connected to the relative density, since the higher the relative density, the higher the Young modulus, the higher the stress at which the plateau is observed and the lower the deformation at which the densification starts.

Behaviour under tensile mode

Under uniaxial tensile mode, plastic foams present a linear elasticity region—where the cell edges rotate towards the tensile axis by plastic bending—, up to a yield point followed by a rise on the stress until fracture. A schematic tensile stress-strain curve of such a material is presented in Figure I.29.

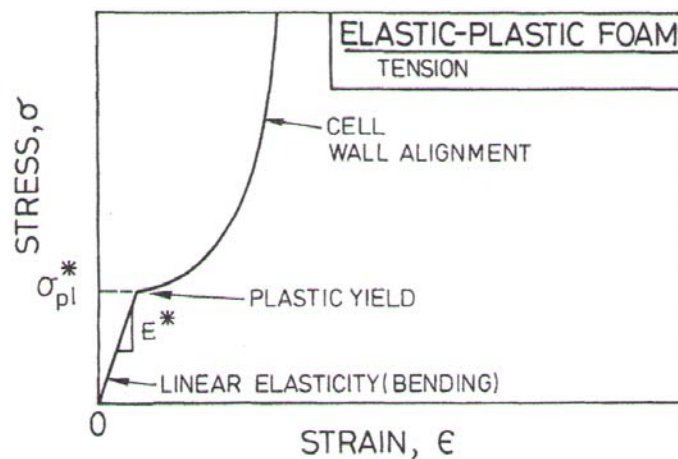


Figure I.29. Schematic tensile stress curves for an elastic-plastic foam, from [102].

Similarly as in compression mode, the initial linear elasticity in uniaxial tensile mode—at low strain values—is mainly caused by cell-wall bending plus cell-wall stretching for closed-

cell foams. The stiffness is determined by the cell-edge bending for open-cell foams, and by the edge bending, wall stretching and pressure of the enclosed gas for closed-cell foams [102]. Further strain in the elastic region leads to higher alignment (bending) of the cell-edges—rotating towards the axis direction—what produces an increase on stiffness and hence, a non-linear elastic behaviour. The plastic collapse in tension differs from the one in compression because after the alignment of the edges, further strain requires the plastic extension of the cell-walls or edges. Moreover, the brittle behaviour of rigid polymeric foams reveals a fast crack's propagation under tensile modes, producing catastrophic failures with low deformation—brittle fracture behaviour—. Therefore, the final fracture in tension is mainly produced by the propagation of a single crack.

1.6. Cellular composites

Cellular composites—abbreviated as CellFRC, as proposed by Sorrentino et al. [104]—are composite materials that have a cellular polymer as a matrix. CellFRCs present very good mechanical properties per unit mass, higher impact strength and toughness, and can imply costs reduction in the matrix polymer. The efficiency of reinforcing foams with fibres depends on the geometrical parameters of the fibres, the content, the orientation, the intrinsic properties and the fibre/matrix interaction [99]. Moreover, also the density of the foam plays a key role, since a general concern about the excessive size of the fibres compared to the cell walls is taken in the literature. Due to that, most studies focus in fibres of small length and diameter to be used as reinforcement.

Concerning to CellFRC with thermoplastic matrices that fall into the green composites category—this is a biopolymer reinforced with natural fibres—, the literature review revealed a predominance of disentangled short cellulosic fibres used in the reinforcement of starch, PLA and PHA matrices, mainly. Generally, the cellulosic fibres applied act as nucleating agents and increase the melt viscosity [99], thus affecting the processing conditions required. Often, certain limitation/inhibition of the expansion is observed due to its presence—depending on the fibre content—, although higher cell densities and smaller cells are obtained. In the literature, these CellFRC materials are produced by means of different foaming techniques and a variety of conditions, and in most cases the reinforcements are applied as loose fibres, thus presenting a lack of an effective network of fibres, although some examples using fibre structures as reinforcements can be found.

Cellular composites reinforced with loose fibres

In this sense, starch from several origins has been reinforced with cellulosic fibres (such as flax or hemp, among others) and foamed by baking techniques [105–108] or extrusion foaming [109,110]. PLA reinforced with cellulose fibres, ranging from the micro to the macroscale, have been foamed by extrusion and injection foaming [111–113]. Gas dissolution foaming has also been used for the production of PLA-based CellFRC in which the fibres are structured in pre-forms [99] or NW [114]. Regarding the PHA family, PHBV and its blends with other polymers, such as polybutyrate adipate terephthalate (PBAT), have been reinforced with cellulosic fibres and foamed by injection foaming [115,116] and gas dissolution foaming [117].

Soykeabkaew et al. studied in [106] starch-based composite foams produced by hot-mould baking. The reinforcements used were various contents—1 wt.%, 5 wt.% and 10 wt.%—of flax or jute fibres, which were cut to lengths ranging between 2 and 60 mm to achieve determined aspect ratios. A general increase in the flexural stiffness and strength was observed in the reinforced foams compared to the unreinforced ones, despite this was achieved in expense of the flexural strain. SEM images revealed good fibre/matrix interfacial interaction. The moisture content increased with the relative humidity set in the storage conditions due to the hydrophilic nature of starch, which was related to loss of stiffness flexural strength and stain due to a plasticization effect. However, optimal values of the mechanical properties—i.e. flexural strength and strain— were reported at moisture contents of 8-10%, attributed to a brittle-to-ductile transition of the starch-based matrix. The increase in fibre content and aspect ratio—larger surface area—lead to enhancement of the reinforcing effect of the fibres, as well as the orientation of the fibres. Jute fibres provided higher improvement than flax fibres because of their smaller diameter and density.

Javadi and co-workers presented two works of PHBV-based composite foams obtained by microcellular injection-moulding using supercritical N₂ as blowing agent. On the one hand, in [115] presented a study of the effect of different treatments— mercerization, silane treatment and a combination of both—applied to coir fibres in the properties of PHBV/coir microcellular composites. With the addition of 10 wt.% of fibres and the foaming process, weight reductions of around 9% where achieved. The fibre addition increased cell density and decreased cell size, explained by the nucleating effect of the fibres, what also enhanced the crystallinity of the fibre reinforced foams. Moreover, the fibre addition caused an improvement in the specific toughness of the foams, non-significant differences in stiffness, and a reduction of the specific strength—thus attributed to weak fibre/matrix adhesion—. The treatments enhanced the storage modulus of the composites measured by DMA, thus probably due to improved bonding. In this sense, silane treatment seemed to be the most effective in improving specific toughness. On the other hand, they studied in [116] the mechanical and thermal properties of PHBV/PBAT composites reinforced with recycled wood fibres (RWF) foamed by means of the previously mentioned microcellular injection technique, reaching density reductions of around 10%. The fibres were used untreated and with a silane coupling agent, although the results revealed that the treatment did not performed a significative improvement in the fibre/matrix adhesion. In general terms, the fibres acted as nucleating agents, inducing heterogeneous nucleation, high cell density and

small cell size in the microcellular composites. The addition of 10 wt.% of RWF increased the crystallinity, the specific stiffness and the specific tensile strength; and reduced the specific toughness and strain. They also reported an improvement of the thermal stability because of the addition of 2 wt.% of nanoclays, which did not played any other relevant role.

Kaisansgri et al. reported in [107] some properties of a biodegradable CellFRC made of cassava starch, chitosan and kraft fibres by means of a hot mould baking process. The main application suggested for this fibre-reinforced foam was production of packaging trays. They evaluated the influence of the blend in colorimetric properties, and the effect of interaction of kraft fibre and chitosan concentration in density, moisture content, mechanical properties and other water related parameters. The addition of kraft fibre content was found to yield higher density and tensile strength but slightly higher elongation; meanwhile the addition of chitosan decreased density, improved the mechanical properties and increased the foam hydrophilicity. The addition of 30% of kraft fibre and 4% of chitosan to the cassava starch improved the mechanical properties, reaching similar values than those of the typical polystyrene foams normally used in this application, although with higher water absorption and solubility.

Srithep et al., in [117], reported the production of PHBV/nanofibrillated cellulose (NFC) foams by CO₂ gas dissolution foaming, reaching the CO₂ saturation at room temperature and a pressure of 5.52 MPa. A fast drop pressure followed by a sudden temperature rise—in an oil-bath—was used to produce the thermodynamic instability required for the development of the cellular structure. In general terms, NFC addition increased the stiffness of the PHBV matrix, as observed by DMA and tensile testing. However, increasing contents of NFC led to a progressive reduction of the toughness. Moreover, NFC addition increased crystallinity and reduced the thermal stability. Regarding the behaviour against CO₂—of special interest for the foaming process—, the addition of the fibres decreased its absorption degree, thus attributed to the high crystallinity of the fibre added to the already high crystallinity of the PHBV, that acted as a CO₂ barrier. Moreover, the desorption diffusivity increased, probably due to a lower molecular weight—result of the degradation—and to the fibre/matrix interface acting as a fast-escape channel for the gas. Due to all that, they stated that the addition of NFC inhibited the foamability.

Recently, Zafar et al. [113] produced PLA foams reinforced with willow-fibres by means of supercritical-N₂-aided injection moulding. The willow fibre bundles presented a length of 0.5-2 mm. From the analysis of SEM images, an insufficient fibre/matrix bonding was

reached. Heterogeneous nucleation promoted by the fibre addition led to the increase in the cell density and the decrease in cell size. The resistance for the cell growth was attributed to the increase in melt viscosity and stiffness of the matrix. The addition of the willow fibres led to a general increase in the specific tensile and flexural stiffness, but to a reduction in the specific tensile and flexural strength because of a poor stress-transfer as a consequence of the poor fibre/matrix compatibility. The foamed samples presented lower specific properties than their solid counterparts, what was attributed to stress-concentration effect of the cells. Regarding the impact behaviour, the addition of the cellulosic fibre led to an increase in brittleness if compared to the unreinforced foam. However, in all cases the impact resistance of the foams was higher than for the respective solids, thus explained by the energy absorption and crack-propagation preventive role of the microcells. The thermal degradation was impoverished with the fibre addition and further reduced for the cellular composites. Besides this, the crystallisation rate and crystallinity were improved with the presence of the fibres.

Bocz et al. used in [111] a supercritical-CO₂ assisted extrusion foaming to produce PLA foams. They investigated the effects of addition of chain extender, talc additives and further addition of 5 wt.% of cellulosic fibres with a length of ~200 µm. The additives revealed to increase the melt viscosity, later even improved by the fibre addition. The crystallisation behaviour was also affected. The addition of the fibres promoted a heterogeneous nucleation and increased crystallinity—as was observed in most of the previously commented cases—, but also widened the processing window to obtain PLA foams. Smaller cells, non-uniform cell distribution and high open-cell ratio were achieved. The porosity was observed to increase with the reduction of the temperature at the die, and fibre reinforced foams of ~95% of porosity could be produced. However, the fibre addition caused a reduction of the compressive strength of the obtained foams—compared to those with additives but without fibres—, thus attributed to a weak fibre/matrix interaction.

Cellular composites reinforced with structures of fibres

According to the literature, only relatively short fibres—typically up to 20 mm—have been processed by extrusion or injection foaming, meanwhile longer fibres—typically up to 60 mm—have been processed in hot-mould baking, batch foaming or other discontinuous processes. All the previous cases used loose fibres for reinforcement. In this sense, both the length and the structure of the fibres are limiting factors for techniques such as extrusion

foaming and injection foaming due to the intrinsic limitations of the process itself. CellFRC reinforced with textile fabrics or structured fibres obtained by gas dissolution foaming techniques can overcome fibre length or fibre volume content limitations of the previous mentioned production techniques.

Mooney et al. reported in [114] the production of porous sponges by using a nonwoven structure of PGA (polyglycolic acid) fibres embedded in a PLGA (PLA-PGA copolymer) matrix in the form of a disc produced by compression moulding. Then, the disc was foamed by gas dissolution with CO₂ at 5.5 MPa and room temperature in a pressure vessel. A 72-h gas saturation step and further fast depressurisation (~15 s) were performed, what produced the thermodynamic instability that led to the development of the porosity. SEM imaging confirmed the presence of pores and fibres in the fracture surface. Nonetheless, the production of such a cellular composite was not the focus of their work and hence, the reinforced foam was not further characterised; although the authors pointed o better mechanical properties expected with such a processing method.

Qiu et al. successfully developed in [118] composites of cellular epoxy matrix and 3D woven carbon structure reinforcement by means of N₂ gas dissolution in pressure quenching moulding followed by temperature curing of the epoxy resin. The density reduction was of a significant 28-37% depending on the textile structure. The cellular composites showed improved specific tensile strength and modulus. Under bending conditions, the failure of the composites was observed to have a layer-to-layer fracture instead of the catastrophic fracture shown by the solid counterparts. Impact tests revealed better energy absorption at lower-speed impacts for the cellular composites than for the solid composites, and equal properties at higher-speed impacts, thus attributed to different fracture mechanisms.

Neagu et al. presented in [99] study regarding the potential of wood fibres of high aspect ratio in the reinforcement of PLA foams. They used 2-5 mm-long birch kraft pulp fibres—treated and untreated—to produce precursors of PLA and wood fibres by a wet route similar to the processes used in paper production. Then, they foamed the precursors—containing 1, 5 and 10 wt.%—by means of a gas-dissolution batch foaming using supercritical CO₂, at high pressure, relatively short saturation times (10 min) and high temperature (185 °C). The expansion was achieved by fast depressurisation and cooling. A decrease in the expansion ratio with the increase in the fibre content was observed. The fibres produced a change in the foam morphology, and the cellular structure showed to be inhomogeneous. Also the increase in fibre content led to a decrease in the cell size, attributed to the fibres acting as

nucleating sites; despite some large voids could also be observed. In this sense, they observed the importance of the compaction in the precursor fabrication, and specimens of 20 wt.% revealed insufficient matrix impregnation. They also reported a trend in the increase of the foam density with the increase in fibre content, thus pointing to its clear influence in the expansion ratios. Mechanically, the foams were anisotropic and presented a wide distribution in the results owing to their inhomogeneous microstructure. Foams with fibre content of the 5 wt.% or higher presented greater specific stiffness in the transverse direction compared to the unreinforced foams, but no mechanical improvement was observed in the foam rise direction. They stated that the wood fibres showed reinforcing potential in foams given that the fibres tend to organize in the foam structure providing support in the cell walls.

More recently, Sorrentino et al. used in [104] a solid state gas dissolution foaming technique to produce novel lightweight thermoplastic composites—named CellFRC—of PEN (polyethylene naphthalate) matrix and glass fibre fabric reinforcement, with addition of expandable graphite particles to act as nucleating agents. The control of the foaming process and the moulding conditions lead to reaching tuneable cell sizes. The presence of these particles enhanced the formation of very small cells of a diameter smaller in size than the glass fibres of the reinforcement. The foaming reduced the density of the composites around a 40% with respect to their solid counterparts. Despite the flexural modulus and strength were reduced in value, the density reduction led to excellent results of the specific mechanical properties for the CellFRC. Moreover, the impact testing revealed great dissipation of the impact energy, mainly due to compressive deformation of the cellular structure in the zone under the impact, and due to compression, tensile and shear deformation in the adjacent area. Therefore, they stated that the presence of small bubbles within the matrix can have the interesting effect of enhancing the specific properties and improving the impact resistance of the final CellFRC.

Thus, the interesting results and challenges detected in this literature review—covering the topic of cellular composites—encourage the research in such a sort of lightweight solutions exploring the use of textile structures of natural fibres.

References

- [1] Mohanty AK, Misra M, Drzal LT. *Natural Fibers, Biopolymers, and Biocomposites*. CRC Press; 2005. doi:10.1201/9780203508206.
- [2] Mokhothu TH, John MJ. Review on hygroscopic aging of cellulose fibres and their biocomposites. *Carbohydr Polym* 2015;131:337–54. doi:10.1016/j.carbpol.2015.06.027.
- [3] Pickering KL, Efendy MGA, Le TM. A review of recent developments in natural fibre composites and their mechanical performance. *Compos Part A Appl Sci Manuf* 2016;83:98–112. doi:10.1016/j.compositesa.2015.08.038.
- [4] Ahmad F, Choi HS, Park MK. A review: Natural fiber composites selection in view of mechanical, light weight, and economic properties. *Macromol Mater Eng* 2015;300:10–24. doi:10.1002/mame.201400089.
- [5] John M, Thomas S. Biofibres and biocomposites. *Carbohydr Polym* 2008;71:343–64. doi:10.1016/j.carbpol.2007.05.040.
- [6] Ardanuy M, Claramunt J, Toledo Filho RD. Cellulosic fiber reinforced cement-based composites: A review of recent research. *Constr Build Mater* 2015;79:115–28. doi:10.1016/j.conbuildmat.2015.01.035.
- [7] Dicker MPM, Duckworth PF, Baker AB, Francois G, Hazzard MK, Weaver PM. Green composites: A review of material attributes and complementary applications. *Compos Part A Appl Sci Manuf* 2014;56:280–9. doi:10.1016/j.compositesa.2013.10.014.
- [8] Chou W, Ko F. *Textile structural composites*. vol. 1. Elsevier S. New York: Elsevier Science & Technology Books; 1989.
- [9] Larrodé E. *Materiales Compuestos*. Barcelona: Reverte; 2003.
- [10] Russell SJ. *Handbook of Nonwovens*. Manchester: CRC Press, Woodhead Publishing; 2007.
- [11] Albrecht W, Fuchs F, Kittelmann W. *Nonwoven Fabrics*. Weinheim: Wiley-VCH; 2003.
- [12] Anandjiwala RD, Boguslavsky L. Development of Needle-punched Nonwoven Fabrics from Flax Fibers for Air Filtration Applications. *Text Res J* 2008;78:614–24.
- [13] Ghane M, Saghafi R, Zarrebini M, Semnani D. Evaluation of Bending Modulus of Needle-Punched Fabrics Using Two Simply Supported Beam Method. *Fibres Text East Eur* 2011;19:89–93.
- [14] Ventura H, Ardanuy M, Capdevila X, Cano F, Tornero JA. Effects of needling parameters on some structural and physico-mechanical properties of needle-punched nonwovens. *J Text Inst* 2014;1–11. doi:10.1080/00405000.2013.874628.
- [15] Biagiotti J, Puglia D, Kenny JM. A Review on Natural Fibre-Based Composites-Part I. *J Nat Fibers* 2004;1:37–68. doi:10.1300/J395v01n02_04.
- [16] Satyanarayana KG, Arizaga GGC, Wypych F. Biodegradable composites based on lignocellulosic fibers—An overview. *Prog Polym Sci* 2009;34:982–1021. doi:10.1016/j.progpolymsci.2008.12.002.
- [17] López-Manchado MA, Arroyo M. Fibras naturales como refuerzos de matrices poliméricas. *Rev plásticos Mod* 2003;594–600.
- [18] Wambua P, Ivens J, Verpoest I. Natural fibres: Can they replace glass in fibre reinforced plastics? *Compos Sci Technol* 2003;63:1259–64. doi:10.1016/S0266-3538(03)00096-4.
- [19] Biagiotti J, Puglia D, Kenny JM. A Review on Natural Fibre-Based Composites-Part I. *J Nat Fibers* 2004;1:37–68. doi:10.1300/J395v01n02_04.

- [20] Dittenber DB, GangaRao HVS. Critical review of recent publications on use of natural composites in infrastructure. *Compos Part A Appl Sci Manuf* 2012;43:1419–29. doi:10.1016/j.compositesa.2011.11.019.
- [21] Saheb DN, Jog JP. Natural fiber polymer composites: A review. *Adv Polym Technol* 1999;18:351–63. doi:10.1002/(SICI)1098-2329(199924)18:4<351::AID-ADV6>3.3.CO;2-O.
- [22] Bledzki A. Composites reinforced with cellulose based fibres. *Prog Polym Sci* 1999;24:221–74. doi:10.1016/S0079-6700(98)00018-5.
- [23] Lei Y, Wu Q, Yao F, Xu Y. Preparation and properties of recycled HDPE/natural fiber composites. *Compos Part A Appl Sci Manuf* 2007;38:1664–74. doi:10.1016/j.compositesa.2007.02.001.
- [24] George M, Chae M, Bressler DC. Composite materials with bast fibres: Structural, technical, and environmental properties. *Prog Mater Sci* 2016;83:1–23. doi:10.1016/j.pmatsci.2016.04.002.
- [25] Morshed MM, Alam MM, Daniels SM. Plasma Treatment of Natural Jute Fibre by RIE 80 plus Plasma Tool. *Plasma Sci Technol* 2010;12:325–9. doi:10.1088/1009-0630/12/3/16.
- [26] Azwa ZN, Yousif BF, Manalo AC, Karunasena W. A review on the degradability of polymeric composites based on natural fibres. *Mater Des* 2013;47:424–42. doi:10.1016/j.matdes.2012.11.025.
- [27] Beckermann GW, Pickering KL. Engineering and evaluation of hemp fibre reinforced polypropylene composites: Fibre treatment and matrix modification. *Compos Part A Appl Sci Manuf* 2008;39:979–88. doi:10.1016/j.compositesa.2008.03.010.
- [28] Ho M, Wang H, Lee J-H, Ho C, Lau K, Leng J, et al. Critical factors on manufacturing processes of natural fibre composites. *Compos Part B Eng* 2012;43:3549–62. doi:10.1016/j.compositesb.2011.10.001.
- [29] Pickering KL, editor. *Properties and Performance of Natural-Fibre Composites*. First. Cambridge: Woodhead Publishing Limited; 2008.
- [30] Faruk O, Bledzki A, Fink H, Sain M. Biocomposites reinforced with natural fibers: 2000–2010. *Prog Polym Sci* 2012;37:1552–96. doi:10.1016/j.progpolymsci.2012.04.003.
- [31] Fan M, Weclawski B. Long natural fibre composites. *Adv. High Strength Nat. Fibre Compos. Constr.*, Elsevier; 2017, p. 141–77. doi:10.1016/B978-0-08-100411-1.00006-6.
- [32] Charlet K, Baley C, Morvan C, Jernot JP, Gomina M, Bréard J. Characteristics of Hermès flax fibres as a function of their location in the stem and properties of the derived unidirectional composites. *Compos Part A Appl Sci Manuf* 2007;38:1912–21. doi:10.1016/j.compositesa.2007.03.006.
- [33] Yan L, Chouw N, Jayaraman K. Flax fibre and its composites – A review. *Compos Part B Eng* 2014;56:296–317. doi:10.1016/j.compositesb.2013.08.014.
- [34] Bos HL. *The potential of flax fibres as reinforcement for composite materials*. Eindhoven University of Technology, 2004.
- [35] Kozłowski RM, Mackiewicz-Talarczyk M, Allam AM. Bast fibres: flax. In: Kozłowski RM, editor. *Handb. Nat. Fibres, Vol. 1 Types, properties factors Affect. Breed. Cultiv.* 1st ed., Woodhead Publishing Limited; 2012, p. 56–113. doi:http://dx.doi.org/10.1533/9780857095503.1.56.
- [36] Nechwatal A, Mieck K-P, Reußmann T. Developments in the characterization of natural fibre properties and in the use of natural fibres for composites. *Compos Sci Technol* 2003;63:1273–9. doi:10.1016/S0266-3538(03)00098-8.
- [37] Summerscales J, Dissanayake N, Virk A, Hall W. A review of bast fibres and their

- composites. Part 2 – Composites. *Compos Part A Appl Sci Manuf* 2010;41:1336–44. doi:10.1016/j.compositesa.2010.05.020.
- [38] Rastogi V, Samyn P. Bio-Based Coatings for Paper Applications. *Coatings* 2015;5:887–930. doi:10.3390/coatings5040887.
- [39] Laycock B, Halley P, Pratt S, Werker A, Lant P. The chemomechanical properties of microbial polyhydroxyalkanoates. *Prog Polym Sci* 2014;39:397–442. doi:10.1016/j.progpolymsci.2013.06.008.
- [40] Shanks RA, Hodzic A, Wong S. Thermoplastic biopolyester natural fiber composites. *J Appl Polym Sci* 2004;91:2114–21. doi:10.1002/app.13289.
- [41] Reddy CSK, Ghai R, Rashmi, Kalia VC. Polyhydroxyalkanoates: An overview. *Bioresour Technol* 2003;87:137–46. doi:10.1016/S0960-8524(02)00212-2.
- [42] Chanprateep S. Current trends in biodegradable polyhydroxyalkanoates. *J Biosci Bioeng* 2010;110:621–32. doi:10.1016/j.jbiosc.2010.07.014.
- [43] Wang B, Sharma-Shivappa RR, Olson JW, Khan SA. Production of polyhydroxybutyrate (PHB) by *Alcaligenes latus* using sugarbeet juice. *Ind Crops Prod* 2013;43:802–11. doi:10.1016/j.indcrop.2012.08.011.
- [44] Martínez V, Herencias C, Jurkevitch E, Prieto MA. Engineering a predatory bacterium as a proficient killer agent for intracellular bio-products recovery: The case of the polyhydroxyalkanoates. *Sci Rep* 2016;6:24381. doi:10.1038/srep24381.
- [45] Keshavarz T, Roy I. Polyhydroxyalkanoates: bioplastics with a green agenda. *Curr Opin Microbiol* 2010;13:321–6. doi:10.1016/j.mib.2010.02.006.
- [46] Serafim LS, Lemos PC, Albuquerque MGE, Reis MAM. Strategies for PHA production by mixed cultures and renewable waste materials. *Appl Microbiol Biotechnol* 2008;81:615–28. doi:10.1007/s00253-008-1757-y.
- [47] Abdelwahab MA, Flynn A, Chiou B-S, Imam S, Orts W, Chiellini E. Thermal, mechanical and morphological characterization of plasticized PLA–PHB blends. *Polym Degrad Stab* 2012;97:1822–8. doi:10.1016/j.polymdegradstab.2012.05.036.
- [48] Poirier Y, Nawrath C, Somerville C. Production of Polyhydroxyalkanoates, a Family of Biodegradable Plastics and Elastomers, in Bacteria and Plants. *Nat Biotech* 1995;13:142–50.
- [49] Steinbüchel A, Lütke-Eversloh T. Metabolic engineering and pathway construction for biotechnological production of relevant polyhydroxyalkanoates in microorganisms. *Biochem Eng J* 2003;16:81–96. doi:10.1016/S1369-703X(03)00036-6.
- [50] Masani MYA, Parveez GKA, Izawati AMD, Lan CP, Siti Nor Akmar A. Construction of PHB and PHBV multiple-gene vectors driven by an oil palm leaf-specific promoter. *Plasmid* 2009;62:191–200. doi:10.1016/j.plasmid.2009.08.002.
- [51] Suriyamongkol P, Weselake R, Narine S, Moloney M, Shah S. Biotechnological approaches for the production of polyhydroxyalkanoates in microorganisms and plants - a review. *Biotechnol Adv* 2007;25:148–75. doi:10.1016/j.biotechadv.2006.11.007.
- [52] Tsuda H. Generation of poly- β -hydroxybutyrate from externally provided acetate in rice root. *Plant Physiol Biochem* 2012;50:35–43. doi:10.1016/j.plaphy.2011.09.019.
- [53] Wróbel M, Zebrowski J, Szopa J. Polyhydroxybutyrate synthesis in transgenic flax. *J Biotechnol* 2004;107:41–54. doi:10.1016/j.jbiotec.2003.10.005.
- [54] Gurunathan T, Mohanty S, Nayak SK. A review of the recent developments in biocomposites based on natural fibres and their application perspectives. *Compos Part A Appl Sci Manuf* 2015;77:1–25. doi:10.1016/j.compositesa.2015.06.007.

- [55] Chen G-Q. A microbial polyhydroxyalkanoates (PHA) based bio- and materials industry. *Chem Soc Rev* 2009;38:2434–46. doi:10.1039/b812677c.
- [56] Bugnicourt E, Cinelli P, Lazzeri A, Alvarez V. Polyhydroxyalkanoate (PHA): Review of synthesis, characteristics, processing and potential applications in packaging. *Express Polym Lett* 2014;8:791–808. doi:10.3144/expresspolymlett.2014.82.
- [57] Avérous L, Pollet E. Biodegradable Polymers. In: Avérous L, Pollet E, editors. *Environ. Silic. Nano-Biocomposites*, vol. 50, Springer London; 2012, p. 13–39. doi:10.1007/978-1-4471-4108-2_2.
- [58] Castilho LR, Mitchell DA, Freire DMG. Production of polyhydroxyalkanoates (PHAs) from waste materials and by-products by submerged and solid-state fermentation. *Bioresour Technol* 2009;100:5996–6009. doi:10.1016/j.biortech.2009.03.088.
- [59] Niaounakis M. *Biopolymers: Processing and Products*. Plastics D. William Andrew; 2014.
- [60] Mekonnen T, Mussone P, Khalil H, Bressler D. Progress in bio-based plastics and plasticizing modifications. *J Mater Chem A* 2013;1:13379. doi:10.1039/c3ta12555f.
- [61] Bledzki AK, Jaszkiwicz A. Mechanical performance of biocomposites based on PLA and PHBV reinforced with natural fibres – A comparative study to PP. *Compos Sci Technol* 2010;70:1687–96. doi:10.1016/j.compscitech.2010.06.005.
- [62] Sudesh K, Abe H, Doi Y. Synthesis, structure and properties of polyhydroxyalkanoates: biological polyesters. *Prog Polym Sci* 2000;25:1503–55. doi:10.1016/S0079-6700(00)00035-6.
- [63] Luo L, Wei X, Chen G-Q. Physical properties and biocompatibility of poly(3-hydroxybutyrate-co-3-hydroxyhexanoate) blended with poly(3-hydroxybutyrate-co-4-hydroxybutyrate). *J Biomater Sci Polym Ed* 2009;20:1537–53. doi:10.1163/092050609X12464345023041.
- [64] Wang S, Chen W, Xiang H, Yang J, Zhou Z, Zhu M. Modification and potential application of short-chain-length polyhydroxyalkanoate (SCL-PHA). *Polymers (Basel)* 2016;8. doi:10.3390/polym8080273.
- [65] Crétois R, Follain N, Dargent E, Soulestin J, Bourbigot S, Marais S, et al. Poly(3-hydroxybutyrate-co-4-hydroxybutyrate) based nanocomposites: influence of the microstructure on the barrier properties. *Phys Chem Chem Phys* 2015;17:11313–23. doi:10.1039/c4cp05524a.
- [66] Wang Y-W, Mo W, Yao H, Wu Q, Chen J, Chen G-Q. Biodegradation studies of poly(3-hydroxybutyrate-co-3-hydroxyhexanoate). *Polym Degrad Stab* 2004;85:815–21. doi:10.1016/j.polymdegradstab.2004.02.010.
- [67] Yamane H, Terao K, Hiki S, Kimura Y. Mechanical properties and higher order structure of bacterial homo poly (3-hydroxybutyrate) melt spun fibers. *Polymer (Guildf)* 2001;42:3241–8.
- [68] Ishii D, Ying TH, Yamaoka T, Iwata T. Characterization and Biocompatibility of Biopolyester Nanofibers. *Materials (Basel)* 2009;2:1520–46. doi:10.3390/ma2041520.
- [69] Sudesh K, Abe H. *Crystalline and Solid-State Structures of Polyhydroxyalkanoates (PHA)*. *Pract. Guid. to Microb. Polyhydroxyalkanoates*, Smithers Rapra Technology; 2010.
- [70] Gordeyev S, Nekrasov Y. Processing and mechanical properties of oriented poly (β -hydroxybutyrate) fibers. *J Mater Sci Lett* 1999;18:1691–2.
- [71] Pan P, Inoue Y. Polymorphism and isomorphism in biodegradable polyesters. *Prog Polym Sci* 2009;34:605–40. doi:10.1016/j.progpolymsci.2009.01.003.
- [72] Tsui A, Wright Z, Frank CW. Prediction of gas solubility in poly(3-hydroxybutyrate-co-3-hydroxyvalerate) melt to inform process design and resulting foam microstructure. *Polym Eng Sci* 2013;1–13. doi:10.1002/pen.23822.

- [73] Chodak I. Polyhydroxyalkanoates: Origin, Properties and Applications. In: Belgacem MN, Gandini A, editors. *Monomers, Polym. Compos. from Renew. Resour.*, Elsevier; 2008, p. 451–77. doi:10.1016/B978-0-08-045316-3.00022-3.
- [74] Schmack G, Jehnichen D, Vogel R, Tändler B. Biodegradable fibers of poly (3-hydroxybutyrate) produced by high-speed melt spinning and spin drawing. *J Polym Sci Part B Polym Phys* 2000;38:2841–50.
- [75] Fernandes EG, Pietrini M, Chiellini E. Bio-based polymeric composites comprising wood flour as filler. *Biomacromolecules* 2004;5:1200–5. doi:10.1021/bm034507o.
- [76] Li Y, Ma H, Shen Y, Li Q, Zheng Z. Effects of resin inside fiber lumen on the mechanical properties of sisal fiber reinforced composites. *Compos Sci Technol* 2015;108:32–40. doi:10.1016/j.compscitech.2015.01.003.
- [77] Madsen B, Lilholt H. Physical and mechanical properties of unidirectional plant fibre composites—an evaluation of the influence of porosity. *Compos Sci Technol* 2003;63:1265–72. doi:10.1016/S0266-3538(03)00097-6.
- [78] Madsen B, Thygesen A, Lilholt H. Plant fibre composites – porosity and volumetric interaction. *Compos Sci Technol* 2007;67:1584–600. doi:10.1016/j.compscitech.2006.07.009.
- [79] Madsen B, Thygesen A, Lilholt H. Plant fibre composites – porosity and stiffness. *Compos Sci Technol* 2009;69:1057–69. doi:10.1016/j.compscitech.2009.01.016.
- [80] Bagherpour S. *Fibre Reinforced Polyester Composites*. Polyester, InTech; 2012. doi:10.5772/48697.
- [81] Mohammed L, Ansari MNM, Pua G, Jawaid M, Islam MS. A Review on Natural Fiber Reinforced Polymer Composite and Its Applications. *Int J Polym Sci* 2015;2015. doi:10.1155/2015/243947.
- [82] Faruk O, Bledzki AK, Fink H-P, Sain M. Progress Report on Natural Fiber Reinforced Composites. *Macromol Mater Eng* 2014;299:9–26. doi:10.1002/mame.201300008.
- [83] Barkoula NM, Garkhaïl SK, Peijs T. Biodegradable composites based on flax/polyhydroxybutyrate and its copolymer with hydroxyvalerate. *Ind Crops Prod* 2010;31:34–42. doi:10.1016/j.indcrop.2009.08.005.
- [84] Kalia S, Thakur K, Celli A, Kiechel M a., Schauer CL. Surface modification of plant fibers using environment friendly methods for their application in polymer composites, textile industry and antimicrobial activities: A review. *J Environ Chem Eng* 2013;1:97–112. doi:10.1016/j.jece.2013.04.009.
- [85] Zille A, Oliveira FR, Souto AP. Plasma Treatment in Textile Industry. *Plasma Process Polym* 2014;n/a-n/a. doi:10.1002/ppap.201400052.
- [86] Shishoo R. *Plasma Technologies for Textiles*. Elsevier Science; 2007.
- [87] Jelil RA. A review of low-temperature plasma treatment of textile materials. vol. 50. Springer US; 2015. doi:10.1007/s10853-015-9152-4.
- [88] Yuan X, Jayaraman K, Bhattacharyya D. Effects of plasma treatment in enhancing the performance of woodfibre-polypropylene composites. *Compos Part A Appl Sci Manuf* 2004;35:1363–74. doi:10.1016/j.compositesa.2004.06.023.
- [89] Bozaci E, Sever K, Sarikanat M, Seki Y, Demir A, Ozdogan E, et al. Effects of the atmospheric plasma treatments on surface and mechanical properties of flax fiber and adhesion between fiber-matrix for composite materials. *Compos Part B Eng* 2013;45:565–72. doi:10.1016/j.compositesb.2012.09.042.
- [90] Claramunt J, Ardanuy M, García-Hortal JA. Effect of drying and rewetting cycles on the structure and physicochemical characteristics of softwood fibres for reinforcement of

- cementitious composites. *Carbohydr Polym* 2010;79:200–5. doi:10.1016/j.carbpol.2009.07.057.
- [91] Ardanuy M, Claramunt J, Ventura H, Manich AM. Effect of Water Treatment on the Fiber–Matrix Bonding and Durability of Cellulose Fiber Cement Composites. *J Biobased Mater Bioenergy* 2015;9:486–92. doi:10.1166/jbmb.2015.1545.
- [92] Claramunt J, Ardanuy M, García-Hortal JA, Filho RDT. The hornification of vegetable fibers to improve the durability of cement mortar composites. *Cem Concr Compos* 2011;33:586–95. doi:10.1016/j.cemconcomp.2011.03.003.
- [93] Solorzano E, Rodriguez-Perez MA. Cellular materials. In: Lehmann D, Busse M, Herrmann AS, Kayvantash K, editors. *Struct. Mater. Process. Transp.*, Weinheim, Germany: Wiley-VCH Verlag GmbH & Co. KGaA; 2013, p. 371–4. doi:10.1002/9783527649846.
- [94] Eaves D. *Handbook of Polymer Foams*. Rapra Technology Limited; 2004.
- [95] Laguna-Gutiérrez E. *Understanding the foamability of complex polymeric systems by using extensional rheology*. Universidad de Valladolid, 2016.
- [96] Takahashi S, Hassler JC, Kiran E. Melting behavior of biodegradable polyesters in carbon dioxide at high pressures. *J Supercrit Fluids* 2012;72:278–87. doi:10.1016/j.supflu.2012.09.009.
- [97] Villalobos M, Awojulu a., Greeley T, Turco G, Deeter G. Oligomeric chain extenders for economic reprocessing and recycling of condensation plastics. *Energy* 2006;31:3227–34. doi:10.1016/j.energy.2006.03.026.
- [98] Ludwiczak J, Kozłowski M. Foaming of Polylactide in the Presence of Chain Extender. *J Polym Environ* 2015;23:137–42. doi:10.1007/s10924-014-0658-7.
- [99] Neagu RC, Cuenoud M, Berthold F, Bourban P-E, Gamstedt EK, Lindstrom M, et al. The potential of wood fibers as reinforcement in cellular biopolymers. *J Cell Plast* 2012;48:71–103. doi:10.1177/0021955X11431172.
- [100] Jeon B, Kim HK, Cha SW, Lee SJ, Han M-S, Lee KS. Microcellular foam processing of biodegradable polymers — review. *Int J Precis Eng Manuf* 2013;14:679–90. doi:10.1007/s12541-013-0092-0.
- [101] Jacobs LJM, Kemmere MF, Keurentjes JTF. Sustainable polymer foaming using high pressure carbon dioxide: a review on fundamentals, processes and applications. *Green Chem* 2008;10:731–8. doi:10.1039/B801895B.
- [102] Gibson LJ, Ashby MF. *Cellular Solids: Structure and properties*. 2nd ed. Cambridge: Cambridge University Press; 1999.
- [103] Campo-Arnáiz RA, Rodríguez-Pérez MA, Calvo B, De Saja JA. Extinction coefficient of polyolefin foams. *J Polym Sci Part B Polym Phys* 2005;43:1608–17. doi:10.1002/polb.20435.
- [104] Sorrentino L, Cafiero L, D’Auria M, Iannace S. Cellular thermoplastic fibre reinforced composite (CellFRC): A new class of lightweight material with high impact properties. *Compos Part A Appl Sci Manuf* 2014;64:223–7. doi:10.1016/j.compositesa.2014.05.016.
- [105] Lawton J., Shogren R., Tiefenbacher K. Aspen fiber addition improves the mechanical properties of baked cornstarch foams. *Ind Crops Prod* 2004;19:41–8. doi:10.1016/S0926-6690(03)00079-7.
- [106] Soykeabkaew N, Supaphol P, Rujiravanit R. Preparation and characterization of jute- and flax-reinforced starch-based composite foams. *Carbohydr Polym* 2004;58:53–63. doi:10.1016/j.carbpol.2004.06.037.
- [107] Kaisangsri N, Kerchoechuen O, Laohakunjit N. Biodegradable foam tray from cassava starch blended with natural fiber and chitosan. *Ind Crops Prod* 2012;37:542–6.

- doi:10.1016/j.indcrop.2011.07.034.
- [108] Lopez-Gil A, Silva-Bellucci F, Velasco D, Ardanuy M, Rodriguez-Perez MA. Cellular structure and mechanical properties of starch-based foamed blocks reinforced with natural fibers and produced by microwave heating. *Ind Crops Prod* 2015;66:194–205. doi:10.1016/j.indcrop.2014.12.025.
- [109] Bénézet J-C, Stanojlovic-Davidovic A, Bergeret A, Ferry L, Crespy A. Mechanical and physical properties of expanded starch, reinforced by natural fibres. *Ind Crops Prod* 2012;37:435–40. doi:10.1016/j.indcrop.2011.07.001.
- [110] Guan J, Hanna MA. Functional properties of extruded foam composites of starch acetate and corn cob fiber. *Ind Crops Prod* 2004;19:255–69. doi:10.1016/j.indcrop.2003.10.007.
- [111] Bocz K, Tábi T, Vadas D, Sauceau M, Fages J, Marosi G. Characterisation of natural fibre reinforced PLA foams prepared by supercritical CO₂ assisted extrusion. *Express Polym Lett* 2016;10:771–9. doi:10.3144/expresspolymlett.2016.71.
- [112] Boissard CIR, Bourban P-E, Tingaut P, Zimmermann T, Manson J -a. E. Water of functionalized microfibrillated cellulose as foaming agent for the elaboration of poly(lactic acid) biocomposites. *J Reinf Plast Compos* 2011;30:709–19. doi:10.1177/0731684411407233.
- [113] Zafar MT, Zarrinbakhsh N, Mohanty AK, Misra M, Ghosh AK. Biocomposites based on poly(Lactic acid)/willow-fiber and their injection moulded microcellular foams. *Express Polym Lett* 2016;10:176–86. doi:10.3144/expresspolymlett.2016.16.
- [114] Mooney DJ, Baldwin DF, Suh NP, Vacanti JP, Langer R. Novel approach to fabricate porous sponges of poly(D,L-lactic-co-glycolic acid) without the use of organic solvents. *Biomaterials* 1996;17:1417–22.
- [115] Javadi A, Srithep Y, Pilla S, Lee J, Gong S, Turng L-S. Processing and characterization of solid and microcellular PHBV/coir fiber composites. *Mater Sci Eng C* 2010;30:749–57. doi:10.1016/j.msec.2010.03.008.
- [116] Javadi A, Srithep Y, Lee J, Pilla S, Clemons C, Gong S, et al. Processing and characterization of solid and microcellular PHBV/PBAT blend and its RWF/nanoclay composites. *Compos Part A Appl Sci Manuf* 2010;41:982–90. doi:10.1016/j.compositesa.2010.04.002.
- [117] Srithep Y, Ellingham T, Peng J, Sabo R, Clemons C, Turng L-S, et al. Melt compounding of poly (3-hydroxybutyrate-co-3-hydroxyvalerate)/nanofibrillated cellulose nanocomposites. *Polym Degrad Stab* 2013;98:1439–49. doi:10.1016/j.polymdegradstab.2013.05.006.
- [118] Qiu Y, Xu W, Wang Y, Zikry MA, Mohamed MH. Fabrication and characterization of three-dimensional cellular-matrix composites reinforced with woven carbon fabric. *Compos Sci Technol* 2001;61:2425–35. doi:10.1016/S0266-3538(01)00164-6.

CHAPTER II

MATERIALS AND METHODS

CHAPTER CONTENTS

II.1.	Materials	123
II.1.1.	Flax	123
II.1.2.	PHA matrix	124
II.1.3.	Blowing agents	124
II.1.4.	Chain extender	125
II.1.5.	Products for flax treatment	125
II.2.	Production techniques	126
II.2.1.	Nonwoven production	126
II.2.2.	Surface treatments	127
II.2.2.1.	Wet/dry cycling	127
II.2.2.2.	Plasma treatments	128
II.2.3.	Melt compounding	130
II.2.4.	Composite production	131
II.2.5.	Foaming techniques	133
II.2.5.1.	Extrusion foaming	133
II.2.5.2.	Pressure quench batch foaming	134
	Summary of the production techniques	135
II.3.	Characterisation methods	137
II.3.1.	Composition and microstructural characterisation	137
II.3.1.1.	Fibre content determination	137
II.3.1.2.	Density and open cell content	137
II.3.1.3.	SEM	138
II.3.2.	Mechanical characterisation techniques	139
II.3.2.1.	Tensile testing	139
II.3.2.2.	Macro-mechanical modelling methods	140
II.3.2.3.	Compression testing	144
II.3.2.4.	DMA	144
II.3.2.5.	Charpy impact tests	146
II.3.3.	Thermal characterisation techniques	146
II.3.3.1.	DSC	146
II.3.3.2.	TGA	147
II.3.4.	Techniques related with water absorption properties	147


II.3.4.1.	Moisture content.....	147
II.3.4.2.	Water retention.....	147
II.3.4.3.	Contact angle.....	148
II.3.4.4.	Hydrothermal testing.....	148
II.3.4.5.	Kinetics of the water absorption	149
II.3.5.	Other techniques	149
II.3.5.1.	DRX.....	149
II.3.5.2.	Rheometry.....	150
II.3.5.3.	XPS	150
	Summary of the characterisation methods	150
	References	152

II.1. Materials

II.1.1. Flax

The flax fibres used in this thesis were medium quality fibres—non-refined and tangled—provided by Fibres Recherche Développement in Technopole de l'Aube in Champagne (France). The main physical-chemical properties of these flax fibres are presented in Table II.1.

Table II.1. Properties of the flax fibres

Length ^a	≤ 6 cm	
Diameter ^b	98 ± 26 μm	
Density (ρ_f) ^a	1.46 g/cm ³	
Stiffness (E) ^b	30.4 GPa	
Strength (σ_{max}) ^b	730 MPa	
Chemical composition ^a :		
Cellulose content	$77.1 \pm 0.0\%$	
Hemicelluloses content	$6.7 \pm 0.2\%$	
Lignin content	$2.6 \pm 0.2\%$	
Content of gums, fatty acids, waxes and others	$13.1 \pm 0.3\%$	
Minerals content	$0.5 \pm 0.0\%$	
Residual shive content	$15.8 \pm 2.3\%$	

Flax fibres, as received.

^a Data provided by the supplier

^b Data obtained by fibre characterisation

The diameter, stiffness and strength values were determined as the average properties of 50 fibres. Each fibre—identified with a reference—was glued to a paper structure as shown in Figure II.1. The observations were performed by means of a Jenaval optical microscope (Carl Zeiss JENA, Deutschland) equipped with an Invenio 3D digital camera (Deltapix, Denmark). The diameter was measured in 3 points using the Dpx View Pro software (Deltapix, Denmark). Then, each fibre was tested in a MTS dynamometer (MTS systems, USA) equipped with pneumatic clamps and a loading cell of 10 N, at a speed of 2 mm/min

with a clamp distance of 20 mm. For the determination of stiffness and maximum strength of each fibre, the area used was calculated—assuming a circular section—using the smallest diameter measured, since the weakest section was considered as the responsible of the fibre failure.

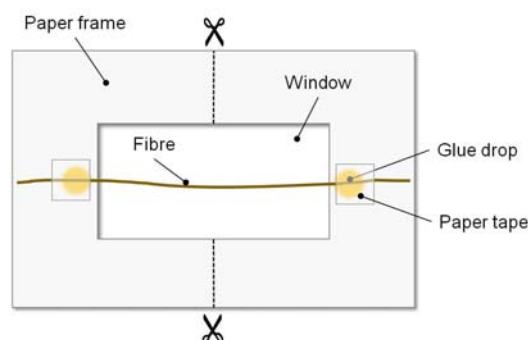


Figure II.1. Scheme of fibre preparation for its characterisation. The paper frame is cut after the sample is clamped in the dynamometer.

II.1.2. PHA matrix

The PHA used in this thesis was the thermoforming grade Mirel P3001, a poly(3-hydroxybutyrate-co-4-hydroxybutyrate)—P3HB4HB—proprietary copolymer formulation, provided in pellets-form by Metabolix Inc. (USA). It will be referred to as PHB hereafter. The most relevant properties are: biodegradability—as certified by the manufacturer—; density of 1.29 g/cm^3 —according to the manufacturer—; melting point around $169 \text{ }^\circ\text{C}$ —determined by DSC—. The mechanical properties were evaluated in tensile testing performed in a 5.500R6025 universal testing machine (Instron, UK), according to the ISO527 1A standard, revealing a maximum strength of 24 MPa and a Young modulus of 1.6 GPa.

II.1.3. Blowing agents

Both chemical and physical blowing agents (CBA and PBA, respectively) were used to produce the foaming of the biopolymer.

Chemical blowing agent used in extrusion foaming

Hydrocerol BIH 40 from Clariant GmbH (Germany) was used as blowing agent in the extrusion foaming. This endothermic CBA masterbatch is presented in pellet form, and has a main decomposition temperature between $135 \text{ }^\circ\text{C}$ and $170 \text{ }^\circ\text{C}$ —according to DSC

characterisation—, mainly attributed to the formation of CO₂ gas although some water can also be produced in the process. This range of decomposition temperatures is compatible with the processing conditions required for the resins used.

Physical blowing agent used in batch foaming

CO₂ gas of 99.99% purity, provided by Rivoira SpA (Italy), was used for the gas dissolution batch foaming technique. Carbon dioxide presents good gas solubility in polymers—also in PHAs [1]—. In the experimental section, the CO₂ gas was used both in subcritical and supercritical state (scCO₂). Supercritical state in CO₂ is achieved when the temperature is higher than 31.1 °C and the pressure higher than 7.39 MPa, and its use in gas dissolution foaming is of interest due to expected effects of melting temperature depression and plasticization. In fact, solubility of scCO₂ in PHAs has been observed to rapidly dissolve with the increase in pressure, and to decrease the melting temperature—at a rate around 1.3 °C/MPa—up to 24 MPa [2].

II.1.4. Chain extender

An epoxy functional oligomeric acrylic additive [3], Joncryl ADR-4368 chain extender (CE) from BASF (Germany), is used in solid flake form with a dosage of 1 wt.%. According to the literature, this CE has been successfully used in PLA foaming [4] and to enhance the thermal and rheological properties of PHBV [5].

II.1.5. Products for flax treatment

Distilled water was used to perform the wet-dry cycling treatment.

Argon gas of 99.999% purity, provided by Air Liquide España (Spain), was used for plasma treatment of the flax fibres, to produce surface etching and surface activation [6].

Ethylene gas of 99.99% purity, provided by Air Liquide España (Spain), was used in order to obtain a plasma-polymerised ethylene layer onto the NW fabrics [7].

II.2. Production techniques

The samples production required several techniques which are described in this section. A small basis about each production technique is given to the reader in order to ensure a proper comprehension of the thesis.

Briefly, the nonwoven (NW) samples used in Chapter III were produced by means of needle-punching and then treated for their study. Chapter IV deals with the foamability of the neat matrix, where the extrusion foaming was used to produce the samples. Regarding Chapter V, solid composite materials were produced by film-stacking with the reinforcements obtained in Chapter III. Finally, in Chapter VI, the previous solid composites were foamed by means of gas foaming dissolution.

II.2.1. Nonwoven production

Flax nonwoven fabrics were prepared on a laboratory double needle-punching machine OUG-II-6 (Dilo, Germany), equipped with universal card clothing, cross-lapper and needle-punching loom (Figure II.2), in the Weaving Laboratory of the Textile Division of the Department de Ciència dels Materials i Enginyeria Metal·lúrgica-CMEM (UPC, Terrassa-Barcelona, Spain).

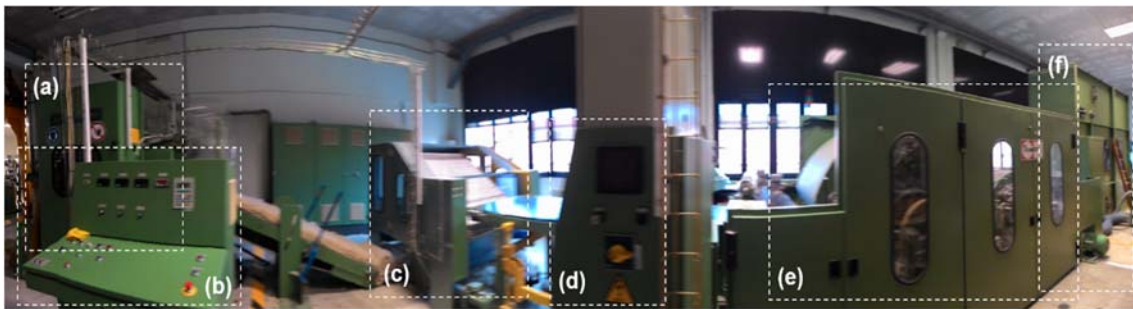


Figure II.2. Image of the needle-punching machine showing the processing units. Fibre tufts are fed in the opener (f), disaggregated and parallelised in the carding system (e) and cross-lapped to form a batt in (c). These units are controlled by (d). The batt is finally consolidated in the needle-loom (a), controlled by (b).

Preliminary [12] and parallel [13] studies helped to determine the optimal processing conditions to produce NW structures with a compromise between mechanical properties—for composite reinforcement—and permeability—to ensure the matrix penetration into the structure—. Therefore, an optimized NW structure of $284 \pm 23 \text{ g/m}^2$ and thickness of $1.9 \pm 0.1 \text{ mm}$ was prepared with the conditions presented in Table II.2.

Table II.2. Needling conditions

Feeding speed	2.30 m/min
Delivery speed	3.15 m/min
Stroke frequency	1200 strokes/min
Needling depth	8 mm
Bed-gap	12 mm

II.2.2. Surface treatments

II.2.2.1. Wet/dry cycling

In previous studies of the research group the wet/dry cycling—also known as hornification—has been shown to: clean the fibre surface, reduce the water retention values, enhance the thermal properties and produce some fibre shrinkage in cellulosic fibres, thus leading to improvement of their dimensional stability [14,15]. Therefore, with the aim of stabilising the flax fibres—i.e. avoiding dimensional changes produced because of moisture/water absorption, this treatment was used in the reinforcement NW structures. This treatment was performed in the Fibres and Polymers Laboratory at the Textile Division of the CMEM (UPC, Terrassa-Barcelona, Spain).

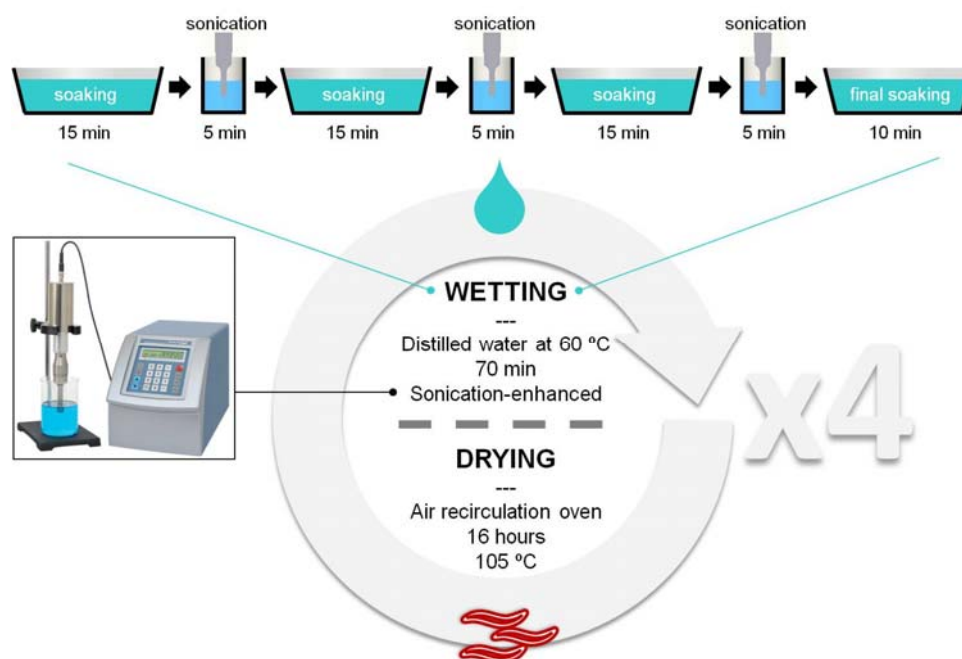


Figure II.3. Scheme of the wet/dry treatment, with detailed wetting cycle.

The treatment consisted of a wetting of the NW sample in water followed by drying, thus repeated 4 times (Figure II.3). The wetting step was performed using distilled water at 60 °C. In this step, intervals of 15 min of soaking were intercalated with intervals of 5 min of sonication-enhanced wetting, thus with a total duration of 70 min. A FB-705 high power ultrasonic probe (Fischer Scientific, USA), was used to that purpose. After each wetting cycle, the NW was dried in a UNB 400 oven (Memmet, Germany) at 105 °C for 16 h.

II.2.2.2. Plasma treatments

In general terms, plasma techniques are divided into two groups: low pressure plasma and atmospheric plasma technologies. For the NW treatment, both types of plasma techniques were used: low pressure plasma (Figure II.4) and a Corona plasma (Figure II.8), which falls in the atmospheric plasma classification.

On the one hand, low pressure plasma was used to treat the NW following two main paths: increase of hydrophobicity—by means of ethylene plasma—, and hydrophilicity increase—using argon plasma—. Treatments were performed in a Junior Advanced PLC radiofrequency plasma reactor (Europlasma, Belgium), operating at 13.56 MHz. To that purpose, the NW specimen was introduced in the reactor chamber, and a vacuum pump was used to reduce the pressure of the reactor up to 50 mtorr ($6 \cdot 10^{-3}$ MPa). Then, the gas was introduced at constant flow rate. Once the stabilisation of the reactor pressure was achieved—at ~ 150 mtorr ($2 \cdot 10^{-2}$ MPa)—, the plasma was initiated. The NW specimen was exposed for the desired time to the action of plasma. Several conditions of exposure time, gas used and combination treatments are evaluated in Chapter III.

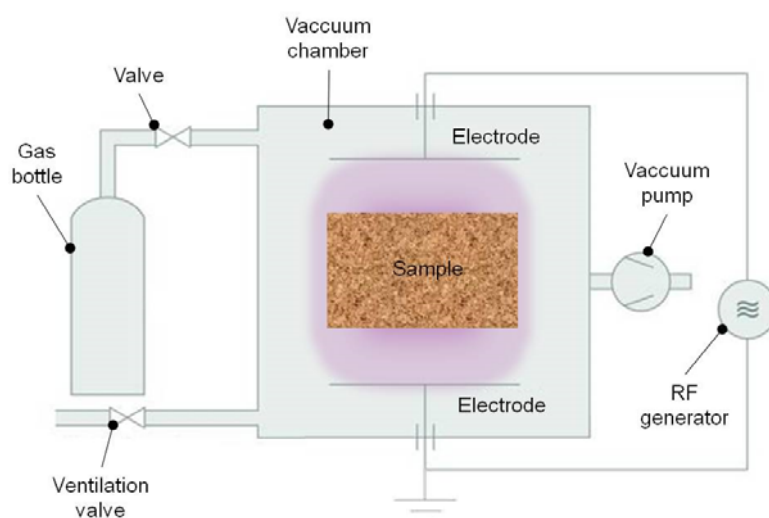


Figure II.4. General scheme of the low pressure plasma device.

The aim of the treatment with ethylene gas was to produce the plasma-polymerization on the target surface. Plasma-polymerized ethylene films are said to present basically a random structure with short chains, some degree of cross-linking and even free radicals (Figure II.5), thus differing from the conventional concept of linear and structured ethylene. However, despite the irregular structure of these films, the flax NW is expected to show an increased hydrophobicity [16].

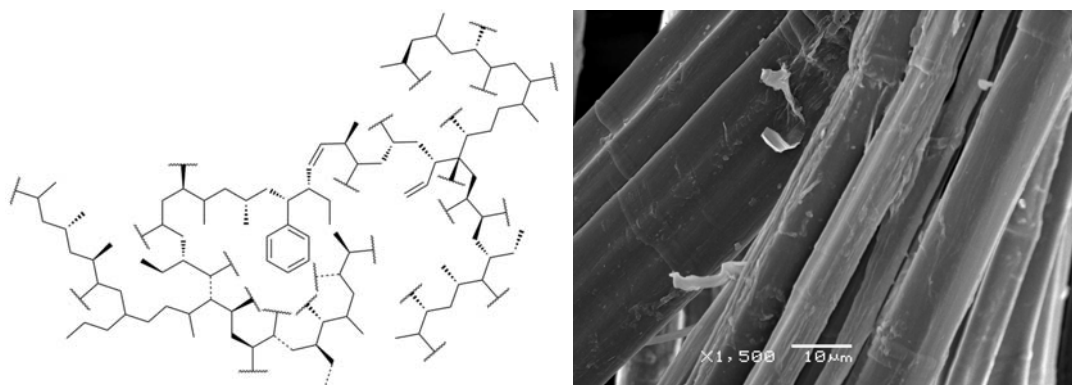


Figure II.5. Hypothesized model of plasma-polymerized ethylene film (right), and SEM image of the flax fibres after plasma polymerisation, showing flake-like structures attributed to ethylene film formation (left).

Regarding the argon-plasma, it is worth mentioning that it can induce molecular fragmentation in cellulose—by cleavage of the pyranosidic ring (Figure II.6)—what leads to the creation of activated sites capable to react with other molecules. Due to that, after the argon plasma, two effects were expected:

- ex-situ post plasma oxidation [6] leading to an increase of the hydrophilic groups (Figure II.7)
- better adhesion of the plasma-polymerised coating—when applied before the ethylene plasma—due to the reaction of the active sites with the ethylene gas molecules.

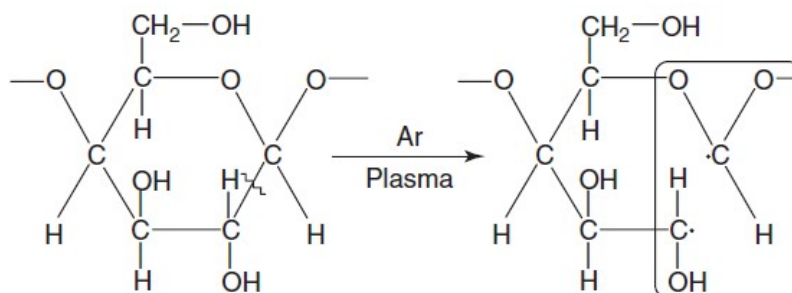


Figure II.6. Plasma-induced fragmentation of the cellulose, from [17].

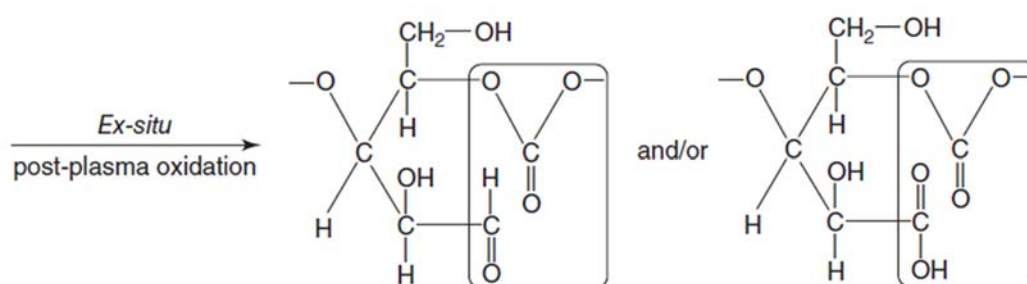


Figure II.7. Ex-situ post-plasma oxidation reactions proposed by Hua et al. [6], from [17].

On the other hand, the Corona plasma treatments (Cr) were carried out by means of an FG-2 Corona plasma (Ahlbrandt, Germany) using air as a plasma gas (Figure II.8). In this case, the NW samples were attached to a rotating cylinder, and exposed to the action of the air plasma. The distance between the electrode and the fabric could be adjusted—10 mm in this case—and power, speed and incident current were kept constant during the treatment. Various exposure times and conditions are also evaluated in Chapter III.

Considering the oxygen present in air, the Corona treatment is expected to generate an increase of hydrophilic groups in the fibre surface due to oxidation reactions.

The plasma treatments were performed in the Ecofinishing laboratory at the Textile Division of the CMEM (UPC, Terrassa-Barcelona, Spain).

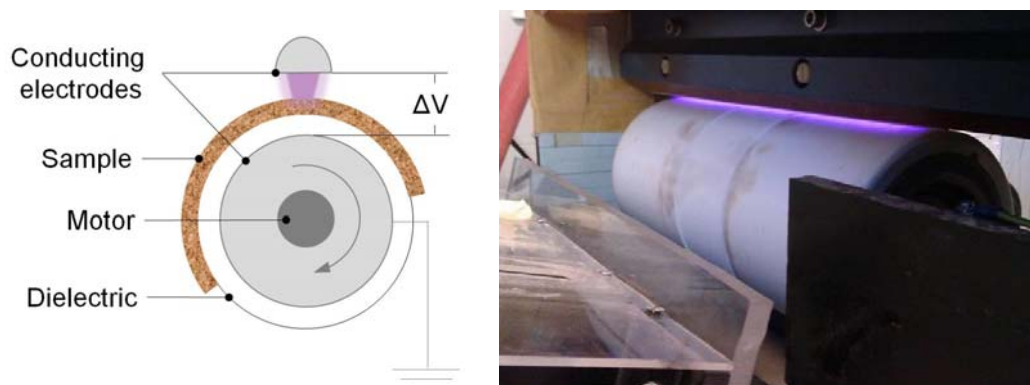


Figure II.8. Corona plasma scheme (left) and equipment (right).

II.2.3. Melt compounding

The addition of the chain extender to the matrix was performed by melt compounding, in a Teach-line ZK 25 T co-rotating twin-screw extruder (Collin, Germany) given that it provides higher mixing capability. The melt compounding was produced in the CellMat Laboratory of the FMC (UVa, Valladolid, Spain).

The PHB was previously dried in vacuum drying oven VacioTem TV (JP-Selecta, Spain), at 50 °C for 12 h under vacuum to eliminate the moisture content, since PHAs are sensible to hydrolytic degradation—specially at high temperatures—. To ensure the homogeneity of the result, mixtures of 1 wt.% of CE additive and 99 wt.% of matrix pellets are prepared in small portions of 100 g—stored in a desiccator—, and progressively feed in the extruder (Figure II.9).

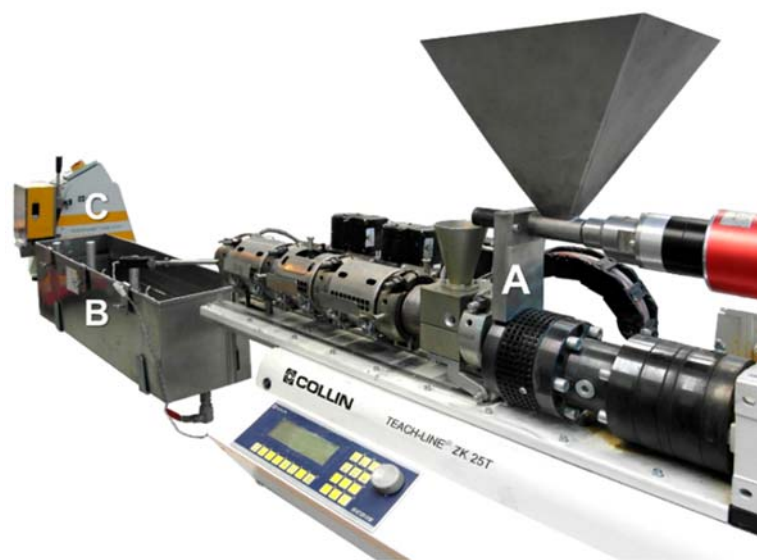


Figure II.9. Melt compounding line, formed by the extruder (A), the water bath cooling (B) and the pelletiser unit (C).

The temperature profile used is a reverse temperature profile according to the manufacturer specifications, in which the temperature is regulated in five points of the process, starting at 170 °C in the zone near the feeder, 165 °C, 160 °C, 155 °C and 150 °C at the exit of the die. The screw speed is kept at 70 rpm, and the dosage speed at 80% of the former. At the exit of the dye, a water bath is placed to produce the cooling of the extrudate before entering into the pelletizer to obtain the modified-matrix pellets.

II.2.4. Composite production

The film-staking method was used to produce composite materials. This is a well-known, simple and effective technique method to obtain sandwich structures, in which a sandwich of matrix-films and NW reinforcements is hot-pressed to achieve a laminar material.

The composite samples used in Chapter IV were prepared in a Remtex hot-plate press (Remtex, Spain) in the CellMat Laboratory (UVa, Valladolid, Spain), meanwhile the

composite samples used in Chapter VI were prepared in the P 300P hot plate press (Collin, Germany) in the Istituto per i Polimeri, Compositi e Biomateriali-IPCB of the Italian National Research Council (CNR, Portici-Naples, Italy).

The film production is schematised in Figure II.10. The pellets were placed inside a mould, heated at 175 °C for 5 min to ensure an appropriate melt state, hot pressed under 50 MPa for 5 minutes with the aim of avoiding the formation of bubbles of air trapped, and then cooled down under 50 MPa at 40 °C for 5 minutes.

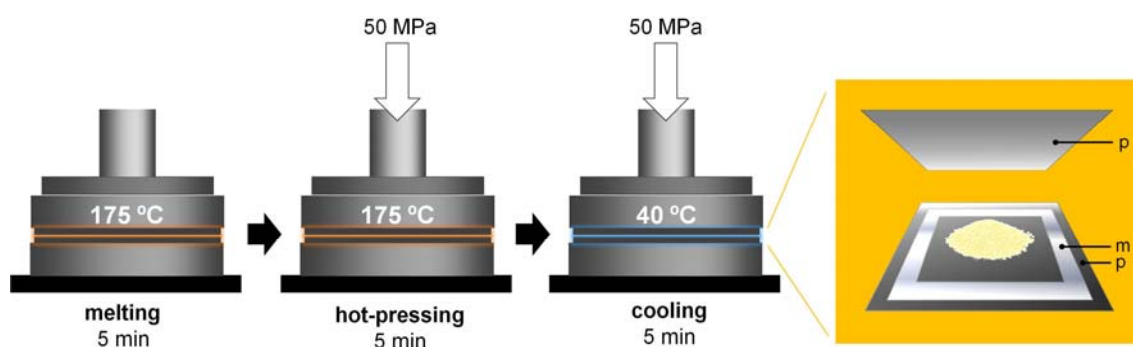


Figure II.10. Scheme of the film production with conditions. In the image on the right, p refers to a steel plate and m to the aluminium mould.

For the composite production (Figure II.11), the NW was placed between two pieces of the previously-produced films inside a mould, heated for 6 min—to ensure an appropriate melt state—, hot pressed under 50 MPa for 4 minutes more—to obtain a good fibre impregnation and low porosity—, and then cooled down up to low temperatures (≤ 40 °C) under 50 MPa—to avoid deformation of the composite sheet—. The use of a 1 mm-thick mould led to the obtaining of composite sheets of equal thickness with an average fibre content around 20 wt.%.

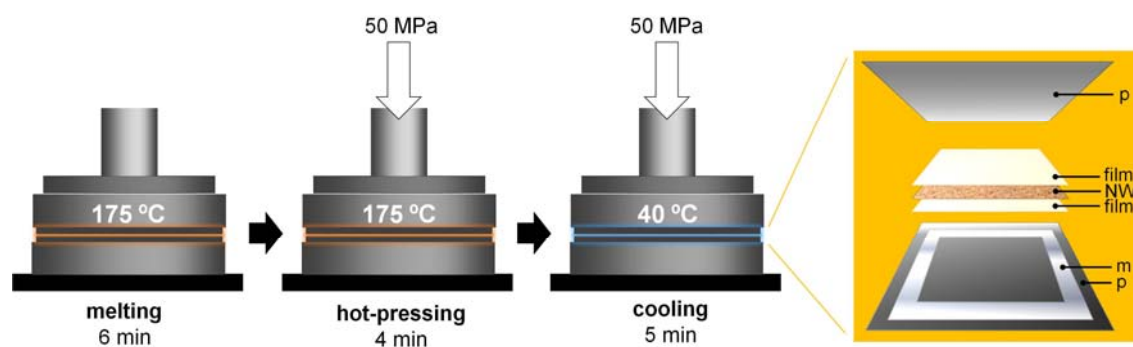


Figure II.11. Scheme of the film-stacking configuration and conditions for composite production. In the image on the right, p refers to a steel plate and m to the aluminium mould.

II.2.5. Foaming techniques

From all the available foaming techniques for thermoplastic materials, two were used to produce cellular materials in this thesis. On the one hand, the foamability of the matrix was evaluated by extrusion foaming in Chapter V. On the other hand, the gas dissolution technique in batch foaming—using a pressure-quench method—was used to foam the composites, since the morphology of the reinforcement—i.e. textile structure—limited the potential processing technologies. In Chapter VI, the pressure quench method was optimised to that purpose.

II.2.5.1. Extrusion foaming

Extrusion foaming is a continuous production technique habitually used in both research and industry owing to the extended knowledge of the method and relative simplicity. In general terms, extrusion foaming consists in the dissolution of gas into a polymer, which has been previously brought to a highly viscous or melt state with the help of temperature and shear action of the extruder. The sudden drop of pressure that is reached when the polymer exits through the die causes the instability of the gas dissolved, what undergoes into nucleation of gas bubbles and further growth (Figure II.12).

PHB foams were produced by extrusion foaming—in the aforementioned Teach-line ZK 25 T co-rotating twin-screw extruder (Collin, Germany)—using an endothermic chemical blowing agent, air cooling or water quenching systems—for cooling of the samples—, and chain extender use, with the aim to evaluate the viability of the biopolymer to achieve further cellular structures in composites. This study was accomplished in the CellMat Laboratory (UVa, Valladolid, Spain).

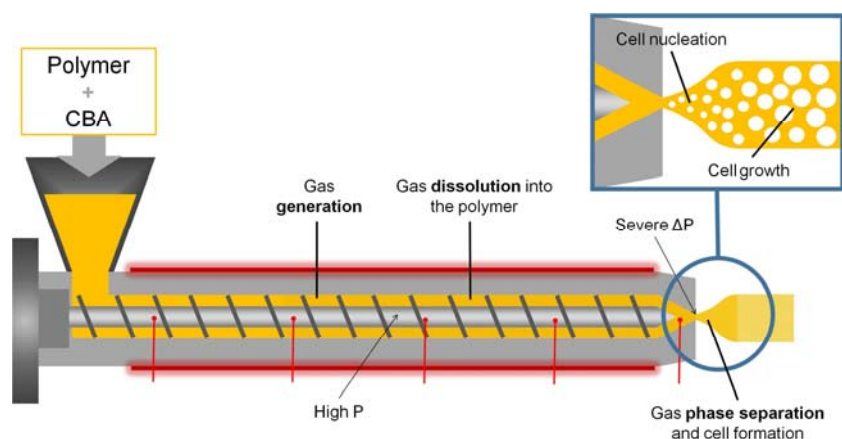


Figure II.12. Principle of extrusion foaming.

The PHB and the CBA were previously dried in vacuum drying oven VacioTem TV (JP-Selecta, Spain), at 50 °C for 12 h under vacuum. The processing parameters in the extruder were those used for the melt compounding: a reverse extrusion profile linearly decreasing from 170 °C in the hopper to 150 °C in the die, screw-speed of 70 rpm and 80% of dosage. The mixture of matrix, CBA and CE—in some of the samples—, in small amounts of 100 g of mixture to enhance the homogeneity of the extrudate, were progressively feed in the extruder hopper. CBA contents ranged from 0 wt.% to 5 wt.% of masterbatch, and the CE addition was either of 0 wt.% or 1 wt.% (Figure II.13).

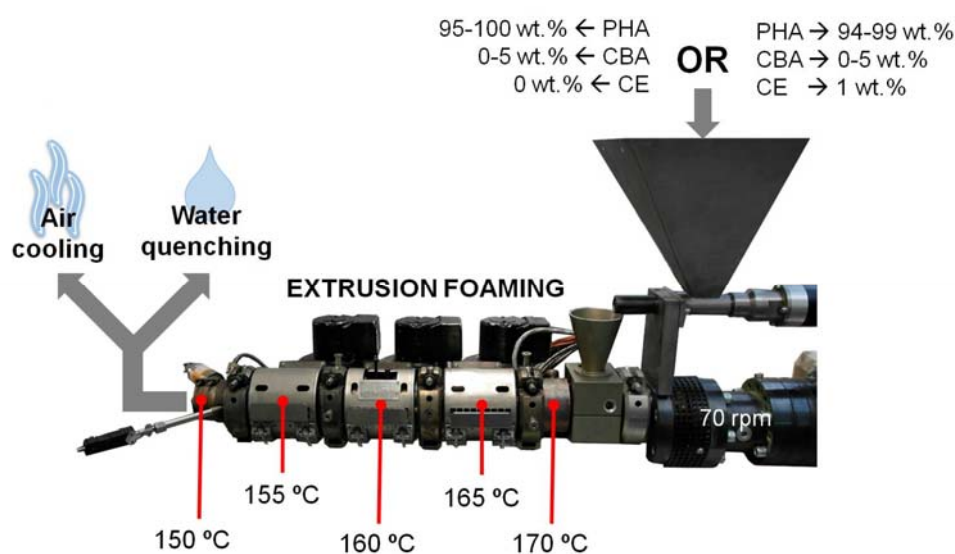


Figure II.13. Scheme of the samples preparation for evaluation of the matrix foamability.

At the exit of the die, which had a 4 mm-diameter profile, specimens of a length of ~20-25 cm were collected. As soon as collected, half of the specimens were water-quenched in a water bath at room temperature, and the other half were laid on a metal tray in order to achieve a slower cooling. In all cases sample were cooled under no-stress. All thus effects are studied in Chapter V.

II.2.5.2. Pressure quench batch foaming

Batch foaming is a discontinuous foaming process that gives a good control of the foaming conditions. Due to that, it is mainly used in research to investigate the foaming behaviour of polymers, although also has some industrial applications.

In general terms, batch foaming consists in the dissolution until saturation of a gas in a polymer, which is normally in rubbery or melt state—for amorphous and semi-crystalline

thermoplastics, respectively—, at a given pressure and temperature. The expansion is produced due to a phase separation, forced because of a loss of the thermodynamic equilibrium that can be produced by a sudden pressure drop or a temperature increase. In the present work, the pressure quench method is used to produce cellular fibre-reinforced composites—CellFRC, [18]—using the aforementioned solid composites as precursors (Figure II.14).

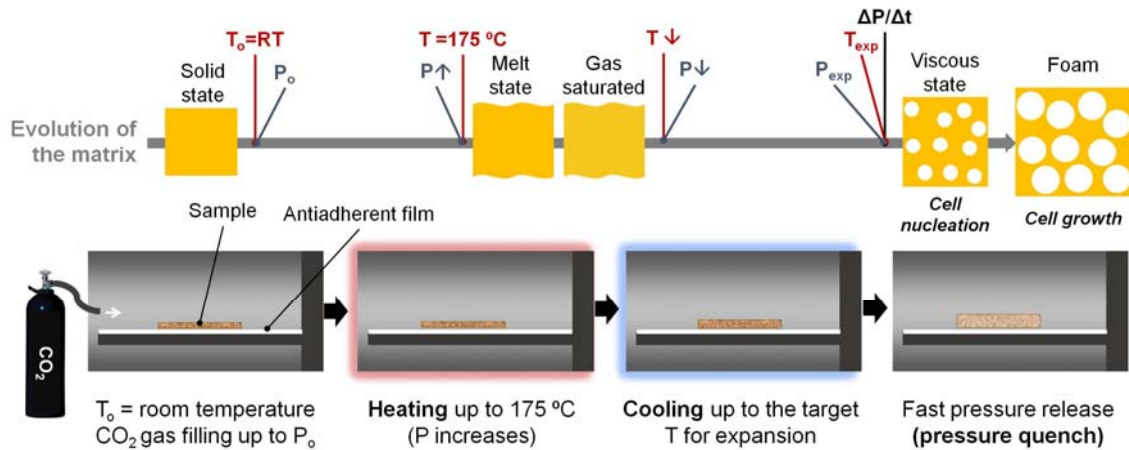


Figure II.14. Foamed composites production by means of the pressure quench method.

To obtain the foamed composites, the solid composite precursors—previously dried overnight at $80\text{ }^\circ\text{C}$ —were placed in the high pressure vessel, which was closely tightened and filled with an initial pressure of CO_2 gas. Once the pressure was stabilized, the temperature was raised up to $175\text{ }^\circ\text{C}$ while checking the pressure and temperature to ensure the target conditions at the expansion point. A saturation time of three minutes was left after reaching the melting temperature of $175\text{ }^\circ\text{C}$, and then the vessel was cooled up to the expansion temperature. This expansion was achieved by a fast pressure release of 40 MPa/s performed with the help of a fast valve. Further details of the process are given in Chapter VI. Regarding this study, the samples were in prepared in the ICPB (CNR, Portici-Naples, Italy).

II.2.6. Summary of the composite techniques

A general scheme concerning the composite samples production is presented in Figure II.15.

Go to next page

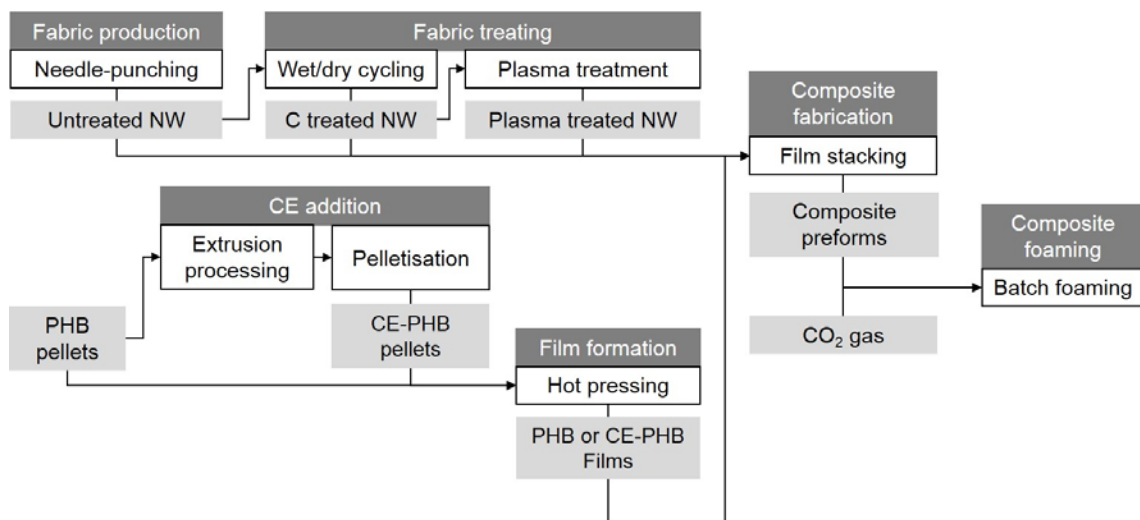


Figure II.15. General scheme of the composite samples production.

II.3. Characterisation methods

II.3.1. Composition and microstructural characterisation

II.3.1.1. Fibre content determination

The fibre content on the PHB/flax composites was determined by extracting the PHB. To that purpose, the specimens were first dried for 16 h at 105 °C in a UNB 400 oven (Memmet, Germany), cooled up to room temperature in a desiccator for 2 h and weighed in a Mettler XS 204 scale (Mettler-Toledo SAE, Spain), to record the dry-weight of the composite sample. Then, the specimens were immersed in chloroform at 60 °C for 45 min under the action of a magnetic-stirrer to dissolve the PHB. The precipitated fibres were filtered, washed 3 times with chloroform, dried again—following the aforementioned conditions- and weighed to record the final dry-weight of the fibres. The fibre content was determined as the ratio between the dry-weight of the fibres and the dry-weight of the composite sample.

II.3.1.2. Density and open cell content

Density of the polymeric foams in Chapter V was determined by the water-displacement method based on Archimedes' principle (Equation (II.1)).

$$\rho_{\text{foam}} = \frac{W}{P} \cdot \rho_o \quad (\text{II.1})$$

where w is the weight of the sample in air, P is the buoyancy of the sample under distilled water—difference between the weight in air and the weight in water—, and ρ_o is the density of the distilled water at the measurement temperature. A Mettler AT261 scale of a resolution of 0.0001 g (Mettler Toledo SAE, Spain), with a density determination kit was used. The density was the average value from three measurements.

The density of the composites and foamed composites in chapters IV and VI was determined geometrically—mass divided by volume—owing to the hydrophilicity of the flax fibres.

Relative density (ρ_{rel})—defined as the ratio between the foam's density and the solid's density—was also calculated.

The open-cell content (f) was determined by means of Equation (II.2):

$$f = \frac{V_s - V_q}{V_s \left(1 - \frac{\rho_{\text{foam}}}{\rho_{\text{solid}}} \right)} = \frac{V_s - V_q}{V_s (1 - \rho_{\text{rel}})} \quad (\text{II.2})$$

where V_s is the external volume of the tested sample (i.e. volume determined by the water-displacement method or geometrically) and V_q corresponds to the volume of the solid plus the gas volume of the unconnected cells—i.e. pycnometric volume—. Determination of V_q was performed by means of an AccuPyc II 1340 gas pycnometer (Micromeritics, USA), with nitrogen gas at 0.134 MPa and equilibration rate at 689 Pa.

II.3.1.3. SEM

Scanning electron microscopy (SEM) was used to characterise the surface morphology of the fibres, the microstructure and surface of composite samples, and the cellular structure of foams (Figure II.16). SEM observations were performed in a Jeol-820 SEM (Jeol, Japan). Fragile fractures were required to evaluate their microstructure, and thence the samples were immersed in liquid nitrogen (-195.8 °C), broken while frozen, and then covered with a thin conductive gold layer of several nanometres. For evaluation of the surface, the samples were directly coated with the conductive layer.

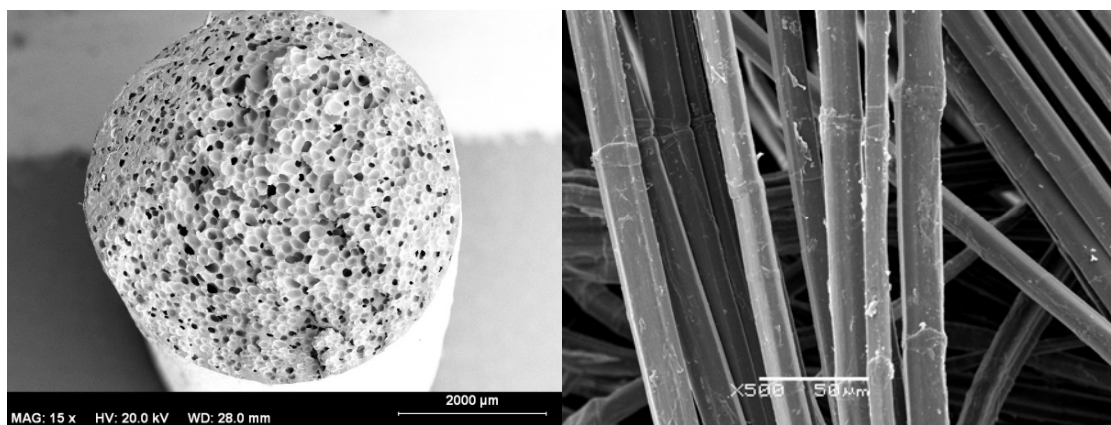


Figure II.16. SEM image of flax fibres' surface (left) and of a NW structure (right).

For the characterisation of the cell structure—based on the determination of the cell size and cell density—SEM images of fragile fractures of the foams or cellular composites are used. A user-interactive specific script for the ImageJ software, developed in CellMat Laboratory by Pinto et al. [19], is used to evaluate around 100 cells per sample from SEM images. From the average cell diameter obtained from the image, the program applies the

required corrections to determine the cell size in 3D (ϕ). The cell density per solid volume (N_0) is determined according to Equation (II.3):

$$N_0 = \frac{6}{\pi\phi^3} \frac{V_p}{1 - V_p} \quad (\text{II.3})$$

where V_p is the porous fraction, calculated as $V_p = 1 - \rho_{\text{rel}}$.

II.3.2. Mechanical characterisation techniques

II.3.2.1. Tensile testing

Tensile tests based in standards were used to characterise the NW, the solid composites and the extruded foams. All the tests in samples containing fibres were performed in the cross-direction.

Regarding the NW mechanical characterisation, breaking force was determined following UNE-EN ISO 13934-1 standard (Figure II.17). The tests were performed in an MTS dynamometer (MTS Systems, USA) with a load cell of 5 kN, at a displacement rate of 5 mm/min, with a pre-load of 1 N, using special clamps for textile testing.

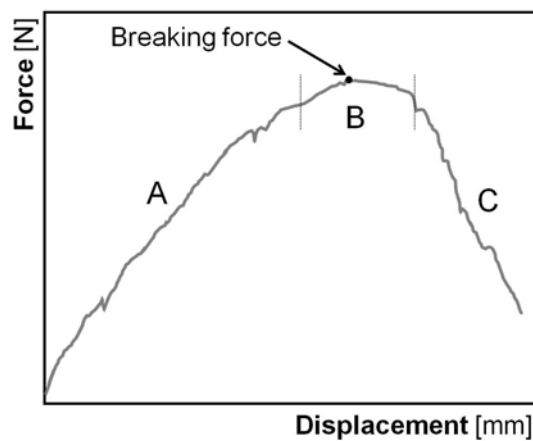


Figure II.17. Typical force-displacement curve of a NW sample. In the beginning, the curve shows progressive force increase with displacement (A). In this region, the NW structure is stretched, flax fibres aligned and stressed, and partial break of entanglement points can take place. Then, a maximum is reached, where the entanglement points are lost (B), thus leading to slip of the fibres (C), where the force values correspond, mainly, to friction between fibres.

The samples from extrusion foaming and the solid composites were characterised in a 5.500R6025 universal testing machine (Instron, UK), following ISO527 1A tensile testing

standard. On the one hand, five specimens of foams obtained by extrusion foaming—with a non-standard shape and a length of 15 cm—were tested to determine average maximum stress (σ_{\max}) and average ultimate tensile strength (σ_{UTS}) (Figure II.18 left). The sectional area of each specimen was estimated from 4 measurements. On the other hand, the solid composites were tested in the form of dumbbell test specimens, at a displacement rate of 5 mm/min. From the curves obtained, experimental values of stiffness (E) and tensile strength (σ_{\max}) were determined (Figure II.18 right).

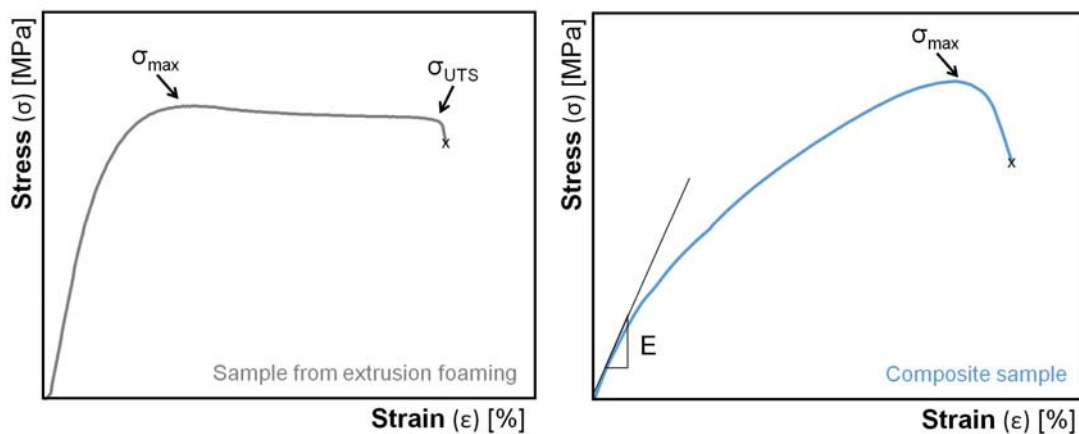


Figure II.18. Examples of stress-strain curves of a foam obtained by extrusion foaming (left) and a solid composite (right).

II.3.2.2. Macro-mechanical modelling methods

There are several existing models for the stiffness (E) and strength (σ) prediction. The most widely accepted model for unidirectional-continuous-fibre-reinforced composites is the general rule of mixtures:

$$P_c = V_f P_f + V_m P_m \quad (\text{II.4})$$

where P refers to the property—commonly E or σ —, V is the fraction volume of each component, and the subscripts c , m and f refer composite, matrix and fibres, respectively. However, this model is not useful for composites reinforced with non-unidirectional and discontinuous fibres, where the modified-rule-of-mixtures models are recommended.

Stiffness and strength modelling of non-porous composite materials

For E_c calculation, the Cox-Krenchel model can be used:

$$E_c = \eta_l \eta_o V_f E_f + V_m E_m \quad (\text{II.5})$$

where E_c refers to the stiffness of the composite, η_l and η_o are fibre length and fibre orientation distribution factors, respectively, and refer to the partial contributions of the fibres which present an ineffective length or a not optimal orientation with respect to the load.

The η_l factor—which corresponds to the shear lag model proposed by Cox [20]—can be calculated as:

$$\eta_l = 1 - \frac{\tanh \frac{\beta L}{2}}{\frac{\beta L}{2}} \text{ where } \beta = \frac{2}{D} \left[\frac{2G_m}{E_f \ln \sqrt{\pi/X_i V_f}} \right]^{1/2} \quad (\text{II.6})$$

where L and D are the fibre length and diameter, respectively, G_m is the shear modulus of the matrix—which can be estimated as $G_m = E_m / 2(1+\nu)$, taking 0.4 as Poisson's ratio (ν)—, X_i is related to the geometrical arrangement of the fibres—a value of 4.0 can assumed if a squared packing is considered [21]—, and the other parameters follow the aforementioned nomenclature. However, η_l can also be considered as 1 when the fibre aspect ratio (L/D) is much greater than 50 [22].

Regarding the η_o factor, it was proposed by Krenchel [23] as:

$$\eta_o = \sum_n a_n \cos^4 \varphi_n \quad (\text{II.7})$$

where a_n is the fraction of fibres which have an angle φ_n with respect to the loading axis. However, the η_o has already been derived in the literature for stiffness calculation, and a value of 3/8 can be assumed for in-plane random orientation of the fibres [22–26], as would be the case of NW-reinforced composites obtained by film staking, where the fibres trend to configure in a two-dimensional distribution.

Similarly, the Kelly-Tyson model is commonly used for σ calculation:

$$\sigma_c = \eta_o^* \eta_{LS} V_f \sigma_f + V_m \sigma_m \quad (\text{II.8})$$

where σ refers to the strength—considering that σ_m is the stress in the matrix at the failure strain of the fibre—and η_{LS} is the Kelly-Tyson's fibre length efficiency factor, which can be calculates as:

$$\eta_{LS} = \frac{1}{V_f} \left(\sum_i \left[\frac{L_i V_i}{2L_c} \right] + \sum_j \left[V_j \left(1 - \frac{L_c}{2L_j} \right) \right] \right) \text{ where } L_c = \frac{\sigma_f D}{2\tau_y} \quad (\text{II.9})$$

where the first summation term—with i subscripts—refers to the fibres shorter than the critical length (L_c), the second—with j subscripts—refers to the fibres of a length greater

than the L_c , and the τ_y is the fibre-matrix interfacial shear strength—a value of 10 MPa was estimated from the literature [27]. Moreover, despite the η_o generally refers to the fibre orientation factor—a $\eta_o = 3/8$ was establish for the E calculation—, it has also been found in the literature that Thomason et al. proposed the use of $\eta_o = 0.2$ as a fitting parameter in this model—without physical meaning—, achieving a better agreement [28]. Similarly, Garkhail et al. proposed an efficiency factor k to be included, thus leading to a $k \cdot \eta_o = 0.2$ with good results also in this Kelly-Tyson model [25]. Due to that, a value of $\eta_o^* = 0.2$ —marked with an asterisk in order to differentiate the non-physical meaning of the term—has been used for σ_c determination in the present work.

Stiffness and strength modelling of porous composite materials

Cox-Krenchel (Equation (II.5)) and Kelly-Tyson (Equation (II.8)) models consider the matrix and the fibre as all the phases of the composite ($V_f + V_m = 1$). However, mechanical models that consider the porosity ($V_p + V_f + V_m = 1$) tend to offer a better approach for the prediction of the stiffness in composites reinforced with natural fibres [29,30], thus owing to the hollow nature of the cellulosic fibres and the technical difficulties for achieving a material without voids. Due to that, models which take into account the porosity are of special interest for the prediction of the properties in composites reinforced with natural bast fibres [31].

The effect of porosity on material stiffness can be approximated by a very simple model, as proposed by Madsen and Lilholt [29]:

$$E_c = E_d \cdot (1 - V_p)^2 \quad (\text{II.10})$$

where E_c refers to the stiffness of the porous material, E_d to the stiffness of the material at fully density (no porosity), and V_p to the porosity volume fraction. In this sense, the E_d can be estimated from the fibre weight fraction (W_f) as:

$$E_d = \eta_1 \eta_o \frac{\frac{W_f}{\rho_f} + \frac{(1 - W_f)}{\rho_m}}{\frac{W_f}{\rho_f} + \frac{(1 - W_f)}{\rho_m}} E_f + \frac{\frac{(1 - W_f)}{\rho_m}}{\frac{W_f}{\rho_f} + \frac{(1 - W_f)}{\rho_m}} E_m \quad (\text{II.11})$$

where ρ_f and ρ_m refers to the density of the fibres and the matrix, respectively. And the V_p can be calculated as:

$$V_p = 1 - \rho_c \cdot \left(\frac{W_f}{\rho_f} + \frac{(1 - W_f)}{\rho_m} \right) \quad (\text{II.12})$$

Madsen et al. [22] proposed an extended version of this model, which included a variable exponent (n_E) in the porosity factor:

$$E_c = (\eta_l \eta_o V_f E_f + V_m E_m) \cdot (1 - V_p)^{n_E} \quad (\text{II.13})$$

where n_E is a porosity efficiency exponent. This n_E exponent, which quantifies the stress concentration effect of porosity in composites, is taken as an empirical parameter which can be obtained by fitting the predicted values to the experimental data. A n_E equal to 0 would mean that the effect of porosity is only the reduction of the volumetric fractions of the matrix and the fibre, although a n_E of 2 has been reported to offer a good fitting to a broad range of natural fibre reinforced composites [22]. Since the model requires the V_p , V_f and V_m , Madsen et al. developed equations For the calculation of each volumetric factor [32]:

$$V_p = \frac{W_f \rho_m \alpha_{pf} + (1 - W_f) \rho_f \alpha_{pm}}{W_f \rho_m (1 + \alpha_{pf}) + (1 - W_f) \rho_f (1 + \alpha_{pm})} \quad (\text{II.14})$$

$$V_f = \frac{W_f \rho_m}{W_f \rho_m (1 + \alpha_{pf}) + (1 - W_f) \rho_f (1 + \alpha_{pm})} \quad (\text{II.15})$$

$$V_m = \frac{(1 - W_f) \rho_f}{W_f \rho_m (1 + \alpha_{pf}) + (1 - W_f) \rho_f (1 + \alpha_{pm})} \quad (\text{II.16})$$

where α_{pf} and α_{pm} are the fibre and matrix correlated porosities, respectively. These equations consider the relationship between the fibre content and the porosity, and the factors α_{pf} and α_{pm} —which can be back calculated from experimental data [33]—estimate the contribution of each sort of porosity [29,32]. However, in the present work—in which the models are used for comparative purposes with experimental data—the V_p has been calculated using Equation (II.12), and V_f and V_m have been estimated from the fibre weight fraction as:

$$V_f = \frac{\frac{W_f \cdot w_c}{v_c}}{\rho_f} \quad (\text{II.17})$$

$$V_m = \frac{\frac{(1 - W_f) \cdot w_c}{v_c}}{\rho_m} \quad (\text{II.18})$$

where w_c is the weight (mass) of the composite sample and v_c is the external volume of the composite sample.

Similarly, in the present work, the use of the porosity term $(1 - V_p)^n$ has been considered for σ_c prediction adapting the Kelly-Tyson model presented in Equation (II.8):

$$\sigma_c = (\eta_o^* \eta_{LS} V_f \sigma_f + V_m \sigma_m) \cdot (1 - V_p)^{n_\sigma} \quad (\text{II.19})$$

where n_{σ} refers to the porosity efficiency exponent, that can take different values than the aforementioned n_E .

II.3.2.3. Compression testing

The compression properties of the foams obtained by extrusion foaming were evaluated in a 5.500R6025 universal testing machine (Instron, UK). Six cylindrical specimens per sample were cut with parallel sides at the required height (h) to achieve a diameter/height ratio of 0.75. Compression tests were performed at a speed of $h/10$ mm/min—that was ~ 0.5 mm/min—until reaching 70% of strain in the samples. Mean values of stress at 25% ($\sigma_{25\%}$) and at 50% ($\sigma_{50\%}$) of the strain, and the collapse stress at the plateau (σ_{pl}) were obtained from the compression curves.

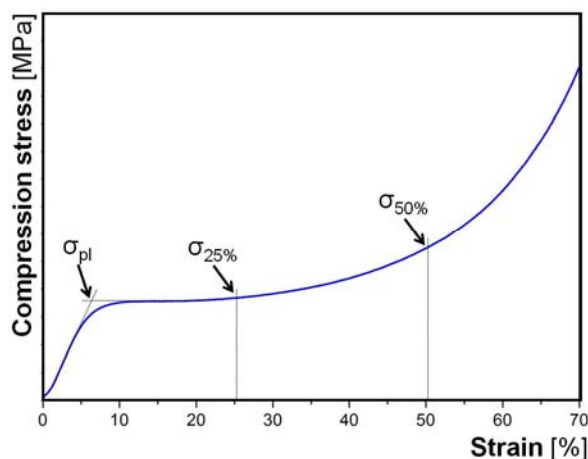


Figure II.19. Typical compression curve of a foam.

II.3.2.4. DMA

Dynamic-mechanical analysis is a key tool for the study of polymers, which permits the evaluation of the complex phenomena that this kind of materials present due to their viscoelastic nature. In the present work, DMA flexural test have been performed both in isothermal mode at room temperature and in a temperature scan mode.

DMA analysis at room temperature

Dynamic-mechanical (DMA) tests were performed at room temperature in a DMTA 7 (Perkin–Elmer, USA) to determine the stiffness of solid and foamed composites in Chapter VI under flexural mode. To that purpose, a three point bending kit of 20 mm span was used

to measure specimens of 22 mm x 6 mm x (thickness), using three specimens per sample and both sides. The forces were adjusted to obtain an amplitude in the indenter displacement of $20 \pm 2 \mu\text{m}$ under low strain values ($\leq 0.08\%$), and the values were taken after 3 min after. A criteria for the static force of “120% the dynamic force” was set, and the frequency of oscillation used was 1 Hz. Flexural modulus (E) and the loss tangent (δ) were recorded.

Dynamic-Mechanical Thermal Analysis (DMTA)

The DMTA tests were performed using the same equipment and load forces established for the DMA analysis previously described. The storage modulus (E'), loss modulus (E'') and loss tangent ($\tan \delta$) were recorded (Figure II.20) during the heating from $-25 \text{ }^\circ\text{C}$ to $90\text{-}130 \text{ }^\circ\text{C}$ at a rate of $3 \text{ }^\circ\text{C}/\text{min}$.

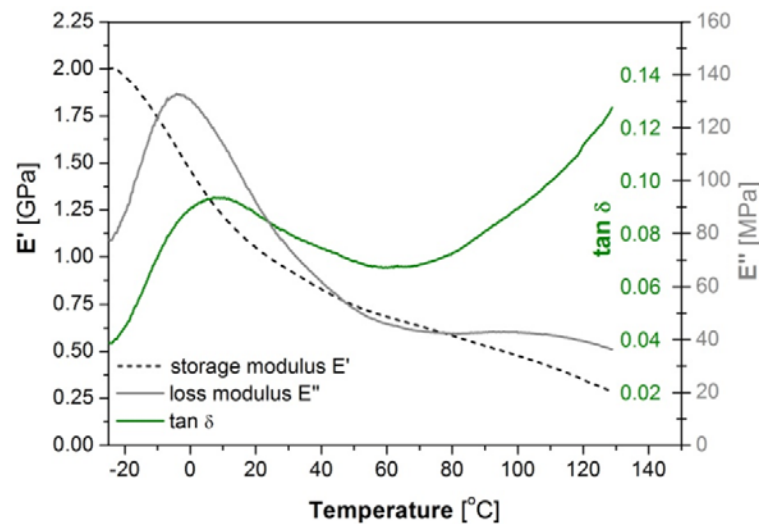


Figure II.20. Example of the DMTA curves obtained for the composites under study.

To evaluate the results, the E' , E'' and $\tan \delta$ curves were analysed, and the intensity of the transition (S), glass transition temperature (T_g), intensity of the $\tan \delta$ peak ($\tan \delta_{\max}$) and the full-width at half-maximum (FWHM) of the $\tan \delta$ peak were determined [34]:

- S refers to the mobility and content of the amorphous phase, and is a helpful parameter to study the effect of the fibre addition, since higher S values point to higher mobility or higher content of the amorphous phase [34]. The parameter is defined as:

$$S = \frac{E'_b - E'_a}{E'_a} \quad (\text{II.20})$$

where E'_b denotes the storage modulus before and E'_a that after the glass transition. In this case, the E'_b is taken as $-20 \text{ }^\circ\text{C}$ and E'_a as $30 \text{ }^\circ\text{C}$ for all samples.

- The glass transition temperature (T_g) was defined as the maximum of the E'' curves.
- The area and intensity of the $\tan \delta$ peaks reveal information about the energy dissipation capabilities, while the FWHM refers to the homogeneity of the amorphous phase, where a wider $\tan \delta$ peak points to higher inhomogeneity [34,35].

II.3.2.5. Charpy impact tests

Charpy impact tests of the foamed samples obtained by extrusion foaming were performed, for comparative purposes only, in a Frank Charpy impact tester 53.566 (Frank, n.a.) with a hammer of 4 J, setting an anvil distance of 39 mm. Ten specimens per sample—of a length of 50 mm—were tested. Energy values were corrected considering the sectional area of each specimen.

II.3.3. Thermal characterisation techniques

II.3.3.1. DSC

The differential scanning calorimetry (DSC) is a useful technique to determine melting temperatures and crystallinity, as well as to reveal differences in the samples produced during processing—thermal story—. DSC analysis are used in Chapter V to study differences due to the extrusion foaming processing, and in Chapter VI to study the foamed composites.

The DSC data were recorded on a DSC-862 (Mettler Toledo SAE, Spain). A three-cycle DSC was performed in all the essays, under nitrogen flow of 60 mL/min: first heating cycle from $-40\text{ }^\circ\text{C}$ to $200\text{ }^\circ\text{C}$ at $10\text{ }^\circ\text{C}/\text{min}$ with 3 min of annealing at $200\text{ }^\circ\text{C}$; cooling cycle from $200\text{ }^\circ\text{C}$ to $-40\text{ }^\circ\text{C}$ at $10\text{ }^\circ\text{C}/\text{min}$ or $20\text{ }^\circ\text{C}/\text{min}$; second heating cycle from $-40\text{ }^\circ\text{C}$ to $200\text{ }^\circ\text{C}$ at $10\text{ }^\circ\text{C}/\text{min}$.

Melting temperatures (T_m) and crystallisation temperatures (T_c) were obtained as the maximum of the peaks from the endothermic and exothermic curves, respectively.

Crystallinity percentage (χ) of all samples was estimated from melting enthalpy (ΔH_m) and crystallisation enthalpy (ΔH_c) as:

$$\chi = \frac{\Delta H}{w \cdot \Delta H^0} \quad (\text{II.21})$$

where w is the real weight fraction of the polymer (corrected according to the amount of fibres and/or additives), ΔH is the heat at the melting or crystallisation point, and ΔH^0 is the heat of fusion or crystallisation of 100% crystalline polymer.

It is worthy to note that complex melting behaviours were observed in most of the samples, even revealing cold crystallisation in some cases (Figure II.21).

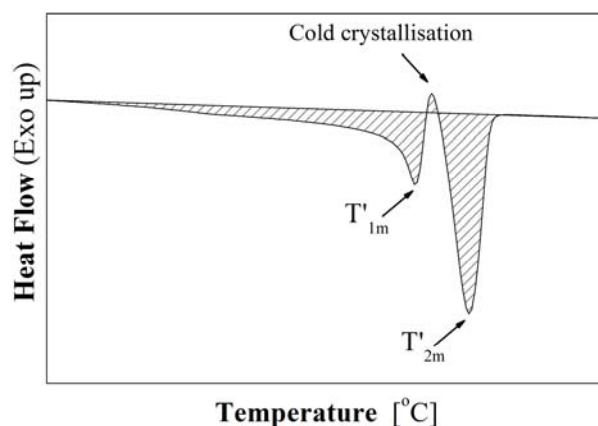


Figure II.21. Example of complex melting behaviour in DSC.

II.3.3.2. TGA

The thermal gravimetric analysis (TGA) was used to evaluate thermal stability. The assays were performed in a TGA/SDTA 861 equipment (Mettler-Toledo SAE, Spain). Samples of about 5.5 mg were heated from room temperature up to 750 °C with heating rates of 10-20 °C/min under nitrogen atmosphere at a flow rate of 60 mL/min, while recording the weight loss.

II.3.4. Techniques related with water absorption properties

II.3.4.1. Moisture content

Moisture-regain values of the treated NW samples in Chapter III were determined following the DIN 54351 standard.

The moisture loss for the foamed composites in Chapter IV was determined from the first slight drop found between room temperature and 170 °C from the TGA curves.

II.3.4.2. Water retention

The water retention values of the NW before and after treatment were determined. Briefly, the method consists in a 4 hours-long water saturation of the samples—which was vacuum-assisted to ensure the saturation—, followed by a centrifugation to remove the excess of water, and then the determination of the “wet” and “dry” weights (w_{wet} and w_{dry} , respectively). Centrifugation was performed in a UJ III centrifuge (Herauschrist, Germany),

at 2600 rpm for 15 min in glass tubes with drainage. After this step, the wet weights were recorded, with a resolution of 0.1 mg, in a Mettler XS 204 scale (Mettler-Toledo SAE, Spain). Then, samples were dried at 105 °C for 16 h in a UNB 400 oven (Memmet, Germany), and weighed again to record the dry weight. The WRV (%) was determined as:

$$\text{WRV} = 100 \frac{W_{\text{wet}} - W_{\text{dry}}}{W_{\text{dry}}} \quad (\text{II.22})$$

II.3.4.3. Contact angle

The static contact angle measurement (Figure II.22) is a useful technique to evaluate the effect of the plasma treatments, since all the treatments performed have the aim of modifying the wettability of the surface sample. To that purpose, a drop shape analyser DSA 100 (Krüss, Germany) was used to deposit water droplets of 5 μL on the fabric surface. A camera records the droplet on the fabric surface, and both the time in which the droplets are absorbed and the contact angles are measured. For the latter, the analysis is performed with the help of the software Drop Shape Analysis DSA3 (Krüss, Germany). As can be observed in Figure II.22, the difficulty of the contact angle measurement in the NW fabrics is the set of the baseline.



Figure II.22. Contact angle measurement.

II.3.4.4. Hydrothermal testing

A hydrothermal test was performed for aging evaluation on the solid composites in Chapter IV. The specimens for the hydrothermal tests were first weighed after drying at 50 °C for 24 h, and then immersed for 100 h in distilled water at 65 °C \pm 2 °C or at room temperature (\sim 23 °C). During the immersion, the specimens—three per sample—were regularly extracted from the water, gently wiped, and weighed to calculate the percentage of water uptake at the measuring time (M_t) as:

$$M_t = [(m_t - m_0)/m_0] \cdot 100 \quad (\text{II.23})$$

where m_0 refers to the mass of the dry sample and m_t refers to the mass of the wet sample at the measuring time. After each measurement, the specimens were immediately immersed again in water. M_s was determined as the saturation point in the water uptake curves.

II.3.4.5. Kinetics of the water absorption

The analysis of the diffusion mechanism and kinetics was performed according to Fick's law. The sorption curves can be fitted as:

$$M_t/M_s = kt^n \quad (\text{II.24})$$

where k and n are constants. The diffusion mechanism can be determined by their shape, since the value of the n exponent, for a planar geometry such as the composites under study reveals, if the diffusion is: pseudo-Fickian or less-Fickian ($n < 0.5$), Fickian ($n = 0.5$), non-Fickian or anomalous ($0.5 < n < 1$), Case II ($n = 1$) or Super Case II ($n > 1$) [36,37].

On the other hand, the diffusion coefficient (D) in Fick's model reveals, according to the present work, the ability of the water fluid molecules to penetrate inside the composite structure. For specimens of flat sheet geometry, and in earlier stages of the water sorption when $M_t/M_s \leq 0.5$, D can be estimated as:

$$D = \pi(\theta h/4M_s)^2 \quad (\text{II.25})$$

where h is the specimen thickness and θ is the slope of the initial portion of the absorption curve M_t against \sqrt{t} .

II.3.5. Other techniques

II.3.5.1. DRX

X-ray diffractography was performed in some of the NW samples with different treatment conditions to obtain the crystalline-to-amorphous ratio (CrI), in order to determine if the treatments applied affect the crystallinity of the samples. These diffractograms of a scan range (2θ) from 5 to 50° were obtained at a scan speed of $5.0^\circ/\text{min}$ with an X-ray tube producing monochromatic Cu $K\alpha$ radiation. The CrI was calculated according to the Segal empirical method [38] by means of the Equation (II.26):

$$\text{CrI}(\%) = \frac{(I_{002} - I_{\text{am}})}{I_{002}} \times 100 \quad (\text{II.26})$$

where I_{002} is the maximum intensity (in arbitrary units) of the diffraction from the (002) plane at $2\theta = 22.6^\circ$; and I_{am} is the intensity of the background scatter measured at $2\theta = 19^\circ$.

II.3.5.2. Rheometry

The viscosity of the matrices and solid composites was evaluated by rheometry measurements in a AR 2000 EX rheometer (TA Instruments, USA), equipped with electrically heated parallel plates of 25 mm of diameter and a gap was set to 1 mm. The linear viscoelastic regime could be obtained for the matrices despite the composites did not reveal a linear region. Due to that, the matrices were evaluated—for a comparative of the degradation rate—, in a time-sweep assay performed in the linear viscoelastic regime, at angular frequency of 1 rad/s, fixed strain of 2% and temperature of 165 °C, under air atmosphere to simulate of the processing conditions.

On the one hand, for the evaluation of the effect of the fibres addition, the dependence of viscosity with shear rate was measured for the neat matrices and a fibre-reinforced composite. The steady state flow curves at 175 °C were obtained, measuring the viscosity under shear rates between 0.001 and 10 rad/s in nitrogen atmosphere, in this case.

II.3.5.3. XPS

The X-ray photoelectron spectroscopy is an excellent technique for characterisation of the effects of the plasma treatments, since permits to analyse the surface chemistry of the first nanometres of the sample. The tests were performed in a SPECS system (SPECS, Germany), equipped with a monochromatic Al K α XR50 anode operating at 100 W and a Phoibos 150 MCD-9 detector. The survey spectrum taken at 1 eV and high resolution spectra of C1s, O1s and N1s taken at 0.1 eV were recorded. The charge correction was performed with the C1s peak at 284.8 eV. A pressure lower than 10⁻⁷ Pa was maintained in the chamber. The relative error for XPS determination is about 0.5%. The composition was obtained from average values on measurements performed in two different points. Atomic fractions (%) were calculated using peak areas normalized on the basis of acquisition parameters after background subtraction. The O/C ratios were calculated considering the atomic fractions.

II.3.6. Summary of the characterisation methods

A summary of characterisation techniques used in each chapter is given in Table II.3.

Table II.3. Characterisation techniques use, for chapters

<i>Technique</i>	<i>Chapter</i>	<i>Technique</i>	<i>Chapter</i>
Cellular microstructure analysis ^a	V, VI	Hydrothermal testing ^d	IV
Charpy ^a	V	Moisture regain ^d	III
Compression testing ^a	V	Open cell content ^a	V, VI
Density ^a	V, VI	Rheometry ^a	IV, VI
DMA ^a	VI	SEM ^{a,e}	III, VI, V, VI
DRX ^b	III	Tensile testing ^{a,e}	III, IV, V
DSC ^a	V, VI	TGA ^a	III, IV
Contact angle ^c	III	Water retention values ^d	III
		XPS ^f	III

Performed at: ^a CellMat Laboratory, Universidad de Valladolid (UVa); ^b Instrumental Techniques Laboratory, UVa; ^c Textile Ecofinishing Laboratory, Universitat Politècnica de Catalunya (UPC); ^d Fibres and Polymers Laboratory, UPC; ^e Textile Physics Laboratory, UPC; ^f Barcelona Research Center of Multiscale Science and Engineering, UPC.

References

- [1] Wright ZC, Frank CW. Increasing cell homogeneity of semicrystalline, biodegradable polymer foams with a narrow processing window via rapid quenching. *Polym Eng Sci* 2014;54:2877–2886. doi:10.1002/pen.23847.
- [2] Takahashi S, Hassler JC, Kiran E. Melting behavior of biodegradable polyesters in carbon dioxide at high pressures. *J Supercrit Fluids* 2012;72:278–87. doi:10.1016/j.supflu.2012.09.009.
- [3] Villalobos M, Awojulu A, Greeley T, Turco G, Deeter G. Oligomeric chain extenders for economic reprocessing and recycling of condensation plastics. *Energy* 2006;31:3227–34. doi:10.1016/j.energy.2006.03.026.
- [4] Ludwiczak J, Kozłowski M. Foaming of Polylactide in the Presence of Chain Extender. *J Polym Environ* 2015;23:137–42. doi:10.1007/s10924-014-0658-7.
- [5] Duangphet S, Szegda D, Song J, Tarverdi K. The Effect of Chain Extender on Poly(3-hydroxybutyrate-co-3-hydroxyvalerate): Thermal Degradation, Crystallization, and Rheological Behaviours. *J Polym Environ* 2013;22:1–8. doi:10.1007/s10924-012-0568-5.
- [6] Hua ZQ, Sitaru R, Denes F, Young RA. Mechanisms of oxygen- and argon-RF-plasma-induced surface chemistry of cellulose. *Plasmas Polym* 1997;2:199–224. doi:10.1007/BF02766154.
- [7] Aguilar-Rios A. Improving the bonding between henequen fibers and high density polyethylene using atmospheric pressure ethylene-plasma treatments. *Express Polym Lett* 2014;8:491–504. doi:10.3144/expresspolymlett.2014.53.
- [8] Russell SJ (Stephen J., Textile Institute (Manchester E. Handbook of nonwovens. CRC Press; 2007.
- [9] Albrecht W, Fuchs F, Kittelmann W. *Nonwoven Fabrics*. Weinheim: Wiley-VCH; 2003.
- [10] Anandjiwala RD, Boguslavsky L. Development of Needle-punched Nonwoven Fabrics from Flax Fibers for Air Filtration Applications. *Text Res J* 2008;78:614–24.
- [11] Ghane M, Saghafi R, Zarrebini M, Semnani D. Evaluation of Bending Modulus of Needle-Punched Fabrics Using Two Simply Supported Beam Method. *Fibres Text East Eur* 2011;19:89–93.
- [12] Ventura H, Ardanuy M, Capdevila X, Cano F, Tornero JA. Effects of needling parameters on some structural and physico-mechanical properties of needle-punched nonwovens. *J Text Inst* 2014;1–11. doi:10.1080/00405000.2013.874628.
- [13] Claramunt J, Ventura H, Fernández-Carrasco L, Ardanuy M. Tensile and Flexural Properties of Cement Composites Reinforced with Flax Nonwoven Fabrics. *Materials (Basel)* 2017;10:215. doi:10.3390/ma10020215.
- [14] Claramunt J, Ardanuy M, García-Hortal JA. Effect of drying and rewetting cycles on the structure and physicochemical characteristics of softwood fibres for reinforcement of cementitious composites. *Carbohydr Polym* 2010;79:200–5. doi:10.1016/j.carbpol.2009.07.057.
- [15] Claramunt J, Ardanuy M, García-Hortal JA, Filho RDT. The hornification of vegetable fibers to improve the durability of cement mortar composites. *Cem Concr Compos* 2011;33:586–95. doi:10.1016/j.cemconcomp.2011.03.003.
- [16] Esteves Magalhães WL, Ferreira de Souza M. Solid softwood coated with plasma-polymer for water repellence. *Surf Coatings Technol* 2002;155:11–5. doi:10.1016/S0257-8972(02)00029-4.
- [17] Shishoo R. *Plasma Technologies for Textiles*. Elsevier Science; 2007.

- [18] Sorrentino L, Cafiero L, D'Auria M, Iannace S. Cellular thermoplastic fibre reinforced composite (CellFRC): A new class of lightweight material with high impact properties. vol. 64. 2014. doi:10.1016/j.compositesa.2014.05.016.
- [19] Pinto J, Solorzano E, Rodriguez-Perez MA, De Saja JA. Characterization of the cellular structure based on user-interactive image analysis procedures. *J Cell Plast* 2013;49:555–75. doi:10.1177/0021955X13503847.
- [20] Cox HL. The elasticity and strength of paper and other fibrous materials. *Br J Appl Phys* 1952;3:72.
- [21] Thomason, J. L.; Vlug MA. The influence of fibre length and concentration on the properties of glass fibres reinforced polypropylene 2 Thermal properties.pdf. *Compos Part A Appl Sci Manuf* 1996;27:477–84. doi:10.1016/1359-835X(95)00065-A.
- [22] Madsen B, Thygesen A, Lilholt H. Plant fibre composites – porosity and stiffness. *Compos Sci Technol* 2009;69:1057–69. doi:10.1016/j.compscitech.2009.01.016.
- [23] Krenchel H. Fibre reinforcement: theoretical and practical investigations of the elasticity and strength of fibre-reinforced materials. Copenhagen: Akademisk Forlag; 1964.
- [24] Thomason JL, Vlug MA. Influence of fibre length and concentration on the properties of glass fibre-reinforced polypropylene: Part 1. Tensile and flexural modulus. *Compos Part A Appl Sci Manuf* 1996;27:477–84. doi:10.1016/1359-835X(95)00065-8.
- [25] Garkhail SK, Heijenrath RWH, Peijs T. Mechanical properties of natural-fibre-mat-reinforced thermoplastics based on flax fibres and polypropylene. *Appl Compos Mater* 2000;7:351–72. doi:10.1023/A:1026590124038.
- [26] Van Den Oever MJA, Bos HL, Van Kemenade MJJM. Influence of the Physical Structure of Flax Fibres on the Mechanical Properties of Flax Fibre Reinforced Polypropylene Composites. *Appl Compos Mater* 2000;7:387–402. doi:10.1023/A:1026594324947.
- [27] Wong S, Shanks RA, Hodzic A. Effect of additives on the interfacial strength of poly(l-lactic acid) and poly(3-hydroxy butyric acid)-flax fibre composites. *Compos Sci Technol* 2007;67:2478–84. doi:10.1016/j.compscitech.2006.12.016.
- [28] Thomason JL, Vlug MA, Schipper G, Krikor HGLT. Influence of fibre length and concentration on the properties of glass fibre-reinforced polypropylene: Part 3. Strength and strain at failure. *Compos Part A Appl Sci Manuf* 1996;27:1075–84. doi:10.1016/1359-835X(96)00066-8.
- [29] Madsen B, Lilholt H. Physical and mechanical properties of unidirectional plant fibre composites—an evaluation of the influence of porosity. *Compos Sci Technol* 2003; 63:1265–72. doi:10.1016/S0266-3538(03)00097-6.
- [30] Summerscales J, Dissanayake N, Virk A, Hall W. A review of bast fibres and their composites. Part 2 – Composites. *Compos Part A Appl Sci Manuf* 2010;41:1336–44. doi:10.1016/j.compositesa.2010.05.020.
- [31] Summerscales J, Virk A, Hall W. A review of bast fibres and their composites: Part 3 – Modelling. *Compos Part A Appl Sci Manuf* 2013;44:132–9. doi:10.1016/j.compositesa.2012.08.018.
- [32] Madsen B, Thygesen A, Lilholt H. Plant fibre composites – porosity and volumetric interaction. *Compos Sci Technol* 2007;67:1584–600. doi:10.1016/j.compscitech.2006.07.009.
- [33] Thygesen A. Properties of hemp fibre polymer composites - An optimisation of fibre properties using novel defibration methods and fibre characterisation Title. Royal Veterinary and Agricultural University, Technical University of Denmark, 2006. doi:(Risø-PhD; No. 11(EN)).

- [34] Díez-Gutiérrez S, Rodríguez-Perez MA, De Saja JA, Velasco JI. Dynamic mechanical analysis of injection-moulded discs of polypropylene and untreated and silane-treated talc-filled polypropylene composites. *Polymer (Guildf)* 1999;40:5345–53. doi:10.1016/S0032-3861(98)00754-X.
- [35] Manikandan Nair K., Thomas S, Groeninckx G. Thermal and dynamic mechanical analysis of polystyrene composites reinforced with short sisal fibres. *Compos Sci Technol* 2001;61:2519–29. doi:10.1016/S0266-3538(01)00170-1.
- [36] Crank J. *The Mathematics of Diffusion*. 2nd ed. Clarendon Press; 1975.
- [37] Karimi M. *Diffusion in Polymer Solids and Solutions*. Mass Transf. Chem. Eng. Process., InTech; 2011. doi:10.5772/23436.
- [38] Segal L, Creely JJ, Martin AE, Conrad CM. An Empirical Method for Estimating the Degree of Crystallinity of Native Cellulose Using the X-Ray Diffractometer. *Text Res J* 1959;29:786–94. doi:10.1177/004051755902901003.

CHAPTER III

TREATMENT OF FLAX-NONWOVEN

FABRICS

CHAPTER CONTENTS

Abstract	159
III.1. Introduction.....	161
III.2. Experimental section.....	163
III.2.1. Materials.....	163
III.2.2. Nonwoven preparation.....	163
III.2.3. Nonwoven treatment.....	163
III.2.3.1. Wet/dry cycling treatment.....	163
III.2.3.2. Plasma treatments	163
III.2.4. Characterization of the NW fibres	165
III.2.4.1. Surface characterization	165
III.2.4.2. Wetting properties	165
III.2.4.3. Thermal stability.....	166
III.2.4.4. Fibre crystallinity	166
III.2.4.5. Mechanical properties.....	166
III.3. Results and discussion.....	167
III.3.1. Surface characterization.....	167
III.3.1.1. SEM analysis	167
III.3.1.2. XPS Analysis.....	170
III.3.2. Wetting Properties.....	176
III.3.2.1. Water Retention Values	176
III.3.2.2. Moisture Regain	176
III.3.2.3. Contact Angles	177
III.3.3. Thermal Stability.....	178
III.3.4. Fibre crystallinity.....	180
III.3.5. Mechanical properties	181
III.3.6. Considerations for Reinforcement Applications	183
III.4. Conclusions.....	184
References	185

Abstract

This research analyzes the effects of different treatments on flax nonwoven (NW) fabrics intended for composite reinforcement. The treatments applied were of two different kinds: a wet/dry cycling which helps to stabilize the cellulosic fibres against humidity changes and plasma treatments with air, argon and ethylene gases considering different conditions and combinations, which produce variation on the chemical surface composition of the NWs. The resulting changes in the chemical surface composition, wetting properties, thermal stability and mechanical properties were determined. Variations in surface morphology could be observed by scanning electron microscopy (SEM). The results of the X-ray photoelectron spectroscopy (XPS) showed significant changes to the surface chemistry for the samples treated with argon or air (with more content on polar groups on the surface) and ethylene plasma (with less content of polar groups). Although only slight differences were found in moisture regain and water retention values (WRV), significant changes were found on the contact angle values, thus revealing hydrophilicity for the air-treated and argon-treated samples and hydrophobicity for the ethylene-treated ones. Moreover, for some of the treatments the mechanical testing revealed an increase of the NW breaking force.

This part of the work was published in open-access as *Effects of Wet/Dry-Cycling and Plasma Treatments on the Properties of Flax Nonwovens Intended for Composite Reinforcing*, Ventura, H.; Claramunt, J.; Navarro, A.; Rodríguez-Pérez, M.A.; Ardanuy, M. *Materials* (MDPI). Vol. 9, num. 2, p. 93:1-93:18, issued on 3 February 2016. doi: 10.3390/ma9020093

Available at: <http://www.mdpi.com/1996-1944/9/2/93>

III.1. Introduction

During the last few years, there has been growing interest in the development of more sustainable and eco-friendly composite materials. In this sense, natural fibres have been proposed as an interesting option for the reinforcement of not only polymeric matrices [1–4] but also for other ceramic matrices such as cements [5]. Cellulosic or vegetable fibres are non-hazardous, renewable, biodegradable, and have low density and well-balanced stiffness, toughness and strength, allowing the development of composite materials with good performance at relatively low cost [5].

Despite all of the aforementioned advantages, one of the main drawbacks of these fibres is their high hydrophilicity, which makes them very sensitive to water. Cellulosic fibres have a cellulose structure and other hydrophilic components with an affinity for water, which favours penetration of the same in the amorphous regions of the fibres. The amount of moisture that can be absorbed, depending on environmental conditions, can vary between 5% and 20% by dry weight. Therefore, one of the main problems to be solved for composites reinforced with cellulosic fibres is the fibre-matrix interaction which is weakened by the dimensional changes of the fibres due to the absorption and desorption of water. One possible treatment used to minimize the dimensional changes due to this effect is the previous modification of fibres with a wet/dry treatment. It is well known that drying and rewetting cycles in water cause shrinkage of the cellulosic fibres and a reduction in water retention values due to the formation of hydrogen bonds in the cellulose [6,7].

On the other hand, this hydrophilicity also affects the interface adhesion with matrices. In general terms, the interaction with cementitious matrices is positive but becomes a problem for most polymeric matrices which are more hydrophobic. The treatments commonly used to improve the compatibility and surface contact and hence the fibre-matrix adhesions are chemical or enzymatic. Nevertheless, these techniques are costly and complex and use high amounts of water and chemicals, which make them poorly applicable to consumer goods. One method that requires less energy, reduces the use of hazardous substances and avoids the generation of wastes is plasma surface treatment, which confers various surface properties, such as increased reactivity of the surface. Plasma treatments physically and chemically modify the fibre surface without any variation in the intrinsic properties of the fibres. The main advantages of the use of plasma technologies are: the minimal use of chemical products—gases or precursors—and energy—no need to dry—; water is not required, thus avoiding residual waters and their treatment; and they can be

applied in continuous processes. The main limitations are due to difficulties in controlling the atmospheric plasma and the investment costs, despite the latter being progressively reduced with the increasing demand. On the other hand, plasma-induced grafting and plasma polymerization techniques can provide diverse surface properties [8,9]. It is possible to achieve increased hydrophilicity in cellulosic fibres [10–13] or to obtain hydrophobic cotton fibres with plasma polymerization processes [14,15].

The aim of this study is to evaluate the effects of more eco-friendly methods for the functionalisation of flax nonwovens (NWs) intended for composite reinforcing. On the one hand, plasma treatments can be considered as eco-friendly solutions due to the minimal use of chemicals, lower use of energy and no use of water, as stated before. Moreover, these plasma treatments can be appropriately optimized to affect only the fibre surface, thus avoiding the major loss of mechanical properties—unlike other more aggressive chemical treatments—. On the other hand, the wet/dry cycling has the advantage of being a very simple treatment that only requires water—with no other hazardous substances—to achieve better fibre stabilization. As aforementioned, the effects of these treatments on cellulosic fibres have already been studied in the literature. However, to the authors' knowledge, no studies dealing with their combination have already been done. Both the stability and the adhesion of the reinforcement are important factors that can affect to the durability of a composite. Therefore, in this study, various surface plasma treatments with previous wet/dry cycling treatments have been applied and evaluated by means of morphology and chemical characterization, water absorption behaviour, and thermal and mechanical properties.

III.2. Experimental section

III.2.1. Materials

Flax fibres with an average length of 6 cm were provided by Fibres Reserche Development, of the Technopole de l'Aube en Champagne (Troyes, France). For plasma treatments, argon gas (99.999% of purity) and ethylene gas (99.99% of purity) were acquired from Air Liquide España (Madrid, Spain).

III.2.2. Nonwoven preparation

NW fabric samples were prepared on a DILO OUG-II-6 pilot plant of double needle-punching machine, equipped with universal card clothing, a cross-lapper, a batt feeder and a needle-punching loom (DILO Group, Eberbach, Germany). The flax fibres were first opened and carded to form a thin web, which was laid by the cross-laying method to form batts. These batts were consolidated on the needle-punch to form the nonwoven mats. The optimized NW structure of 284 ± 23 g/m² and thickness of 1.9 ± 0.1 mm with high entanglement was prepared. The processing parameters to prepare these nonwovens were evaluated in previous research [16].

III.2.3. Nonwoven treatment

III.2.3.1. Wet/dry cycling treatment

The wet/dry cycling treatment (C) was performed by repetition of a two-step process. For the first step, NW were soaked in distilled water at 60 °C for 70 min under sonication. For the second step, the wet NW were dried in an oven with air recirculation at 105 °C for 16 h. A total of four wet/dry cycles applied to the samples.

III.2.3.2. Plasma treatments

Low pressure and corona plasma treatments were carried out in this study. Table III.1 shows the reference and main characteristics of the treatments used.

For low pressure plasma, the NWs were treated by means of a Europlasma Junior Advanced PLC radiofrequency (RF) plasma reactor (Europlasma, Oudenaarde, Belgium), operating at 13.56 MHz and using argon (Ar) and ethylene (Et) gases at constant flow rate of 20 and 30 sccm, respectively. The plasma treatment procedure was as follows: first, the NW

specimen was introduced into the reactor chamber and a vacuum of 50 mtorr was applied; then, the controlled flow of gas was injected, and the pressure inside the reactor was maintained at around 150 mtorr. At this point, the RF 50W-power plasma was initiated, and the NW specimen was exposed for the time previously specified in Table III.1. Samples treated with both gases were first treated with argon, which was purged before further treatment with ethylene gas. This double treatment was performed without opening the reactor chamber—with no vacuum loss—.

Corona plasma treatments (Cr) were carried out by means of an Ahlbrandt FG-2 corona plasma (Ahlbrandt System GmbH, Lauterbach, Germany) using air as a plasma gas. The distance between the electrode and the fabric was adjusted to 10 mm and power, speed and incident current were kept constant during the treatment at 400 W, 20 rpm and 2 A, respectively. Treatment time is also specified in Table III.1.

Table III.1. Sample references and description of the treatment conditions applied.

Reference	Wet/dry treatment (Cycles)	Corona plasma (min)	Argon plasma (min)	Ethylene plasma (min)
NW SC	0	-	-	-
NW C	4	-	-	-
NW C-Et10	4	-	-	10
NW C-Ar5	4	-	2.5 + 2.5	-
NW C-Ar10	4	-	5 + 5	-
NW C-Ar20	4	-	10 + 10	-
NW C-Ar30	4	-	15 + 15	-
NW C-Ar5-Et5	4	-	5	5
NW C-Ar5-Et10	4	-	5	10
NW C-Cr20	4	20	-	-
NW C-Cr1010	4	10 + 10	-	-
NW C-Cr1010-Et10	4	10 + 10	-	10

Note: Plasma treatments were applied to one side (n) or to both sides ($n + n$) of the NW, so n refers to treatment time per side.

III.2.4. Characterization of the NW fibres

III.2.4.1. Surface characterization

Both the morphology and chemical composition of the fibre surface of the treated and untreated fibres was studied.

For the morphology analysis, images of the surface of the fibres were obtained by means of a JEOL-820 SEM (JEOL USA Inc., Peabody, MA, USA).

For the chemical composition, the X-ray photoelectron spectroscopy (XPS) technique was used. XPS measurements were performed in a SPECS system (SPECS GmbH, Berlin, Germany), equipped with a monochromatic Al K α anode XR50 operating at 100 W and a Phoibos 150 MCD-9 detector. The pass energy was set at 25 eV. The following sequence of spectra was recorded: survey spectrum taken at 1 eV, and high resolution spectra of C1s, O1s and N1s taken at 0.1 eV. The charge correction was performed with the C1s peak at 284.8 eV. A pressure lower than 10^{-7} Pa was maintained in the chamber. The relative error for XPS determination is about 0.5%. Each sample was analyzed at two different places and the average composition was calculated. Atomic fractions (%) were calculated using peak areas normalized on the basis of acquisition parameters after background subtraction. The O/C ratios were calculated considering the atomic fractions.

III.2.4.2. Wetting properties

For characterization of the wetting properties of all the NW samples, water-retention values, moisture-regain values and contact angle assays were used.

WRV were determined based on a standard ASTM D 2402-01 [34]. To ensure the water saturation of the samples, the specimens underwent vacuum-assisted immersion for 4 h. To remove excess water, the samples were centrifuged at 2600 rpm for 15 min. Moisture-regain values were determined following the DIN 54351 standard [35].

The static contact angle measurements were performed with a Krüss DSA 100 goniometer (KRÜSS GmbH, Hamburg, Germany). NW samples were laid flat on a clean, dry glass support without mechanical stress and 5 μ L water droplets were deposited on the fabric surface. The time taken to absorb these water droplets was recorded. Contact angles were obtained from further analysis with the Drop Shape Analysis DSA3 software (KRÜSS GmbH, Hamburg, Germany).

III.2.4.3. Thermal stability

The thermal stability was determined by thermal gravimetric analysis (TGA) using the Mettler TGA/SDTA 861 equipment (Mettler-Toledo S.A.E., L'Hospitalet de Llobregat, Spain). Samples weighing about 5.5 mg were heated in the temperature range from 25 to 750 °C with a heating rate of 20 °C/min under nitrogen atmosphere (at a flow of 60 mL/min).

III.2.4.4. Fibre crystallinity

X-ray diffractograms were obtained in a Bruker Discover D8 X-ray diffractometer (Bruker Company, Billerica, MA, USA), at a scan speed of 5.0 degree/min, in a scan range (2θ) from 5 to 50°, and with an X-ray tube producing monochromatic Cu K α radiation.

The CrI, which corresponds to the crystalline-to-amorphous ratio, was calculated according to the Segal empirical method [17] by the following equation:

$$\text{CrI}(\%) = \frac{(I_{002} - I_{\text{am}})}{I_{002}} \times 100 \quad (\text{III.1})$$

where I_{002} is the maximum intensity (in arbitrary units) of the diffraction from the (002) plane at $2\theta = 22.6^\circ$; and I_{am} is the intensity of the background scatter measured at $2\theta = 19^\circ$.

III.2.4.5. Mechanical properties

For the analysis of mechanical properties, tensile tests based on UNE-EN ISO 13934-1 standard [37] were performed to determine the changes in the breaking force of the NW. The tests were performed in an MTS dynamometer (MTS Systems, Eden Prairie, MN, USA) with a load cell of 5 KN, at a displacement rate of 5 mm/min. The nonwovens were tested in the cross-direction.

III.3. Results and discussion

The original NW (SC) was treated with several methods: wet/dry cycling (C), low pressure argon plasma (Ar), low pressure ethylene plasma (Et) and air corona plasma (Cr), in several conditions. Table III.1 shows the references of the samples and a description of the treatments and combinations applied.

III.3.1. Surface characterization

III.3.1.1. SEM analysis

Surface morphology of the fibres was observed by scanning electron microscopy (SEM). As shown in Figure III.1, after the wet/dry cycling, the fibres presented a rougher surface while the untreated sample had the typical appearance of flax fibres with smoother surfaces. However, despite some shrinkage was expected, it could not be observed due to the high variability in the diameters of fibres.

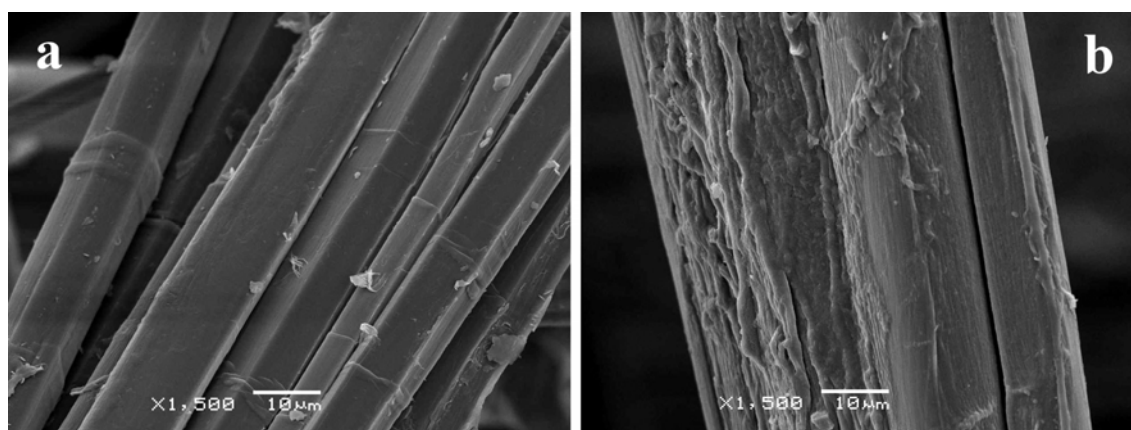


Figure III.1. SEM images of (a) untreated; and (b) wet/dry cycled flax bundles taken at 10 kV and $\times 1500$ magnification.

The low pressure Ar treatment led to an increase in surface roughness when increasing the treatment time, as expected. Figure III.2 shows these differences on the surface roughness of samples after 5, 10, 20 and 30 min of Ar-plasma treatment at high magnification. This is consistent with the fibre surface etching produced by Ar-plasma [18,19]. Moreover, some small craters of around 0.5–1 μm could be observed in the NW C-Ar30 sample (Figure III.3), thus attributed to the aforementioned etching following longer exposure times.

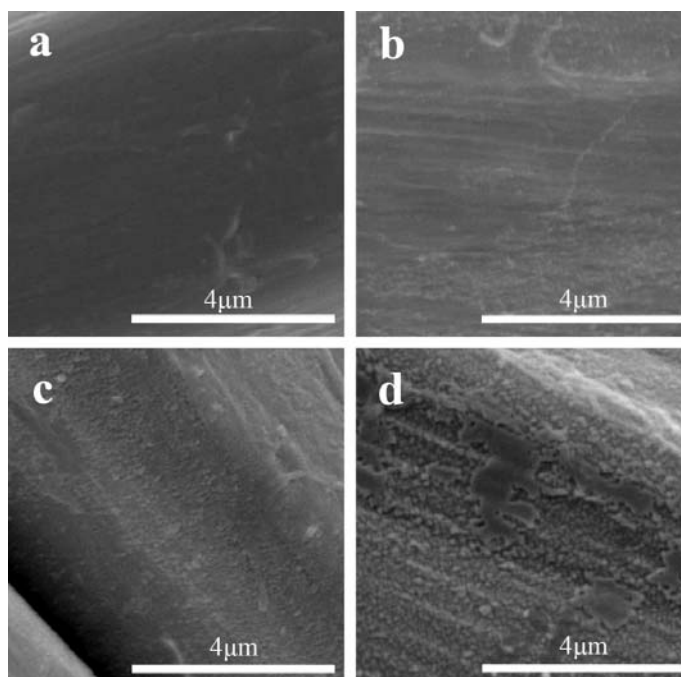


Figure III.2. Effect on the surface roughness of the fibre due to increasing time in Ar-plasma treatment of samples: (a) NW C-Ar5; (b) NW C-Ar10; (c) NW C-Ar20; and (d) NW C-Ar30. SEM images were taken at 10 kV and $\times 10,000$ magnification.

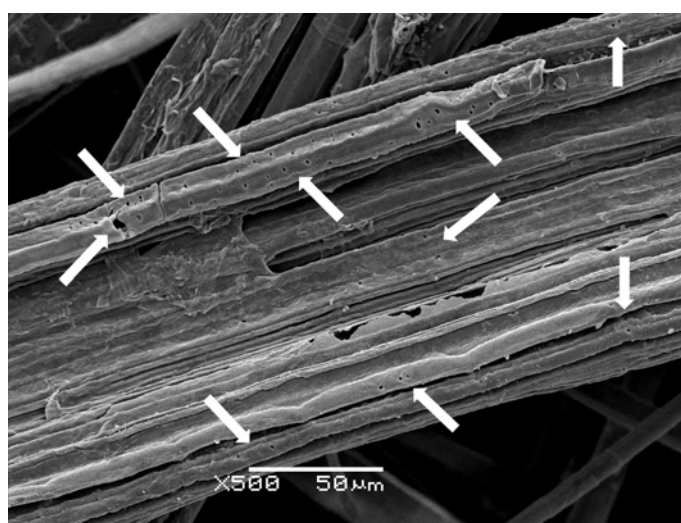


Figure III.3. SEM image of the sample NW C-Ar30 taken at 10 kV and $\times 500$ magnification. Arrows mark the craters formed.

Samples in which air corona plasma treatment was applied also presented high roughness (Figure III.4), although some differences could be observed between treating the NW for 20 min on one side only (NW C-Cr20) and treating it for 10 min on each side (NW C-Cr1010). The NW C-Cr20 presented higher levels of damage on the fiber surface of the treated side, which was attributed to the higher etching caused by the plasma.

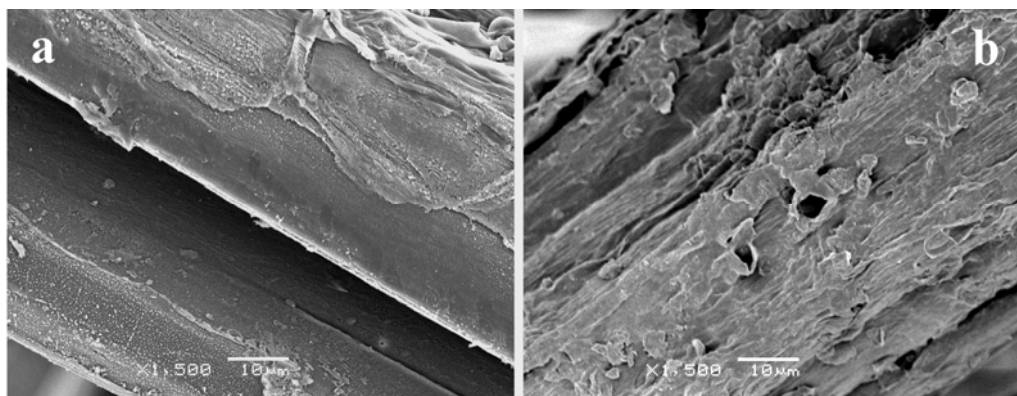


Figure III.4. SEM image of surfaces of samples (a) NW C-Cr1010; and (b) NW C-Cr20 taken at 10 kV and $\times 1500$ magnification.

When using further low pressure Et-plasma treatments, fibre morphology did not change significantly. Only flake-like attachments could be observed, which were attributed to partial lifting of thin ethylene layers that polymerized on the surface of the fibres (Figure III.5). The polymer deposition in the surface was more clearly observed in samples with higher roughness (Figure III.6).

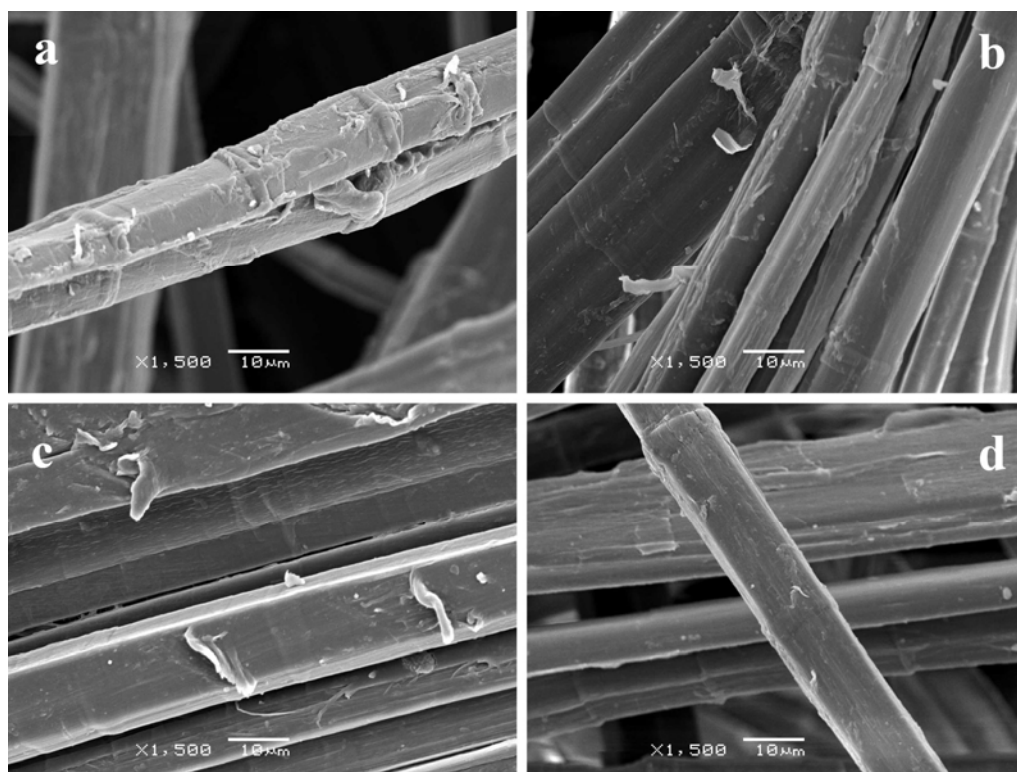


Figure III.5. SEM image of surfaces of samples (a) NW C-Ar5-Et5; (b) NW C-Ar5-Et10; (c) NW C-Cr1010-Et10; and (d) NW C-Et10 taken at 10 kV and $\times 1500$ magnification.

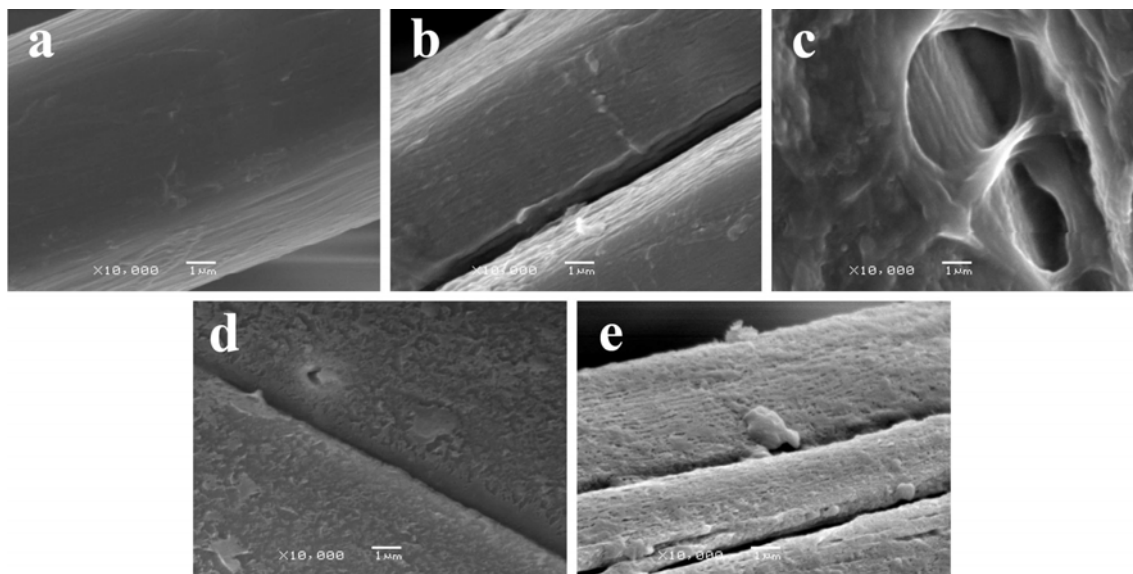


Figure III.6. Comparative SEM images taken at 10 kV and $\times 10,000$ magnification, of the surfaces of samples (a) NW C-Ar5; (b) NW C-Ar5-Et5; and (c) NW C-Ar5-Et10; and (d) NW C-Cr1010; and (e) NW C-Cr1010-Et10.

III.3.1.2. XPS Analysis

Plasma treatments generate new reactive groups on the surface and, at the same time, remove other chemical groups due to surface etching. Therefore, XPS analyses are required to provide clear information about chemical composition. In the survey scans of XPS spectra, the major elements identified were carbon (C1s) followed by oxygen (O1s) with a negligible amount of nitrogen, as expected [19]. Results are presented in Table III.2.

As far as the O/C ratio is concerned, it has to be pointed out that initial ratio of 0.23 was slightly increased to 0.27 due to the wet/dry cycling treatment. This could be attributed to the loss of lignin during the treatment process, since O/C ratios have been previously related to the amount of lignin in the literature [20].

Further treatment with low pressure Ar-plasma and air corona plasma increased O/C ratios, in agreement with previous work [21]. In general terms, plasma treatments produced an enhancement of the surface reactivity due to free-radicals, and/or energetic and reactive states of surface atoms. As a result, more oxygen atoms could be attached to the surface in post-plasma oxidation processes. In this case, Ar-treatments showed higher effectiveness of surface oxidation in the samples of the study. However, some inconsistencies were found in the Ar-plasma samples. With increasing treatment time, the O/C ratios were expected to increase, but samples NW C-Ar10 and NW C-Ar30 did not follow the expected trend. This

could be associated with the aging of the treatment [9,10] produced due to unavoidable contact with the ambient air during storage and a longer time delay between preparation and the XPS analysis. For that reason, samples NW C-Ar10 and NW C-Ar30 were not considered for further analysis of XPS results. For air corona plasma-treated samples, NW C-Cr20 and NW C-Cr1010 had similar results; therefore, only NW C-Cr1010 was considered for further XPS analysis.

Table III.2. Elemental composition percentage and oxygen to carbon (O/C) ratios for all the nonwoven (NW) samples obtained by X-ray photoelectron spectroscopy (XPS).

Reference	Elemental Composition (Atomic %)			O/C Ratio
	C1s	O1s	N1s	
NW SC	80.9	18.4	0.7	0.23
NW C	78.2	20.8	1.1	0.27
NW C-Et10	93.6	6.4		0.07
NW C-Ar5	65.4	33.4	1.2	0.51
NW C-Ar10	72.0	27.0	1.0	0.37
NW C-Ar20	61.5	37.3	1.2	0.61
NW C-Ar30	70.4	28.6	0.9	0.41
NW C-Ar5-Et5	80.3	18.7	1.0	0.23
NW C-Ar5-Et10	94.8	5.2		0.05
NW C-Cr20	73.9	25.0	1.1	0.34
NW C-Cr1010	72.9	26.0	1.2	0.36
NW C-Cr1010-Et10	93.9	6.2		0.07

When further treatment with low pressure Et-plasma was performed, the C and H elements of the ethylene gas were expected to cover the surface, producing an increase of

C1s, a reduction of O1s—note the drastic reduction of the O/C ratios—, and even the fading of N1s for all samples treated with a final 10 min Et-plasma. This indicates that the plasma polymerization would have achieved good coverage of the fibres.

The analysis of high resolution spectrum for C1s revealed two kinds of composition (Figure III.7) of the three main peaks—for the samples treated with 10 min of Et-plasma—or four main peaks—for the rest of samples—. Those peaks were found at characteristic bending energies, corresponding with the results in the literature [19–21]: C1, which is mainly associated with C–C and C–H bonds, was found at 284.9 ± 0.2 eV; C2, associated with C–OH and C–O–C bonds, at 286.5 ± 0.4 eV; C3, associated with C=O and O–C–O bonds, at 288.4 ± 0.3 eV; and finally, C4, associated with O–C=O bonds, at 289.7 ± 0.5 eV. For comparative purposes, C1, C2, C3 and C4 peaks of all samples are shown in Figure III.8. Differences in the height of these peaks revealed information about the loss or gain of specific bonds, and was thus compared with the reaction mechanisms to plasma treatments suggested in the literature [9,22].

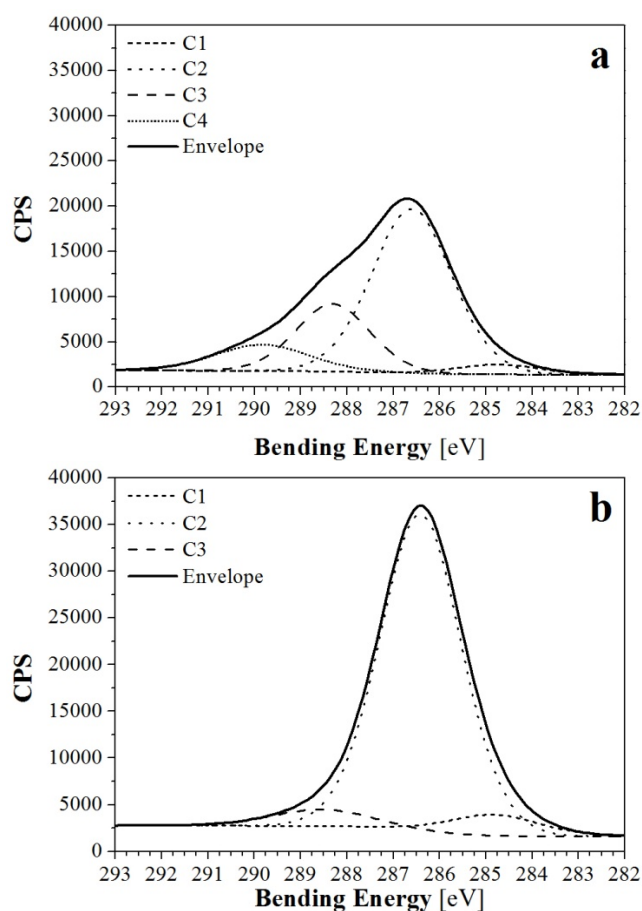


Figure III.7. Deconvoluted curves of XPS C1s peaks of (a) NW C-Cr1010; and (b) NW C-Cr1010-Et10 samples. CPS stands for counts per second as a measure of the intensity.

No significant differences between NW SC and NW C samples were found. Comparison of C4 and C1 peaks (Figure III.8-C4 and Figure III.8-C1, respectively) showed equally low contents of O=C=O bonds and very similar contents for C-C linkages, respectively. Only a slight difference in C2 (Figure III.8-C2) and C3 (Figure III.8-C3) was found, showing lower C-OH and higher C=O and O-C-O contents for the treated sample, which could correspond to higher oxidation.

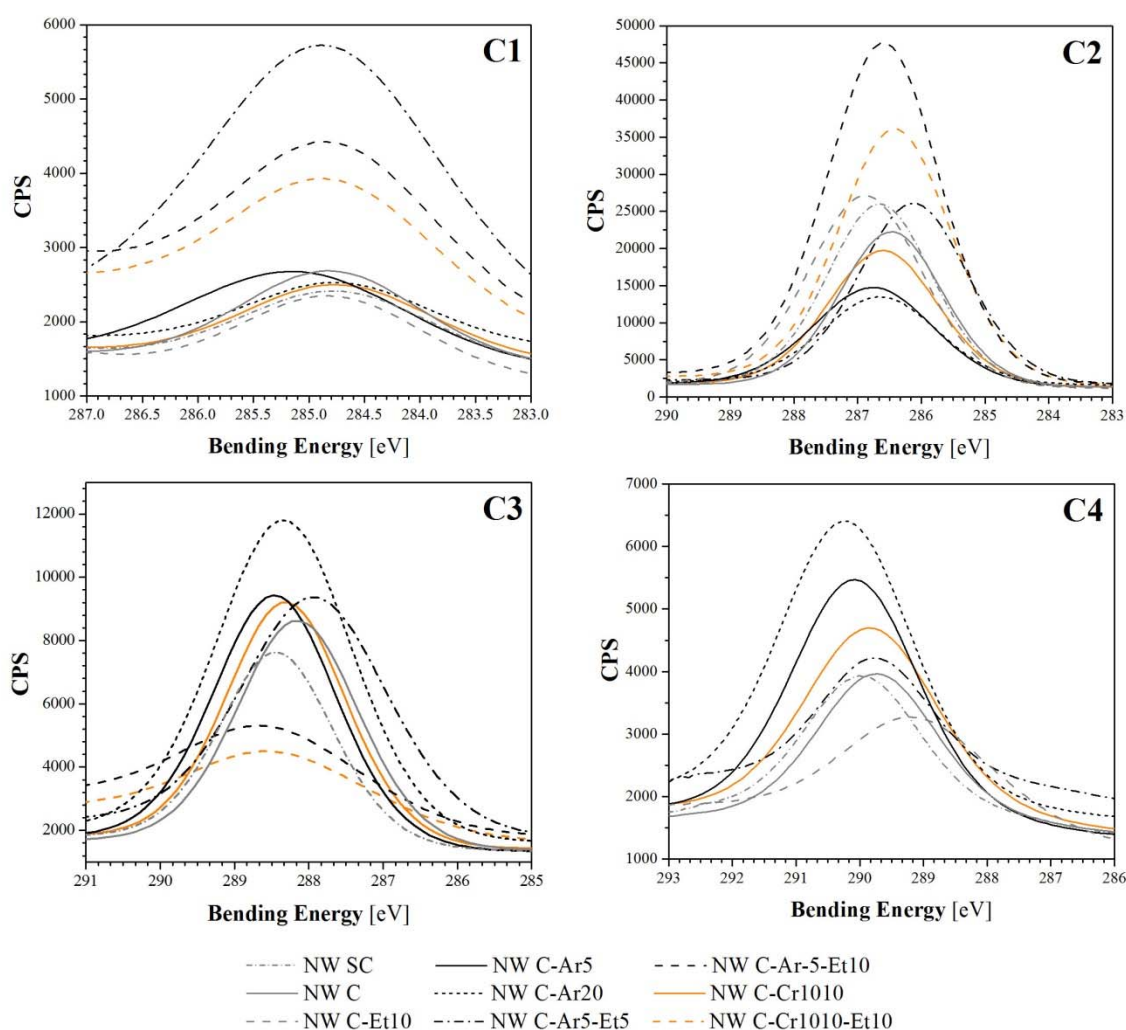


Figure III.8. Comparative of the C1s peaks found in the deconvolution curves for the C1, C2, C3 and C4 peaks of all samples.

For low pressure Ar-plasma and air corona plasma treatments, similar trends were found, despite Ar-plasma treatments being more effective and samples revealing higher oxidation. On the one hand, Ar-plasma treatment of cellulosic fibres has been suggested to produce the cleavage of C-C bonds, which generates active groups capable of reacting with oxygen in

post-plasma oxidation, thus leading to the formation of C=O and O–C–O groups [22], but also to a loss of C–OH groups. This would explain the lower C–OH curves in Figure III.8-C2 and the higher C=O and O–C–O curves in Figure III.8-C3 for the Ar-plasma-treated samples. On the other hand, the modification produced by the air corona plasma could be associated with the oxygen plasma reaction, since oxygen is the second major component in air. In this case, oxygen plasma has been associated with more intense C–O–C scission reactions and some cross-linking, thus producing a decrease in the C–OH and C–O–C peaks and an increase of O–C–O bonds [22,23]. Therefore, the results obtained for C=O and O–C–O groups in Figure III.8-C3 would confirm the post-plasma oxidation for Ar-treated samples and possible small cross-linking in the air corona plasma-treated samples.

Moreover, all samples presented similar contents of C–C and C–H bonds (Figure III.8-C1), with the exception of samples NW C-Ar5-Et5, NW C-Ar5-Et10 and NW C-Cr1010-Et10, which showed higher contents of C–C and C–H bonds, probably due to the effect of ethylene plasma polymerization. In this sense, the ethylene layer showed the expected good adhesion, and also revealed minor oxidation of the samples. However, for the NW C-Et10 sample, the adhesion of this ethylene layer is expected to be worse due to the lack of a previous argon or corona activation step. This could explain the differences in the results for this sample with respect to the other Et-plasma-treated samples.

Finally, the O–C=O bonds (Figure III.8-C4) should also be attributed to oxidation products, and, therefore, samples with oxidation presented high curves, while those with the ethylene layer did not show any signals.

The analysis of the O1s spectrum revealed differences between those samples with large exposure to Et-plasma and the rest of the samples. On the one hand, all samples treated for 10 min with Et-plasma presented a deconvolution with two peaks of lower intensity than the rest of the samples, at 534.0 ± 0.3 eV (O2) and 535.3 ± 0.2 eV (O3). Thus, they were associated to –O–C bonds and to absorbed water, respectively. As an example, the deconvoluted curves for the sample NW C-Ar5-Et10 have been represented in Figure III.9b. On the other hand, the rest of the samples presented also a deconvolution of two peaks: one of lower intensity found at 533.1 ± 0.2 eV (O1), and other of higher intensity found at 534.6 ± 0.2 eV (O2). In this case, the peaks were associated to –C=O and –O–C, respectively. As an example, the deconvoluted curves for the sample NW C-Ar5 have been represented in Figure III.9a.

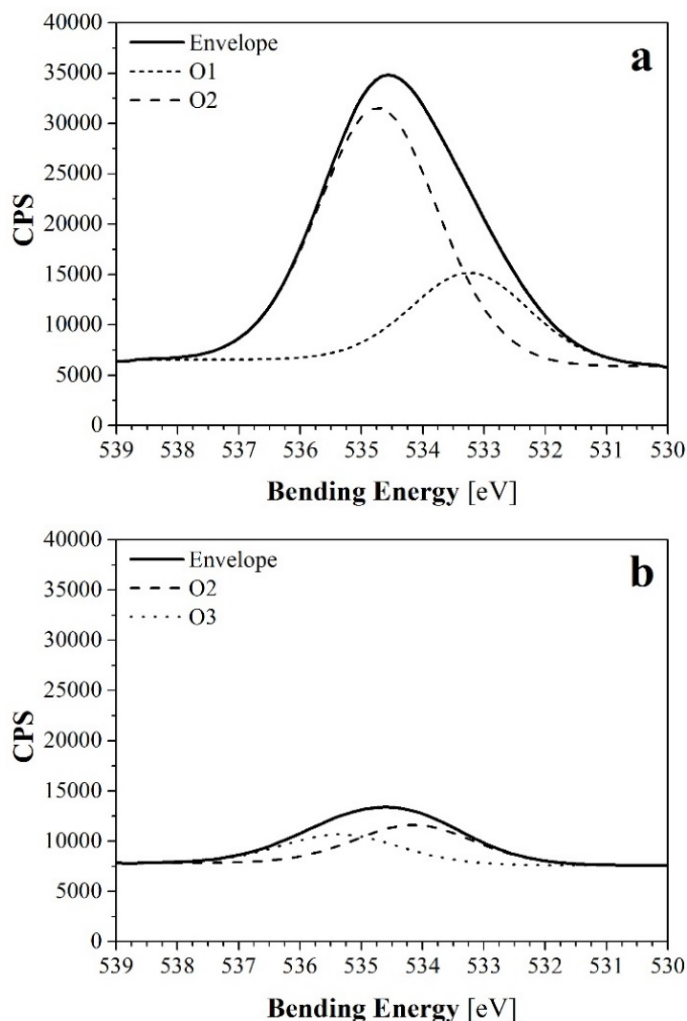


Figure III.9. Deconvoluted curves of XPS O1s peaks of (a) NW C-Ar5; and (b) NW C-Ar5-Et10.

The presence of $-O-C$ bonds has to be related both to cellulose's own nature and to the *in situ* and post-plasma oxidation phenomena. On the one hand, for the fibres treated with Et-plasma, the fact that its intensity is clearly lower—see the O2 peaks in Figure III.9—is consistent with the C1 results, since the ethylene plasma polymerization would be hiding the fibre and avoiding the oxidation. The water presence related to O3 in these samples can be due to moisture absorption. On the other hand, for the rest of the samples, the intensities for the O2 peaks showed an increasing trend: first the untreated and the wet/dry cycled samples, then the corona plasma-treated samples, and finally the samples treated with Ar-plasma, which presented the higher intensities. A similar trend was observed in the O1 peak. In general terms, the larger intensities for those peaks can be related to the surface activation produce by the plasma treatments, what helped the *in situ* or post-plasma oxidation to fix the oxygen atoms to the fibres' surface. The Ar-plasma treatment showed to be more effective

than the corona plasma-treatment. In addition, the larger presence of $-C=O$ groups in Ar-plasma treated samples—when compared to the original NW—is consistent with the results obtained for the C1s analysis.

III.3.2. Wetting Properties

III.3.2.1. Water Retention Values

As shown in Table III.3 and, as expected, the water retention value (WRV) decreased significantly after performing the wet/dry cycling treatment on the fabrics. Although high standard deviations of the values denote a certain irregularity that can be attributed to both the fibres and the treatments, the WRV were clearly reduced from $33.0\% \pm 1.7\%$ for the untreated sample, and to half of this—average of $15.1\% \pm 6.4\%$ of water retention—in all samples treated with the wet/dry cycling. This irreversible loss of water retention capacity and swelling, as a result of the wet/dry cycling, is related to the collapse and hardening of the outer walls of fibres [24].

Further plasma treatments did not show significant effects, since the variations presented were smaller than the deviations.

III.3.2.2. Moisture Regain

The moisture regain values of the samples ranged from 5.3% to 3.9%, with standard deviations of around 0.2. The highest value (5.3%) was found for the untreated NW (NW SC). After the wet/dry cycling treatment, there was a reduction in moisture regain, with a value of 4.4% for the NW C sample. This decrease is consistent with previous research, since the fiber is compacted, therefore presenting greater difficulty in absorbing any moisture present in the air.

Further plasma treatments helped to slightly reduce these values, which were similar in all cases, to around 4.1% moisture regain. No clear differences between the moisture regain of Ar-plasma and corona plasma samples were observed, or for further treatment with Et-plasma. Only in the case of the lowest value could a clear difference between the moisture regain of the previous step—4.4% for the NW C sample—and the further treatment with Et-plasma—3.9% for NW C-Et10—be observed, thus indicating that ethylene plasma polymerization helped to reduce the water uptake of the fibres, as expected for the creation of a more hydrophobic surface.

Table III.3. Characterization results for NW. WRV: water retention values; MR: moisture regain; CA: contact angle; At: absorption time; F_R: breaking force; ε_R: strain at break.

Reference	WRV (%)	MR (%)	CA (°)	At	F _R (N)	ε _R (%)
NW SC	33.0 ± 1.7	5.3	115	>1 h	12.0 ± 0.4	4.7 ± 2.2
NW C	14.8 ± 7.3	4.4	116	>1 h	11.4 ± 5.0	39.8 ± 13.0
NW C-Et10	10.8 ± 4.2	3.9	116	>1 h	12.7 ± 3.9	47.6 ± 0.8
NW C-Ar5	16.0 ± 5.8	4.0	108	30 min	14.9 ± 6.9	52.6 ± 11.5
NW C-Ar10	16.5 ± 9.0	4.2	94	15 min	15.8 ± 0.6	58.7 ± 2.0
NW C-Ar20	15.9 ± 6.4	4.2	94	36 s	16.7 ± 0.2	47.4 ± 9.8
NW C-Ar30	18.9 ± 5.3	4.0	83	4s	13.5 ± 3.7	81.0 ± 11.8
NW C-Ar5-Et5	14.1 ± 7.5	4.1	117	>1 h	17.8 ± 5.7	47.9 ± 11.2
NW C-Ar5-Et10	12.2 ± 6.9	4.1	116	>1 h	29.0 ± 1.6	53.2 ± 0.8
NW C-CR1010	17.2 ± 5.9	4.2	80	50 ms	12.8 ± 2.0	41.7 ± 4.0
NW C-CR20	15.0 ± 8.1	4.1	74	5 ms	7.9 ± 1.1	56.9 ± 15.7
NW C-CR1010-Et10	15.0 ± 7.5	4.1	127	>1 h	28.7 ± 1.2	38.2 ± 2.4

III.3.2.3. Contact Angles

The initial contact angle of the untreated NW (NW SC) was around 115°, with completely hydrophobic behaviour, since the drop remained stable on the surface for more than 1 h. The wet/dry cycled sample (NW C) did not show large variation in the contact angle nor absorption time, and a further treatment with Et-plasma polymerization for 10 min (NW C-Et10) failed to produce any change in these parameters.

However, when the Ar-plasma was used after the wet/dry cycling, the contact angles and the time taken to absorb the deposited drop were increasingly reduced when the treatment was longer, which resulted in general hydrophilicity. For Ar-plasma treatments between 5 and 30 min, contact angles were progressively reduced up to 28° and the time required for absorption of the deposited drop was also reduced from more than 1 h—previous conditions to the Ar-plasma, corresponding to the NW C sample—by up to 4 s. Therefore, higher hydrophilicity was obtained, which is consistent with the results in the literature [10,12,13,21]. An increase in water affinity is produced due to oxidation of the surface. After the creation of reactive groups on the fibre surface, these groups tend to react with air to

form peroxide and other oxygen-containing groups [11,19,21,25–28]. The contact with air was unavoidable during manipulation after the plasma activation, and it was therefore expected that the adhesion of polar groups took place.

Nonetheless, for NW C-Ar5-Et5 and NW C-Ar5-Et10 samples, after a wet/dry cycling and 5 min treatment with Ar-plasma, the ethylene plasma polymerization took place on the surface of the NW fibres for 5 or 10 min. This led to the generation of a hydrophobic surface, which is consistent with the results in the literature [14], outbalancing the hydrophilicity generated with the previous step and recovering the initial contact angles ($\sim 116^\circ$) and absorption time (>1 h).

Similar results were observed for samples in which corona plasma was used, since oxidation species in the air used as plasma gas helped to form hydrophilic groups on the surface. Initial treatment with air corona plasma clearly increased the samples' water affinity, reducing both contact angles and the time required to absorb the water droplet compared to the results of the only wet/dry cycled samples (NW C). However, the further treatment of Et-plasma polymerization helped to seal the fibres' surfaces against water; as a result, both the contact angle and absorption time increased, corresponding to a more hydrophobic surface.

III.3.3. Thermal Stability

TGA was performed in all samples, obtaining similar curves in all cases—see selected examples in Figure III.10—; the main results are summarized in Table III.4.

From these curves, a slight improvement in stability due to the fibre treatment was observed between 250 and 350 °C, with the original NW SC presenting higher weight loss—around 10% higher—compared with all of the other treated samples. Between 375 and 650 °C, however, only small differences were observed, which were mainly attributed to the degradation of lignin [29]. On the other hand, between 675 and 750 °C, some differences were recorded, corresponding with the final residue. When comparing the untreated sample (NW SC) with the wet/dry cycled sample (NW C), an increase of the solid residue by 18% was recorded. Further treatments with Ar-plasma and Ar-plasma and Et-plasma did not present better results than the NW C sample. In fact, increasing the treatment time of Ar-plasma progressively reduced the solid residue, thus resulting in worse thermal stability, with results that were no better than those for the Et-plasma treatments. Nevertheless, corona treatment seemed to stabilize the fibres, since the solid residue was better than the

original value in all cases. The best result was obtained for the NW C-Cr1010 sample, in which the solid residue was almost double that of the NW SC sample.

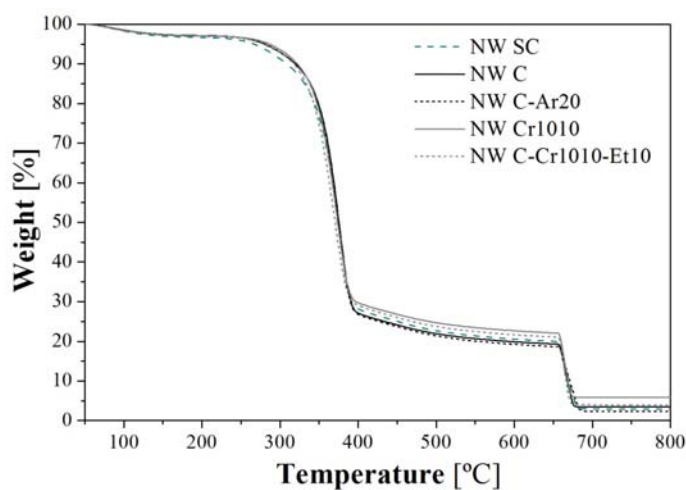


Figure III.10. TGA curves of selected samples. Curve NW C-Ar20 can be considered the representative curve for all Ar-plasma-treated samples (NW C-Ar5, NW C-Ar10, NW C-Ar30, NW C-Ar5-Et5, and NW C-Ar5-Et10) due to their similarity.

Table III.4. Thermogravimetric analysis (TGA) results for the NW.

Reference	Moisture Loss (%)	Inflection Point (°C) 2nd Step	Inflection Point (°C) 3rd Step	Solid Residue (%)
NW SC	2.9	375	677	2.9
NW C	2.5	376	677	3.5
NW C-Et10	2.6	376	675	2.3
NW C-Ar5	2.5	374	677	3.0
NW C-Ar10	2.5	375	676	2.6
NW C-Ar20	2.6	375	677	2.3
NW C-Ar30	2.5	376	674	2.5
NW C-Ar5-Et5	2.5	373	673	2.9
NW C-Ar5-Et10	2.5	372	673	2.9
NW C-CR1010	2.5	374	675	5.9
NW C-CR20	2.5	376	673	3.3
NW C-CR1010-Et10	2.5	369	672	3.9

Note: Moisture or water loss is attributed to the 1st inflection on the TGA curve up to 125 °C.

Despite the fact that only a small variation in thermal stability could be observed in this study, it is possible to find evidence of thermal stability improvement of natural cellulosic fibres by means of plasma treatment in the literature. Relvas et al. [29] found differences of around 14% in the residual weight after an equivalent TGA assay in quiscal fibres between 400 and 800 °C. The higher thermal stability was attributed to the formation of oxygen containing groups, which are more stable, thus avoiding complete degradation.

III.3.4. Fibre crystallinity

Plasma treatments are expected to modify only the fibres' surface. The XPS analysis confirmed that this chemical modification was achieved. However, in order to check that the plasma treatments did only affected its surface chemistry, the crystalline structure was observed by means of XRD. The results of the assays are shown in Figure III.11.

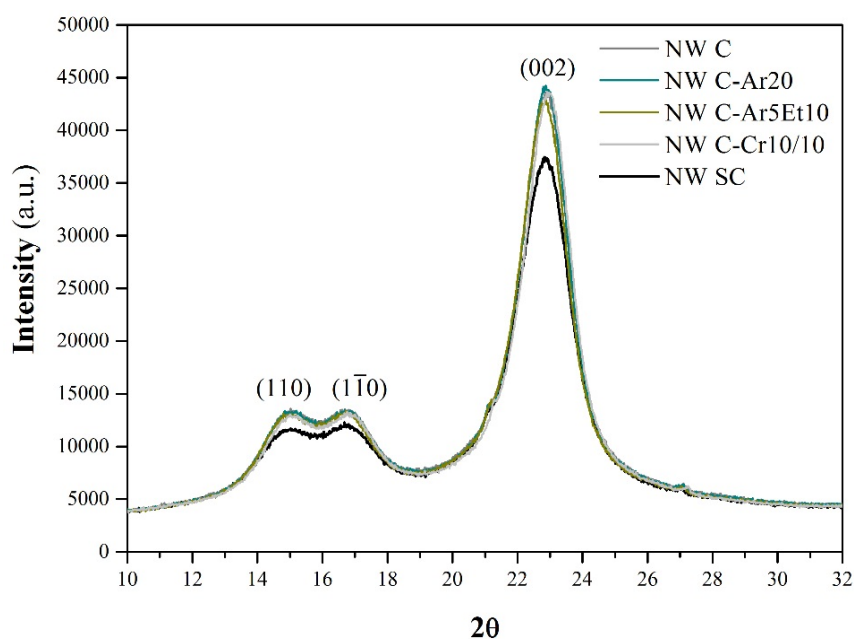


Figure III.11. X-ray diffraction patterns of some selected treated and the untreated samples.

On the one hand, a double-headed peak can be observed around $2\theta = 16^\circ$, that corresponds to (110) and ($1\bar{1}0$) crystallographic planes. The appearance of this double-headed peak is related to high cellulose content, as expected for flax fibers [30]. On the other hand, a higher peak that corresponds to the (002) crystallographic plane of cellulose can also be observed at $2\theta = 22.6^\circ$. The crystallinity indexes for the cellulose (CrI) have been calculated in order to compare the results. The untreated fibres (NW SC) presented a CrI of

81.0%. The rest of the samples, which have the wet/dry cycling treatment in common, presented very similar CrI, around $83.1\% \pm 0.4\%$, which is significantly higher.

The increase of the CrI after a wet/dry cycling treatment is associated with a higher packing on the cellulose crystals [31].

Furthermore, the XRD patterns in Figure III.11 also reveal that the different plasma treatments did not perform significant modifications on the fibres' crystallinity, since it affected mainly the fibres' surface. Despite some microstructural alterations of natural fibres due to plasma treatments having been reported in the literature (Morshed et al. [32] reported an increase on crystallinity and crystal size, for instance), this effect could not be observed in this study.

III.3.5. Mechanical properties

Tensile tests were performed to the NWs in order to evaluate the reinforcing capacities of their structures. Therefore, due to the NW nature, the mechanical behaviour is more similar to the deformation of a net than to the deformation of a solid, where the entanglement degree of the structure plays a key role. During the tensile test, the structure starts to elongate, the fibres are aligned and the entanglement points are stretched up to a maximum force. From this maximum point, the entanglement points are progressively broken, the strength progressively lost, and the aligned fibres start to progressively slide up to a total disentanglement of the section of the specimen. This means that the breakage is slow instead of abrupt; therefore, it is difficult to determine a breaking point. Due to that, this maximum has been considered as the breaking point. Breaking force and strain at break values, given in Table III.3, can be considered as design parameters. High standard deviations reveal the complexity of characterization of NW due to their unavoidable heterogeneity that is added to the irregular nature of the bast flax fibres used in the study.

In order to understand the results and only for comparative reasons, the breaking force values were normalized by the weight of the specimens (Figure III.12).

The wet/dry cycling did not reveal a clear effect in the NW resistance. However, the Ar-plasma seemed to increase the NW resistance when the treatment time was increased up to 20 min. The mechanical improvement of the NW structure after the plasma treatment can be attributed to higher inter-fibre friction. Plasma treatments enhance the roughness of the fibres' surface due to the etching, thus leading to higher friction between fibres [33]. Therefore, it becomes more difficult to separate the entangled fibres, which leads to

increased breaking force [34]. However, sample NW C-Ar30 presented a lower value, probably due to the stress concentration effect of the craters observed previously (Figure III.3). Plasma corona-treated samples presented similar or lower resistance than the original NW. In this case, despite higher roughness is also achieved, the fibre damage generated during the process outweighs the enhancement of the inter-fibre friction. Thus leads to higher fibre breaking during the tensile test, and therefore, to lower breaking forces. In Figure III.12, it can be observed that the results are clearly worse for the sample only treated in one side (NW C-Cr20), in which the treatment was clearly more aggressive (Figure III.4). Furthermore, in the literature, Morshed et al. [32] pointed out that oxygen plasma caused higher stress than argon plasma, which weakens the fibre, affecting its strength and durability; this is consistent with the effects observed in the current study, since oxygen plasma is comparable to the air corona plasma treatment used here.

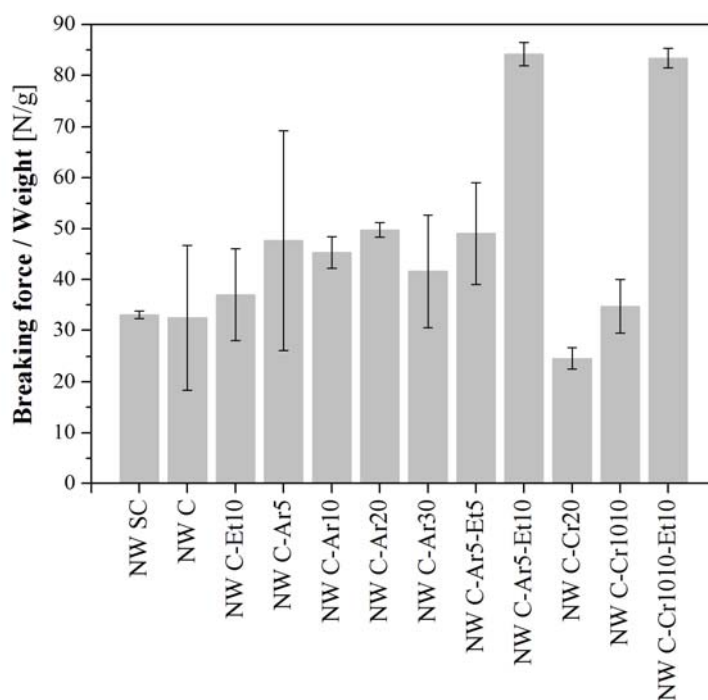


Figure III.12. Breaking force of the NW normalized by the sample weight for comparative purposes only.

Further Et-plasma treatment caused plasma polymerization on the surface of the fibres. In samples with a highly activated surface (after the Ar-plasma or corona plasma treatments), the ethylene created a polymeric layer with good adhesion, thus improving the mechanical properties of the NW with similar results in samples NW C-Ar5-Et10 and NW C-Cr10 10-Et10. Thinner ethylene layers due to shorter exposure times, such as those obtained in NW

C-Ar5-Et5, had less of a reinforcing effect. In the sample in which the surface was not activated (NW C-Et10), the reinforcing effect of the aforementioned layer was barely observed.

In what the strain is concerned with, a clear difference between the untreated samples (NW SC) and all the rest has been observed. The wet/dry cycling seems to be responsible of the higher flexibility and deformation of the NW structure. During the treatment, the cleaning of the fibres reduces the stiffness of the structure, thus helping to enhance the deformation capability of the net and, therefore, to achieve higher strain. Attending to the high irregularity of the fibres and the structure, no clear trends can be observed in to what effects the plasma treatments are concerned.

III.3.6. Considerations for Reinforcement Applications

Overall, on the one hand, it has been observed that wet/dry cycling is a good method to stabilize fibres against changes in humidity. Ar-treatment of up to 20 min is a good way to increase the hydrophilicity when considering NW for the reinforcement of cementitious matrices. Corona treatments would also be helpful in this sense but seem to produce greater damage to the fibres.

On the other hand, if conventional non-polar polymeric matrices—such as PP—are to be used, treatments of stabilization, activation and further plasma polymerization—such as those performed for NW C-Ar5-Et10—should be considered.

However, the requirements of the treatment will depend on the nature of the matrix to be used; some of the treatments presented here could be useful in the reinforcement of other more polar matrices.

III.4. Conclusions

In this study, different treatments were applied in flax-NW fabrics in order to evaluate their feasibility for composite reinforcement regardless of whether the matrix is hydrophobic or hydrophilic. On the one hand, the effectiveness of the wet/dry treatment in the achievement of greater stability against the water absorption of fibres has been observed. On the other hand, different strategies for the plasma treatments have shown very different results, thus indicating that the properties of the reinforcement can be adapted depending on the nature of the matrix. If hydrophilic reinforcement is required, Ar-plasma treatments have shown the most satisfactory results, even helping to enhance the mechanical properties of the NW. However, corona plasma treatments can also be considered, since a balance between cost-effectiveness and simplicity of the treatment can be achieved with fair properties. On the contrary, if hydrophobic reinforcement is required, the Et-plasma treatment of the flax-NW can be an interesting option, although a previous Ar-plasma or corona plasma treatment is recommended, since the latter seems to improve the effectiveness of the former.

References

- [1] Saheb DN, Jog JP. Natural fiber polymer composites: A review. *Adv Polym Technol* 1999;18:351–63. doi:10.1002/(SICI)1098-2329(199924)18:4<351::AID-ADV6>3.3.CO;2-O.
- [2] Thomas S, Pothan LA. *Natural Fibre Reinforced Polymer Composites. From Macro to Nanoscale*. Paris: Old City Publishing; 2009.
- [3] Faruk O, Bledzki A, Fink H, Sain M. Biocomposites reinforced with natural fibers: 2000–2010. *Prog Polym Sci* 2012;37:1552–96. doi:10.1016/j.progpolymsci.2012.04.003.
- [4] Yan L, Chouw N, Jayaraman K. Flax fibre and its composites – A review. *Compos Part B Eng* 2014;56:296–317. doi:10.1016/j.compositesb.2013.08.014.
- [5] Ardanuy M, Claramunt J, Toledo Filho RD. Cellulosic fiber reinforced cement-based composites: A review of recent research. *Constr Build Mater* 2015;79:115–28. doi:10.1016/j.conbuildmat.2015.01.035.
- [6] Claramunt J, Ardanuy M, García-Hortal JA, Filho RDT. The hornification of vegetable fibers to improve the durability of cement mortar composites. *Cem Concr Compos* 2011;33:586–95. doi:10.1016/j.cemconcomp.2011.03.003.
- [7] Ardanuy M, Claramunt J, Ventura H, Manich AM. Effect of Water Treatment on the Fiber–Matrix Bonding and Durability of Cellulose Fiber Cement Composites. *J Biobased Mater Bioenergy* 2015;9:1–7. doi:10.1016/j.jbmb.2015.1545.
- [8] Inagaki N. *Plasma Surface Modification and Plasma Polymerization*. Taylor & Francis; 1996.
- [9] Shishoo R. *Plasma Technologies for Textiles*. Elsevier Science; 2007.
- [10] Sabharwal HS, Denes F, Nielsen L, Young RA. Free-radical formation in jute from argon plasma treatment. *J Agric Food Chem* 1993;41:2202–7. doi:10.1021/jf00035a072.
- [11] Wang CX, Qiu YP. Two sided modification of wool fabrics by atmospheric pressure plasma jet: Influence of processing parameters on plasma penetration. *Surf Coatings Technol* 2007;201:6273–7. doi:10.1016/j.surfcoat.2006.11.028.
- [12] Samanta KK, Jassal M, Agrawal AK. Improvement in water and oil absorbency of textile substrate by atmospheric pressure cold plasma treatment. *Surf Coatings Technol* 2009;203:1336–42. doi:10.1016/j.surfcoat.2008.10.044.
- [13] Zille A, Oliveira FR, Souto AP. Plasma Treatment in Textile Industry. *Plasma Process Polym* 2014;n/a-n/a. doi:10.1002/ppap.201400052.
- [14] Lee SG, Choi S-S, Park WH, Cho D. Characterization of surface modified flax fibers and their biocomposites with PHB. *Macromol Symp* 2003;197:089–100. doi:10.1002/masy.200350709.
- [15] Aguilar-Rios A. Improving the bonding between henequen fibers and high density polyethylene using atmospheric pressure ethylene-plasma treatments. *Express Polym Lett* 2014;8:491–504. doi:10.3144/expresspolymlett.2014.53.
- [16] Ventura H, Ardanuy M, Capdevila X, Cano F, Tornero JA. Effects of needling parameters on some structural and physico-mechanical properties of needle-punched nonwovens. *J Text Inst* 2014;1–11. doi:10.1080/00405000.2013.874628.
- [17] Segal L, Creely JJ, Martin AE, Conrad CM. An Empirical Method for Estimating the Degree of Crystallinity of Native Cellulose Using the X-Ray Diffractometer. *Text Res J* 1959;29:786–94. doi:10.1177/004051755902901003.

- [18] Xu X, Wang Y, Zhang X, Jing G, Yu D, Wang S. Effects on surface properties of natural bamboo fibers treated with atmospheric pressure argon plasma. *Surf Interface Anal* 2006;38:1211–7. doi:10.1002/sia.2378.
- [19] Bozaci E, Sever K, Sarikanat M, Seki Y, Demir A, Ozdogan E, et al. Effects of the atmospheric plasma treatments on surface and mechanical properties of flax fiber and adhesion between fiber-matrix for composite materials. *Compos Part B Eng* 2013;45:565–72. doi:10.1016/j.compositesb.2012.09.042.
- [20] Johansson L-S, Campbell JM, Koljonen K, Stenius P. Evaluation of surface lignin on cellulose fibers with XPS. *Appl Surf Sci* 1999;144–145:92–5.
- [21] Yuan X, Jayaraman K, Bhattacharyya D. Effects of plasma treatment in enhancing the performance of woodfibre-polypropylene composites. *Compos Part A Appl Sci Manuf* 2004;35:1363–74. doi:10.1016/j.compositesa.2004.06.023.
- [22] Hua ZQ, Sitaru R, Denes F, Young RA. Mechanisms of oxygen- and argon-RF-plasma-induced surface chemistry of cellulose. *Plasmas Polym* 1997;2:199–224. doi:10.1007/BF02766154.
- [23] Johansson K. Plasma modification of natural cellulosic fibres. In: Shishoo R, editor. *Plasma Technol. Text.*, Cambridge: Woodhead Publishing Limited; 2007, p. 247–81.
- [24] Claramunt J, Ardanuy M, García-Hortal JA. Effect of drying and rewetting cycles on the structure and physicochemical characteristics of softwood fibres for reinforcement of cementitious composites. *Carbohydr Polym* 2010;79:200–5. doi:10.1016/j.carbpol.2009.07.057.
- [25] Wang B, Sharma-Shivappa RR, Olson JW, Khan SA. Production of polyhydroxybutyrate (PHB) by *Alcaligenes latus* using sugarbeet juice. *Ind Crops Prod* 2013;43:802–11. doi:10.1016/j.indcrop.2012.08.011.
- [26] Wang C, Chen J-R. Studies on surface graft polymerization of acrylic acid onto PTFE film by remote argon plasma initiation. *Appl Surf Sci* 2007;253:4599–606. doi:10.1016/j.apsusc.2006.10.014.
- [27] Morent R, De Geyter N, Verschuren J, De Clerck K, Kiekens P, Leys C. Non-thermal plasma treatment of textiles. *Surf Coatings Technol* 2008;202:3427–49. doi:10.1016/j.surfcoat.2007.12.027.
- [28] Keller A. Compounding and mechanical properties of biodegradable hemp fibre composites. *Compos Sci Technol* 2003;63:1307–16. doi:10.1016/S0266-3538(03)00102-7.
- [29] Relvas C, Castro G, Rana S, Fangueiro R. Characterization of Physical, Mechanical and Chemical Properties of Quiscal Fibres: The Influence of Atmospheric DBD Plasma Treatment. *Plasma Chem Plasma Process* 2015. doi:10.1007/s11090-015-9630-0.
- [30] Tserki V, Zafeiropoulos NE, Simon F, Panayiotou C. A study of the effect of acetylation and propionylation surface treatments on natural fibres. *Compos Part A Appl Sci Manuf* 2005;36:1110–8. doi:10.1016/j.compositesa.2005.01.004.
- [31] Fang L, Catchmark JM. Structure characterization of native cellulose during dehydration and rehydration. *Cellulose* 2014;21:3951–63. doi:10.1007/s10570-014-0435-8.
- [32] Morshed MM, Alam MM, Daniels SM. Plasma Treatment of Natural Jute Fibre by RIE 80 plus Plasma Tool. *Plasma Sci Technol* 2010;12:325–9. doi:10.1088/1009-0630/12/3/16.
- [33] Jazbec K, Šala M, Mozetič M, Vesel A, Gorjanc M. Functionalization of Cellulose Fibres with Oxygen Plasma and ZnO Nanoparticles for Achieving UV Protective Properties. *J Nanomater* 2015;2015:1–9. doi:10.1155/2015/346739.

- [34] Pivec T, Persin Z, Kolar M, Maver T, Dobaj A, Vesel A, et al. Modification of cellulose non-woven substrates for preparation of modern wound dressings. *Text Res J* 2014;84:96–112. doi:10.1177/0040517513483855.

CHAPTER IV

**MECHANICAL PERFORMANCE AND AGING
OF PHB/FLAX FABRIC COMPOSITES**

CHAPTER CONTENTS

Abstract	193
IV.1. Introduction.....	195
IV.2. Experimental section.....	197
IV.2.1. Materials	197
IV.2.2. Sample preparation.....	197
IV.2.2.1. Production and treatment of the reinforcements.....	197
IV.2.2.2. Composite fabrication	197
IV.2.3. Hydrothermal aging.....	198
IV.2.3.1. Kinetics of the water absorption	198
IV.2.4. Characterization of the composites	199
IV.2.4.1. Tensile test	199
IV.2.4.2. Thermal characterisation.....	199
IV.2.4.3. Morphologic characterisation.....	199
IV.3. Results and discussion.....	200
IV.3.1. Water uptake and kinetics of water absorption.....	200
IV.3.2. Analysis of the mechanical performance	203
IV.3.2.1. Macromechanical modelling.....	203
IV.3.2.2. Mechanical behaviour of the unaged samples	205
IV.3.2.3. Effects of aging on composites' mechanical properties	206
IV.3.3. Thermal characterisation	207
IV.3.4. Aging effect on the morphology of the composites	209
IV.4. Conclusions	211
References	212

Abstract

This research analyses the effect of hydrothermal aging on the water uptake and mechanical performance of biocomposites based on polyhydroxybutyrate (PHB) and flax fibre reinforcement in the form of nonwoven (NW) fabrics. The effectiveness of various surface treatments—wet/dry cycling (C), argon plasma (Ar), ethylene plasma and combinations—of these NW in the improvement of the mechanical properties of the composites is also evaluated. The water uptake during aging was analysed at both room temperature and 65 °C. Moreover, the composites were characterised before and after the aging to determine its effects on the morphology, thermal behaviour and tensile properties. It was found that the water diffusion was mainly influenced by the fibre content, and no significant differences were found in the effects of the NW treatments. Although the highest tensile stiffness and strength was found for the composites prepared with the Ar-treated NW, the C treatment was the most effective to prevent the loss of tensile performance after aging.

IV.1. Introduction

Composites of biopolymeric matrix and reinforcement of natural cellulosic fibres are of special interest because of their environmentally beneficial properties [1–3].

Concerning the thermoplastic matrices, biopolymers such as starch, polylactic acid (PLA) or polyhydroxyalkanoates (PHAs) are very common [4–6]. The latter are a family of bacterial polyesters [7–9] obtained from renewable resources, that are biodegradable and of interest for a wide range of applications [8,9], although their current high price—compared to commodity polymers—limits their commercial use.

The addition of cellulosic bast fibres—such as flax: renewable, biodegradable, with good mechanical properties, low density and low cost—as reinforcement in a PHA matrix leads to a completely biodegradable solution with increased mechanical performance and an expected lower cost. This natural fibre reinforcement can be applied in several forms: short fibres, woven fabrics, multiaxial fabrics or nonwoven fabrics among others. The use of nonwoven (NW) fabrics is interesting owing to their low production costs. Besides, this kind of reinforcement can be easily incorporated via film stacking methods.

Nonetheless, such natural fibre reinforcements present two main drawbacks in polymeric matrix: the poor fibre–matrix adhesion, and the sensitivity to water due to the hydrophilic nature of these fibres.

Regarding the fibre–matrix adhesion, in general terms, PHAs show better adhesion to cellulosic fibres than polyolefins, given the similar chemical nature of the fibres and the matrix, both with a polar character [9]. However, modification of the cellulosic fibres can further improve the compatibility with the PHA-matrix and reduce their sensitivity to water [4]. These techniques can be of diverse nature: chemical, physical, physical–chemical, or mechanical [10,11]. Among all these, plasma treatments are gaining interest for fibre treatment since they require no water, less energy, minimum use of chemical products and can be applied in continuous processes. Moreover, the plasma technologies can provide diverse surface properties by plasma-induced grafting, plasma polymerization or plasma etching without affecting the bulk properties of the fabrics. Plasma techniques have already been used for the increase of hydrophilicity and hydrophobicity of cellulosic fibres [12]. For instance, on the one hand, argon plasma has been reported to increase the surface roughness of flax fibres due to an etching effect, as well as to increase polar groups on the surface, thus enhancing the adhesion of the fibres to other polyester resins [13]. On the other hand, the use of ethylene plasma for treatment of flax fibres has been reported to increase the contact

angle—thus meaning higher hydrophobicity—and to enhance the interfacial strength between the fibres and polyhydroxybutyrate—PHB, a member of the PHAs' family—[14].

Regarding the water sensitivity, the moisture absorption in natural fibre-reinforced composites causes, among others, swelling of the fibres, leading to damage in the matrix and fibre debonding. Therefore, the efficiency of the load-transfer is reduced, thus influencing the mechanical performance of the composites and their long-term durability [15,16]. A possible treatment to decrease this effect is a wet/dry cycling treatment, since it is well known that this causes shrinkage and a reduction in the water retention values of the cellulosic fibres [17–19]. In this sense, hydrothermal aging is a tool to perform accelerated tests of water absorption in composites, which makes it possible to evaluate the degradation of the composites' properties. For this reason, this technique has been employed by many authors to study the effects of water absorption on the mechanical and thermal properties, molecular weight and morphology of natural fibre-reinforced composites [20–24]. However, to the author's knowledge, the evaluation of aging in PHA-based biocomposites, in which the reinforcement—of cellulosic fibres—is treated with combined wet/dry cycling and plasma treatments, has not yet been reported.

The aim of this study is to evaluate the effects of hydrothermal aging on the tensile and thermal properties of PHA-based composites reinforced with flax fibre NWs with various surface treatments. Moreover, the effectiveness of these treatments—wet/dry cycling (C), argon (Ar) plasma, ethylene (Et) plasma and some combinations—in the improvement of the mechanical properties is also evaluated.

IV.2. Experimental section

IV.2.1. Materials

Flax technical fibres with an average length of 6 cm were provided by Fibres Recherche Développement of the Technopole de l'Aube en Champagne (France). The biopolymer used as matrix was Mirel P3001 thermoforming grade provided by Metabolix (USA), designated hereafter as PHB. For plasma treatments, argon gas (99.999% of purity) and ethylene gas (of 99.99% purity) were acquired from Air Liquide España (Spain).

IV.2.2. Sample preparation

IV.2.2.1. Production and treatment of the reinforcements

NW fabric samples with a weight of 284 ± 23 g/m² and a thickness of 1.9 ± 0.1 mm were prepared on a DILO OUG-II-6 pilot plant of a double needle-punching machine, under the processing parameters determined in previous research [25].

The NW fabrics were further treated with wet/dry cycling (C), argon plasma (Ar) and ethylene plasma (Et) following the conditions used in previous research [26]. Briefly, the C treatment consists of 4 cycles of soaking the NW in distilled water under sonication and further oven-drying at 105 °C. The plasma treatments consist of placing the NW between the electrodes inside the plasma chamber, further pumping of the air until vacuum is achieved, and then the desired gas under constant flux is excited for a specified time by supplying energy to the electrodes. A total of 5 kinds of flax nonwoven fabrics were used as reinforcement, one of them in the original conditions, and the other four treated under the conditions specified in Table IV.1.

IV.2.2.2. Composite fabrication

The film stacking method was used to prepare biopolymer composites by means of a Remtex hot-plates press. The NW was placed between two 0.5 mm-thick PHB sheets, heated at 175 °C for 5 minutes and hot pressed under 10 tonnes at 175 °C for 5 minutes, followed by cooling under 10 tonnes at 30 °C for 10 minutes. 1 mm-thick composite sheets with an average fibre content of 21.1 ± 2.3 wt.% were obtained and named according to the reinforcement used in each sample. The composite sheets were machined to obtain standard dumbbell specimens to perform the tensile tests before and after aging in water.

The fibre fraction—in wt.%—was determined by extracting the PHB matrix in chloroform at 60 °C for 45 minutes. The precipitated fibres were washed 3 times with chloroform, dried at 105 °C for 6 h, cooled in a desiccator for 2 h and then weighed.

Table IV.1. Treatment conditions applied to the NW fabrics used as reinforcements.

Reference	Wet/dry treatment [cycles]	Argon plasma [min]	Ethylene plasma [min]
NW_Untreated	0	-	-
NW_C	4	-	-
NW_C-Et10	4	-	10
NW_C-Ar20	4	10 + 10	-
NW_C-Ar5-Et10	4	5	10

Note: Plasma treatments were applied to one side (n) or to both sides ($n + n$) of the NW, so each n value refers to treatment-time per side.

IV.2.3. Hydrothermal aging

A hydrothermal test was performed for aging evaluation on the composite samples and the matrix. The specimens for the hydrothermal tests were first weighed after drying at 50 °C for 24 h, and then immersed for 100 h in distilled water at 65 °C \pm 2 °C—around the matrix's heat deflection temperature at 1.8 MPa—or at room temperature (RT), around 23 °C. Three specimens per sample and temperature were used to determine the percentage of water uptake at the measuring time (M_t) and the water saturation capability (M_s). To that purpose, during the 100 h immersion, the specimens were regularly extracted from the water, gently wiped, and weighed to calculate the water uptake by means of Equation (IV.1):

$$M_t = [(m_t - m_0)/m_0] \cdot 100 \quad (\text{IV.1})$$

where m_0 refers to the mass of the dry sample and m_t refers to the mass of the wet sample at the measuring time. After each measurement, the specimens were immediately immersed again in water. M_s was determined as the saturation point in the water uptake curves.

IV.2.3.1. Kinetics of the water absorption

The analysis of the diffusion mechanism and kinetics was performed according to Fick's law. The diffusion mechanism can be revealed by the shape of the sorption curves—represented by Equation (IV.2), where k and n are constants—, since the value of the n

exponent reveals if the diffusion is—in a planar geometry—pseudo-Fickian or less-Fickian ($n < 0.5$), Fickian ($n = 0.5$), non-Fickian or anomalous ($0.5 < n < 1$), Case II ($n = 1$) or Super Case II ($n > 1$) [27,28].

$$M_t/M_s = kt^n \quad (IV.2)$$

The n and k values for each sample were determined by linear regression analysis, adjusting the experimental data to Equation (IV.3).

$$\log(M_t/M_s) = \log(k) + n \log(t) \quad (IV.3)$$

On the other hand, the diffusion coefficient (D) in Fick's model reveals the ability of the water molecules—in this case—to penetrate inside the composite structure. For specimens of a flat sheet geometry in earlier stages of the water sorption—thus meaning $M_t/M_s \leq 0.5$ —Equation (IV.4) can be used to estimate the D values:

$$D = \pi (\theta h/4M_s)^2 \quad (IV.4)$$

where h is the specimen thickness and θ is the slope of the initial portion of the absorption curve M_t against \sqrt{t} .

IV.2.4. Characterization of the composites

IV.2.4.1. Tensile test

Dumbbell test specimens were tested under tensile configuration using an Instron 5.500R6025 universal testing machine, under Standard ISO 527 1A conditions at a displacement rate of 5 mm/min. From the curves obtained, experimental values of stiffness (E) and tensile strength (σ_{\max}) were determined.

IV.2.4.2. Thermal characterisation

Thermogravimetric analysis (TGA) was performed in order to determine the effect of the addition of fibres and the aging on the thermal stability. The analyses were performed in a Mettler TGA/SDTA 861 equipment at a heating rate of 10 °/min from 30 °C to 600 °C under nitrogen atmosphere at a flow of 60 mL/min.

IV.2.4.3. Morphologic characterisation

Images of the surface of both aged and unaged specimens were obtained with a Jeol-820 SEM, and further compared in order to evaluate the damage produced by the hydrothermal aging test.

IV.3. Results and discussion

IV.3.1. Water uptake and kinetics of water absorption

As expected, hydrothermal tests revealed a higher water uptake of the composites when compared to the matrix due to the effect of the cellulosic fibres. As shown in Figure IV.1, the water saturation capability (M_s) was around 4–6% for all the composites, and around 0.5–1% for the neat matrix (PHB) at the aging temperatures studied. These values are consistent with the results found in previous research for composites with similar amounts of cellulosic fibres [22,23,29].

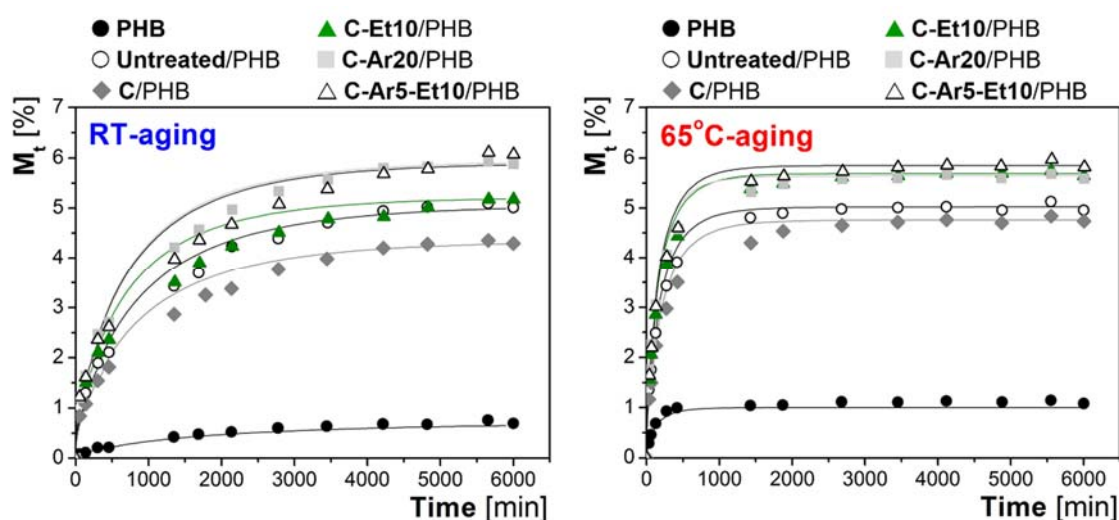


Figure IV.1. Water uptake (M_t) curves for the aging at RT (left) and at 65 °C (right). Solid lines—which describe a Fickian diffusion—have been presented to guide the eye.

The gradual rise in saturation mass with the increasing fibre weight fraction (Figure IV.2) reveals that the differences observed between the behaviour of the samples in Figure IV.1 are mainly due to the fibre content rather than to the effect of the surface treatments. In this sense, the treatments barely affected the water absorption of the composites. Lin et al. [30] studied wood-flour/PP composites and also observed a high dependence of the filler content on the moisture absorption. However, they applied coupling agents—to the matrix, and to the wood-flour as treatments—which improved the interfacial bonding, thus reducing the water uptake. Similar results were obtained by Joseph et al. [31] in sisal fibre/PP composites, where the moisture absorption increased with the fibre content, and decreased due to addition of coupling agents, thus attributed to an improved fibre/matrix adhesion. This latter could not be observed in this study, probably owing to a general better affinity of the

matrix—which presents few hydrophilic groups—with the flax fibres, which could be shielding the effect of the plasma treatments.

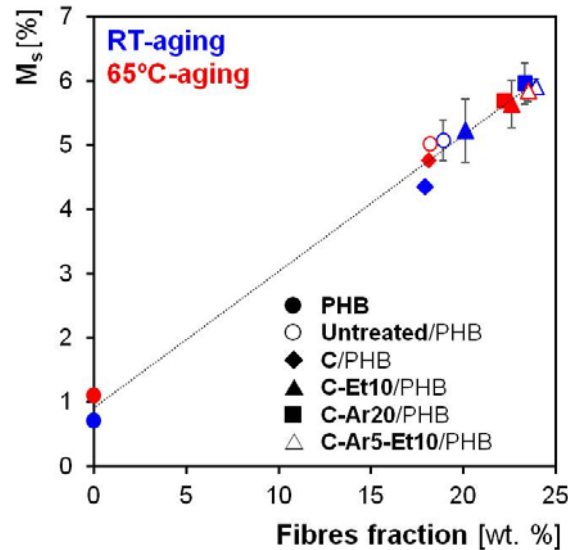


Figure IV.2. Saturation water uptake (M_s) results against average fibre content of each sample.

Symbol colours refer to the aging temperature: RT (blue) or 65 °C (red).

Regarding the kinetics of the water absorption, as expected, faster water absorption at higher temperatures was observed for all the materials (see Figure IV.1). As shown, the saturation of the curve—achievement of the M_s —was observed after 5500 minutes at RT, while only around 3500 minutes were required to reach it at 65 °C.

In order to determine the diffusion mechanism, the n exponents were estimated with good adjustment as revealed by the R^2 values presented in Table IV.2. For the PHB, the n values approached 0.5, thus pointing to a Fickian diffusion behaviour for the neat matrix, as shown by the good agreement between the experimental values and the corresponding curves for Fickian diffusion (Figure IV.1). However, the n values of the composites—similar to those found in the literature for similar composites [23,29,31]—were lower than 0.5. Therefore, a pseudo-Fickian diffusion mechanism is expected, meaning that the initial slope of water uptake persists for a shorter time than in Fickian diffusion [27], and hence the water uptake curves differ from this, as shown in Figure IV.1. On the other hand, the composites seemed to approach a Fickian behaviour with the increase of temperature.

The diffusion coefficients (D) were calculated with good adjustments according to the R^2 values presented in Table IV.2. In Figure IV.3, the D values for water diffusion at RT and 65 °C of the neat matrix and the composites are plotted against the fibre weight fraction.

Here, a high dependence on the fibre fraction is observed, while the effect of the NW treatments on the diffusion behaviour is not clear. Otherwise, the increase in the water temperature caused a general increase of the diffusion coefficient, attributed to a higher mobility of the polymeric chains, which leads to an easier penetration of the water molecules into the material. Regarding the differences between the composites and the matrix, at RT the water diffusion in the matrix was clearly lower than in the composites, while the opposite trend was observed at high temperatures. This could be ascribed to a higher deflection temperature for the composites. No explanation was found for that phenomenon, although similar results were observed in other studies [22].

Table IV.2. Water uptake values of: n and the adjusted R^2 ; saturation mass (M_s); slope of M_t vs \sqrt{t} curve (θ), diffusion coefficient (D) and the adjusted R^2 .

Sample reference	Aging T	$M_t/M_s = kt^n$		M_s [%]	$D = \pi(\theta h/4M_s)^2$		
		n	R^2		$\cdot 10^{-4} \theta$ [g/g·s ^{-0.5}]	$\cdot 10^{-12} D$ [m ² /s]	R^2
PHB	RT	0.5381	0.9486	0.71 ±0.04	0.130	0.65	0.9847
	65 °C	0.5032	0.9793	1.11 ±0.03	0.757	9.21	0.9977
Untreated /PHB	RT	0.3960	0.9828	5.07 ±0.31	1.330	1.35	0.9941
	65 °C	0.4570	0.9955	5.02 ±0.08	2.840	6.27	0.9998
C/PHB	RT	0.4009	0.9952	4.35 ±0.05	1.144	1.36	0.9964
	65 °C	0.4425	0.9914	4.76 ±0.07	2.544	5.61	0.9992
C-Et10 /PHB	RT	0.3533	0.9916	5.22 ±0.49	1.534	1.69	0.9931
	65 °C	0.4031	0.9934	5.64 ±0.36	3.559	7.83	0.9988
C-Ar20 /PHB	RT	0.3966	0.9966	5.95 ±0.32	1.717	1.62	0.9963
	65 °C	0.4259	0.9966	5.69 ±0.07	3.356	6.83	0.9994
C-Ar5-Et10/PHB	RT	0.3700	0.9953	5.91 ±0.11	1.697	1.61	0.9947
	65 °C	0.4252	0.9944	5.85 ±0.17	3.449	6.83	0.9998

Go to next page

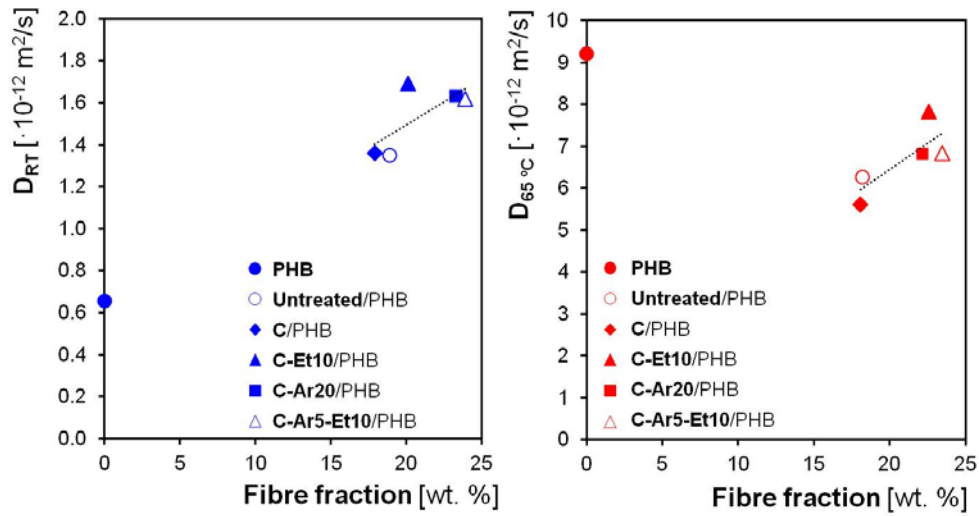


Figure IV.3. Diffusion coefficient at RT (left) and 65 °C (right) against average fibre content of each sample. The linear regression fitting for the composite samples has been included to guide the eye.

IV.3.2. Analysis of the mechanical performance

IV.3.2.1. Macromechanical modelling

For the composites under study, considering that the flax fibres have an average length of 6 cm, have a lumen (hollow section) and present a random in-plane distribution in the nonwoven fabric structure, two types of models have been considered as appropriate.

On the one hand, the Cox–Krenchel model (Equation (IV.5)) and the Kelly–Tyson model (Equation (IV.6)) can be used to predict for E_c and σ_c , respectively, since they include corrective factors for the fibre length (η_l and η_{LS}) and fibre orientation (η_o). These models consider only two phases in the composite ($V_f + V_m = 1$) and the E_c and σ_c are defined as:

$$E_c = \eta_l \eta_o V_f E_f + V_m E_m \quad (\text{IV.5})$$

$$\sigma_c = \eta_o \eta_{LS} V_f \sigma_f + V_m \sigma_m \quad (\text{IV.6})$$

where V_x is the volumetric fraction of the component, E_x is the elastic modulus, and σ_x is the maximum strength; and the subscripts for components are c for composite, f for fibre, and m for matrix.

However, in the composites prepared in this study, porosity can play an important role in reducing the mechanical properties. For that reason, other models that take into account the porosity ($V_f + V_m + V_p = 1$) can be used to predict E_c and σ_c [32]. Madsen et al., included a porosity-related factor $(1-V_p)^n$ in the modified rule of mixtures (Equation (IV.5)) to predict the stiffness of plant fibre composites [33]:

$$E_c = (\eta_l \eta_o V_f E_f + V_m E_m) \cdot (1 - V_p)^n \quad (\text{IV.7})$$

where the subscript p is for porosity, and n is a porosity efficiency exponent.

Similarly, the use of such term in Equation (IV.6) can be considered for σ_c prediction:

$$\sigma_c = (\eta_o \eta_{LS} V_f \sigma_f + V_m \sigma_m) \cdot (1 - V_p)^n \quad (\text{IV.8})$$

In this study, the stiffness and maximum strength values of the fibres and the matrix were determined by tensile testing: $E_f = 30.4$ GPa, $E_m = 1.6$ GPa, $\sigma_f = 730.2$ MPa. The σ_m required for composite modelling is the stress in the matrix at the failure strain of the fibre, which was determined from the tensile testing: $\sigma_m = 22.2$ MPa.

For the E_c and σ_c prediction with Equations (IV.7) and (IV.8), the volume fractions can be determined as:

$$V_p = 1 - \rho_c \cdot \left(\frac{W_f}{\rho_f} + \frac{(1 - W_f)}{\rho_m} \right) \quad (\text{IV.9})$$

$$V_f = \frac{\frac{W_f \cdot w_c}{\rho_f}}{v_c} \quad (\text{IV.10})$$

$$V_m = \frac{\frac{(1 - W_f) \cdot w_c}{\rho_m}}{v_c} \quad (\text{IV.11})$$

where ρ_x refers to the density of the component, W_f to the fibre weight fraction, and w_c is the weight of the composite sample and v_c its volume, geometrically determined.

Regarding the corrective factors:

η_l (Cox fibre length distribution factor) was calculated as:

$$\eta_l = \left[1 - \frac{\tanh(\beta L/2)}{\beta L/2} \right] \text{ where } \beta = \frac{2}{D} \left[2G_m / \left(E_f \ln \sqrt{\frac{\pi}{\chi_i V_f}} \right) \right]^{1/2} \quad (\text{IV.12})$$

considering: fibre diameter $D = 98$ μm , fibre length $L = 60$ mm, average $V_f = 0.19$, $\chi_i = 4$, $E_f = 30.4$ GPa, and $G_m = E_m / 2(1 + \nu)$ where $E_m = 1.6$ GPa and the Poisson's ratio $\nu = 0.4$; thus giving a η_l of 0.929.

η_o (Krenchel fibre orientation factor) was assumed to be 3/8 for in-plane random orientation of the fibres in E_c calculation [33–38], although a fitting value of $\eta_o = 0.2$ —with no physical meaning—was used for determination of σ_c [35–38].

η_{LS} (Kelly–Tyson’s fibre length efficiency factor) was calculated following Equation (IV.13), where the first term refers to fibres shorter than the critical length (L_c), and the second to those fibres longer than L_c .

$$\eta_{LS} = \frac{1}{V_f} \left(\sum_i \left[\frac{L_i V_i}{2L_c} \right] + \sum_j \left[V_j \left(1 - \frac{L_c}{2L_j} \right) \right] \right) \text{ where } L_c = \frac{\sigma_f D}{2\tau_y} \quad (\text{IV.13})$$

To that purpose, it was considered that all the fibres ($L = 60 \text{ mm}$) were longer than the critical length ($L_c = 35.8 \text{ mm}$)—thus meaning that $V_i = 0$ —, and they had an average $D = 98 \text{ }\mu\text{m}$, $\sigma_f = 730 \text{ MPa}$ and $\tau_y = 10 \text{ MPa}$ [36,39]; thus giving a η_{LS} of 0.702.

Finally, the porosity efficiency exponent n was set to 2 [33].

IV.3.2.2. Mechanical behaviour of the unaged samples

The experimental values of the stiffness and maximum strength of the unaged composite samples with respect to the fibre content are plotted in Figure IV.4.

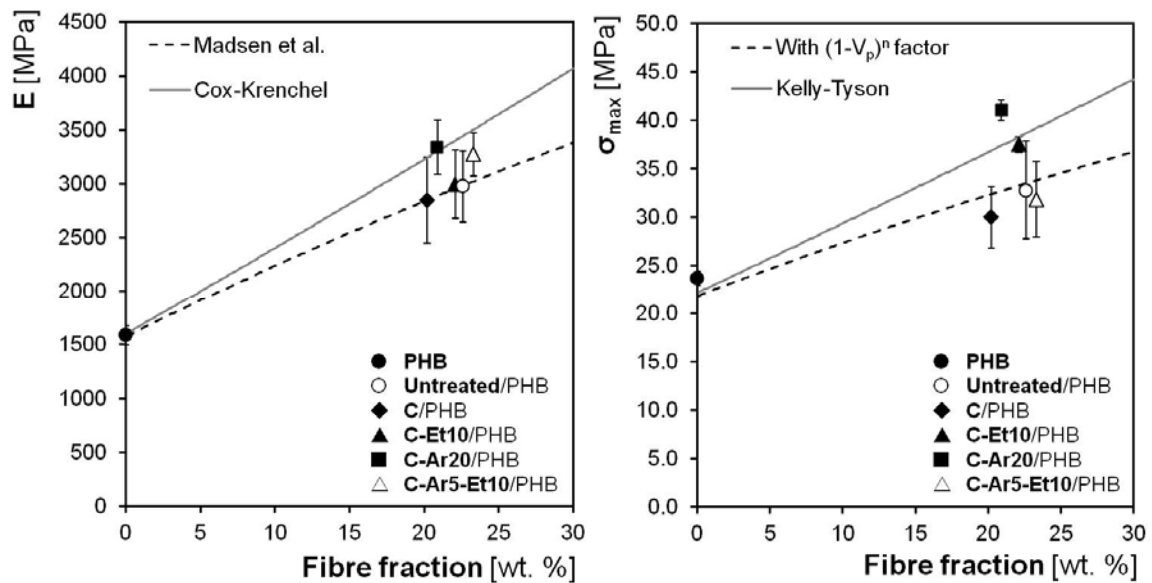


Figure IV.4. Stiffness (E) and tensile strength (σ_{max}) values for unaged samples (data points), comparing different models (lines).

The high standard deviations (SD) found were attributed to the irregular nature of the reinforcement. The predictions according to the aforementioned models are also included in Figure IV.4. Volume fractions in the models considering porosity were determined as proposed by Madsen et al. [33,40].

As shown, all the composites presented E values around 3 GPa, which is 100% higher than the stiffness of the neat PHB. This is attributed to the higher E values of the fibres with respect to the neat matrix. A similar stiffness increase has been obtained in other biocomposites of similar nature such as PHBV/wood fibres [41], PHBV/bamboo fibres [42] or PHBV/pineapple fibres [43]. On the other hand, the stiffness values seemed to be unaffected by the NWs' treatments. This was also observed in the literature for other modifications in cellulosic fibres [44,45]. Comparing the experimental results with the Cox–Krenchel and Madsen et al. models, it was found that the latter performs a more accurate prediction, since it considers the porosity.

Regarding the composite strength, the addition of the reinforcement led to a moderate increase in strength of nearly 25% with respect to the PHB, thus indicating a good interface between the fibres and the matrix. In the literature, the strength of other biocomposites has been reported to have very variable results with respect to the matrix's—both increased [43] and reduced [41,42,46]—, thus pointing to the importance of the fibre–matrix compatibility. Considering the SD, all the samples presented similar values around 30 MPa except the C-Ar20/PHB, which reached a σ_{\max} of 41.0 ± 1.1 MPa. The strength results presented much variability with respect to both models, attributed to the high sensitivity of the composite strength to the stress-transfer, which is difficult to model due to the irregular nature of the reinforcement structures.

Therefore, the NW C-Ar20 reinforcement yielded the best overall mechanical results on the composites, thus pointing to better stress-transfer. The argon plasma treatment in flax fibres is expected to produce an increase of polar groups such as $-\text{C}-\text{OH}$, $-\text{C}=\text{O}$, $-\text{COOH}$, which could be creating primary or secondary bonds with the hydroxybutyrate groups of the matrix. Also, the surface roughness produced by the plasma etching [26] could be contributing to a better wettability. All this could be improving the fibre–matrix interaction and hence the effectiveness of the reinforcement.

IV.3.2.3. Effects of the aging on the composites' mechanical properties

In Figure IV.5, the E and σ_{\max} values before and after the hydrothermal aging are compared. As can be seen, aging had a severe effect on all the composites—which suffered considerable loss of stiffness and strength—but barely affected the PHB, which presented even higher E and σ_{\max} values after aging. On the other hand, none of the models presented a

good prediction of the properties after aging, although the models considering the porosity were closer to the experimental values.

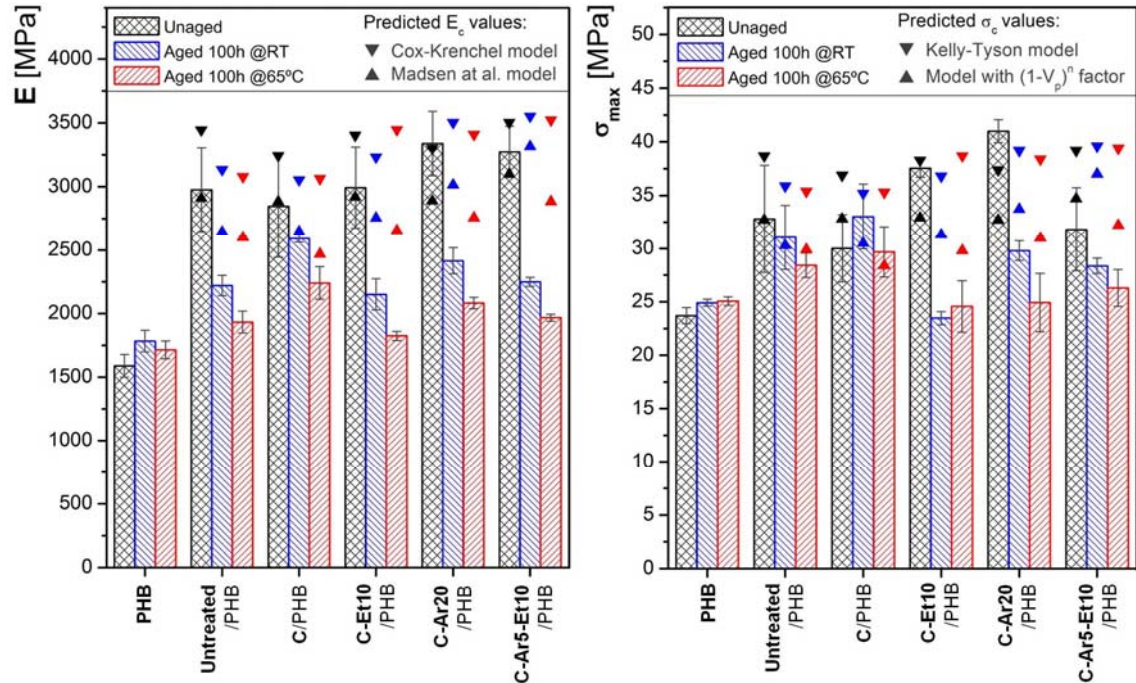


Figure IV.5. Stiffness (E) and tensile strength (σ) graphs comparing unaged and aged samples (bars), and models' predictions (points).

The loss in the mechanical properties was more severe for the higher aging temperature—especially in the σ —, owing to higher water uptake and damage—see section IV.3.4—, and reveals an impoverishment of the stress-transfer between the matrix and the fibres. This is explained by the swelling of the fibres, which produces microcracks in the fibre–matrix interface, debonding of the fibre and matrix damage [15]. However, the composite reinforced with the nonwoven subjected to a wet/dry cycling (C/PHB) seemed to have better resistance to aging, showing the lowest decrease in stiffness and equal values of strength after the hydrothermal testing. This is attributed to the effectiveness of the single treatment, given that the purpose of the wet/dry cycling is to stabilise the fibre against moisture variations [47].

IV.3.3. Thermal characterisation

Regarding the TGA, the matrix and the fibres presented a one-step decomposition around 295 °C and 375 °C, respectively, as can be observed in Figure IV.6.

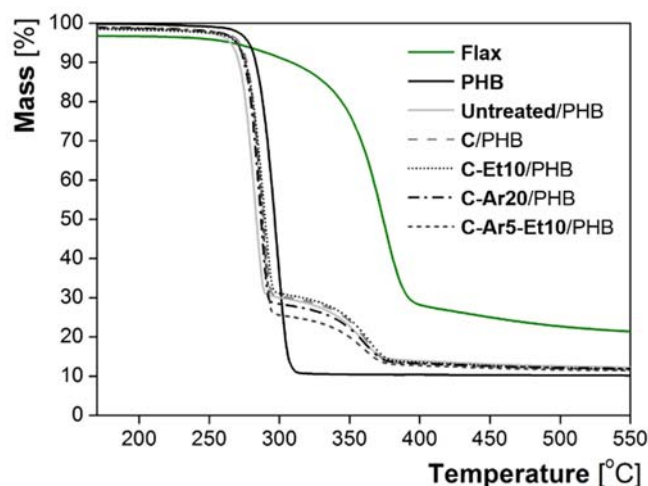


Figure IV.6. Comparison of TGA curves for all unaged samples.

The composites presented a two-step decomposition with two maximums at around 285 °C and 363 °C: the first maximum is associated with the degradation temperature (T_d) of the matrix and the second one (T_d') is associated with the degradation of the fibres. The TGA curves also revealed a weight loss between 30 °C and 170 °C, attributed to the moisture content (m_{loss}), which was clearly higher for the original fibres than for the PHB matrix, and of an intermediate range for the composites. The values are presented in Table IV.3.

Although the fibres presented a higher decomposition temperature, the mixture of both components led to composites with lower thermal resistance than the neat matrix. This was also observed in hemp/PP composites [48], doum fibre/LDPE composites [49], and wood-fibre/PHBV composites [50]. One possible explanation is a larger degradation of the PHB during the composite preparation, given that the films for film-stacking had to be first produced by hot-pressing. Another possibility would be that the presence of water—revealed by the moisture content obtained from the TGA curves—could be enhancing the hydrolytic degradation of the matrix.

The effect of the aging on the thermal properties was performed in selected samples: C/PHB and C-Ar20/PHB. On the one hand, an increasing trend in moisture content with aging was observed, which would be in accordance with the fibre debonding—thus promoting water storage in the interfaces—and hence, with the worsening of the mechanical properties. On the other hand, the T_d of the composites presented an increase with aging. The fibre–matrix interaction can accelerate the degradation process of the components, as observed by Araújo et al. [51]. Therefore, the increase of the thermal resistance with aging could be a consequence of a poorer interaction due to fibre debonding.

Table IV.3. Main parameters of the thermal characterisation

Sample	Aging	m_{loss} [%]	T_d [°C]	T_d' [°C]
PHB	Unaged	0.2	294.4	-
	RT	0.2	297.3	-
	65 °C	0.2	295.9	-
Flax NW fabric	-	2.9	374.9	-
Untreated /PHB	Unaged	1.3	280.1	360.5
C /PHB	Unaged	1.2	285.0	362.0
	RT	1.4	288.3	366.6
	65 °C	1.4	290.9	364.3
C-Et10 /PHB	Unaged	1.5	286.9	363.6
C-Ar20 /PHB	Unaged	1.0	283.8	361.9
	RT	1.7	287.9	365.0
	65 °C	1.9	292.6	359.8
C-Ar5-Et10 /PHB	Unaged	1.2	285.2	360.3

IV.3.4. Aging effect on the morphology of the composites

Figure IV.7 shows the SEM images of the surfaces of the unaged and aged composites. Although the unaged composites presented a coarse surface and even small cracks due to superficial fibres, the volume, length and depth of these cracks increased due to the hydrothermal testing according to the hardening of the aging conditions. As explained before, the formation, propagation and expansion of cracks is related to the swelling of the fibres during the aging process.

Therefore, the images presented some relationship between the water uptake and the cracks observed in the surface: samples with higher water uptake (C-Et10/PHB, C-Ar20/PHB, and C-Ar5-Et10/PHB) had larger and deeper cracks than samples with smaller M_s values (C/PHB and untreated/PHB). Moreover, the mechanical properties after aging also present some relationship with the damage observed in Figure IV.7 and the corresponding water uptakes, with a loss according to M_s , that is, with higher damage.

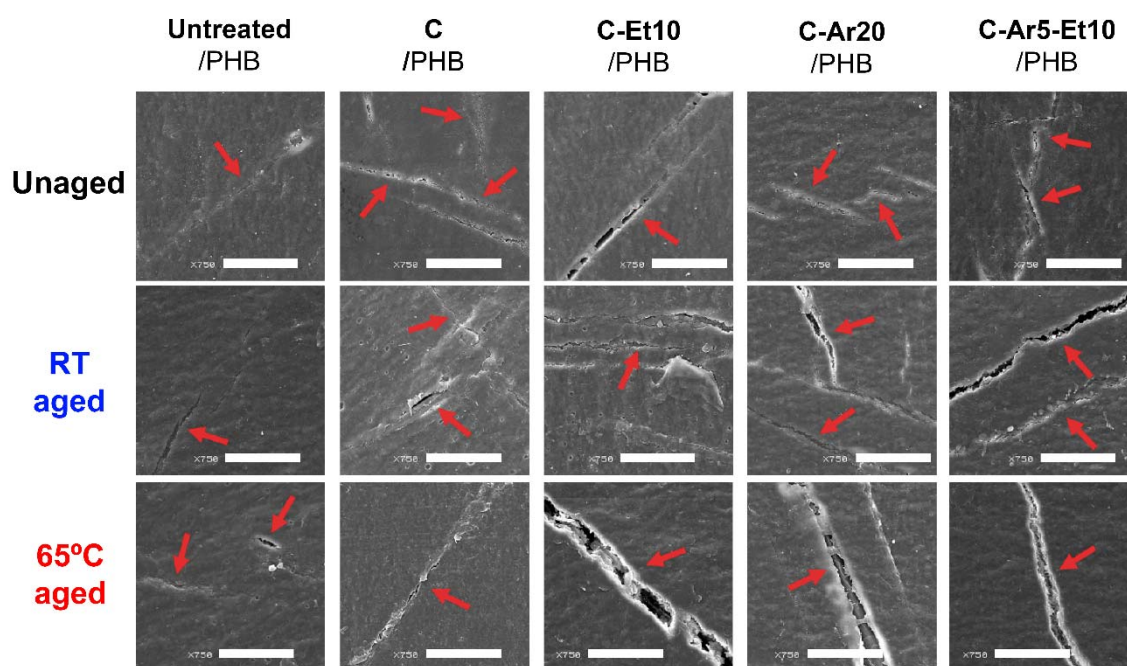


Figure IV.7. SEM images of the surfaces of unaged, aged for 100 h at RT and aged for 100 h at 65 °C samples, obtained at 10.0 keV at x750 magnification. Scale bars are 50 μm .

IV.4. Conclusions

In this study, the effects of hydrothermal aging on the water uptake and water absorption kinetics, as well as the tensile and thermal properties of PHB reinforced with flax NW fabrics, have been evaluated. The incorporation of the reinforcements produced an increase in the water uptake with respect to the neat matrix, showing high sensitivity to small variations in the fibre contents. The different surface treatments applied to the NW fabrics did not influence the water uptake, and proved to be ineffective in preventing water absorption.

The water diffusion, with a pseudo-Fickian behaviour for the composites, increased with the aging temperature.

Regarding the mechanical properties, in the unaged state all the composites presented higher stiffness and strength than the neat matrix. The C-Ar20/PHB composite presented the best overall mechanical improvement in the unaged state, thus pointing to better adhesion. Nonetheless, aging had severe effects in reducing the mechanical properties of most of the samples due to fibre debonding and matrix damage. The C/PHB composite presented the best resistance to aging, with a lower loss of stiffness and strength, thus pointing to wet/dry cycling as an effective treatment for stabilisation of the reinforcement and improvement of this sort of composite. Finally, the SEM images showed a connection between the water uptake and the damage observed.

References

- [1] Faruk O, Bledzki A, Fink H, Sain M. Biocomposites reinforced with natural fibers: 2000–2010. *Prog Polym Sci* 2012;37:1552–96. doi:10.1016/j.progpolymsci.2012.04.003.
- [2] Barkoula NM, Garkhail SK, Peijs T. Biodegradable composites based on flax/polyhydroxybutyrate and its copolymer with hydroxyvalerate. *Ind Crops Prod* 2010; 31:34–42. doi:10.1016/j.indcrop.2009.08.005.
- [3] Bledzki A. Composites reinforced with cellulose based fibres. *Prog Polym Sci* 1999;24:221–74. doi:10.1016/S0079-6700(98)00018-5.
- [4] Satyanarayana KG, Arizaga GGC, Wypych F. Biodegradable composites based on lignocellulosic fibers—An overview. *Prog Polym Sci* 2009;34:982–1021. doi:10.1016/j.progpolymsci.2008.12.002.
- [5] Bhowmick M, Mukhopadhyay S, Alagirusamy R. Mechanical properties of natural fibre-reinforced composites. *Text Prog* 2012;44:85–140. doi:10.1080/00405167.2012.676800.
- [6] Faruk O, Bledzki AK, Fink H-P, Sain M. Progress Report on Natural Fiber Reinforced Composites. *Macromol Mater Eng* 2014;299:9–26. doi:10.1002/mame.201300008.
- [7] Laycock B, Halley P, Pratt S, Werker A, Lant P. The chemomechanical properties of microbial polyhydroxyalkanoates. *Prog Polym Sci* 2014;39:397–442. doi:10.1016/j.progpolymsci.2013.06.008.
- [8] Reddy CSK, Ghai R, Rashmi, Kalia VC. Polyhydroxyalkanoates: An overview. *Bioresour Technol* 2003;87:137–46. doi:10.1016/S0960-8524(02)00212-2.
- [9] Shanks RA, Hodzic A, Wong S. Thermoplastic biopolyester natural fiber composites. *J Appl Polym Sci* 2004;91:2114–21. doi:10.1002/app.13289.
- [10] Kabir MM, Wang H, Lau KT, Cardona F. Chemical treatments on plant-based natural fibre reinforced polymer composites: An overview. *Compos Part B Eng* 2012;43:2883–92. doi:10.1016/j.compositesb.2012.04.053.
- [11] Kalia S, Thakur K, Celli A, Kiechel MA, Schauer CL. Surface modification of plant fibers using environment friendly methods for their application in polymer composites, textile industry and antimicrobial activities: A review. *J Environ Chem Eng* 2013;1:97–112. doi:10.1016/j.jece.2013.04.009.
- [12] Johansson K. Plasma modification of natural cellulosic fibres. In: Shishoo R, editor. *Plasma Technol. Text.*, Cambridge: Woodhead Publishing Limited; 2007, p. 247–81.
- [13] Bozaci E, Sever K, Sarikanat M, Seki Y, Demir A, Ozdogan E, et al. Effects of the atmospheric plasma treatments on surface and mechanical properties of flax fiber and adhesion between fiber-matrix for composite materials. *Compos Part B Eng* 2013;45:565–72. doi:10.1016/j.compositesb.2012.09.042.
- [14] Lee SG, Choi S-S, Park WH, Cho D. Characterization of surface modified flax fibers and their biocomposites with PHB. *Macromol Symp* 2003;197:089–100. doi:10.1002/masy.200350709.
- [15] Azwa ZN, Yousif BF, Manalo AC, Karunasena W. A review on the degradability of polymeric composites based on natural fibres. *Mater Des* 2013;47:424–42. doi:10.1016/j.matdes.2012.11.025.
- [16] Mokhothu TH, John MJ. Review on hygroscopic aging of cellulose fibres and their biocomposites. *Carbohydr Polym* 2015;131:337–54. doi:10.1016/j.carbpol.2015.06.027.
- [17] Brancato AA. Effect of progressive recycling on cellulose fiber surface properties. Georgia Institute of Technology, 2008.

- [18] Bertoniere NR, King WD. Effect of Scouring / Bleaching, Caustic Mercerization, and Liquid Ammonia Treatment on the Pore Structure of Cotton Textile Fibers. *Text Res J* 1989;59:114–21.
- [19] Kongdee A, Bechtold T, Burtscher E, Scheinecker M. The influence of wet/dry treatment on pore structure-the correlation of pore parameters, water retention and moisture regain values. *Carbohydr Polym* 2004;57:39–44. doi:10.1016/j.carbpol.2004.03.025.
- [20] Dhakal HN, Zhang ZY, Richardson MOW. Effect of water absorption on the mechanical properties of hemp fibre reinforced unsaturated polyester composites. *Compos Sci Technol* 2007;67:1674–83. doi:10.1016/j.compscitech.2006.06.019.
- [21] Hu R-H, Sun M, Lim J-K. Moisture absorption, tensile strength and microstructure evolution of short jute fiber/poly lactide composite in hygrothermal environment. *Mater Des* 2010;31:3167–73. doi:10.1016/j.matdes.2010.02.030.
- [22] Gil-Castell O, Badia JD, Kittikorn T, Strömberg E, Martínez-Felipe A, Ek M, et al. Hydrothermal ageing of polylactide/sisal biocomposites. Studies of water absorption behaviour and Physico-Chemical performance. *Polym Degrad Stab* 2014;108:212–22. doi:10.1016/j.polymdegradstab.2014.06.010.
- [23] Badia JD, Kittikorn T, Strömberg E, Santonja-Blasco L, Martínez-Felipe A, Ribes-Greus A, et al. Water absorption and hydrothermal performance of PHBV/sisal biocomposites. *Polym Degrad Stab* 2014;108:166–74. doi:10.1016/j.polymdegradstab.2014.04.012.
- [24] Le Duigou A, Bourmaud A, Baley C. In-situ evaluation of flax fibre degradation during water ageing. *Ind Crops Prod* 2015;70:190–200. doi:10.1016/j.indcrop.2015.03.049.
- [25] Ventura H, Ardanuy M, Capdevila X, Cano F, Tornero JA. Effects of needling parameters on some structural and physico-mechanical properties of needle-punched nonwovens. *J Text Inst* 2014;1–11. doi:10.1080/00405000.2013.874628.
- [26] Ventura H, Claramunt J, Navarro A, Rodriguez-Perez M, Ardanuy M. Effects of Wet/Dry-Cycling and Plasma Treatments on the Properties of Flax Nonwovens Intended for Composite Reinforcing. *Materials (Basel)* 2016;9:93. doi:10.3390/ma9020093.
- [27] Crank J. *The Mathematics of Diffusion*. 2nd ed. Clarendon Press; 1975.
- [28] Karimi M. *Diffusion in Polymer Solids and Solutions*. Mass Transf. Chem. Eng. Process., InTech; 2011. doi:10.5772/23436.
- [29] Espert A, Vilaplana F, Karlsson S. Comparison of water absorption in natural cellulosic fibres from wood and one-year crops in polypropylene composites and its influence on their mechanical properties. *Compos Part A Appl Sci Manuf* 2004;35:1267–76. doi:10.1016/j.compositesa.2004.04.004.
- [30] Lin Q, Zhou X, Dai G. Effect of hydrothermal environment on moisture absorption and mechanical properties of wood flour-filled polypropylene composites. *J Appl Polym Sci* 2002;85:2824–32. doi:10.1002/app.10844.
- [31] Joseph PV, Rabello MS, Mattoso LHC, Joseph K, Thomas S. Environmental effects on the degradation behaviour of sisal fibre reinforced polypropylene composites. *Compos Sci Technol* 2002;62:1357–72. doi:10.1016/S0266-3538(02)00080-5.
- [32] Summerscales J, Virk A, Hall W. A review of bast fibres and their composites: Part 3 – Modelling. *Compos Part A Appl Sci Manuf* 2013;44:132–9. doi:10.1016/j.compositesa.2012.08.018.
- [33] Madsen B, Thygesen A, Lilholt H. Plant fibre composites – porosity and stiffness. *Compos Sci Technol* 2009;69:1057–69. doi:10.1016/j.compscitech.2009.01.016.
- [34] Thomason JL, Vlug MA. Influence of fibre length and concentration on the properties of

- glass fibre-reinforced polypropylene: Part 1. Tensile and flexural modulus. *Compos Part A Appl Sci Manuf* 1996;27:477–84. doi:10.1016/1359-835X(95)00065-8.
- [35] Thomason JL, Vlug MA, Schipper G, Krikor HGLT. Influence of fibre length and concentration on the properties of glass fibre-reinforced polypropylene: Part 3. Strength and strain at failure. *Compos Part A Appl Sci Manuf* 1996;27:1075–84. doi:10.1016/1359-835X(96)00066-8.
- [36] Peijs T, Garkhail S, Heijenrath R, Van Den Oever M, Bos H. Thermoplastic composites based on flax fibres and polypropylene: Influence of fibre length and fibre volume fraction on mechanical properties. *Macromol Symp* 1998;127:193–203. doi:10.1002/masy.19981270126.
- [37] Van Den Oever MJA, Bos HL, Van Kemenade MJJM. Influence of the Physical Structure of Flax Fibres on the Mechanical Properties of Flax Fibre Reinforced Polypropylene Composites. *Appl Compos Mater* 2000;7:387–402. doi:10.1023/A:1026594324947.
- [38] Garkhail SK, Heijenrath RWH, Peijs T. Mechanical properties of natural-fibre-mat-reinforced thermoplastics based on flax fibres and polypropylene. *Appl Compos Mater* 2000;7:351–72. doi:10.1023/A:1026590124038.
- [39] Wong S, Shanks RA, Hodzic A. Effect of additives on the interfacial strength of poly(l-lactic acid) and poly(3-hydroxy butyric acid)-flax fibre composites. *Compos Sci Technol* 2007;67:2478–84. doi:10.1016/j.compscitech.2006.12.016.
- [40] Madsen B, Thygesen A, Lilholt H. Plant fibre composites – porosity and volumetric interaction. *Compos Sci Technol* 2007;67:1584–600. doi:10.1016/j.compscitech.2006.07.009.
- [41] Peterson S, Jayaraman K, Bhattacharyya D. Forming performance and biodegradability of woodfibre–Biopol™ composites. *Compos Part A Appl Sci Manuf* 2002;33:1123–34. doi:10.1016/S1359-835X(02)00046-5.
- [42] Singh S, Mohanty AK, Sugie T, Takai Y, Hamada H. Renewable resource based biocomposites from natural fiber and polyhydroxybutyrate-co-valerate (PHBV) bioplastic. *Compos Part A Appl Sci Manuf* 2008;39:875–86. doi:10.1016/j.compositesa.2008.01.004.
- [43] Luo S, Netravali AN. Interfacial and mechanical properties of environment-friendly “green” composites made from pineapple fibers and poly(hydroxybutyrate-co-valerate) resin. *J Mater Sci* 1999;34:3709–19. doi:10.1023/A:1004659507231.
- [44] Javadi A, Srithep Y, Lee J, Pilla S, Clemons C, Gong S, et al. Processing and characterization of solid and microcellular PHBV/PBAT blend and its RWF/nanoclay composites. *Compos Part A Appl Sci Manuf* 2010;41:982–90. doi:10.1016/j.compositesa.2010.04.002.
- [45] Javadi A, Srithep Y, Pilla S, Lee J, Gong S, Turng L-S. Processing and characterization of solid and microcellular PHBV/coir fiber composites. *Mater Sci Eng C* 2010;30:749–57. doi:10.1016/j.msec.2010.03.008.
- [46] Salim YS, Abdullah AA-A, Nasri CSSM, Ibrahim MNM. Biosynthesis of poly(3-hydroxybutyrate-co-3-hydroxyvalerate) and characterisation of its blend with oil palm empty fruit bunch fibers. *Bioresour Technol* 2011;102:3626–8. doi:10.1016/j.biortech.2010.11.020.
- [47] Claramunt J, Ardanuy M, García-Hortal JA. Effect of drying and rewetting cycles on the structure and physicochemical characteristics of softwood fibres for reinforcement of cementitious composites. *Carbohydr Polym* 2010;79:200–5. doi:10.1016/j.carbpol.2009.07.057.
- [48] Beckermann GW, Pickering KL. Engineering and evaluation of hemp fibre reinforced polypropylene composites: Fibre treatment and matrix modification. *Compos Part A Appl Sci Manuf* 2008;39:979–88. doi:10.1016/j.compositesa.2008.03.010.
- [49] Arrakhiz FZ, El Achaby M, Malha M, Bensalah MO, Fassi-Fehri O, Bouhfid R, et al. Mechanical and thermal properties of natural fibers reinforced polymer composites:

- Doum/low density polyethylene. *Mater Des* 2013;43:200–5.
doi:10.1016/j.matdes.2012.06.056.
- [50] Singh S, Mohanty AK. Wood fiber reinforced bacterial bioplastic composites: Fabrication and performance evaluation. *Compos Sci Technol* 2007;67:1753–63.
doi:10.1016/j.compscitech.2006.11.009.
- [51] Araújo JR, Waldman WR, De Paoli MA. Thermal properties of high density polyethylene composites with natural fibres: Coupling agent effect. *Polym Degrad Stab* 2008;93:1770–5.
doi:10.1016/j.polymdegradstab.2008.07.021.

CHAPTER V

**EVALUATION OF THE FOAMABILITY OF THE
PHB MATRIX**

CHAPTER CONTENTS

Abstract	221
V.1. Introduction.....	223
V.2. Experimental section.....	225
V.2.1. Materials	225
V.2.2. Sample preparation.....	225
V.2.3. Characterization methods.....	226
V.2.3.1. Rheological characterisation	226
V.2.3.2. Density.....	227
V.2.3.3. Open cell content.....	227
V.2.3.4. Characterisation of the cellular structure.....	227
V.2.3.5. Differential scanning calorimetry.....	227
V.2.3.6. Compression tests	228
V.2.3.7. Tensile tests.....	228
V.2.3.8. Charpy impact tests.....	228
V.3. Results and discussion.....	229
V.3.1. Rheological characterization	229
V.3.2. Density	229
V.3.3. Cellular morphology.....	230
V.3.4. Thermal behaviour analysis.....	234
V.3.4.1. Crystallinity degree	234
V.3.4.2. Melting and crystallisation temperatures	236
V.3.5. Mechanical properties	237
V.3.5.1. Compression testing results.....	237
V.3.5.2. Tensile testing results.....	240
V.3.5.3. Impact testing results.....	241
V.4. Conclusions	242
References	243

Abstract

Bacterial polyesters such as polyhydroxyalkanoates (PHAs) are of great interest for a large number of applications both because of their properties and because they come from renewable resources, despite having a higher cost than commodity polymers. Their foaming—although it presents some difficulties—could be an option to increase their competitiveness. In this work, two strategies have been studied to enhance the poly(3-hydroxybutyrate-*co*-4-hydroxybutyrate) (P3HB4HB) foamability by extrusion foaming. The effect of the cooling system (water-quenching or air-cooling), chain extender (CE) addition and chemical blowing agent (CBA) amount were evaluated. Density, cellular morphology, mechanical and thermal properties were studied. Optimal density reduction was achieved with use of CE and 3–4 wt.% of CBA masterbatch. The most effective strategy on density reduction was the addition of CE, while the water quenching had only a slight influence on the samples in which CE was not present. CE addition decreased the viscosity and the degradation rate of the polymer, thus leading to lighter foams with larger cells but with equal or even slightly better resistance to compressive and tensile stress, in general terms.

This part of the work is a post-print adapted version of the publication *Effect of chain extender and water-quenching on the properties of poly(3-hydroxybutyrate-co-4-hydroxybutyrate) foams for its production by extrusion foaming*, Ventura, H.; Laguna-Gutiérrez, E.; Rodríguez-Pérez, M.A.; Ardanuy, M. *European Polymer Journal*. Vol. 85, p. 14-25, issued on 1 October 2016. doi: 10.1016/j.eurpolymj.2016.10.001

Available at: <http://linkinghub.elsevier.com/retrieve/pii/S0014305716303743>

V.1. Introduction

PHAs are a family of microbial biodegradable bacterial biopolyesters [1–3] that are obtained from renewable resources, and are of interest for a wide range of applications from packaging to biomedical industries [2,3]. However, due to its current high price compared with other commodity polymers, PHAs' commercial use is currently limited to those applications in which the biodegradability or biocompatibility properties are capable of outbalancing the cost of the PHA resin.

A possible strategy to reduce the amount of polymer required for a certain application, and therefore, the cost of the final good, is the weight reduction obtained from foaming the solid material leading to a foam with improved specific mechanical properties [4]. Nonetheless, the foaming of PHAs has some difficulties, since most PHAs are intrinsically difficult to foam because of a narrow processing window and a low melt strength, which leads to a tendency towards cell coalescence and collapse at high expansion [5].

Among all the foaming techniques, one of the most widely used is extrusion foaming due to its low cost for the production of continuous foams and high productivity. With this technique, blowing agents can be physical (PBAs) or chemical (CBAs). PHAs have already been foamed with super critical CO₂ gas as PBA [6], with exothermic CBAs such as azodicarbonamide (ADA) [5,7], or with more eco-friendly endothermic CBAs mainly based on sodium bicarbonate (SB) and citric acid [5,8,9]. The use of PBAs requires extruders with PBA-pumping systems and, in some cases, screws with special profiles, thus meaning that special processing machinery is necessary. Due to that, this study focuses on the use of CBAs, which allows its foam-processing in conventional extruder machines.

The aforementioned endothermic CBAs, which release CO₂ gas, have been shown to achieve lower density-PHA foams than exothermic CBAs such as ADA, which release N₂ gas [5]. Nevertheless, the use of endothermic CBAs has some drawbacks. The thermal decomposition of SB produces water in addition to CO₂, which can lead to an hydrolytic degradation of PHAs—an effect that is more noticeable at high processing temperatures [5,10–12] or large residence times [13] in which PHAs also suffer from thermal degradation. Both thermal and hydrolytic degradation of PHAs are caused by random chain scission, and hence, a decrease in the molecular weight is produced [10], which reduces not only the properties of the polymer but also its foamability. Therefore, both the CBA and the process itself adversely affect the resulting foam.

On the other hand, it is known that branched structures can enhance the melt strength and, therefore, the foamability of polymers. Epoxy-functionalised chain extenders (CEs) can be used to increase the molecular weight and melt viscosity, and also to improve the melt strength by means of chain branching and chain extension in other polymers [14]. The use of CEs for foamability improvement has already been proved in other biodegradable polyesters, such as PLA. In some cases, their addition increased the molecular weight, enhanced melt viscosity and improved the cellular structure by promoting the formation of a large amount of uniform small cells [15–18]. Furthermore, the use of CEs in PHAs has been reported to increase thermal stability, thus widening the processing window to improve sheet extrusion or foaming processes [19]. Nonetheless, to the authors' knowledge, only a few articles have focused on the influence of these CEs in the properties of PHAs; and even fewer have focused on the variation of cellular structure and mechanical properties of PHA foams due to CE addition.

Another proposal for improving PHA foamability when produced via extrusion foaming is water-quenching [5]. Wright and Frank [5] found an improvement in the cellular structure of extruded PHA SB-blown foams when water-quenching post-extrusion was performed, since foams presented better cellular homogeneity and higher cell density. This was explained based on controlling the crystallinity due to the fast cooling rate produced by the water-quenching. Nevertheless, these authors did not study the effect of the use of a chain extender and no analysis of the effects on the mechanical properties was performed.

From the large family of PHAs, poly(3-hydroxybutyrate) (PHB) and its copolymers such as poly(3-hydroxybutyrate-*co*-3-hydroxyvalerate) (PHBV), poly(3-hydroxybutyrate-*co*-4-hydroxybutyrate) (P3HB4HB), or poly(3-hydroxybutyrate-*co*-hydroxyhexanoate) (PHBHHx) are the most widely studied. Regarding PHAs' foaming, the aforementioned research is mainly focused on PHBV and, in fewer cases, on PHBHHx. Nevertheless, to the authors' knowledge, none has focused on the PHB copolymer used in this study (P3HB4HB).

The aim of this study was to evaluate the combinations of the two strategies (water quenching and addition of chain extender) to enhance P3HB4HB extrusion foamability using an endothermic CBA, since their immediate application to the current processing technologies would be simple. The effects on the foamability of CBA content, chain extender addition and the cooling system were evaluated by means of cellular structure characterisation and analysis of the thermal and mechanical properties.

V.2. Experimental section

V.2.1. Materials

The poly(3-hydroxybutyrate-*co*-4-hydroxybutyrate) used for this research was Mirel P3001—thermoforming grade, Metabolix Inc., USA—. The chemical blowing agent (CBA) used was Hydrocerol BIH40E in masterbatch form from Clariant GmbH, Germany. Joncryl ADR-4368-C—FDA approved grade, kindly provided by BASF, Germany—was used as the chain extender (CE).

V.2.2. Sample preparation

Foamed samples were produced directly by extrusion foaming in a Collin Co-rotating Twin-screw Extruder ZK 25 T. PHA and CBA were previously dried at 50 °C for 16 h in a P-Selecta Vacuum Drying Oven VacioTem TV. A reverse extrusion profile was used, linearly decreasing from 170 °C in the hopper to 150 °C in the die. The screw-speed was fixed to 70 rpm. The feeding and mass flow rates at these conditions were estimated to be around 71 ± 3 g/min. The pressure measured at the die was in the range of 6.1 ± 3 MPa. At the exit of the die—with a circular profile of 4-mm diameter—, 50–60 specimens of each sample—with a length of ~20–25 cm—were collected. Half of the specimens were water-quenched in a water bath at 23 ± 1 °C after few seconds (5–10 s) of their exit through the die—referred to as W—. The other specimens were air-cooled at room temperature—referred to as A—. Sample cooling was done under no stress. After cooling, all the specimens were kept in standard conditions of temperature and relative humidity— 23 ± 2 °C, $50 \pm 10\%$ RH—. Twelve different compositions were obtained by varying the CBA amount—six levels, from 0 to 5 wt.%—, CE amount—two levels: 0 and 1 wt.%—, and the cooling system used—air or water—, as shown in Table V.1.

Go to next page

Table V.1. Composition and reference of the samples prepared (CBA=Chemical Blowing Agent; CS=Cooling System; CE=Chain Extender; A=Air cooling; W=Water quenching).

	<i>Ref.</i>	<i>CBA</i> ¹ (wt%)	<i>CE</i> (wt%)	<i>CS</i>		<i>Ref.</i>	<i>CBA</i> ¹ (wt%)	<i>CE</i> (wt%)	<i>CS</i>
0CE/A	0CBA-0CE/A	0	0	A	0CE/W	0CBA-0CE/W	0	0	W
	1CBA-0CE/A	1	0	A		1CBA-0CE/W	1	0	W
	2CBA-0CE/A	2	0	A		2CBA-0CE/W	2	0	W
	3CBA-0CE/A	3	0	A		3CBA-0CE/W	3	0	W
	4CBA-0CE/A	4	0	A		4CBA-0CE/W	4	0	W
	5CBA-0CE/A	5	0	A		5CBA-0CE/W	5	0	W
1CE/A	0CBA-1CE/A	0	1	A	1CE/W	0CBA-1CE/W	0	1	W
	1CBA-1CE/A	1	1	A		1CBA-1CE/W	1	1	W
	2CBA-1CE/A	2	1	A		2CBA-1CE/W	2	1	W
	3CBA-1CE/A	3	1	A		3CBA-1CE/W	3	1	W
	4CBA-1CE/A	4	1	A		4CBA-1CE/W	4	1	W
	5CBA-1CE/A	5	1	A		5CBA-1CE/W	5	1	W

¹ CBA content refers to wt.% of the masterbatch

V.2.3. Characterization methods

V.2.3.1. Rheological characterisation

For the evaluation of the effect of CE addition, a rheological characterisation using oscillatory shear rheometry was performed. In order to compare samples with the same thermal history, P3HB4HB and the mixture—P3HB4HB and 1 wt.% of CE—were extruded following the processing conditions described in section V.2.2. After the extrusion, the samples were collected, air-cooled and dried for 12 h at 50 °C under vacuum. Then, the samples obtained were moulded into 1 mm-thick discs at 175 °C under 10,000 kg for 3 min in a Remtex Hot Plate Press. The assays were performed in a TA Instruments Rheometer AR 2000 EX, equipped with electrically heated parallel plates of 25 mm of diameter. The gap was set to 1 mm. The time-sweep was performed with an angular frequency of 1 rad/s and a fixed strain of 2% at a temperature of 165 °C, which was in the linear viscoelastic regime.

Since the objective was to study the degradation rate of the two samples, the atmosphere used was air instead of nitrogen, for a better simulation of the processing conditions.

V.2.3.2. Density

Density was determined by the water-displacement method, based on Archimedes' principle, obtaining an average value from three measurements. Relative density (ρ_{rel})—defined as the ratio between the foam's density and the solid's density—was also calculated.

V.2.3.3. Open cell content

The open-cell content (f) was determined using a Micromeritics Gas Pycnometer AccuPyc II 1340 with nitrogen gas at 0.134 MPa and equilibration rate at $0.689 \cdot 10^{-6}$ MPa, by means of Equation (V.1):

$$f = \frac{V_s - V_q}{V_s \left(1 - \frac{\rho_{\text{foam}}}{\rho_{\text{solid}}} \right)} \quad (\text{V.1})$$

where V_s is the external volume of the tested sample—i.e. volume determined by the water-displacement method—, V_q corresponds to the volume of the solid plus the gas volume of the unconnected cells—i.e. pycnometric volume—, ρ_{foam} is the foam's density, and ρ_{solid} is the density of the solid phase ($\rho_s = 1290 \text{ kg/m}^3$).

V.2.3.4. Characterisation of the cellular structure

For the characterisation of cellular structure, SEM images of fragile fractures were taken in a JEOL Scanning Electron Microscope JSM 820. Cellular structure analysis was performed using only images of the centre of the specimens. A user-interactive image analysis adaptation of the ASTM D3576-04 method was used [20]. Cell size (mean cell diameter) and cell density (per solid volume unit, N_0) were determined in section and transversal directions from 100–150 cells.

V.2.3.5. Differential scanning calorimetry

The differential scanning calorimetry (DSC) data were recorded on a Mettler DSC-862. A three-cycle DSC was performed under nitrogen flow of 60 mL/min: first heating cycle from $-40 \text{ }^\circ\text{C}$ to $200 \text{ }^\circ\text{C}$ at $10 \text{ }^\circ\text{C}/\text{min}$ with 3 min of annealing at $200 \text{ }^\circ\text{C}$; cooling cycle from $200 \text{ }^\circ\text{C}$

to -40 °C at 20 °C/min; second heating cycle from -40 °C to 200 °C at 10 °C/min. Melting temperatures (T_m) and crystallisation temperatures (T_c) were obtained as the maximum of the peaks from the endothermic and exothermic curves, respectively. Crystallinity percentage (χ) of all samples was estimated from melting enthalpy (ΔH_m) and crystallisation enthalpy (ΔH_c) according to Equation (V.2):

$$\chi = \frac{\Delta H}{w \cdot \Delta H^0} \quad (\text{V.2})$$

where w is the weight fraction of P3HB4HB in each case, ΔH is the heat at the melting or crystallisation peak, and ΔH^0 is the heat of fusion or crystallisation of 100% crystalline PHB, which is considered to be 146 J/g [21].

V.2.3.6. Compression tests

Compression tests were performed in an Instron Universal Testing Machine 5.500R6025. Six specimens of each sample were cut at a height (h) of around 5 mm, resulting in cylindrical specimens with parallel sides with a diameter/height ratio of 0.75. The tests were performed at a speed of $h/10$ mm/min (~ 0.5 mm/min) up to a strain of the 70%. Values of stress at 25% and 50% of the strain ($\sigma_{25\%}$ and $\sigma_{50\%}$, respectively) and the collapse stress at the plateau (σ_{pl}) were obtained from the curves for each specimen.

V.2.3.7. Tensile tests

Tensile tests were performed in an Instron Universal Testing Machine 5.500R6025 following ISO527 1A standard. Five no-standard-shaped specimens of each sample were tested. The cylindrical extrudate specimens were first cut to a length of 15 cm and then the sectional area was calculated in order to adjust each test result with the corresponding specimen. Mean values of maximum stress (σ_{max}) and ultimate tensile strength (σ_{UTS}) were calculated. A high scatter of the maximum strain data was observed, which is related to the brittleness of the samples; therefore, the data related to the strain was not considered.

V.2.3.8. Charpy impact tests

Charpy impact tests for comparative purposes were performed in a Frank Charpy Impact Tester 53.566, with a 4 J hammer and an anvil distance of 39 mm. Ten specimens of each sample, cut to a length of 50 mm, were tested. Energy values were corrected, taking into account the sectional area of each specimen.

V.3. Results and discussion

V.3.1. Rheological characterization

The complex viscosity versus time is presented in Figure V.1. Initial complex viscosity values were 2192 Pa·s for the neat polymer and 1638 Pa·s for the polymer with CE. This first viscosity data reveals that the addition of CE produces a decrease in the complex viscosity, which is relevant to explain the cellular morphology and will be described in section V.3.3.

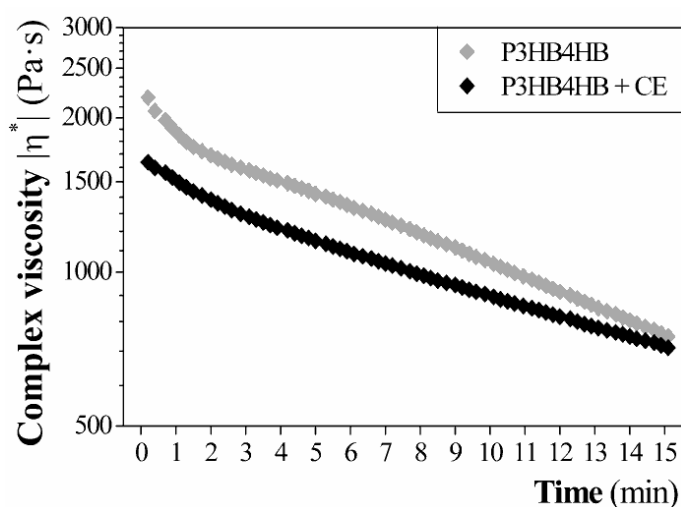


Figure V.1. Complex viscosity against time.

Moreover, complex viscosity is also related to the degradation of the polymer. As can be seen in Figure V.1, the most dramatic differences were revealed in the first minutes. For instance, after 2 min, the complex viscosity modulus of the neat polymer decreased 23%, while for the polymer with CE, the decrease was of 15%. This is related to a lower degradation rate when the CE is added. It has to be taken into account that the residence time of the material in the extruder during the foaming process was around 2–3 minutes. Therefore, although the CE addition produced a decrease in viscosity, the degradation rate was also reduced, thus leading to a less degraded polymer with expected better properties.

V.3.2. Density

Density values are shown in Figure V.2. As expected, increasing amounts of CBA led to lower densities. Density values of near 750 kg/m³ could be obtained with the addition of 3 wt.% CBA and 1 wt.% of CE.

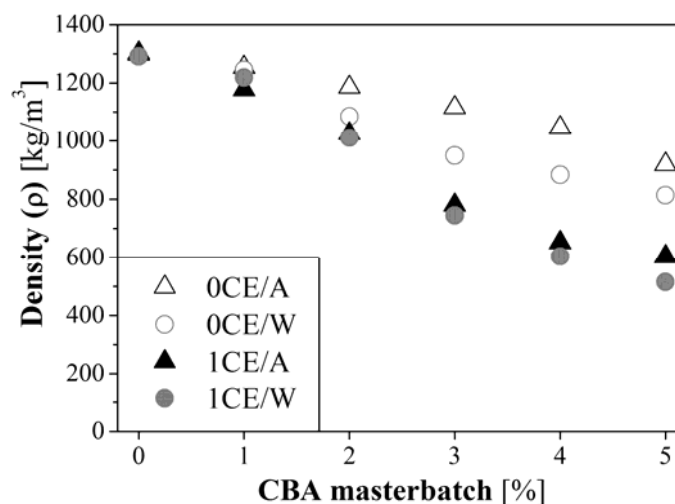


Figure V.2. Density against CBA amount.

For the 0CE series—without chain extender: cooled in air (Δ) or water (\circ)—, an almost linear reduction in the density was observed. Since the water-quenching (\circ) produced faster solidification with lower contraction, and samples without the chain extender achieved lower densities with this cooling system. However, for the 1CE series — with chain extender: \blacktriangle and \bullet —, the differences due to the cooling system were negligible. The largest decrease in density was observed for CBA contents of 3 wt.% or higher when the CE was used. As aforementioned, the addition of CE produced a reduction on the viscosity, thus leading to higher expansion rates as will be discussed in section 3.2. Moreover, CE addition also reduced the degradation rate of the polymer, what could have led to a less degraded polymer present in the cell walls, thus leading to a better stability.

In the literature, the chain extender was presumed to enhance the polymer conditions for foaming, such as increased polymer viscosity, molecular weight or melt strength [18,19,22,23]. Although in this study a reduction in viscosity was observed as a consequence of the CE addition, other properties such as melt strength or molecular weight could have been improved, thus intensifying the effect of the decrease in degradation previously discussed.

V.3.3. Cellular morphology

In general terms, the P3HB4HB foams of this study presented closed-cell structures with more regular pores in the inner part that tended to reduce in size and to lose the apparent isotropy when approaching the foam skin. However, some coalescence was observed. Foams with high CBA content showed coalescence in the inner part, where the heat was easily

retained. In this sense, significant amounts of connected pores were observed in some cases. 4CBA-1CE/W 5CBA-1CE/A and 5CBA-1CE/W samples presented 15%, 27% and 62% of open-cell content, respectively, while negligible open-cell content of 6% or lower was found in the rest of the samples. Figure V.3 shows cellular structure of sample 5CBA-1CE/W, which presented massive coalescence in the centre and some irregularities in the skin due to the collapse, thus explaining the high open-cell content of 62%.

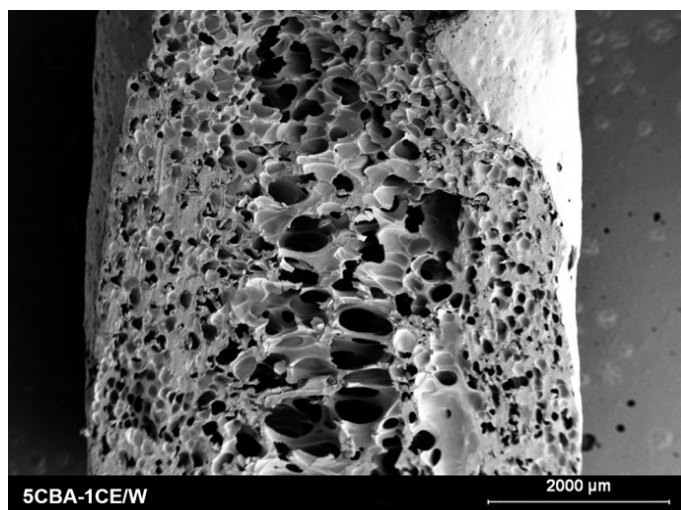


Figure V.3. SEM image of transversal (bias) fracture of specimen 5CBA-1CE/W showing a poor cellular structure in the central area.

Moreover, samples containing the chain extender—corresponding to the higher expansions—showed acceptable cellular structures up to the addition of 4% of CBA. Further increases in CBA content led to large coalescence in the centre of the samples as well as very irregular surfaces. According to the literature, a large amount of soluble gas would have been translated into high cell density, but at certain point the nucleated cells would have reached their maximum growth, and a further increase in the blowing agent would have led to coalescence and collapse of the cells [5,7,16].

The evolution of cellular structure for the four series when increasing CBA content can be observed in Figure V.4. The cellular morphologies are in accordance with the density results mentioned previously.

Go to next page

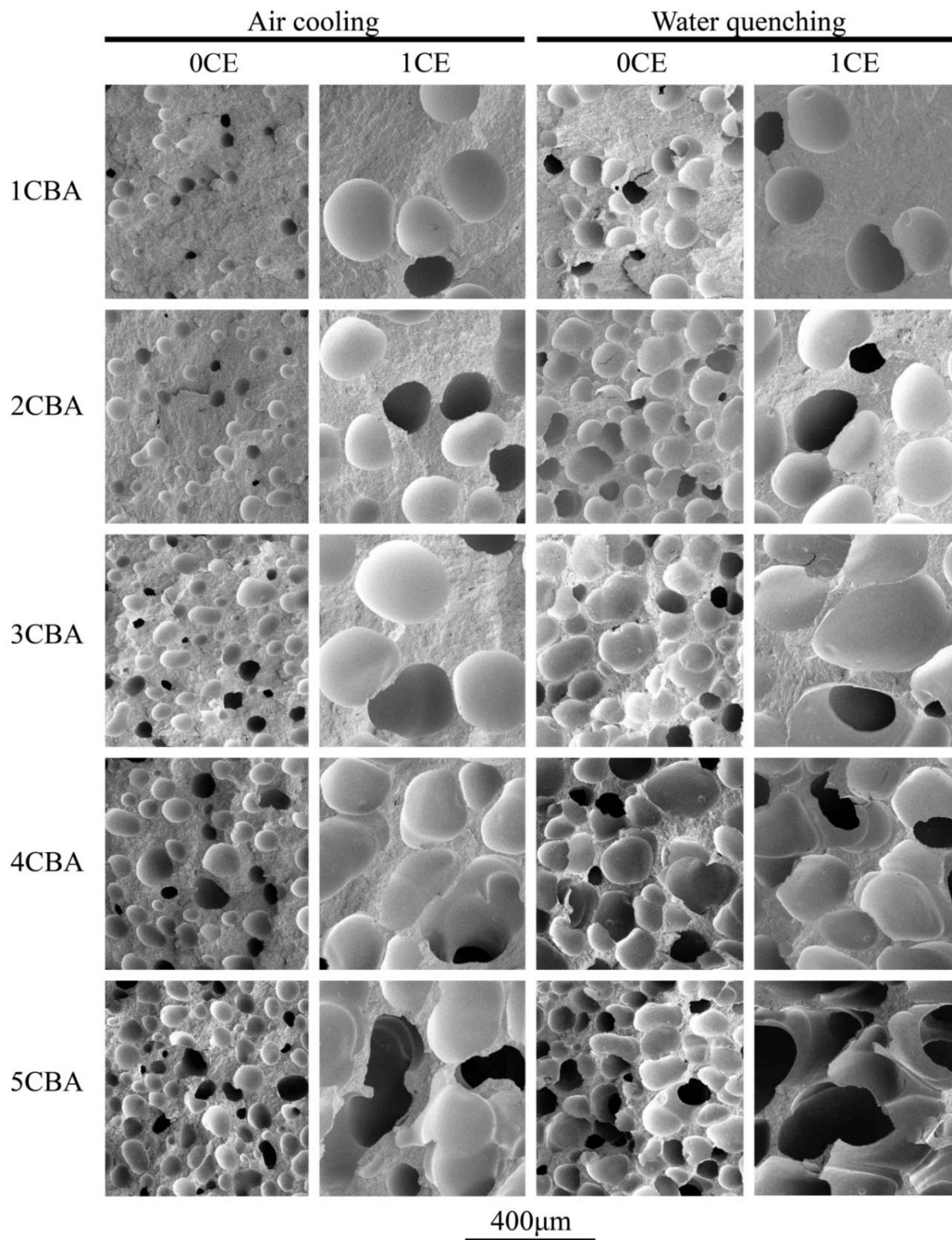


Figure V.4. SEM images showing the evolution of the cellular structure in the samples section when increasing CBA content. (Magnification: 50X).

The data from the cellular structure analysis, in transversal and section directions, is presented in Figure V.5. In general terms, the 0CE series presented larger cell densities (10^5 – 10^6 cells/cm³) and smaller pores with diameters between 50–80 μ m; and the 1CE series presented lower cell densities (10^4 – 10^5 cells/cm³) with cells three-times larger than the 0CE series, of a diameter between 150–200 μ m. Cell density (N_0) initially showed a fast growth with increasing CBA content in each series. Further narrowing or even recession of this trend was produced due to cell growth, coarsening and later coalescence.

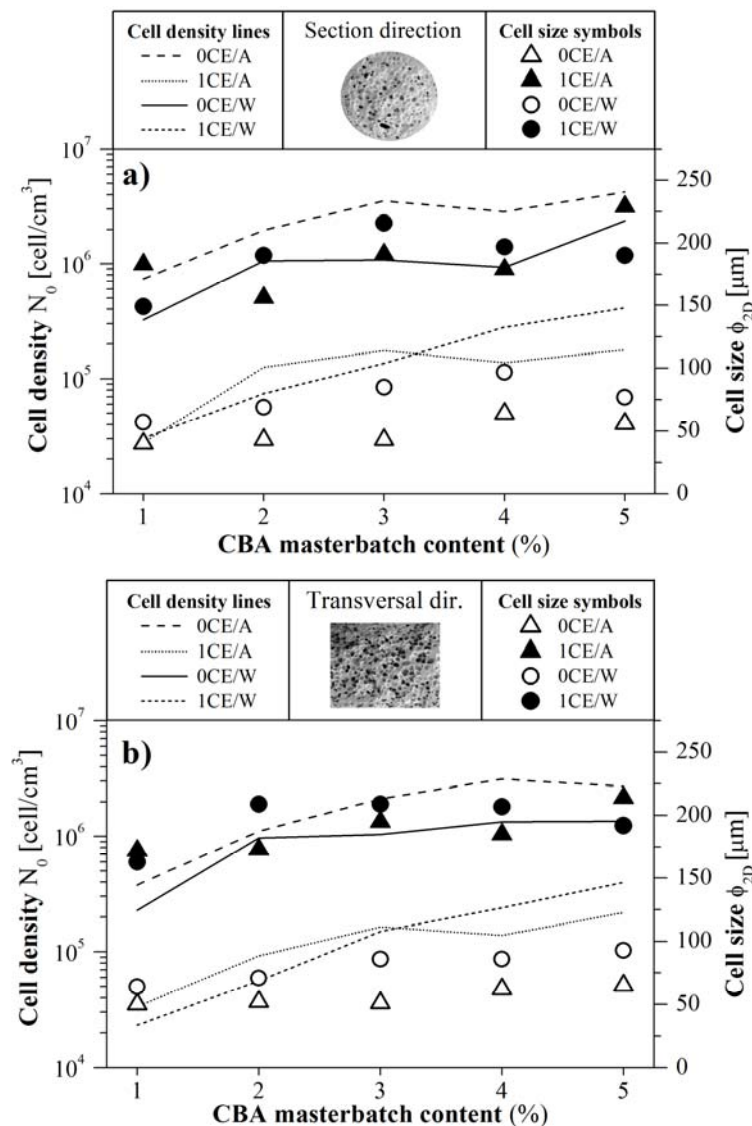


Figure V.5. Graphic summary of the cellular structure analysis in the a) section direction and b) transversal direction, containing the cell density and cell size evolution with increasing the CBA.

On the one hand, the effect of the cooling system was observed in the cell size for the 0CE series, although it was not significant in the cell size of the 1CE series. The 0CE series

presented cell sizes that were on average 50% larger in the water-quenched samples when compared to the air-cooled samples, thus explaining the slightly lower densities—see Figure V.2—. Shrinkage of the specimens was clearly observed during cooling in the air-cooled samples, which could lead to the differences observed in the cell size. However, differences in the cell size due to the cooling system were not relevant for the 1CE series. Moreover, similar trends in cell density evolution—of the 0CE series on one side, and of the 1CE series on the other—revealed similar cell formation and growing regardless of the cooling system used.

On the other hand, the addition of CE led to coarser cellular structures. The cell growth process is known to be related to the viscosity of the polymer melt [24], since low viscosity values favour the cell growth rate. Therefore, the lower initial complex viscosity observed for the 1CE series—see section V.3.1—enhanced the cell growth rate, leading to more expanded foams with larger cells, as observed in Figure V.2, Figure V.4 and Figure V.5. Moreover, the addition of CE also produced a decrease in the crystallisation temperature—see section V.3.4.2—, leading to a slower solidification of the foams. Therefore, a prolonged evolution of the cellular structure in terms of coalescence, coarsening and collapse took place, thus also promoting the coarser structures observed in Figure V.4.

V.3.4. Thermal behaviour analysis

V.3.4.1. Crystallinity degree

In the first heating cycle (χ_m), the values of crystallinity degree obtained from all series showed a rising trend with decreasing relative density (Figure V.6a). This general increase could be attributed to differences in the thermal properties of the foamed samples. In general terms, the reduction of density is translated into a decrease in the thermal conductivity [25], and thus to larger times at high temperature. Therefore, the heat retention enhanced the crystal formation, thus explaining the increasing trend with the decrease of the density. Moreover, as shown in Figure V.6a, the air-cooled series— Δ and \blacktriangle —presented slightly higher χ_m values than water-quenched series— \circ and \bullet —in the first heating cycle, as expected, due to lower cooling rates [26]. However, once the sample is completely melted—at the end of the first heating cycle—the cellular structure is lost, thus levelling the thermal behaviour of all specimens. Thus, the following cycles presented scattered and more flat trends, as shown for the crystallinity of the second heating cycle in Figure V.6b.

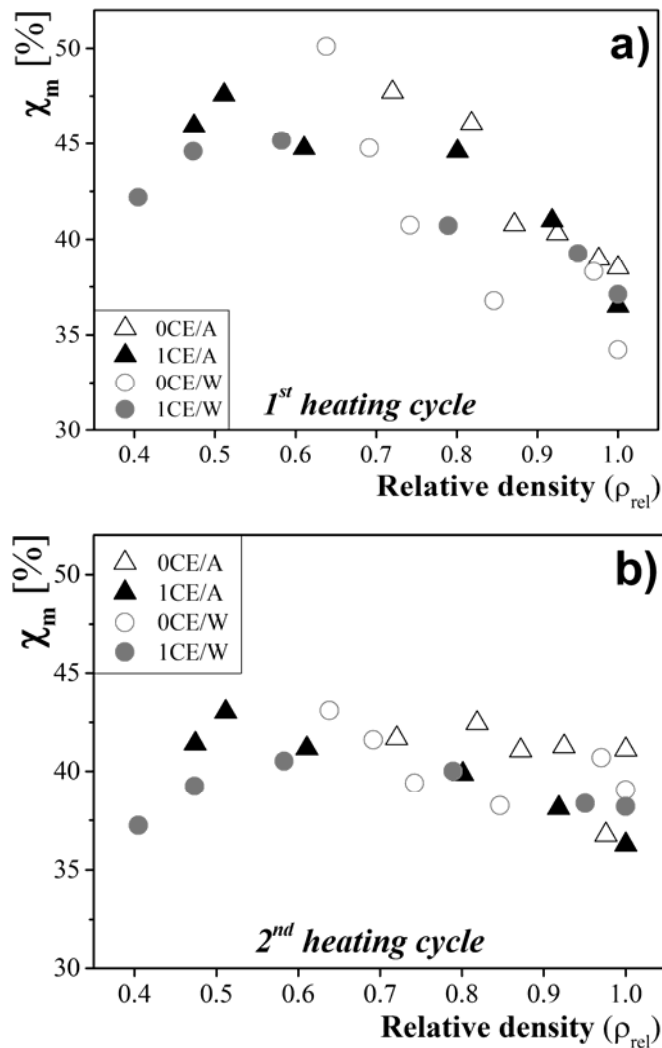


Figure V.6. χ_m percentages for the a) first heating cycle and b) second heating cycle against relative density.

The addition of CE had no clear effect on the crystallinity, since χ_m values of the 1CE-series were over those of the 0CE-series, as can be seen in Figure V.6. Nonetheless, in the literature, Pilla et al. reported a reduction in χ from around 10% in talc-filled PLA foams due to the addition of CE [15], and Ludwiczak and Kozłowski reported, among other effects, even larger reductions in the crystallinity percentage with increased CE in PLA foams [18]. These authors attributed this reduction to the formation of non-linear molecules or branched chains, which mainly difficult the packing of the chains, thus inhibiting the crystal formation. However, the interaction between the P3HB4HB and the chain extender could have been different from the PLA system studied in the literature. Here, the CE could have played only a minor role balancing or counteracting the thermal degradation, thus giving chains of similar properties that would not reveal large differences in chain packing, as in the other studies.

V.3.4.2. Melting and crystallisation temperatures

With regard to the DSC heating curves, a complex melting behaviour was observed—see Figure V.7—, which is consistent with the literature [26–29]. The DSC curves for the first heating cycle presented high dependence on the processing conditions (Figure V.7a) and the CBA content—Figure V.7b, showing the results for the 1CE/A-series as an example—.

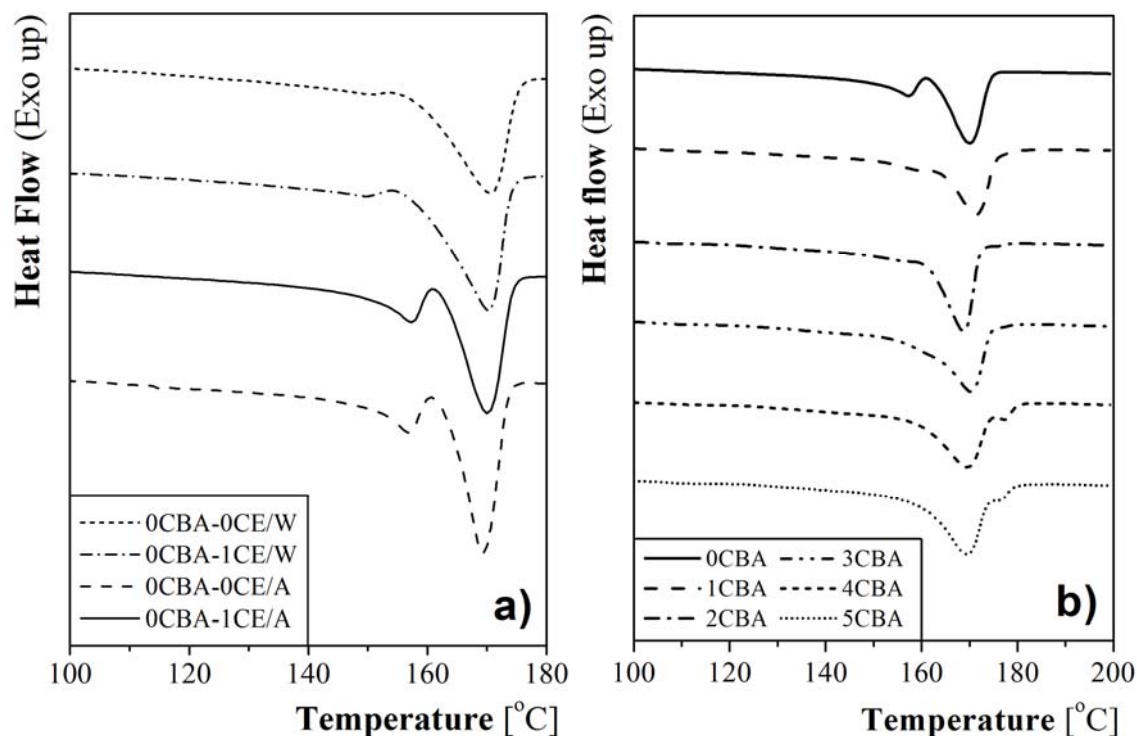


Figure V.7. DSC first heating cycle-curves comparison for a) 0CBA samples; b) 1CE/A-series with increasing CBA contents from top to bottom.

However, in the second heating cycle where all samples were affected by the same thermal history, small variations due to the addition of CE were observed, since the melting peaks were observed at a temperature of 2–3 °C lower compared to the 0CE series. Thus could be associated with the formation of less stable or thicker crystals when the CE is added.

With respect to the maximum crystallisation temperatures (T_c) obtained in the cooling cycle, no differences associated with the CBA amount or cooling system were detected. However, DSC revealed a T_c reduction from 105.4 ± 0.2 °C to 99.9 ± 0.6 °C due to the addition of the CE. This means that the formation of crystals in the series with CE is slower since it needs to reach lower temperatures. This crystallisation delay, due to CE addition, is consistent with the literature [18,19]. For instance, Duangphet et al. reported lower

crystallisation temperatures and a slight decrease in the enthalpies of crystallisation for increasing amounts of Joncryl in PHBV [19].

V.3.5. Mechanical properties

Compression, tensile and impact tests were performed in order to characterise mechanical properties of the obtained foams. Relative properties were plotted against relative density, and the data were fitted to the scaling law using Equation (V.3), with the purpose to guide the eye and ease the comparison of the results.

$$\frac{\text{Foam's property}}{\text{Solid's property}} = C \cdot \left(\frac{\rho_{\text{foam}}}{\rho_{\text{solid}}} \right)^n \quad (\text{V.3})$$

As expected, density reduction was obtained at the expense of reducing the mechanical properties. The mechanical properties of the foams largely depend on the foam's density, but also on the properties of the solid material from which the cell walls are made [30]. Therefore, the less degraded is the polymer, the better mechanical properties of the foam are expected.

As a reference, the properties of all unfoamed samples (0 wt.% content of CBA) were similar: for compression testing, $\sigma_{\text{pl}} = 39.3 \pm 0.8$ MPa, $\sigma_{25\%} = 44.6 \pm 1.8$ MPa and $\sigma_{50\%} = 61.4 \pm 3.7$ MPa; and for tensile testing, $\sigma_{\text{max}} = 25.4 \pm 0.9$ MPa and $\sigma_{\text{UTS}} = 23.5 \pm 1.6$ MPa.

V.3.5.1. Compression testing results

Compression-test curves of all obtained foams show the typical behaviour observed for cellular materials: an initial elastic deformation, in which the cell walls suffer from elastic bending and cell walls suffer some stretching; this is followed by a change in the slope that marks a plateau, which is associated with the collapse of cell walls of the foam; and finally, the progressive densification associated with the compression of the solid matrix, since cell walls have completely collapsed, and hence, cellular structure is lost.

The tangent method was used in σ_{pl} calculations. Samples corresponding to the lower densities—up to 918 kg/m³—presented an elasto-plastic behaviour with a clear plateau [30], probably because the thinner cell walls and higher crystallinity observed in more expanded foams resulted in more brittleness. The rest of the samples—i.e. those corresponding to the higher densities (≥ 949 kg/m³) with thicker cell walls and lower crystallinity—presented a change in the slope, but not a clear plateau. Each series presented a progressive reduction of

the compression curves with increasing CBA content—example in Figure V.8—as a consequence of the density reduction.

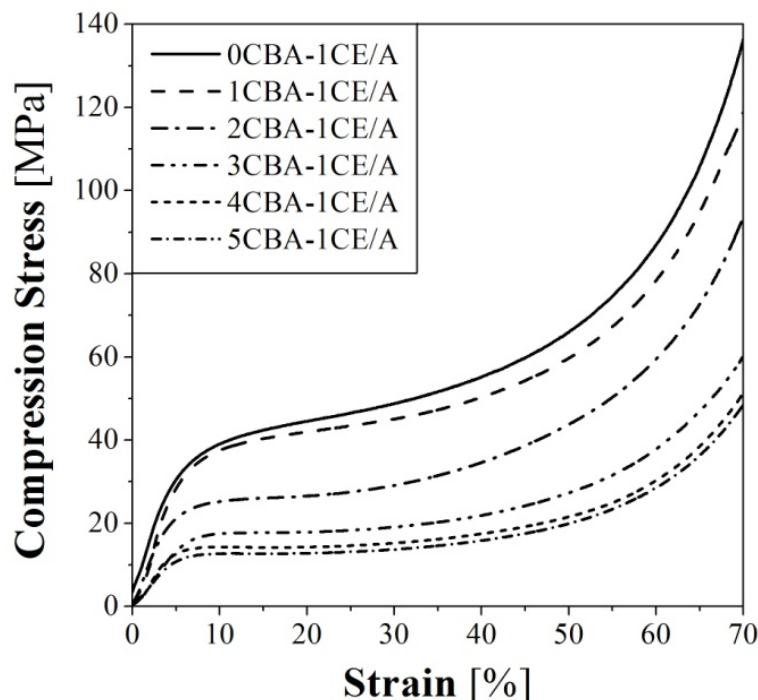


Figure V.8. Compression curves for 1CE/A series, showing the evolution of the behaviour when increasing the CBA amount (average standard deviations were around 8%).

The plot of the measured relative properties against relative density is presented in Figure V.9. A slightly better behaviour of the 1CE/A series can be observed in the compression stress at the plateau (Figure V.9a). However, for larger deformations—at 25% of the strain, Figure V.9b, and at 50% of the strain, Figure V.9c—the mechanical behaviour of all samples was similar, giving superposed curves with small differences that are not forceful given the high standard deviations obtained.

In general terms, the best results in compression mode were obtained with the 1CE/A series, which gave slightly better performance, especially in σ_{pl} . Here, the CE reduced the degradation rate of the polymer and hence, low densities could be achieved. Moreover, a high crystallinity degree was reached due to the slow air-cooling. As previously shown in Figure V.6, the 1CE/A series presented a good χ/ρ ratio that was higher than the water-quenched samples. Therefore, the combined effects of the CE and crystallinity overcame the loss of properties due to the cellular structure, thus explaining the better results. The other series presented very similar trends, regardless of the cooling system or the CE addition, thus pointing to the complexity of the system being studied.

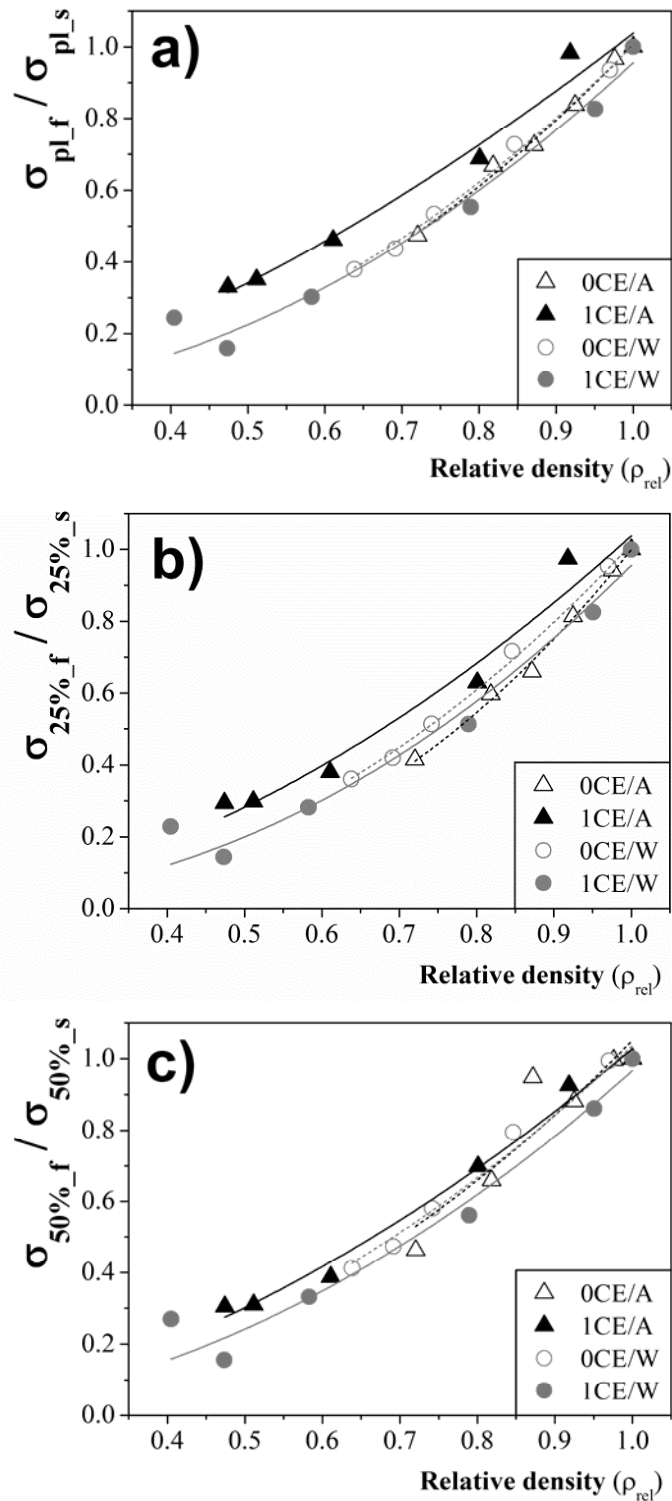


Figure V.9. Representation of relative compression properties: a) relative stress at the plateau σ_{pl} ; b) relative stress at 25% of strain $\sigma_{25\%}$; c) relative stress at 50% of strain $\sigma_{50\%}$; against relative density. Relative refers to the properties of the foam versus the properties of the solid. The fitting lines, which follow the scaling law, have been included to guide the eye.

V.3.5.2. Tensile testing results

Tensile properties decreased when increasing the expansion ratios, as expected, given the reduction of the effective section because of the foam's structure. Maximum stress (σ_{\max}) and ultimate tensile strength values (σ_{UTS}) were recorded, and the SD was 9% and 10%, respectively. Once again, relative properties were represented against relative density (Figure V.10).

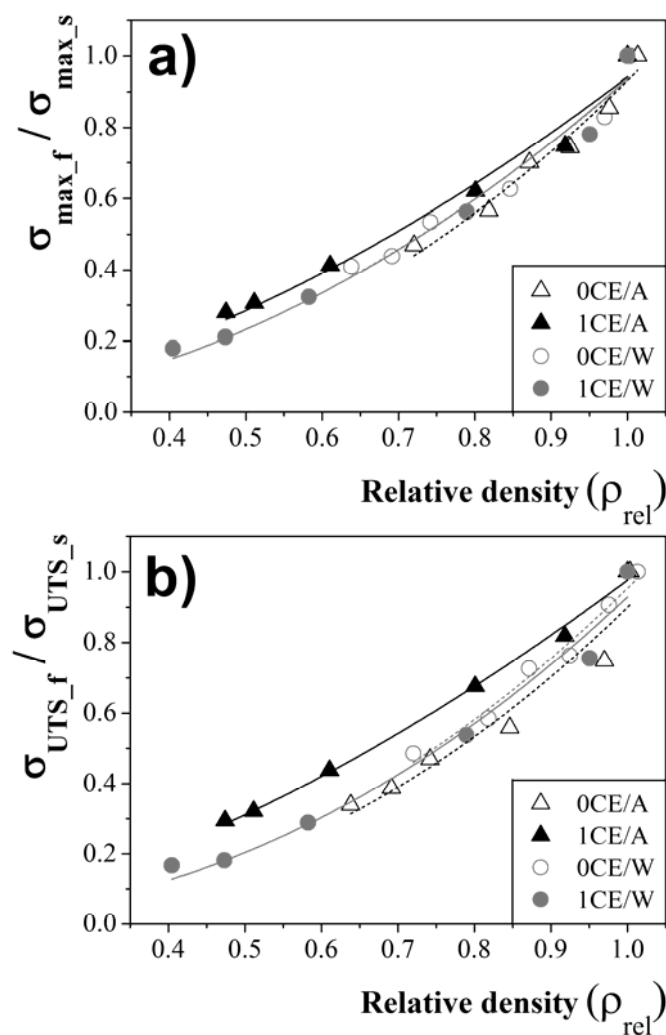


Figure V.10. Representation of relative tensile properties: a) relative maximum strength σ_{\max} ; b) relative ultimate tensile strength σ_{UTS} ; against relative density. Relative refers to the properties of the foam versus the properties of the solid. The fitting lines, which follow the scaling law, have been included to guide the eye.

Considering the high deviations obtained in the tensile tests, the curves in Figure V.10 show very similar behaviours under tensile modes for all the samples, thus the strategies used produced no improvements nor deteriorations in mechanical properties beyond those

expected due to the density's reduction. However, the 1CE/A series presented slightly better results for the ultimate tensile strength (Figure V.10b), associated with a better preservation of the polymer via CE addition. Once again, a good balance between the lower degradation of the polymer and the high crystallinity values achieved could explain the slightly better results, although the cellular structure is not favourable for such a behaviour.

V.3.5.3. Impact testing results

In Figure V.11, a comparison of the results of the impact against density is shown—error bars correspond to standard deviations values—. Taking into account the high deviations, the observed results were within the expected range of the general impact properties of foams. All samples showed very similar behaviour regardless of the CE addition and the cooling system.

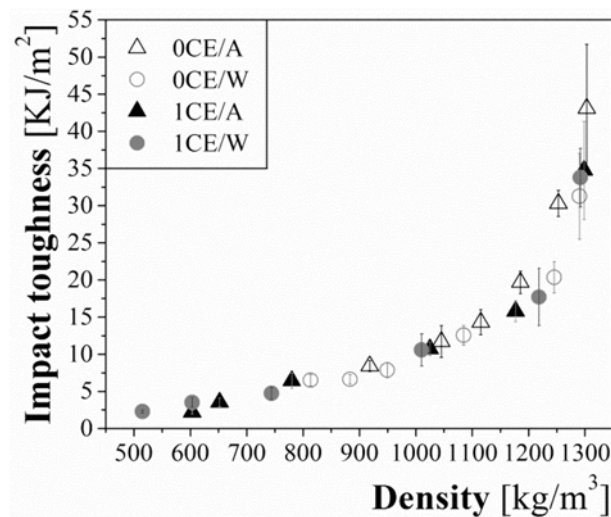


Figure V.11. Impact toughness against density.

In addition to this, the density was the most significant factor in the impact behaviour of the samples, as expected. The addition of only 1 wt.% CBA reduced the density around ~3% and ~8%, causing a decrease of 30% and 50% in the impact toughness of the 0CE and 1CE series, respectively. However, further additions of CBA led to less severe drops in impact toughness. The high standard deviation values impede determining whether other factors, such as crystallinity, have any effect on the impact properties, as might be expected.

V.4. Conclusions

In this study, PHA foams were successfully achieved by extrusion foaming with an endothermic CBA. Effects of the CBA content, as well as the effects of the two strategies—CE-addition and water cooling—were evaluated.

The results revealed a very complex system given, on the one hand, the intrinsic complexity of the polymer under study. On the other hand, opposing processes occurred simultaneously, some of them—such as hydrolytic degradation, CBA decomposition and cellular structure evolution, among others—impoverishing and some of them—such as chain extension and/or branching, and crystallinity variation—enhancing the foam's properties.

Regarding the CE addition, the strategy was more effective, regardless of the cooling system used, since it led to lower densities without producing a negative effect on the mechanical properties—the reduction observed in the mechanical properties was in the range of what was expected due to the decrease in the density—. CE addition led to lower viscosity and coarser cellular morphologies, but at the same time, prevented the polymer degradation—by reducing the degradation rate—, thus leading to a less degraded polymer with better properties.

The water-cooling strategy enhanced the density reduction only when the chain extender was not used, and could not reach the effectiveness of the CE addition.

No clear synergies were observed when combining both strategies.

The mechanical properties were strongly affected by the density reduction, as expected, and were similar for all samples; however, slightly better behaviour was observed for the 1CE/A series. In this sense, it can be concluded that optimal results were obtained with the use of CE (1 wt.%), 3–4 wt.% CBA content, and air cooling, since a balance between the mechanical properties and the density reduction could be achieved here.

References

- [1] Laycock B, Halley P, Pratt S, Werker A, Lant P. The chemomechanical properties of microbial polyhydroxyalkanoates. *Prog Polym Sci* 2014;39:397–442. doi:10.1016/j.progpolymsci.2013.06.008.
- [2] Reddy CSK, Ghai R, Rashmi, Kalia VC. Polyhydroxyalkanoates: An overview. *Bioresour Technol* 2003;87:137–46. doi:10.1016/S0960-8524(02)00212-2.
- [3] Shanks RA, Hodzic A, Wong S. Thermoplastic biopolyester natural fiber composites. *J Appl Polym Sci* 2004;91:2114–21. doi:10.1002/app.13289.
- [4] Rodriguez-Perez MA. Crosslinked Polyolefin Foams: Production, Structure, Properties, and Applications. *Crosslink. Mater. Sci.*, vol. 184, Berlin, Heidelberg: Springer Berlin Heidelberg; 2005, p. 97–126. doi:10.1007/b136244.
- [5] Wright ZC, Frank CW. Increasing cell homogeneity of semicrystalline, biodegradable polymer foams with a narrow processing window via rapid quenching. *Polym Eng Sci* 2014;54:2877–2886. doi:10.1002/pen.23847.
- [6] Le Moigne N, Sauceau M, Benyakhlef M, Jemai R, Benezet J-C, Rodier E, et al. Foaming of poly(3-hydroxybutyrate-co-3-hydroxyvalerate)/organo-clays nano-biocomposites by a continuous supercritical CO₂ assisted extrusion process. *Eur Polym J* 2014;61:157–71. doi:10.1016/j.eurpolymj.2014.10.008.
- [7] Liao Q, Tsui A, Billington S, Frank CW. Extruded foams from microbial poly(3-hydroxybutyrate-co-3-hydroxyvalerate) and its blends with cellulose acetate butyrate. *Polym Eng Sci* 2012;52:1495–508. doi:10.1002/pen.23087.
- [8] Behraves AH, Park CB, Cheung LK, Venter RD. Extrusion of polypropylene foams with hydrocerol and isopentane. *J Eng Appl Sci* 1996;2:1862–7. doi:10.1002/vnl.10153.
- [9] Szegda D, Daungphet S, Song J, Tarverdi K. Extrusion foaming and rheology of PHBV. 8th Int. Conf. Foam Mater. Technol., 2010, p. 6–11.
- [10] Verhoogt H, Ramsay BA, Favis BD, Ramsay JA. The influence of thermal history on the properties of poly(3-hydroxybutyrate-co-12%-3-hydroxyvalerate). *J Appl Polym Sci* 1996;61:87–96. doi:10.1002/(SICI)1097-4628(19960705)61:1<87::AID-APP10>3.0.CO;2-X.
- [11] Chodak I. Polyhydroxyalkanoates: Origin, Properties and Applications. In: Belgacem MN, Gandini A, editors. *Monomers, Polym. Compos. from Renew. Resour.*, Elsevier; 2008, p. 451–77. doi:10.1016/B978-0-08-045316-3.00022-3.
- [12] Cabedo L, Plackett D, Giménez E, Lagarón JM. Studying the degradation of polyhydroxybutyrate-co-valerate during processing with clay-based nanofillers. *J Appl Polym Sci* 2009;112:3669–76. doi:10.1002/app.29945.
- [13] Yamaguchi M, Arakawa K. Effect of thermal degradation on rheological properties for poly(3-hydroxybutyrate). *Eur Polym J* 2006;42:1479–86. doi:10.1016/j.eurpolymj.2006.01.022.
- [14] Villalobos M, Awojulu A, Greeley T, Turco G, Deeter G. Oligomeric chain extenders for economic reprocessing and recycling of condensation plastics. *Energy* 2006;31:3227–34. doi:10.1016/j.energy.2006.03.026.
- [15] Pilla S, Kim SG, Auer GK, Gong S, Park CB. Microcellular extrusion-foaming of polylactide with chain-extender. *Polym Eng Sci* 2009;49:1653–60. doi:10.1002/pen.21385.
- [16] Matuana LM, Faruk O, Diaz CA. Cell morphology of extrusion foamed poly(lactic acid) using endothermic chemical foaming agent. *Bioresour Technol* 2009;100:5947–54. doi:10.1016/j.biortech.2009.06.063.
- [17] Wang J, Zhu W, Zhang H, Park CB. Continuous processing of low-density, microcellular

CHAPTER VI

CELLULAR PHB/FLAX COMPOSITES

CHAPTER CONTENTS**SECTION 1. PRODUCTION PROCESS OF CELLULAR PHB/FLAX COMPOSITES**

Abstract	251
VI.1.1. Introduction	253
VI.1.2. Experimental section	256
VI.1.2.1. Preparation of the solid composite precursors	256
VI.1.2.1.1. Production of the reinforcement fabrics.....	256
VI.1.2.1.2. CE addition to the matrix.....	257
VI.1.2.1.3. Solid composite precursors' fabrication	257
VI.1.2.2. Preparation of the foamed composites.....	257
VI.1.2.3. Samples characterisation	259
VI.1.2.3.1. Rheology of the solid precursors.....	259
VI.1.2.3.2. Density	259
VI.1.2.3.3. Cell size and cell density	259
VI.1.3. Results and discussion	260
VI.1.3.1. Preliminary tests	260
VI.1.3.2. Influence of the presence of fibre	262
VI.1.3.3. Influence of the processing conditions in the CellFRC properties ..	264
VI.1.3.3.1. Density	264
VI.1.3.3.2. Cellular structure.....	265
VI.1.4. Conclusions	269
References	270

SECTION 2. CHARACTERISATION OF CELLULAR PHB/FLAX COMPOSITES

Abstract	275
VI.2.1. Introduction	277
VI.2.2. Experimental section	279
VI.2.2.1. Materials	279
VI.2.2.1.1. Matrix	279
VI.2.2.1.2. Reinforcement.....	279
VI.2.2.1.3. Blowing agent.....	280
VI.2.2.2. Production of the cellular fabric-reinforced composites	280
VI.2.2.2.1. Precursor preparation	280
VI.2.2.2.2. Pressure quench batch foaming.....	280
VI.2.2.3. Design of experiments	281

VI.2.2.4.	Samples characterisation.....	281
VI.2.2.4.1.	Density.....	281
VI.2.2.4.2.	Mechanical characterisation.....	282
VI.2.2.4.3.	DSC analysis.....	285
VI.2.3.	Results and discussion.....	286
VI.2.3.1.	Mechanical behaviour at room temperature.....	286
VI.2.3.2.	Dynamic mechanic thermal behaviour of the C-series.....	290
VI.2.3.3.	DSC results.....	293
VI.2.3.4.	Fibre reinforcing effect.....	295
VI.2.4.	Conclusions.....	296
	References.....	298

SECTION 1

**PRODUCTION PROCESS OF CELLULAR
PHB/FLAX COMPOSITES**

Abstract

The aim of the section of this chapter is to explore the production of cellular lightweight fibre-reinforced composites made of PHB-based matrix reinforced with flax nonwoven fabrics. The pressure quench method with CO₂ gas dissolution is used to foam composite precursors. The foaming conditions are determined from some preliminary tests performed to that purpose. The effect of several factors—matrix modification, reinforcement treatment, expansion temperature and expansion pressure—on density and cellular structure of the samples is evaluated. Homogeneous foamed composites are obtained. The influence of the fibre in the expansion of the samples is discussed. In general terms, the fibres seemed to enhance the foamability but, at the same time, to limit the expansion.

VI.1.1. Introduction

Over the last three decades, awareness about fossil resources' depletion, waste accumulation and other environmental problems has prompted researchers to the search of greener materials with high performance, good enough to replace other less eco-friendly solutions in their applications. Thus has led to the rise of biopolymers. The term "biopolymer" encompasses biodegradable polymers which proceed from oil, non-biodegradable polymers obtained from renewable resources, and bio-based biodegradable polymers. Over all the biopolymers available, polyhydroxyalkanoates (PHAs) biopolyesters are an interesting bio-based biodegradable alternative since the carbon-sources required for their production may not compete with food-crops [1]. This large family of biopolyesters is generated by bacteria under specific feeding conditions. Their properties are of great interest for a large number of applications, but their high price limits nowadays their competitiveness against the so called "commodity polymers" such as polyolefins. The addition of other phases is an interesting strategy to reduce the amount of biopolymer required, and hence, to increase their competitiveness. In this sense, both solid and gaseous phases can be added, to produce composites and foams, respectively.

On the one hand, foaming techniques introduce the gaseous phase as porosity to form a cellular material with lightweight, what reduces the biopolymer fraction. However, PHAs present, generally, an intrinsic difficulty to be foamed owing to their low molecular weight, low melt strength, high crystallinity and narrow processing window, although they have been successfully foamed by injection foaming and extrusion foaming [2–6]. Chain extender additives (CE) have been reported to enhance foamability in biopolyesters such as polylactic acid (PLA) [7–9], poly(3-hydroxybutyrate-co-3-hydroxyvalerate) (PHBV) [10] and poly(3-hydroxybutyrate-co-4-hydroxybutyrate) (P3HB4HB) [3].

On the other hand, addition of solid reinforcements leads to the formation of composite materials with generally improved mechanical properties. According to their shape, the reinforcements can be introduced in the form of fillers, fibres or textile fabrics. Reinforcements based on natural fibres—such as cellulosic fibres—have been shown to increase the stiffness and strength of biopolymers interaction—chemical and/or mechanical—is required. At the same time, the use of the right combination of cellulosic fibres and biopolymers, introduces the possibility of obtaining completely biodegradable composites product solutions with a greener end-of-life. To that purpose, nonwoven fabrics (NW) made of long flax fibres (60 mm) has been used as reinforcement, because of the good

mechanical properties, low density and low cost of the fibres, and because of the low production cost, easier handling and good fibre distribution of the NW structure. Despite a good compatibility between the flax fibres and the PHB-based matrix is expected, the NWs have been treated with wet/dry cycling and further argon plasma to improve fibre-matrix adhesion, as seen in Chapter IV.

The combination of both strategies leads to cellular fibre reinforced composites, abbreviated hereafter as CellFRC [11]. CellFRC have been obtained by different foaming techniques in the literature. In reference to this, some studies regarding CellFRC made of natural fibres and the main biopolymers—starch, PLA and PHAs—, are summarised in Table VI.1. Starch from several origins has been reinforced with cellulosic fibres (such as flax or hemp, among others) and foamed by baking techniques [12–15] or extrusion foaming [16,17]. PLA reinforced with cellulose fibres from the micro to the macroscale have been foamed by extrusion and injection foaming [18–20]. However, the gas dissolution foaming has also been for the production of produce PLA-based CellFRC in which the fibres were structured in preforms [21] or NW [22]. Regarding the PHA family, PHBV and blends, such as the blend with polybutyrate adipate terephthalate (PHBV/PBAT), have been reinforced with cellulosic fibres and foamed by injection foaming [23,24] and gas dissolution foaming [25]. According to these studies, up to 18-mm long fibres have been processed by extrusion foaming. However, the length and the structure of the fibres is a limiting factor for techniques such as extrusion foaming and injection foaming due to the process itself. In this sense, CellFRC reinforced with textile fabrics or structured fibres have been obtained by gas dissolution foaming techniques, as reported by Mooney et al. [22], Qiu et al. [26], Neagu et al. [21] and Sorrentino et al. [11].

Gas dissolution is a foaming batch process that mainly consists on polymer's saturation with a physical blowing agent (gas) at given temperature and pressure inside a pressure vessel, thus forming a single-phase polymer/gas solution; further expansion is achieved when a thermodynamic instability is reached, leading to the evolution of the dissolved gas (phase separation), what promotes the cell nucleation and grow. This gas separation can be induced by a temperature increase—temperature soak method—or by a quick pressure release—pressure quench method—. Given that the gas diffusion takes place mainly through the amorphous regions of the polymer, for semi-crystalline polymers, the gas diffusion is favoured in the melt state, where the crystalline regions are dissolved and the chain mobility is high, although the gas sorption depends inversely on the temperature and directly on the

pressure, all thus affecting on the final properties of the foam. Given that PHB is a semi-crystalline polymer, high temperature saturation and the pressure quench method have been considered for producing green CellFRC.

Table VI.1. Literature review regarding biopolymer/natural fibres CellFRC.

Matrix	Reinforcement (fibre length)	Blowing agent	Foaming method	Ref.
Starch (<i>corn</i>)	Aspen fibres (1-11 mm)	-	Baking	[12]
Starch (<i>tapioca</i>)	Flax fibres (6-60 mm) Jute fibres (2-20 mm)	-	Baking	[13]
Starch (<i>cassava</i>) /chitosan	Kraft fibre	-	Baking	[14]
Starch (<i>wheat</i>)	Barley straw fibres	Water	Microwave heating	[15]
Starch (<i>potato</i>) + talc	Wheat straw fibres (2.7 mm) Cotton linter fibres (18 mm) Cellulose fibres (120 μm) Hemp fibres (15 mm)	Water, CBA	Extrusion foaming	[16]
Starch acetate + talc	Corn cob fibre Cellulose fibre	Ethanol	Extrusion foaming	[17]
PLA + CE, talc	Cellulose fibres (20-200 μm)	scCO ₂	Extrusion foaming	[18]
PLA	Microfibrillated cellulose	CBA, water	Extrusion foaming	[19]
PLA	Willow fibre (0.5-2 mm)	scN ₂	Injection foaming	[20]
PHBV	Coir fibres	scN ₂	Injection foaming	[23]
PHBV/PBAT	Recycled wood fibres	scN ₂	Injection foaming	[24]
PLA	Birch kraft pulp fibres (~2 mm)	scCO ₂	Gas dissolution	[21]
PLA	PGA fibres	CO ₂	Gas dissolution	[22]
PHBV	Nanofibrillated cellulose (200 μm)	CO ₂	Gas dissolution	[25]

CBA: Chemical Blowing Agent; sc: supercritical.

The aim of this study is to explore the production of green cellular lightweight composites of PHB reinforced with flax NW fabrics. To that purpose, the pressure quench method with CO₂ gas dissolution is used to foam the samples. In the first part, preliminary tests are evaluated with two purposes: to determine the conditions in which the lower density values of CellFRC are achieved and to evaluate the influence of the fibre presence in the foaming behaviour of the PHB. In the second part, the effects of several factors—matrix type, reinforcement treatment, expansion temperature and expansion pressure—in the density and cellular structure of the CellFRC samples are discussed.

VI.1.2. Experimental section

The scheme of the sample preparation, which summarises part of the experimental work, is presented in Figure VI.1. The sample preparation requires, first, the NWs production and treatment on the one hand, and the matrix modification—with the CE—and film-formation on the other hand. With that, solid precursors are achieved by film-stacking. Then, the solid precursors are foamed by CO₂ dissolution at high temperature and expansion by quick pressure release. Finally, the resulting CellFRC are characterised.

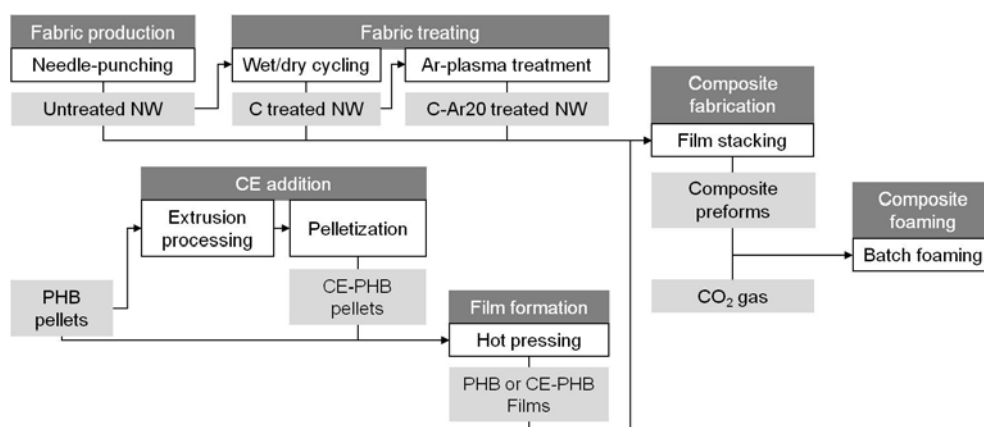


Figure VI.1. Scheme for the samples preparation.

VI.1.2.1. Preparation of the solid composite precursors

VI.1.2.1.1. Production of the reinforcement fabrics

Flax fibres, of average length of 6 cm and average diameter of 98 μm , were provided by Fibres Reserche Development of the Technopole de l'Aube en Champagne (France). NW fabrics of $284 \pm 23 \text{ g/m}^2$ and $1.9 \pm 0.1 \text{ mm}$ of thickness were produced by needle-punching in a DILO OUG-II-6 Pilot Plant (Germany), according to the processing conditions evaluated in previous research [27].

The NW fabrics were used in original conditions (Untreated) and modified with two treatments (C and C-Ar20), as summarised in Figure VI.1. The wet/dry cycling treatment (C), consisted on 4 cycles of sonication-enhanced rewetting with distilled water followed by drying in an air-circulating oven at 105 °C. For the C-Ar20 treatment, the argon plasma etching at low pressure was performed after the wet/dry cycling. For the plasma treatment, argon gas of 99.999% of purity was acquired from Air Liquide España (Spain). The process was performed under vacuum, in a Europlasma Junior Advanced PLC radiofrequency

plasma reactor (Belgium), using argon at constant flow rate of 20 sccm and a power of 50 W. The NW fabric was treated 10 minutes per side. Further information about the treatments can be found in [28].

VI.1.2.1.2. CE addition to the matrix

The thermoforming grade Mirel P3001, from Metabolix Inc. (USA), was used as matrix (referred to as PHB). The pellets were dried at 50 °C overnight in a P-SELECTA Vacuum Drying Oven VacioTem TV (Spain), and mixed with 1 wt.% of the chain extender (CE), Joncryl ADR-4368-C kindly provided by BASF (Germany). The mixture was then processed in a COLLIN ZK 25 T co-rotating twin-screw extruder (Germany), using a reverse temperature profile linearly decreasing from 170 °C to 150 °C at a screw-speed of 70 rpm. The extrudate was cooled in a water bath and pelletized. The modified polymer is referred to hereafter as CE-PHB.

VI.1.2.1.3. Solid composite precursors' fabrication

Both, PHB and CE-PHB were used to produce 0.6 mm-thick films in a COLLIN P 300P Hot Plate Press (Germany). The process consisted on heating at 175 °C for 5 minutes without pressure to melt the polymer and further 5 min under 50 MPa, followed by cooling to room temperature under 50 MPa of pressure. Then, the film-staking method was used to produce the solid composite precursors. Sandwich structures of film-NW-film were conformed in the hot plate press into 1 mm-thick precursors. The temperature was set to 175 °C and the conditions were 6 min under no pressure for melting, 4 min under 50 MPa for the conformation, and final cooling under 50 MPa. Six precursors (with an average fibre fraction of 19.8 ± 1.5 wt.%) were prepared. Regarding the use of the two matrices and the three types of reinforcement, the samples will be referred hereafter as: Untreated/PHB, Untreated/CE-PHB, C/PHB, C/CE-PHB, C-AR20/PHB and C-AR20/CE-PHB. Six specimens of 40 mm x 60 mm were cut from each precursor.

VI.1.2.2. Preparation of the foamed composites

The pressure quench foaming method was used to foam the solid precursors obtained by film-stacking. The samples were dried at 80 °C overnight under vacuum, and placed inside the high-pressure vessel. The dissolution of the blowing agent, the CO₂ gas of 99.9% purity supplied by Rivoira SpA (Italy), was performed at high temperature (above the melting

temperature (T_m) of the polymer, determined as 174.4 °C by DSC). Further foaming was achieved by quick pressure release after a cooling to reach the expansion temperature. For a better understanding, the scheme of pressure and temperature evolution of the general process is represented in Figure VI.2.

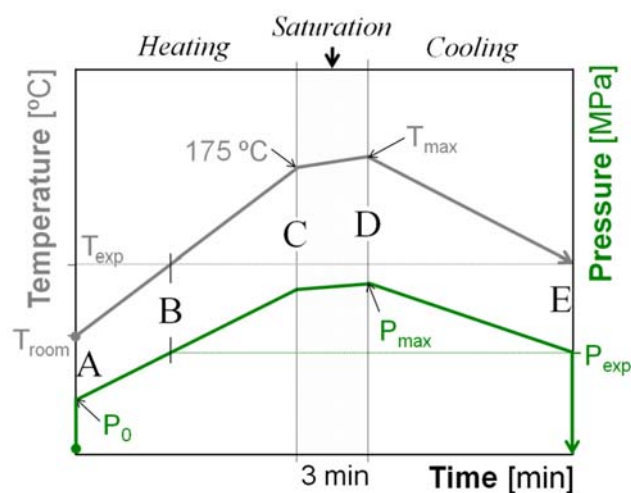


Figure VI.2. Definition of the temperature and pressure curves in the batch foaming process.

The steps A to D were performed as follows:

- (A) The pressure vessel was filled of CO₂ gas with an initial pressure (P_0) in accordance with the expansion pressure (P_{exp}) required. [P_0 were 3.75 ± 0.25 MPa, 6.25 ± 0.25 MPa and 7.25 ± 0.25 MPa for P_{exp} of 5 MPa, 10 and 20 MPa, respectively.]
- (A-C) Heating. The temperature was raised, with the consequent pressure increase, to 175 °C. [The heating rates were determined as 5.8 °C/min, 5.1 °C/min and 4.6 °C/min for expansion pressures of 5, 10 and 20 MPa, respectively.]
- (B) During heating, the pressure was controlled and regulated, if required, to be coincident with the final targeted conditions.
- (C-D) Gas saturation. After reaching 175 °C, a 3-minutes step was set for the CO₂ saturation. The short saturation time is due to the sensitivity of the PHAs to undergo in thermal degradation at temperatures near their melting point.
- (D) Owing to the thermal inertia, maximum temperature (T_{max}) and pressure (P_{max}) were found at the end of the saturation.
- (D-E) Cooling. The vessel was cooled to the targeted T_{exp} at a rate of -4.9 ± 0.3 °C/min.
- (E) Once reached the desired conditions, the expansion was achieved by a fast pressure release at a rate of 40 MPa/s.

Finally, the vessel was quickly opened and the samples extracted to avoid the modification/collapse of the cellular structure.

VI.1.2.3. Samples characterisation

VI.1.2.3.1. Rheology of the solid precursors

For the evaluation of the effect of the fibres addition, the dependence of viscosity with shear rate of the two matrices (PHB and CE-PHB) and the untreated/PHB solid composite was measured. The steady state flow curves at 175 °C were obtained in a TA Instruments Rheometer AR 2000 EX, equipped with electrically heated parallel plates of 25 mm of diameter, with a gap set to 1 mm. The viscosity was measured under shear rates between 0.001 and 10 rad/s in nitrogen atmosphere.

VI.1.2.3.2. Density

Geometric density (ρ) of the samples was determined dividing the mass of the specimen by its external volume (calculated considering its dimensions) before (ρ_{solid}) and after expansion (ρ_{foam}). The relative density (ρ_{rel}) was obtained by the ρ_{foam} by the ρ_{solid} .

VI.1.2.3.3. Cell size and cell density

The mean cell size (ϕ) of the foams was determined with a user-interactive image analysis adaptation of the ASTM D3576-04 method, based on [29], from SEM images of fragile fractures taken in a JEOL Scanning Electron Microscope JSM 820.

The cell density per solid volume (N_o) was determined as $N_o = [(6V_p)/(\pi\phi^3)]/(1-V_p)$, where the porous fraction V_p is calculated as $V_p = 1-(\rho_{\text{foam}}/\rho_{\text{solid}})$.

VI.1.3. Results and discussion

VI.1.3.1. Preliminary tests

The preliminary tests performed in the polymer without fibres had the aim of evaluating the foamability of PHB in the conditions of the study. Some examples of the results are presented in Figure VI.3.

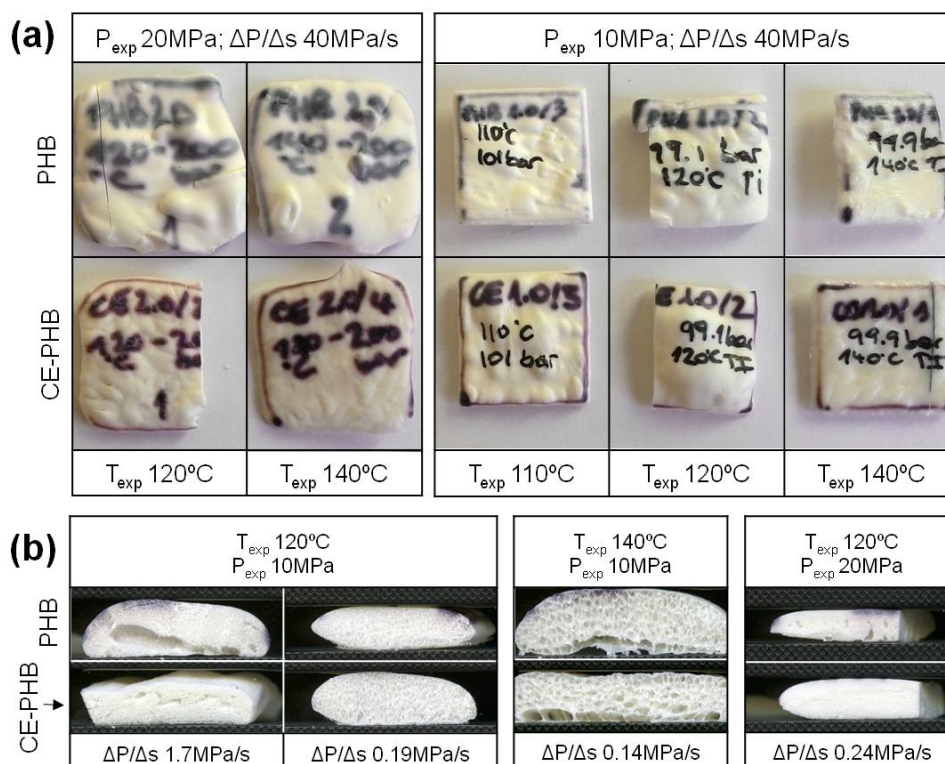


Figure VI.3. Examples of the specimens from the preliminary tests. PHB and CE-PHB without fibres expanded with a quick pressure release (a) and slow pressure release (b).

The expansion tests of the specimens without fibres expanded at quick pressure release (40 MPa/s) were unsuccessful, owing that the samples presented high heterogeneity in the expansion, with large bubbles and/or huge air-traps, as shown in Figure VI.3a. However, when the gas was slowly manually released ($0.15\text{--}0.30 \text{ MPa/s}$), the PHB and CE-PHB samples presented good expansions with more regular cellular structures, as shown in Figure VI.3b. Nonetheless, the conditions for such a slow release—which was critical to achieve the foaming of the matrices—would require an automatic system for the pressure release control to assure the experimental conditions, and hence the study about matrices without fibres could not be extended.

The composites gave more homogeneous expansions regardless the conditions used (Figure VI.4).



Figure VI.4. Comparative of the Untreated/PHB composites before and after expansion.

For preliminary test on composites, T_{exp} ranging from 100 °C to 170 °C, and P_{exp} of 5 MPa, 7.5 MPa, 10 MPa and 20 MPa were tested. The exploratory results are presented in Figure VI.5.

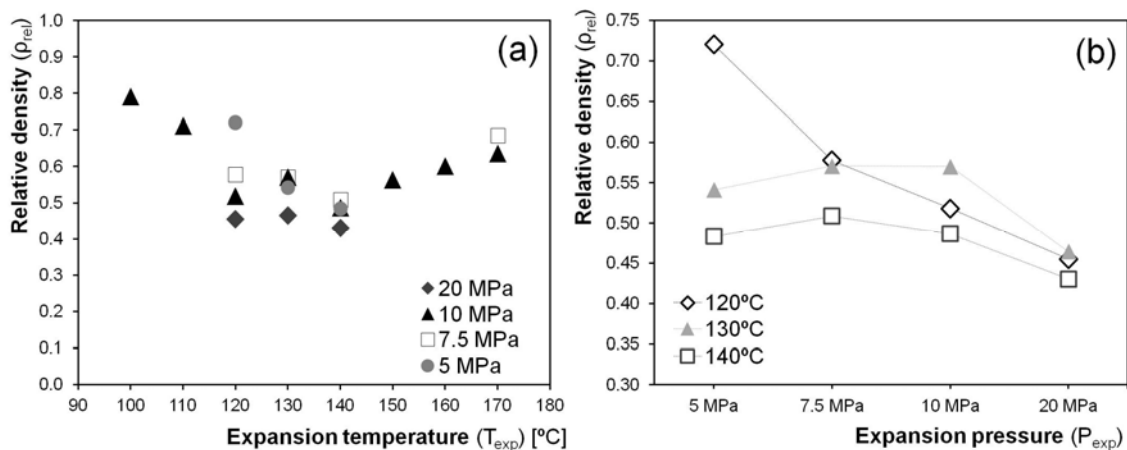


Figure VI.5. Relative density values of the composite samples foamed on the exploratory tests against T_{exp} (a) and P_{exp} (b). In (b), the purpose of lines is to guide the eye, and the P_{exp} axis is categorical (not in scale).

On the one hand, in Figure VI.5a, the relative densities achieved are plotted against the expansion temperatures. A scan of the T_{exp} effect in the relative density was performed at an expansion pressure of 10 MPa. According to this scan, the relative density decreased with the increase in the temperature, reached minimum values between 120 °C and 140 °C, and then started to rise again. On the other hand, in Figure VI.5b, the relative density results for the tests performed at 120 °C, 130 °C and 140 °C at different P_{exp} are presented, where the lower densities observed were achieved for the higher expansion pressure of 20 MPa, regardless the

T_{exp} used. Besides this, the densities were in the same range between 0.45-0.6 for tests performed at any of the temperatures at 10 MPa or 7.5 MPa, and at high temperatures at 5 MPa. No clear differences could be observed between the 7.5 MPa and 10 MPa and hence, the 7.5 MPa expansion pressure was not further considered for the following tests.

The exploratory results helped to define the conditions for the design of experiment. The factors for study of composite foaming were defined as follows. Two matrices—PHB and CE-PHB—and three NW fabrics—untreated, C, and C-Ar20—were used. According to the foamability range observed in Figure VI.5, for the expansion conditions, two temperatures and three pressures were considered under the following combinations: 10 MPa and 20 MPa at 120 °C, and 5 MPa, 10 MPa and 20 MPa at 140 °C. All thus originated 30 different samples which were further characterised according to the methods previously described. The effects of all these factors on the properties of the obtained CellFRC are later discussed.

VI.1.3.2. Influence of the presence of fibre

According to the results of the preliminary tests, the neat matrices revealed some difficulties to foam under the conditions evaluated. Given the intrinsic difficulty for foaming of the PHB, the CE was added with the aim of enhancing its expansion [3]. However, both the PHB and the CE-PHB specimens presented very irregular shapes, with large bubbles and no clear cellular structure, as seen in Figure VI.3. The ineffectiveness of the CE could be, in this case, due to the extra thermal cycle required for the CE addition in the PHB, which was performed by extrusion mixing, thus leading to higher degradation and loss of molecular weight. Anyhow, the lack of cellular structure in both matrices was attributed to a low viscosity, thus owing mainly to the high temperatures required for the process [30] and the effect of the CO₂ in the reduction of the T_m [31], although other possible effects—such as thermal degradation—cannot be discarded. Therefore, the too fluid state of the matrices under the foaming conditions would have led to an uncontrolled evolution of the cell nucleation and grow. Thus means that the driving forces of the gas pressure could not be counterbalanced by the polymer viscosity, what is consistent with the results observed.

Nevertheless, under the same conditions, the foaming of the composites could be easily achieved, showing fairly homogeneous expansions, regular cellular structures and relative densities between 0.45 and 0.6 for most of the specimens expanded at T_{exp} between 120-140 °C and P_{exp} between 5-20 MPa. It must be pointed out, that the homogeneous distribution of the fibres in the precursor was observed to be a key parameter, since areas

with lack of fibres were critical. According to these results, the foamability appeared to improve in the presence of the fibre reinforcement, thus attributed to an increase of the viscosity.

A rheological characterisation was performed in solid samples (with and without fibres) in order to determine possible changes in the viscosity. The steady state flow curves are shown in Figure VI.6.

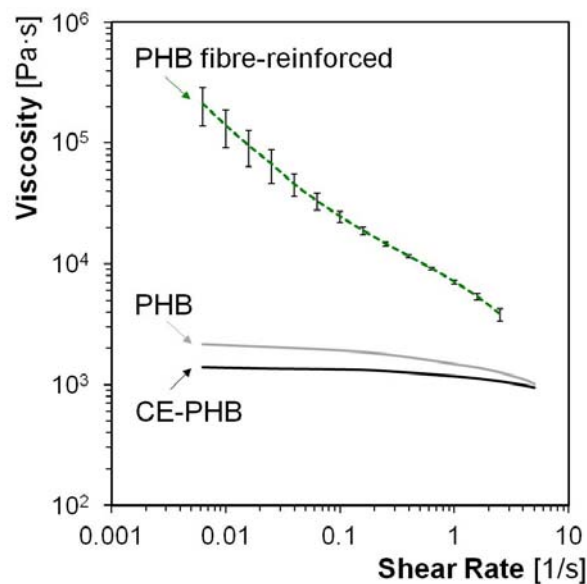


Figure VI.6. Steady state flow curves for the solid materials with and without fibres.

As can be observed, the viscosity curves for the fibre-reinforced materials are around two magnitude orders higher compared to their unreinforced counterparts. The addition of fibres clearly restricted the polymer flow of the material in the melt state, thus supporting the contribution of the viscosity increase in the higher foamability observed for the composites.

According to the scientific literature, the presence of fibres could have also promoted the formation of a more homogeneous cellular structure. In this sense, Boissard et al. produced cellular PLA/micro-fibrillated cellulose composites by extrusion foaming reporting, among other results, increased nucleation and a decrease on the cell size, pointing to a possible nucleating effect of the fibres [19]. Similarly, Javadi et al. reported the decrease in the cell size and increase in the cell density, due to fibre addition, in PHBV/wood fibre foams [24] and PHBV/coir fibre foams [23] obtained by injection moulding with N_2 .

Besides this, as aforementioned, all the samples had similar relative densities, with values between 0.45 and 0.6. Density values were barely lowered despite doubling the expansion pressure from 10 MPa to 20 MPa. In this sense, the flax fabric reinforcement seemed to have

a “constriction effect”, limiting the expansion. Thus could be a consequence of the fabric NW structure, which presents some mechanical entanglement of the long fibres through the fabric thickness due to its fabrication method, where a 3D structure is produced. Moreover, the flax fibres are completely stable at the T_m of the matrix (~ 174 °C). Therefore, the structural integrity of the NW fabric must remain throughout the batch process, thus explaining the shape stability of the specimens, unlike unreinforced foams that could experience cell collapsing between the expansion step and extraction from the vessel.

VI.1.3.3. Influence of the processing conditions in the CellFRC properties

VI.1.3.3.1. Density

The results of the relative density achieved against the expansion pressure have been plotted in Figure VI.7.

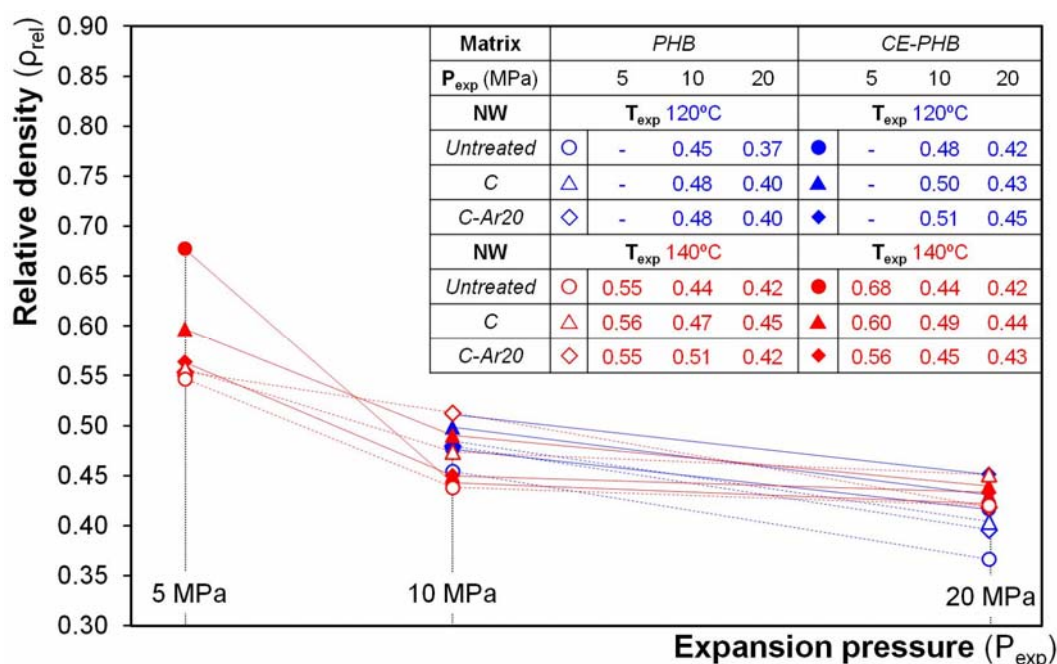


Figure VI.7. Relative densities of the CellFRC obtained according to the variables of study.

All the specimens foamed at the expansion pressures of 10 MPa and 20 MPa presented relative densities in the range from 0.45 to 0.5 and from 0.4 to 0.45, respectively. The very limited density reduction under P_{exp} of 20 MPa with respect to the lower P_{exp} is mainly attributed to the constriction effect of the reinforcement structure, as explained before. The addition of CE, the NWF treatment, and the expansion temperature seemed to present a low influence on the foam density.

Significant variations in density were obtained at P_{exp} of 5 MPa, at which higher densities—lower expansions—were measured. This can be related with the lower solubilization pressure during the gas dissolution process—highly dependant on the expansion pressure—. The lower amount of available gas—blowing agent—reduces the achievable expansion ratio and also the thermodynamic instability during the pressure quench, and hence, the cell nucleation is lower. Moreover, the CO_2 is known to produce a plasticization effect, reducing the viscosity of the matrix, but since the CO_2 content is smaller, this effect is lower and the bubble growth requires to overcome higher forces. For the P_{exp} of 10 MPa, a higher amount of absorbed CO_2 lowered the density levelling the expansion ratio, but higher solubilization pressures—although produced an even lower viscosity—could not result in foam reduction due to the constriction effect of the fibres.

VI.1.3.3.2. Cellular structure

To evaluate the cellular structure, fracture images (obtained by SEM) of the 30 specimens were analysed. In Figure VI.8, some examples are presented, where the cellular structure throughout the thickness can be observed.

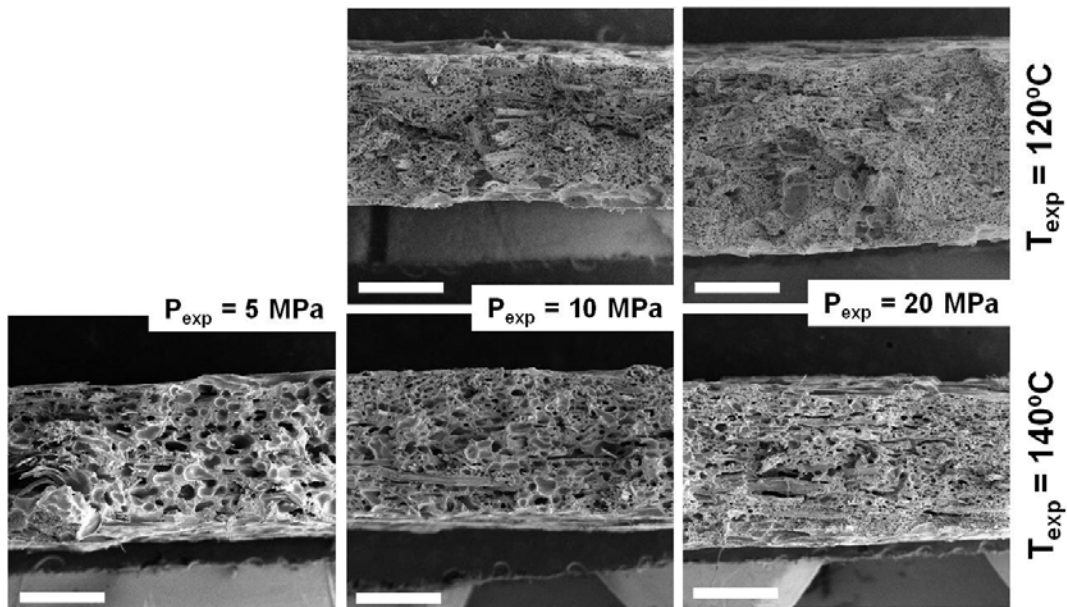


Figure VI.8. SEM images of the C-Ar20/PHB composite series.

In general terms, a good distribution of the fibres through all the specimens was observed. This homogeneity was attributed to the NW nature of the reinforcement fabric and a good consolidation achieved in the precursors during film-stacking. On the other hand,

all the specimens presented variable results concerning to fibre/matrix interaction, since fibre pull-out—what points to a weak fibre/matrix adhesion—and good adhesion in part of the fibres were both observed.

The morphology of cellular structures at higher magnification is presented in Figure VI.9, in order to show the clear differences observed in the cell size and the cell density.

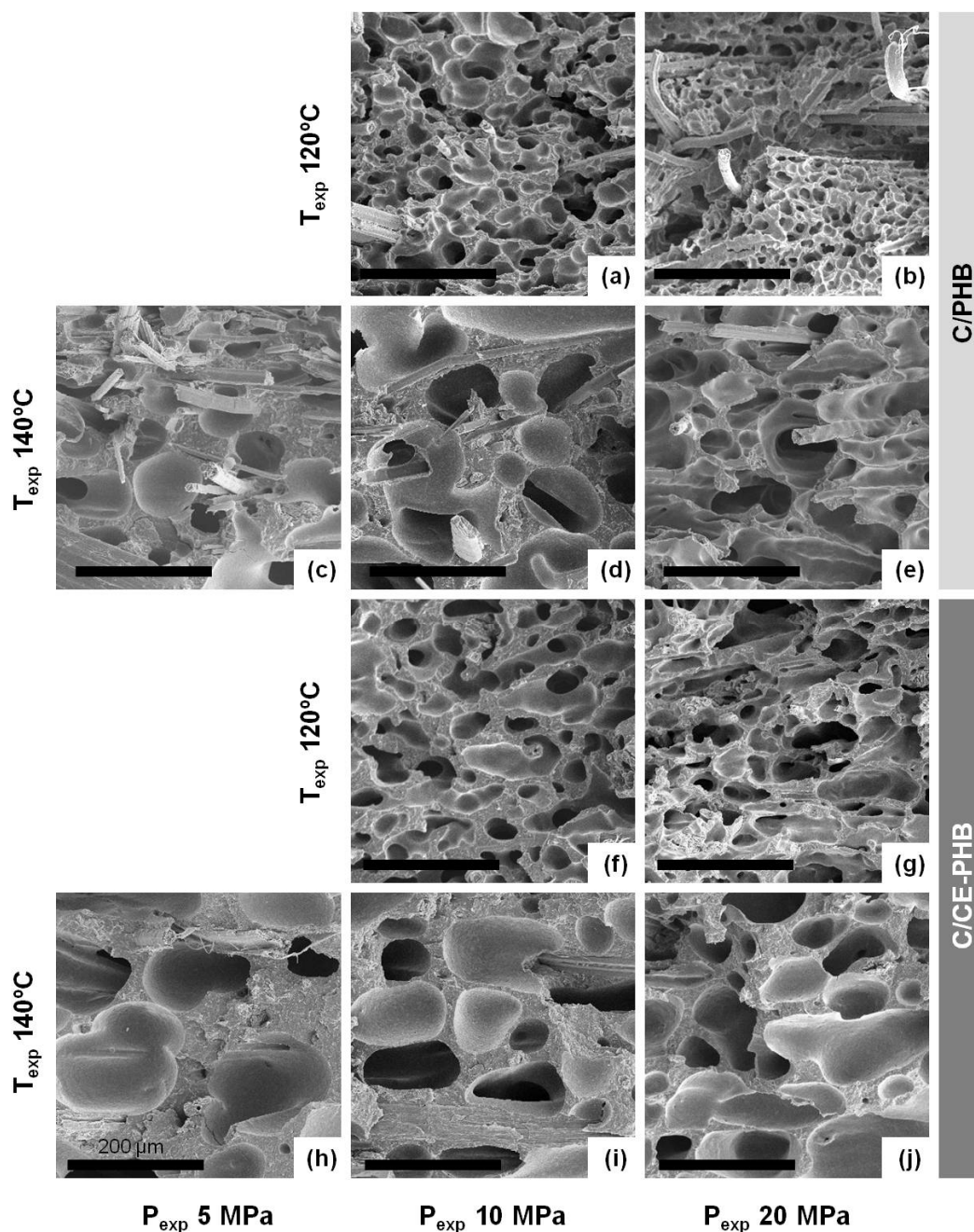


Figure VI.9. SEM images at 100X magnification of the (a)-(e) C/PHB series and (f)-(j) C/CE-PHB series, as an example of the different cellular structures observed regarding the different expansion conditions. Scale bars correspond to 200 μm .

Regarding to the cell size, the results of the cell measurement are presented in Table VI.2. The cell size of the CellFRC samples presented a high variability, with values from $\sim 30 \mu\text{m}$ to $\sim 190 \mu\text{m}$. However, this variability was in accordance with the expansion conditions.

Table VI.2. Cell size values, in μm .

Matrix	PHB			CE-PHB		
	5 MPa	10 MPa	20 MPa	5 MPa	10 MPa	20 MPa
NW	T_{exp} 120 °C			T_{exp} 120 °C		
<i>Untreated</i>	-	61	51	-	68	34
<i>C</i>	-	49	32	-	60	57
<i>C-Ar20</i>	-	40	40	-	62	31
NW	T_{exp} 140 °C			T_{exp} 140 °C		
<i>Untreated</i>	170	129	105	98	104	107
<i>C</i>	116	113	64	168	82	105
<i>C-Ar20</i>	165	116	67	153	187	84

The cell sizes values were higher for the samples expanded at 140 °C (between 60-190 μm) than for the samples expanded at 120 °C (up to $\sim 80 \mu\text{m}$). The coarser structures could also be observed in Figure VI.8 and Figure VI.9, were some of the samples obtained at 140 °C presented larger cells. Besides this, for the samples untreated/PHB, C/PHB and C-Ar20/PHB both at 140 °C, and in all samples at 120 °C—except C-Ar20/PHB—, the cell size decreased with the expansion pressure. For all the samples (except the C/CE-PHB at 140 °C), the cell size for the 20 MPa pressure was equal or smaller than the cell size for the 10 MPa pressure, thus attributed to the higher amount of gas, which caused heavier thermodynamic instability and hence, a higher cell nucleation.

Concerning to the cell density, the results for T_{exp} of 120 °C and 140 °C have been plotted against the P_{exp} in Figure VI.10. First of all, the scales of the cell density in both graphs reveal a clear influence of the temperature. Meanwhile cell density values were in the range of 10^5 - 10^7 cells/cm³ at 140 °C, for 120 °C were in the range of 10^6 - 10^8 cells/cm³. On the other hand, the cell density increased with the increase of the P_{exp}, reaching maximum values for the samples expanded at 20 MPa of pressure. This agrees the classical nucleation theory of cell nucleation, which predicts a higher amount of cells for increasing content of

gas—the solubilization pressure, related to the expansion pressure, is higher—and higher thermodynamic instability. On the other hand, the increase of the cell size with the temperature is translated to a cell density reduction, as expected.

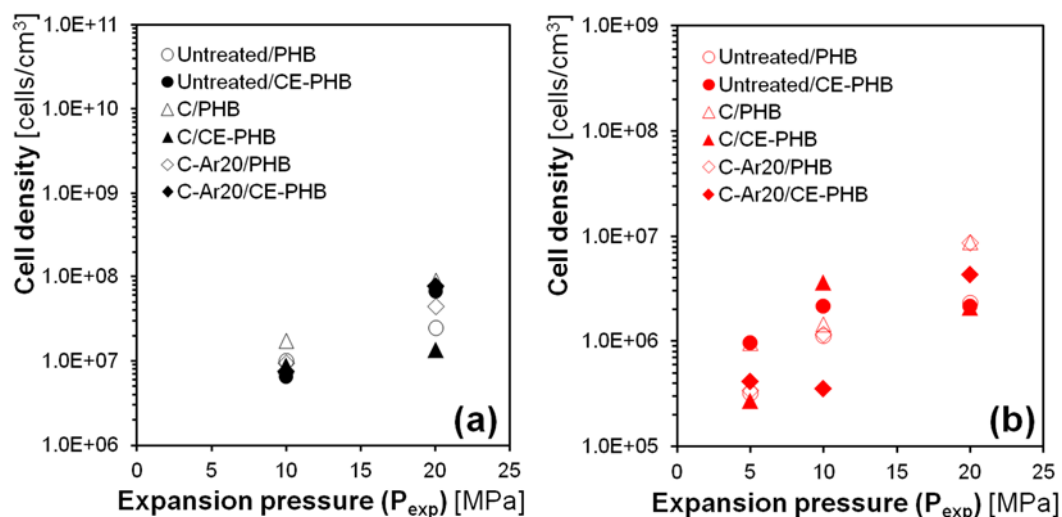


Figure VI.10. Cell densities of the CellFRC for the composites expanded at 120 °C (a) and at 140 °C (b). It is worth to note the difference in the scales.

Finally, despite the cellular structure was highly influenced by the expansion conditions, the treatments in the NW reinforcements did not show any relevant difference for the properties analysed. Neither the use of a chain extended matrix revealed to have any effect in the cellular structure.

VI.1.4. Conclusions

CellFRC of PHB matrix—with or without chain extender additive—and flax NW fabric reinforcements were successfully achieved by CO₂ gas dissolution using the pressure quench method. The CellFRC obtained presented good regularity according to the homogeneity of the precursors. In this sense, the fibres presented a homogeneous distribution through the thickness and a fair fibre-matrix adhesion could be observed. Regarding their effect in the foamability, the presence of the fibre-reinforcement enhanced the viscosity of the polymeric matrix—thus favouring the foaming—, although also limited the total expansion due to constriction effects attributed to the structural integrity of the reinforcement. Regarding the density reduction, the best results were achieved expanding the samples between 120 °C and 140 °C, at pressures of 10 MPa and 20 MPa. In this sense, specimens expanded at 10 MPa and 20 MPa presented similar relative densities around 0.4-0.5 regardless the matrix or reinforcement. However, some differences could be observed in their cellular structure. The specimens presented fewer larger cells with the increase in the expansion temperature—as a consequence of the higher chain mobility enhancing the cell grow and/or their coalescence, and a higher cell density with the increase of the expansion pressure, as a result of a higher gas solubilized and the consequent higher thermodynamic instability after the pressure quench.

Therefore, the CellFRC presented a considerably amount of porous phase and fibre, what reduces the amount of biopolymer required, what could lower the cost of this biodegradable solution, increasing its competitiveness.

References

- [1] Chanprateep S. Current trends in biodegradable polyhydroxyalkanoates. *J Biosci Bioeng* 2010;110:621–32. doi:10.1016/j.jbiosc.2010.07.014.
- [2] Jeon B, Kim HK, Cha SW, Lee SJ, Han M-S, Lee KS. Microcellular foam processing of biodegradable polymers — review. *Int J Precis Eng Manuf* 2013;14:679–90. doi:10.1007/s12541-013-0092-0.
- [3] Ventura H, Laguna-Gutiérrez E, Rodríguez-Perez MA, Ardanuy M. Effect of chain extender and water-quenching on the properties of poly(3-hydroxybutyrate-co-4-hydroxybutyrate) foams for its production by extrusion foaming. *Eur Polym J* 2016;85:14–25. doi:10.1016/j.eurpolymj.2016.10.001.
- [4] Liao Q, Tsui A, Billington S, Frank CW. Extruded foams from microbial poly(3-hydroxybutyrate-co-3-hydroxyvalerate) and its blends with cellulose acetate butyrate. *Polym Eng Sci* 2012;52:1495–508. doi:10.1002/pen.23087.
- [5] Szegda D, Daungphet S, Song J, Tarverdi K. Extrusion foaming and rheology of PHBV. 8th Int. Conf. Foam Mater. Technol., 2010, p. 6–11.
- [6] Wright ZC, Frank CW. Increasing cell homogeneity of semicrystalline, biodegradable polymer foams with a narrow processing window via rapid quenching. *Polym Eng Sci* 2014;54:2877–2886. doi:10.1002/pen.23847.
- [7] Pilla S, Kim SG, Auer GK, Gong S, Park CB. Microcellular extrusion-foaming of polylactide with chain-extender. *Polym Eng Sci* 2009;49:1653–60. doi:10.1002/pen.21385.
- [8] Ludwiczak J, Kozłowski M. Foaming of Polylactide in the Presence of Chain Extender. *J Polym Environ* 2015;23:137–42. doi:10.1007/s10924-014-0658-7.
- [9] Wang J, Zhu W, Zhang H, Park CB. Continuous processing of low-density, microcellular poly(lactic acid) foams with controlled cell morphology and crystallinity. *Chem Eng Sci* 2012;75:390–9. doi:10.1016/j.ces.2012.02.051.
- [10] Duangphet S, Szegda D, Song J, Tarverdi K. The Effect of Chain Extender on Poly(3-hydroxybutyrate-co-3-hydroxyvalerate): Thermal Degradation, Crystallization, and Rheological Behaviours. *J Polym Environ* 2013;22:1–8. doi:10.1007/s10924-012-0568-5.
- [11] Sorrentino L, Cafiero L, D’Auria M, Iannace S. Cellular thermoplastic fibre reinforced composite (CellFRC): A new class of lightweight material with high impact properties. vol. 64. 2014. doi:10.1016/j.compositesa.2014.05.016.
- [12] Lawton J., Shogren R., Tiefenbacher K. Aspen fiber addition improves the mechanical properties of baked cornstarch foams. *Ind Crops Prod* 2004;19:41–8. doi:10.1016/S0926-6690(03)00079-7.
- [13] Soykeabkaew N, Supaphol P, Rujiravanit R. Preparation and characterization of jute- and flax-reinforced starch-based composite foams. *Carbohydr Polym* 2004;58:53–63. doi:10.1016/j.carbpol.2004.06.037.
- [14] Kaisangsri N, Kerdechuen O, Laohakunjit N. Biodegradable foam tray from cassava starch blended with natural fiber and chitosan. *Ind Crops Prod* 2012;37:542–6. doi:10.1016/j.indcrop.2011.07.034.
- [15] Lopez-Gil A, Silva-Bellucci F, Velasco D, Ardanuy M, Rodríguez-Perez MA. Cellular structure and mechanical properties of starch-based foamed blocks reinforced with natural fibers and produced by microwave heating. *Ind Crops Prod* 2015;66:194–205. doi:10.1016/j.indcrop.2014.12.025.
- [16] Bénézet J-C, Stanojlovic-Davidovic A, Bergeret A, Ferry L, Crespy A. Mechanical and

- physical properties of expanded starch, reinforced by natural fibres. *Ind Crops Prod* 2012;37:435–40. doi:10.1016/j.indcrop.2011.07.001.
- [17] Guan J, Hanna MA. Functional properties of extruded foam composites of starch acetate and corn cob fiber. *Ind Crops Prod* 2004;19:255–69. doi:10.1016/j.indcrop.2003.10.007.
- [18] Bocz K, Tábi T, Vadas D, Sauceau M, Fages J, Marosi G. Characterisation of natural fibre reinforced PLA foams prepared by supercritical CO₂ assisted extrusion. *Express Polym Lett* 2016;10:771–9. doi:10.3144/expresspolymlett.2016.71.
- [19] Boissard CIR, Bourban P-E, Tingaut P, Zimmermann T, Manson J-A. E. Water of functionalized microfibrillated cellulose as foaming agent for the elaboration of poly(lactic acid) biocomposites. *J Reinf Plast Compos* 2011;30:709–19. doi:10.1177/0731684411407233.
- [20] Zafar MT, Zarrinbakhsh N, Mohanty AK, Misra M, Ghosh AK. Biocomposites based on poly(Lactic acid)/willow-fiber and their injection moulded microcellular foams. *Express Polym Lett* 2016;10:176–86. doi:10.3144/expresspolymlett.2016.16.
- [21] Neagu RC, Cuenoud M, Berthold F, Bourban P-E, Gamstedt EK, Lindstrom M, et al. The potential of wood fibers as reinforcement in cellular biopolymers. *J Cell Plast* 2012;48:71–103. doi:10.1177/0021955X11431172.
- [22] Mooney DJ, Baldwin DF, Suh NP, Vacanti JP, Langer R. Novel approach to fabricate porous sponges of poly(D,L-lactic-co-glycolic acid) without the use of organic solvents. *Biomaterials* 1996;17:1417–22.
- [23] Javadi A, Srithep Y, Pilla S, Lee J, Gong S, Turng L-S. Processing and characterization of solid and microcellular PHBV/coir fiber composites. *Mater Sci Eng C* 2010;30:749–57. doi:10.1016/j.msec.2010.03.008.
- [24] Javadi A, Srithep Y, Lee J, Pilla S, Clemons C, Gong S, et al. Processing and characterization of solid and microcellular PHBV/PBAT blend and its RWF/nanoclay composites. *Compos Part A Appl Sci Manuf* 2010;41:982–90. doi:10.1016/j.compositesa.2010.04.002.
- [25] Srithep Y, Ellingham T, Peng J, Sabo R, Clemons C, Turng L-S, et al. Melt compounding of poly (3-hydroxybutyrate-co-3-hydroxyvalerate)/nanofibrillated cellulose nanocomposites. *Polym Degrad Stab* 2013;98:1439–49. doi:10.1016/j.polymdegradstab.2013.05.006.
- [26] Qiu Y, Xu W, Wang Y, Zikry MA, Mohamed MH. Fabrication and characterization of three-dimensional cellular-matrix composites reinforced with woven carbon fabric. *Compos Sci Technol* 2001;61:2425–35. doi:10.1016/S0266-3538(01)00164-6.
- [27] Ventura H, Ardanuy M, Capdevila X, Cano F, Tornero JA. Effects of needling parameters on some structural and physico-mechanical properties of needle-punched nonwovens. *J Text Inst* 2014;1–11. doi:10.1080/00405000.2013.874628.
- [28] Ventura H, Claramunt J, Navarro A, Rodriguez-Perez M, Ardanuy M. Effects of Wet/Dry-Cycling and Plasma Treatments on the Properties of Flax Nonwovens Intended for Composite Reinforcing. *Materials (Basel)* 2016;9:93. doi:10.3390/ma9020093.
- [29] Pinto J, Solorzano E, Rodriguez-Perez MA, De Saja JA. Characterization of the cellular structure based on user-interactive image analysis procedures. *J Cell Plast* 2013;49:555–75. doi:10.1177/0021955X13503847.
- [30] Colton JS. The nucleation of microcellular foams in semi-crystalline thermoplastics. *Mater Manuf Process* 1989;4:253–62. doi:10.1080/10426918908956288.
- [31] Takahashi S, Hassler JC, Kiran E. Melting behavior of biodegradable polyesters in carbon dioxide at high pressures. *J Supercrit Fluids* 2012;72:278–87. doi:10.1016/j.supflu.2012.09.009.

SECTION 2

**CHARACTERISATION OF THE CELLULAR
PHB/FLAX COMPOSITES**

Abstract

In this study, biocomposites—made of polyhydroxybutyrate-based matrix and flax nonwoven-fabric reinforcement—foamed by CO₂ gas dissolution, are characterised by means of dynamic mechanical analysis (DMA) and differential scanning calorimetry (DSC). The effects of fibre addition, surface treatment of the reinforcement, use of chain extender additives and foaming conditions are evaluated. The cellular fibre-reinforced composites (CellFRC) presented 140% higher flexural stiffness than unreinforced foams of the same density, with values decreasing with the density following the scaling law. Macro-mechanical models considering porosity fraction presented reasonable fitting to the results obtained. The damping properties increased in CellFRC with higher expansions. The mechanical improvement due to presence of fibres even at higher temperatures was observed in dynamic mechanic thermal analysis of selected samples, and the DSC revealed clear differences in the crystal formation depending on the foaming conditions.

VI.2.1. Introduction

Green composites have gained an increasing interest of both the research and the industry. The awareness about the depletion of fossil sources and the waste accumulation problems have favoured the rise of more eco-friendly solutions. The use of appropriate combination of matrix and reinforcement materials can lead to completely bio-based and biodegradable solutions, thus presenting some advantages in their origin and final disposal. Due to that, biopolymers—such as polylactic acid (PLA) or polyhydroxyalkanoates (PHAs)—reinforced with natural cellulosic fibres (such as flax, hemp or sisal, among others) have focussed the attention of researchers over the last two decades [1–5]. In this sense, the focus is found in “solid” biocomposites, regarding coupling agent addition or fibre treatments to improve fibre/matrix adhesion [6–8], modelling of composite's properties [9–11] and its characterisation [1–3,12,13], mainly. However, some authors have addressed their work to the development of cellular fibre reinforced composites—or CellFRC [14], as will be referred hereafter—, in which the composite consists on a cellular matrix with fibre reinforcement. Concerning to CellFRC biocomposites, biopolymers—such as starch, PLA and PHAs—reinforced with natural cellulosic fibres have been foamed by means of several techniques, such as injection foaming [15–17], extrusion foaming [18–21], or gas dissolution foaming [22–24], among others. Nonetheless, despite the foaming of this kind of materials can lead to several advantages—such as the lightweight or the improvement in thermal and/or acoustic insulation, for instance—, the reduction in density is achieved in detriment of the mechanical properties. In general terms, in foams this behaviour is described by the scaling law:

$$\frac{\text{Foam's property}}{\text{Solid's property}} = C \cdot \left(\frac{\rho_{\text{foam}}}{\rho_{\text{solid}}} \right)^n \quad (\text{VI. 1})$$

where C is a constant that mainly depends on the polymer matrix [25] and n is the density exponent related to the deformation mechanisms and the cellular structure characteristics.

The dynamic mechanical analysis (DMA) is a characterisation technique that allows studying the response of a material to stress or temperature. However, the dynamic mechanical response of composites has a high dependence on interface, content, morphology and nature of the components [26,27].

On the one hand, the complex response of a polymer to an applied force is related to its viscoelasticity, where the storage modulus (E') is related to the elastic response, the loss

modulus (E''), to the viscous response, and the loss tangent ($\tan \delta$) is regarded as a damping factor—giving an idea of the energy dissipation capabilities of the materials—or as an index of viscoelasticity. The complex modulus (E^*) is defined as $E^*=[(E')^2+(E'')^2]^{1/2}$, and is related to the tensile modulus by a correcting factor than can be neglected for $\tan \delta$ values of 0.1 or lower. Therefore, the E^* is often considered as the elastic modulus (E) of the material.

On the other hand, the reinforcements introduced in composites tend to respond as purely elastic systems—if thermally stable at the analysis temperatures—, while the matrix and the fibre/matrix interfaces present a viscoelastic response [28]. Therefore, the addition of the reinforcement in a polymer generally increases the elastic response with respect to the neat polymer, and hence a decrease in the $\tan \delta$ is observed. Moreover, the improvement in the fibre/matrix adhesion is translated into an increase on the elastic response—since the mobility of the polymeric chains is more limited in the fibre/matrix interface—, thus decreasing even more the $\tan \delta$ values of the composite [26].

Regarding to the effects of foaming in the dynamic mechanical response, it must be taken into account that the expansion does not only affect the cellular structure but also the physical characteristics of the matrix—i.e. crystallinity—. Concerning to the modulus, the complex modulus (E^*) is affected by the foam density [29], and hence foaming leads to a lowering of the intensity in the E' and E'' curves with respect to the solids. Otherwise, the $\tan \delta$ curves are independent of the specimen geometry, therefore the relaxation peaks observed depend mainly on the polymeric morphology—crystallinity, lamellar thickness, etc.—, and not on the cellular structure whether low frequencies and strains are used [29].

This work deals with the characterisation of composites with polyhydroxybutyrate (PHB) matrix and flax fibre nonwoven (NW) reinforcement, both the solid and the CellFRC—obtained from these precursor composites—obtained by gas dissolution foaming—pressure quench method—. To that purpose, dynamic mechanical tests at room temperature are performed in order to determine the stiffness of the samples—solid or cellular—, which is compared to macro-mechanical modelling for its validation. On the other hand, dynamic mechanical thermal analysis—referred as DMTA for differentiation of the room temperature tests—are performed to obtain information about thermal transitions occurring in the material—such as the glass transition—, as well as to evaluate the viscoelastic behaviour of selected samples. This is complemented with DSC tests to characterise the melting and crystallisation behaviour.

VI.2.2. Experimental section

VI.2.2.1. Materials

VI.2.2.1.1. Matrix

The thermoforming grade *Mirel P3001* from Metabolix Inc. (USA) was used as matrix—referred hereafter as PHB—. A 1 wt.% of chain extender (CE) additive was mixed to obtain a modified matrix (CE-PHB). The CE used was Joncryl ADR-4368-C, kindly provided by BASF (Germany). The conditions of extrusion mixing used for that process have been previously defined—see previous section—. PHB and CE-PHB were transformed into films of 0.6 mm thickness by means of a COLLIN P 300P Hot Plate Press (Germany) under the following conditions: melting at 175 °C for 5 minutes under no pressure, hot-pressing at 175 °C for 5 minutes under 50 MPa of pressure, and cooling to room temperature under 50 MPa of pressure.

VI.2.2.1.2. Reinforcement

For the reinforcement, flax fibres—with 60 mm of average length, 98 µm of average diameter, an E modulus of an average of 30.4 GPa, and a density of 1.46 g/dm³—, were provided by Fibres Reserche Development, from Technopole de l'Aube in Champagne (France). NW fabrics, of 284 ± 23 g/m² of weight and 1.9 ± 0.1 mm of thickness, were produced with the flax fibres by needle-punching in a DILO OUG-II-6 Pilot Plant (Germany), according to the processing conditions evaluated in previous research [30]. For improvement of the fibre/matrix interaction, the NW fabrics were modified with two kind of surface treatments. Therefore, the NW used were in three different conditions: the original (untreated), treated with wet/dry cycling (C), and treated with wet/dry cycling plus further plasma etching with argon (C-Ar20). Briefly, the wet/dry cycling consists of 4 cycles of wetting in distilled water—enhanced by sonication—followed by oven-drying at 105 °C. For the plasma treatment, argon gas of 99.999% of purity was acquired from Air Liquide España (Spain). The process consisted on placing the samples in the reactor and, under vacuum conditions, generating a plasma of 50 W of power under a constant flow of argon gas at 20 sccm, treating the NW fabric 10 minutes per side. Thus was performed in a Europlasma Junior Advanced PLC Radiofrequency Plasma Reactor (Belgium). Further information about the treatments can be found in [31].

VI.2.2.1.3. Blowing agent

The (physical) blowing agent used to obtain the cellular composites was CO₂ gas, of 99.9% of purity, supplied by Società Ossigeno Napoli (Italy).

VI.2.2.2. Production of the cellular fabric-reinforced composites

VI.2.2.2.1. Precursor preparation

Sandwich structures of film-NW-film were conformed by film-stacking in the hot plate press, under the following conditions: melting at 175 °C for 6 minutes under no pressure, thermoforming at 175 °C for 4 minutes under 50 MPa of pressure, and cooling to room temperature under 50 MPa of pressure. Six different precursors were obtained, with a thickness of 1 mm and an average fibre fraction of 19.8 ± 1.5 wt.%, from the combination of the two matrices and three NW fabrics: untreated/PHB, untreated/CE-PHB, C/PHB, C/CE-PHB, C-AR20/PHB and C-AR20/CE-PHB. Six specimens of 40 mm x 60 mm were cut from each precursor and dried at 80 °C under vacuum overnight previously to their foaming.

VI.2.2.2.2. Pressure quench batch foaming

The cellular biocomposites were obtained by batch foaming process with CO₂ gas dissolution using the pressure quench method. In Figure VI.11, a generalised example of the temperature and pressure evolution is recorded. Briefly, specimens—precursors—were placed in the high-pressure vessel, which was secured and filled with initial pressure (P_0) of CO₂ gas determined by the targeted expansion pressure (P_{exp}). Then, the vessel was heated until reaching 175 °C, with the consequent pressure increase. The heating rates were different depending on the P_0 due to the amount of gas filled. During heating, the conditions were controlled to achieve the targeted P_{exp} at the expansion temperature (T_{exp}). A short saturation time of 3 minutes was set to minimize the thermal degradation of the PHB, after which the vessel was cooled. At the target conditions of T_{exp} and P_{exp} —10 MPa or 20 MPa at 120 °C, and 5 MPa, 10 MPa or 20 MPa at 140 °C—, the expansion was achieved by a quick release of the pressure in rate of 40 MPa/s. The pressure release produced the expansion of the matrix, and then the vessel was opened to take the specimens quickly to avoid the modification of their cellular structure. Further details of the process can be found in the previous section.

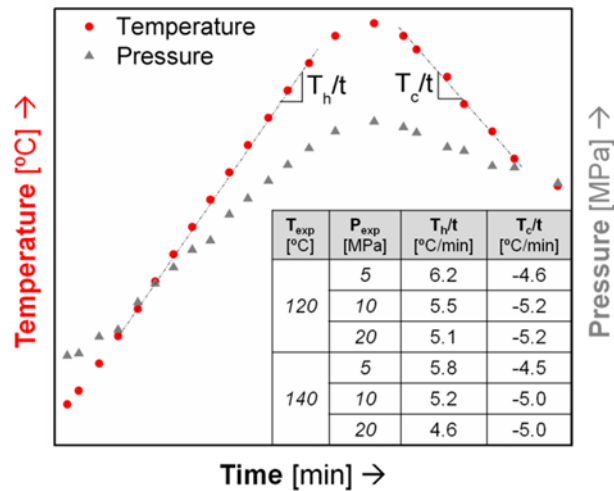


Figure VI.11. Evolution of the temperature and pressure curves in foaming process.

VI.2.2.3. Design of experiments

The factors for study of composite foaming were defined as follows. Two matrices—PHB and CE-PHB—and three NW fabrics—untreated, C, and C-Ar20—were used. According to the foamability range of the material, the conditions considered were two temperatures and three expansion pressures combined as: 10 MPa and 20 MPa at 120 °C; and 5 MPa, 10 MPa and 20 MPa at 140 °C. 30 different specimens with only one replication were obtained.

VI.2.2.4. Samples characterisation

VI.2.2.4.1. Density

The density of the samples was determined dividing the mass of the specimen by its external volume, which was geometrically calculated considering the specimen's dimensions. Densities were measured before (ρ_{solid}) and after expansion (ρ_{foam}). The relative density (ρ_{rel}) was obtained as the ρ_{foam}/ρ_{solid} ratio.

The open-cell content (f) of the composite foams was determined by means of the following equation:

$$f = \frac{v_c - v_q}{v_c \left(1 - \frac{\rho_{foam}}{\rho_{solid}} \right)} \quad (VI.2)$$

where v_c is the volume of the tested composite sample—i.e. external volume—and v_q corresponds to the volume of the solid plus the gas volume of the unconnected cells—i.e.

volume determined by pycnometry—. The v_q measurements were performed in a Micromeritics Gas Pycnometer AccuPyc II 1340 with nitrogen gas at 27.6 kPa and equilibration rate at 0.3 kPa. The solid density was considered to be 1290 kg/m³ and 1280 kg/m³, for PHB and CE-PHB, respectively.

VI.2.2.4.2. Mechanical characterisation

DMA tests at room temperature

The stiffness at room temperature of all the samples was evaluated by dynamic-mechanical (DMA) flexural tests performed in a Perkin–Elmer DMTA 7 equipped with a three point bending kit of 20-mm span. The forces were adjusted to obtain an amplitude in the indenter displacement of $20 \pm 2 \mu\text{m}$ —strain values below 0.08%—. The static force was set as 120% the dynamic force, and the frequency of oscillation used was 1 Hz. The values were taken 3 min after applying the forces. Three specimens per sample, of 22 mm x 6 mm x 1-2 mm thickness—depending on the sample—were measured in their both sides. The complex modulus—considered as the flexural modulus (E) hereafter—and the loss tangent for the solid and foamed samples were obtained.

Macro-mechanical modelling

Mechanical models that consider the porosity tend to offer a better approach for the prediction of the stiffness in composites reinforced with natural fibres [32,33], thus owing to the hollow nature of the cellulosic fibres and the technical difficulties for achieving a material without voids. This is of special interest when dealing with CellFRC, given that a clear effect of stiffness lowering is expected due to the cellular structure of the matrix and hence, due to the increase of void fraction. The experimental E values were compared with values predicted according to models considering the porosity volume fraction (V_p). On the one hand, the effect of porosity on material stiffness can be approximated by a very simple model, as proposed by Madsen and Lilholt [32]:

$$E_c = E_d \cdot (1 - V_p)^2 \quad (\text{VI.3})$$

where E_c refers to the stiffness of the porous material and E_d to the stiffness of the material at fully density—no porosity—. On the other hand, Madsen et al. [34] proposed an extended version of this model, which included a variable exponent (n_E):

$$E_c = (\eta_l \eta_o V_f E_f + V_m E_m) \cdot (1 - V_p)^{n_E} \quad (\text{VI.4})$$

where E_x and V_x are the elastic modulus and the volumetric fraction of the components—the subscripts c, f, m and p refer to composite, fibre, matrix, and porosity—, all respectively; η_1 is the Cox fibre length distribution factor; η_0 is the Krenchel fibre orientation factor; and the n_E is a porosity efficiency exponent.

For the representation of the model in Equation (VI.3), the stiffness of the material at full density E_d was estimated as:

$$E_d = \eta_1 \eta_0 \frac{\frac{W_f}{\rho_f} + \frac{(1-W_f)}{\rho_m}}{\frac{W_f}{\rho_f} + \frac{(1-W_f)}{\rho_m}} E_f + \frac{\frac{(1-W_f)}{\rho_m}}{\frac{W_f}{\rho_f} + \frac{(1-W_f)}{\rho_m}} E_m \quad (\text{VI.5})$$

where W_f is the fibre weight fraction, ρ_f and ρ_m refers to the density of the fibres and the matrix, respectively, and the following considerations were taken: average $W_f = 0.1975$; $E_f = 30.4$ GPa; average $E_m = 1.58$ GPa; $\rho_f = 1.46$ g/cm³ and $\rho_m = 1.29$ g/cm³. Moreover, the Cox fibre length distribution factor (η_1) was estimated to be 1 since the fibre aspect ratio—fibre length/fibre diameter—was much greater than 50 [34]. Finally, the Krenchel fibre orientation factor (η_0) was assumed to be 3/8 given the expected in-plane random orientation of the fibres [34,35].

The model by Madsen et al. presented in Equation (VI.4) was used to predict the E values for each composite sample, which requires a more accurate calculation. To that purpose, V_f , V_m and V_p were estimated by means of the following equations:

$$V_f = \frac{\frac{W_f \cdot w_c}{\rho_f}}{v_c} \quad (\text{VI.6})$$

$$V_m = \frac{\frac{(1-W_f) \cdot w_c}{\rho_m}}{v_c} \quad (\text{VI.7})$$

$$V_p = 1 - \rho_c \cdot \left(\frac{W_f}{\rho_f} + \frac{(1-W_f)}{\rho_m} \right) \quad (\text{VI.8})$$

where w_c is the weight (mass) of the composite sample, ρ_c refers to the density of the composite, and v_c is the aforementioned external volume of the composite sample. The η_1 and η_0 were estimated to be 1 and 0.375, as explained before, and the n_E exponent, which quantifies the stress concentration effect of porosity in composites, is taken as an empirical parameter which can be obtained by fitting the predicted values to the experimental data. Despite a n_E of 2 has been reported to offer a good fitting to a broad range of natural fibre

reinforced composites [34], the n_E gave a better approach when adjusted to the experimental results with a value of 0.7, in this case.

DMTA tests

The DMTA tests were performed with the Perkin-Elmer DMTA 7 also in three point bending mode. The load forces used were those set for the DMA analysis previously described and frequency was 1 Hz. The storage modulus (E'), loss modulus (E'') and loss tangent ($\tan \delta$) were recorded during the heating from $-25\text{ }^\circ\text{C}$ to $90\text{ }^\circ\text{C}$ at a rate of $3\text{ }^\circ\text{C}/\text{min}$.

The intensity of the transition (S) refers to the mobility and content of the amorphous phase, and is a helpful parameter to study the effect of the fibre addition, since higher S values point to higher mobility or higher content of the amorphous phase [36]. The parameter is defined as:

$$S = \frac{E'_b - E'_a}{E'_a} \quad (\text{VI.9})$$

where E'_b denotes the storage modulus before and E'_a that after the glass transition. In this case, the E'_b is taken as $-20\text{ }^\circ\text{C}$ and E'_a as $30\text{ }^\circ\text{C}$ for all samples. The glass transition temperatures (T_g) were defined as the maximum of the E'' curves. The intensity of the $\tan \delta$ peak ($\tan \delta_{\max}$) and the full-width at half-maximum (FWHM) were also determined [36]. In Figure VI.12, the criteria used to determine the FWHM is presented. Meanwhile the area of the $\tan \delta$ and its intensity reveals information about the energy dissipation capabilities, the FWHM refers to the homogeneity of the amorphous phase, where a wider $\tan \delta$ peak points to higher inhomogeneity [27,36].

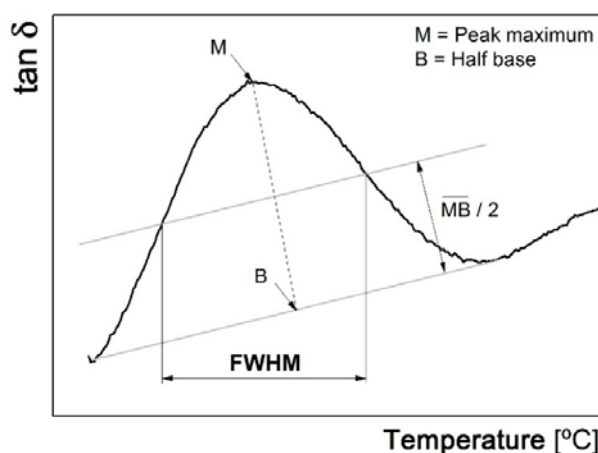


Figure VI.12. Criteria for the determination of the FWHM.

VI.2.2.4.3. DSC analysis

The differential scanning calorimetry (DSC) was performed in a METTLER DSC-862. A three-cycle DSC, under nitrogen flow of 60 mL/min. Three cycles were recorded: the first heating cycle from -40 °C to 200 °C at 10 °C/min followed by a 3 min annealing step at 200 °C; the cooling cycle from 200 °C to -40 °C at 10 °C/min; and the second heating cycle from -40 °C to 200 °C at 10 °C/min. The melting and crystallisation temperatures (T_m and T_c , respectively) were obtained from the peaks in the curves. The crystallinity percentage (χ) was estimated from melting enthalpy (ΔH_m) of the second cycle, and crystallisation enthalpy (ΔH_c) according to Equation (VI.10).

$$\chi = \frac{\Delta H}{w \cdot \Delta H^0} \quad (\text{VI.10})$$

where w is the real weight fraction of the polymer—corrected according to the amount of fibres and/or additives—, ΔH is the heat at the melting or crystallisation point, and ΔH^0 is the heat of fusion or crystallisation of 100% crystalline PHB, taken as 146 J/g [19].

VI.2.3. Results and discussion

VI.2.3.1. Mechanical behaviour at room temperature (DMA results)

The stiffness (flexural E) and $\tan \delta$ values obtained at room temperature for the solid precursors—with and without fibres—are presented in Table VI.3.

Table VI.3. Flexural modulus and $\tan \delta$ values for the matrix and the solid precursors

Sample	E [GPa]	$\tan \delta$
PHB	1.43 \pm 0.14	0.080 \pm 0.009
Untreated/PHB	2.26 \pm 0.40	0.073 \pm 0.015
C/PHB	2.21 \pm 0.44	0.065 \pm 0.007
C-Ar20/PHB	2.07 \pm 0.24	0.070 \pm 0.010
CE-PHB	1.81 \pm 0.14	0.099 \pm 0.005
Untreated/CE-PHB	2.76 \pm 0.54	0.066 \pm 0.010
C/CE-PHB	2.99 \pm 0.35	0.058 \pm 0.006
C-Ar20/CE-PHB	2.55 \pm 0.42	0.061 \pm 0.008

The addition of the reinforcement increased around a 53% the stiffness of the composites with respect to that of the matrix, as can be observed in Table VI.3. In this sense, the high rigidity of the flax fibres enhances the mechanical properties of the matrix. Moreover, the CE addition lead to an increase in the stiffness of the matrix—from 1.4 GPa to 1.8 GPa—; and also the composite precursors with a CE-PHB matrix presented E values a 27% higher than those with PHB matrix. With respect to the effect of the treatment of the NW, the composites presented similar E values—around 2.2 GPa for the PHB series and around 2.8 GPa for the CE-PHB series—, despite slightly higher results were obtained for the untreated and the C-treated NW reinforcements.

A significant decrease of $\tan \delta$ values was observed for the composites with respect to the neat polymer. This effect can be attributed to the effect of the fibres, since the ~20% of reinforcement added should be contributing with a purely elastic response [28] as aforementioned, and hence to the decrease of the viscoelasticity index. Concerning to this, the highest decrease in the $\tan \delta$ of the composites was found for the C-reinforced followed

by C-Ar20–reinforced and untreated–reinforced with the highest value. These differences in the decrease in the loss tangent could be pointing to a more effective stress transfer for the C–reinforced samples due to better fibre/matrix interaction, since an improved fibre/matrix interface bonding should result in a lower mobility of the molecular chains at the fibre/matrix interface, thus reducing the $\tan \delta$ values recorded [26]. In this sense, the improvement of the C-treatment—with regard to the untreated reinforcement—would be explained due to the removal of waxes and lignin, and the increase of C=O and O–C–O groups in the fibre surface [31] capable to react with the ester groups in the hydroxybutyrate.

Concerning to the DMA results for the foamed samples, the obtained E values for all the composite samples have been plotted against the porosity in Figure VI.13, and compared to macro-mechanical models. The determination of the porosity fraction revealed that the solid precursors presented low porosity contents—around 0.05, thus is 5%—due to the hollow nature of the flax fibres. As expected, the E values decreased with the porosity fraction.

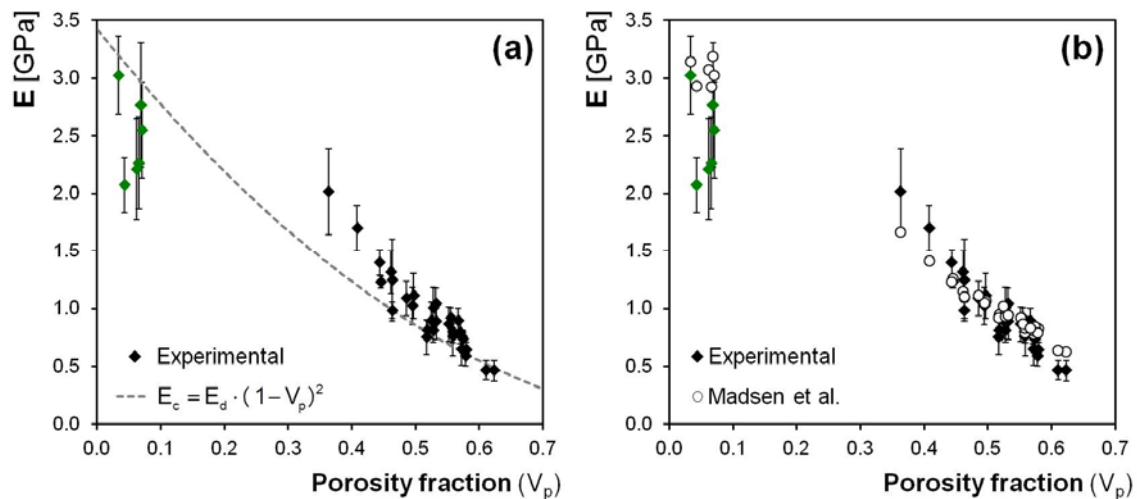


Figure VI.13. Experimental flexural modulus (E_{exp}) against porosity fraction of the samples with compared to: (a) the Madsen and Lilholt model; (b) to the values predicted by means of the Madsen et al. model, considering $n_E = 0.7$. Green points correspond to the experimental E of the precursors.

On the one hand, the correlation between the experimental values and the model presented in Equation (VI.3) is given in Figure VI.13a. Thus consists on a modified rule of mixtures with a simplified term including the porosity—average values of solids’ stiffness have been considering for the line plot—[32]. As shown, it presents a close fitting, with better accuracy for samples with higher porosity contents.

On the other hand, in Figure VI.13b, the E values predicted by means of the Madsen et al. model [34] expressed in Equation (VI.4) are compared to the experimental ones. In this

case, the complexity of the model makes necessary to represent each predicted value in order to consider the fibre content and porosity of each sample. As aforementioned, the n_E exponent initially set as 2, according to the good fitting reported in the literature [34]. However, it gave an unreasonable prediction of the stiffness in CellFRC, being the values determined much lower than the experimental ones. Due to that, the n_E value was adjusted until reaching the optimal fitting, which was found in that case to be 0.7, thus pointing to a lower effect of the porosity in the stress concentration for the samples under study. In general terms, a good approach to the CellFRC stiffness can be achieved under these conditions, although some of the values for the solids (which) are clearly higher than the experimental.

Otherwise, the E values of the CellFRC decreased with the increase of porosity fraction, as expected—since the expansion is achieved in detriment of the stiffness—. As previously mentioned, this behaviour in foams follows the scaling law presented in Equation (VI.1). This defines the relative properties of the foams as a function of a constant (C_1) that depends on the polymer matrix, and the power of the relative density to an exponent (n) that is related to deformation mechanisms and the cellular structure— C_1 is normally up to 1 and n is often around 2, for polymeric foams [37]—. With the aim of observing such a behaviour, the relative E against relative density has been plotted in Figure VI.14, and fitted to the scaling law.

In general terms, the properties of the foamed composites follow such a trend, being the C-series those presenting an overall better agreement with the scaling law. Besides this, the samples expanded at 140 °C present in most cases relative E above those of the samples expanded at 120 °C. Thus can be attributed to differences in the microstructure obtained according the processing conditions, or to higher degradation due to longer heat-exposure—larger processing time—.

Go to next page

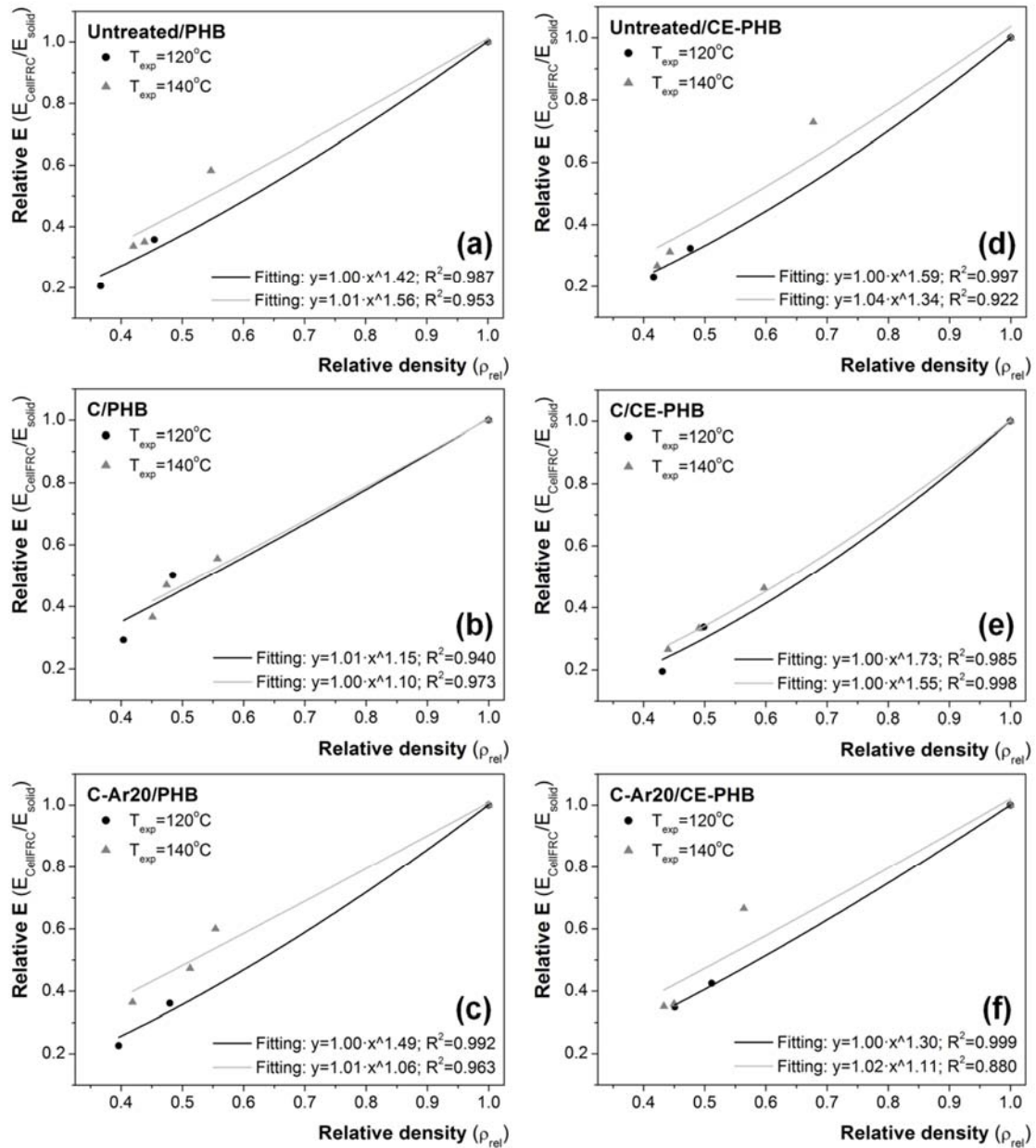


Figure VI.14. Relative E-modulus against relative density plots for the series: (a) untreated/PHB; (b) C/PHB; (c) C-AR20/PHB; (d) untreated/CE-PHB; (e) C/CE-PHB; and (f) C-AR20/CE-PHB.

Concerning to the $\tan \delta$ values, the results of all samples have been plotted against the relative density in Figure VI.15. As can be observed, solid composites ($\rho_{rel} = 1$) presented $\tan \delta$ values around 0.600. However, for the CellFRC, the trend starts to rise with the density reduction: the lower the density, the higher the loss tangent. Therefore, reaching relative densities of 0.6 or lower leads to the progressive increase in the damping properties of the CellFRC at room temperature, thus leading to materials with expected better energy absorption than their solid counterparts. A similar increasing trend with density reduction was observed for polypropylene closed cell foams at high temperatures—around 75 °C—, attributed to gas enclosed in the cells given that the DSC did not revealed differences on the polymer morphology [38]. However, the foams obtained in this study had open cell contents of 62% or higher—most of the specimens were 100% open cell—and therefore the explanation must be found in differences on the polymer microstructure in the foamed composites.

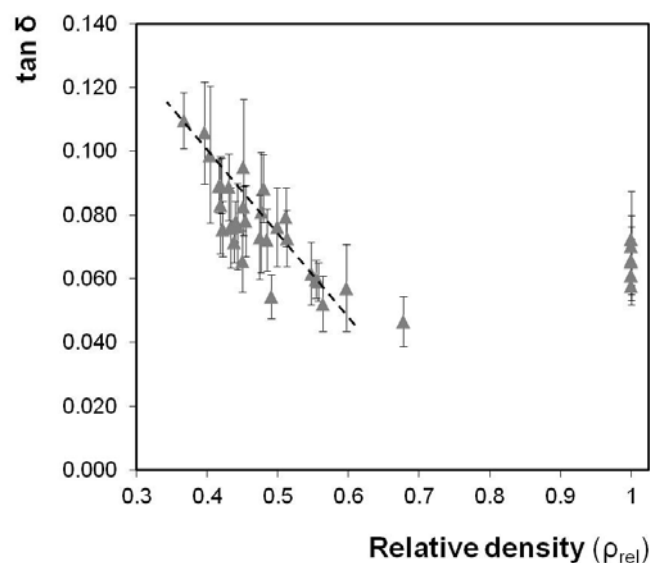


Figure VI.15. Values of $\tan \delta$ against relative density. The dotted line has been added with the aim to guide the eye.

VI.2.3.2. Dynamic mechanic thermal behaviour of the C-series (DMTA results)

The DMTA analysis was used to study the viscoelastic behaviour in selected samples. In this sense, the C-series—more specifically, those expanded at 140 °C—were selected due to an expected better fibre/matrix interaction—according to the lower $\tan \delta$ values recorded—and their closer approach to the scaling law. Moreover, the PHB and CE-PHB matrices, and the C/PHB and C/CE-PHB solids were also added to the analysis for comparative purposes.

Representative DMTA curves of these samples are presented in Figure VI.16 (E') and Figure VI.17 (tan δ). Other data extracted from the DMTA curves is given in Table VI.4.

Storage modulus analysis

On the one hand, for the solid composites, the storage modulus decreased with the increase in temperature, with the most drastic reduction taking place in the glass transition region—between $-25\text{ }^{\circ}\text{C}$ and $\sim 20\text{ }^{\circ}\text{C}$ —, as can be observed in Figure VI.16. This reduction corresponds to chain mobility enhancement of the polymer matrix. However, this E' decrease was significantly less severe for the solid composites than for the neat matrices. This could be attributed to the effect of the fibres—which are thermally-stable at the temperature range evaluated—since the E' drop of the matrix is compensated by the elastic response of the fibres [27].

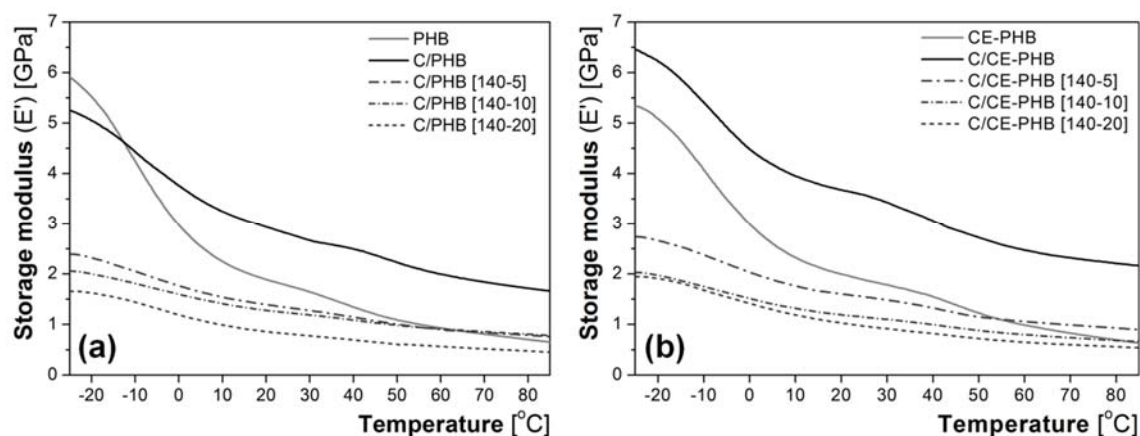


Figure VI.16. Representative E' curves for the PHB series (a) and the CE-PHB series (b).

On the other hand, the foamed samples followed a similar trend than their solid counterparts, with less pronounced E' drops, also due to the presence of fibres. In this sense, some tests performed up to $110\text{ }^{\circ}\text{C}$, revealed that at $110\text{ }^{\circ}\text{C}$ —taking $E'_{-20\text{ }^{\circ}\text{C}}$ as a reference—, the neat matrices were capable to retain only a 7% of the reference, meanwhile the solid composites retained a 29% and the foams a 25%. Thus reveals the significance of the fibre contribution in achieving materials with higher softening temperatures.

S and T_g evaluation

The intensity of the transition (S), measured between $-20\text{ }^{\circ}\text{C}$ and $30\text{ }^{\circ}\text{C}$, is shown in Table VI.4).

Table VI.4. Intensity of the transition (S), glass temperature (T_g), maximum intensity in the $\tan \delta$ peak ($\tan \delta_{max}$), full-width at half-maximum (FWHM) and area of the $\tan \delta$ peak (A) results extracted from the E' , E'' and $\tan \delta$ curves.

<i>Sample</i>	S	T_g [°C]	$\tan \delta_{max}$	$FWHM$
PHB	2.45	-8.6 ±0.6	0.113 ±0.003	28.2
C/PHB	0.90	-3.7 ±0.7	0.083 ±0.007	31.2
C/PHB [140-5]	3.59	-5.4 ±1.3	0.067 ±0.006	29.2
C/PHB [140-10]	3.78	-5.3 ±1.1	0.070 ±0.001	32.0
C/PHB [140-20]	6.30	-2.1 ±1.5	0.094 ±0.008	37.8
CE-PHB	2.09	-8.6 ±0.3	0.129 ±0.015	28.6
C/CE-PHB	0.71	-5.6 ±1.1	0.079 ±0.006	29.2
C/CE-PHB [140-5]	3.00	-4.9 ±0.6	0.073 ±0.001	31.2
C/CE-PHB [140-10]	4.64	-5.5 ±0.7	0.068 ±0.002	32.2
C/CE-PHB [140-20]	6.17	-2.5 ±1.3	0.093 ±0.005	37.6

Regarding the solids, lower S values are found for the composites than for the neat matrices, revealing lower mobility of the amorphous phase. This is in agreement with the E' results, since the rigid reinforcement would limit the mobility of the amorphous phase [36]. According to this, the T_g determined for the solid composites increased with regard to the unreinforced matrix, what is in concordance with a higher difficulty in chain mobility due to the presence of the fibres [24,27].

However, the CellFRC presented higher S , increasing with the expansion pressure—lower density—, meanwhile their T_g values were similar or even higher—especially for the samples expanded at 20 MPa—than those of their solid precursors. This could be explained by a higher content of amorphous phase but that requires higher temperatures to gain mobility—given the increasing T_g values—, possibly produced due to a different organization of the microstructure during the expansion.

Analysis of the $\tan \delta$ peaks

Representative $\tan \delta$ curves have been plotted in Figure VI.17. As can be seen, lower $\tan \delta_{max}$ were found for the solid and foamed composites with respect to the neat polymer.

This decrease on the damping properties for the composites is consistent with the effect of the elastic contribution of the fibres to the viscoelastic response, and with the reduction in the chain mobility [27]. Therefore, the elastic contribution that improves the mechanical properties of the composites is, at the same time, responsible of their lower energy-dissipation capabilities.

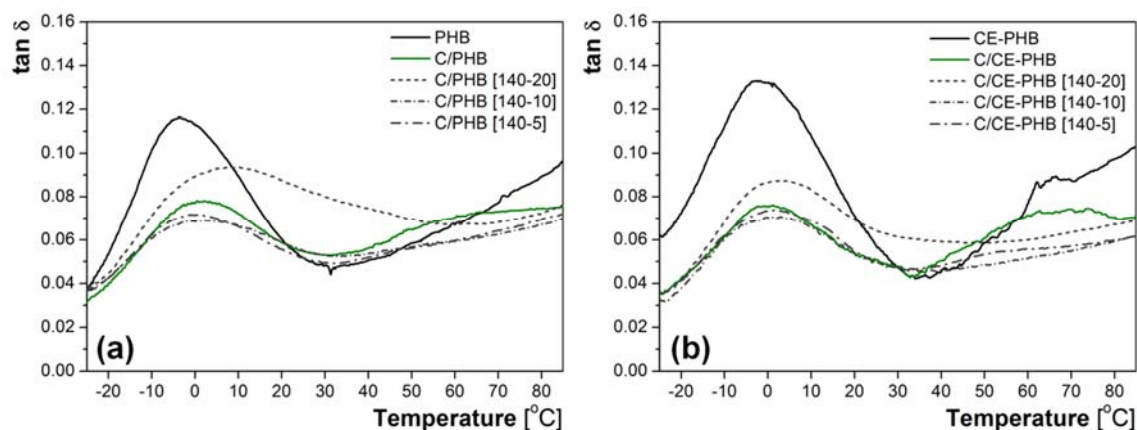


Figure VI.17. Representative $\tan \delta$ curves for the PHB series (a) and the CE-PHB series (b).

Regarding the FWHM values—presented in Table VI.4—, similarity widths between the $\tan \delta$ peaks of all the samples are observed, except in the C/PHB [140-20] and C/CE-PHB [140-20] foams. According to this result, these two CellFRC would present higher inhomogeneity in the amorphous phase than the rest of the samples—which would show similar results—. This can be attributed to differences in the microstructure formation during the processing conditions, as aforementioned. In this sense, these two foams expanded at 20 MPa present unique properties compared to the rest of the samples: highest S values, highest T_g , highest FWHM and higher $\tan \delta_{\max}$ than the other foams.

VI.2.3.3. DSC results

DSC tests were performed in C/PHB series—considering foams expanded at both 120 °C and 140 °C—, and in the C/CE-PHB series—considering only those expanded at 140 °C—, in order to observe differences in the melting and crystallisation behaviour of the samples.

In the first heating, the curves revealed some differences in the crystal formation due to processing conditions, as can be observed in Figure VI.18. As shown, all the samples presented a main melting peak around 168 °C, which is associated to the melting temperature of the polymer. However, a previous secondary peak was observed in some of the samples

between 146 °C and 158 °C, which appeared as a shoulder in the rest of the samples. The presence of two peaks points to re-crystallisation phenomenon during melting, where the smaller peak would correspond to the melting of primary (unstable) crystals formed during processing, and the higher peaks to the melting of recrystallised crystals—partially generated during the own DSC heating—[39]. The differences in the secondary peaks could be corresponding to chain alignment occurred during a fast cell grow in the expansion step. This strain-induced crystallinity could be generating amorphous regions with high inhomogeneity, what could be explaining the higher S and $\tan \delta$ previously explained.

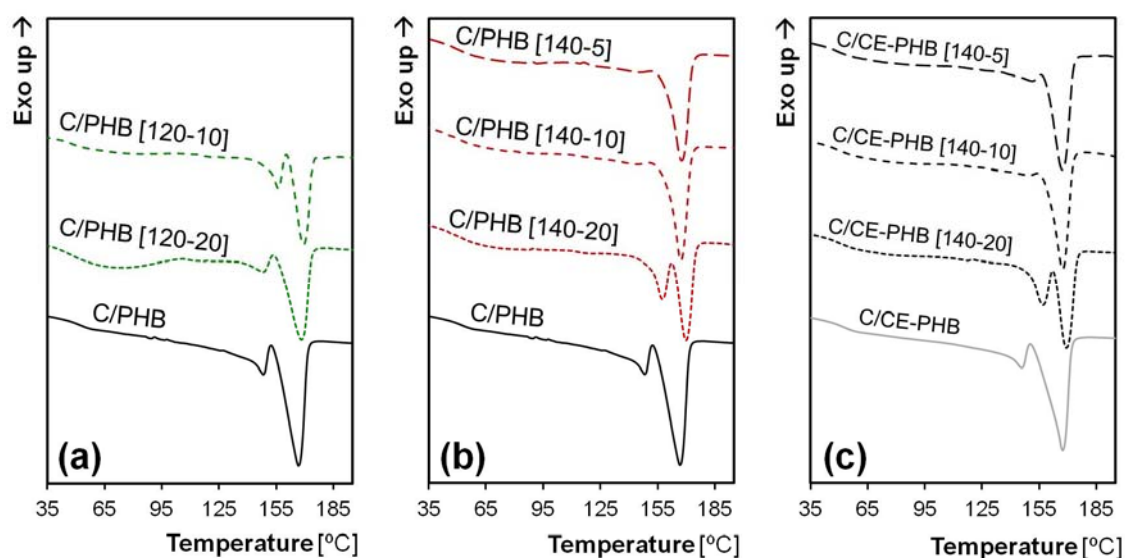


Figure VI.18. Comparison of the DSC curves corresponding to first heating cycle of the C/PHB series expanded at 120 °C (a) and 140 °C (b); and the C/CE-PHB series expanded at 140 °C (c).

With regard to the cooling cycle, all the samples with CE-PHB matrix presented a crystallisation temperature (T_c) of ~ 108 °C, meanwhile for samples with PHB matrix, the T_c was ~ 116 °C, although the effect of the fibres did not reveal any change in this trend. The lowering of the crystallisation temperature due to the addition of CE was observed in previous studies [40]. However, the lower crystallisation temperature seems to not affect the crystallisation during the samples' processing, given the similarity in the curves for the first heating in samples expanded at 140 °C presented in Figure VI.18b and Figure VI.18c.

The crystallinity values obtained from the second heating cycles—corrected according to fibre and/or additives content—determined a χ_c of 48% for the composites and of 36% for the unreinforced matrix. Thus increase of crystallinity points to the fibres presence, which could be performing as nucleating agents for the crystal formation, as reported in the literature [16].

VI.2.3.4. Fibre reinforcing effect

With the aim to estimate the effect of the fibre reinforcement in the increase of the mechanical properties of the CellFRC, a comparative between foams of similar densities was performed. To that purpose, a foam of a density around 535 kg/m^3 of PHB without fibres was produced following the same process explained in the experimental section—2 mm thick specimen foamed at T_{exp} of $120 \text{ }^\circ\text{C}$ and P_{exp} of 10 MPa —, but with a much lower pressure release rate of 0.3 MPa/s . The comparative of the properties of this PHB foam with other PHB-based CellFRC of similar densities is presented in Table VI.5.

Table VI.5. Comparative of flexural modulus (E) values for a foam without reinforcement and other CellFRC of similar characteristics.

Sample*	ρ (kg/m^3)	ρ_{rel}	W_f wt. %	ϕ_{3D} (μm)	E (MPa)
C-Ar20/PHB [120-20] ^b	492	0.40	19.1	40	469 ± 82
C-Ar20/PHB [140-20] ^b	529	0.42	19.1	67	757 ± 165
Untreated/PHB [140-20] ^b	534	0.42	20.5	105	760 ± 34
PHB [120-10] ^a	<u>537</u>	<u>0.42</u>	<u>0</u>	<u>167</u>	<u>318 ± 29</u>
Untreated/PHB [140-10] ^b	540	0.44	20.5	129	793 ± 94
C-Ar20/PHB [140-5] ^b	682	0.55	19.1	165	1245 ± 357

* Samples are denoted as Precursor [T_{exp} (in $^\circ\text{C}$)- P_{exp} (in MPa)]

^a Pressure release rate ($\Delta P/\Delta s$) of 0.3 MPa/s ; unreinforced foam; ^b $\Delta P/\Delta s$ of 40 MPa/s ; foamed composites

Despite the comparative has the limitation of the differences in processing conditions and cell sizes, the CellFRC presented—for similar density values—higher stiffness than the unreinforced foam. As shown in Table VI.5, the untreated/PHB [140-20] and the untreated/PHB [140-10], with practically equal densities, presented 139% and 149% higher E than the PHB [120-10], respectively. Even the C-Ar20/PHB [120-20], with a density 8% lower, presented a stiffness 47% higher than the unreinforced foam. All thus gives promising results in what to the effect of fibre reinforcement is concerned. In this sense, further work has to be done in the tailoring of the properties of both the unreinforced foams and the CellFRC.

VI.2.4. Conclusions

Cellular biocomposites of PHB matrix reinforced with nonwoven flax fabrics have been characterised by means of DMA and DSC. The effects of fibre addition, surface treatment of the reinforcement, use of chain extender additives and foaming conditions have been studied.

The mechanical characterisation of the solids revealed a significant increase in the flexural stiffness due to the addition of the fibre reinforcement regardless the surface treatment applied, although the C-treatment seemed to show slightly higher fibre/matrix interaction. The addition of chain extender also improved the flexural E of the matrix and hence, of the composites. The DMTA analysis showed differences between the unreinforced matrices and the composite solid precursors. On the one hand, the fibres contributed with an elastic response, what increased the storage modulus and decreased the $\tan \delta$ —lower intensities and areas of the peaks—, thus pointing to lower damping properties of the solid composites. On the other hand, the fibres restricted the chain mobility, what increased the T_g and reduced the intensity of the glass transition (S). Moreover, the presence of fibres was found to increase the crystallinity from 36% for the neat matrix to 48% for the composites, and the addition of CE decreased the crystallisation temperature.

Regarding the foamed samples, the CellFRC presented 140% higher flexural stiffness than unreinforced foams of the same density. As expected, the flexural E values decreased with the reduction in the density. Two macro-mechanical models—both considering the porosity fraction in their equations—presented reasonable fitting to the results obtained. The plots of relative stiffness against relative density followed the scaling law, being the samples of the C-series those that presented a better overall adjust. The $\tan \delta$ values taken in DMA tests at room temperature a progressive increase of the viscosity index in samples with relative densities of 0.6 or lower, thus meaning better damping properties. Moreover, the DMTA results revealed, on the one hand, similar effects than the composites due to the fibre addition—increase of T_g , lower E' loss at high temperatures and lower $\tan \delta$ curves compared to the neat matrix—. However, the foaming affected differently some of the parameters evaluated. The intensity of the transition presented increasing values for higher expansions, and similar results were observed for the $\tan \delta$. However, the CellFRC expanded at 20 MPa were the ones that presented extreme values of S, T_g and $\tan \delta$ —peak intensity and width—thus attributed to differences on the crystal formation during processing. In this sense, the DSC analysis revealed the presence of unstable crystals with melting points around

147 °C not shown in other CellFRC obtained at an expansion temperature of 140 °C. However, the first heating DSC curves also presented similar crystal formations for foams obtained at 120 °C. In this sense, further DMTA analysis of those samples should be performed for a better understanding of the effects of processing in the crystal formation and final properties of the CellFRC achieved.

References

- [1] Satyanarayana KG, Arizaga GGC, Wypych F. Biodegradable composites based on lignocellulosic fibers—An overview. *Prog Polym Sci* 2009;34:982–1021. doi:10.1016/j.progpolymsci.2008.12.002.
- [2] Faruk O, Bledzki A, Fink H, Sain M. Biocomposites reinforced with natural fibers: 2000–2010. *Prog Polym Sci* 2012;37:1552–96. doi:10.1016/j.progpolymsci.2012.04.003.
- [3] Gurunathan T, Mohanty S, Nayak SK. A review of the recent developments in biocomposites based on natural fibres and their application perspectives. *Compos Part A Appl Sci Manuf* 2015;77:1–25. doi:10.1016/j.compositesa.2015.06.007.
- [4] Pickering KL, Efendy MGA, Le TM. A review of recent developments in natural fibre composites and their mechanical performance. *Compos Part A Appl Sci Manuf* 2016;83:98–112. doi:10.1016/j.compositesa.2015.08.038.
- [5] George M, Chae M, Bressler DC. Composite materials with bast fibres: Structural, technical, and environmental properties. *Prog Mater Sci* 2016;83:1–23. doi:10.1016/j.pmatsci.2016.04.002.
- [6] Shanks RA, Hodzic A, Wong S. Thermoplastic biopolyester natural fiber composites. *J Appl Polym Sci* 2004;91:2114–21. doi:10.1002/app.13289.
- [7] Kalia S, Kaith BS, Kaur I. Pretreatments of natural fibers and their application as reinforcing material in polymer composites—A review. *Polym Eng Sci* 2009;49:1253–72. doi:10.1002/pen.21328.
- [8] Kabir MM, Wang H, Lau KT, Cardona F. Chemical treatments on plant-based natural fibre reinforced polymer composites: An overview. *Compos Part B Eng* 2012;43:2883–92. doi:10.1016/j.compositesb.2012.04.053.
- [9] Wang C, Chen J-R. Studies on surface graft polymerization of acrylic acid onto PTFE film by remote argon plasma initiation. *Appl Surf Sci* 2007;253:4599–606. doi:10.1016/j.apsusc.2006.10.014.
- [10] Singh S, Mohanty AK. Wood fiber reinforced bacterial bioplastic composites: Fabrication and performance evaluation. *Compos Sci Technol* 2007;67:1753–63. doi:10.1016/j.compscitech.2006.11.009.
- [11] Summerscales J, Virk A, Hall W. A review of bast fibres and their composites: Part 3 – Modelling. *Compos Part A Appl Sci Manuf* 2013;44:132–9. doi:10.1016/j.compositesa.2012.08.018.
- [12] Bledzki AK, Jaszkiwicz A. Mechanical performance of biocomposites based on PLA and PHBV reinforced with natural fibres – A comparative study to PP. *Compos Sci Technol* 2010;70:1687–96. doi:10.1016/j.compscitech.2010.06.005.
- [13] Graupner N, Müssig J. A comparison of the mechanical characteristics of kenaf and lyocell fibre reinforced poly(lactic acid) (PLA) and poly(3-hydroxybutyrate) (PHB) composites. *Compos Part A Appl Sci Manuf* 2011;42:2010–9. doi:10.1016/j.compositesa.2011.09.007.
- [14] Sorrentino L, Cafiero L, D’Auria M, Iannace S. Cellular thermoplastic fibre reinforced composite (CellFRC): A new class of lightweight material with high impact properties. *Compos Part A Appl Sci Manuf* 2014;64:223–7. doi:10.1016/j.compositesa.2014.05.016.
- [15] Zafar MT, Zarrinbakhsh N, Mohanty AK, Misra M, Ghosh AK. Biocomposites based on poly(Lactic acid)/willow-fiber and their injection moulded microcellular foams. *Express Polym Lett* 2016;10:176–86. doi:10.3144/expresspolymlett.2016.16.
- [16] Javadi A, Srithep Y, Pilla S, Lee J, Gong S, Turng L-S. Processing and characterization of

- solid and microcellular PHBV/coir fiber composites. *Mater Sci Eng C* 2010;30:749–57. doi:10.1016/j.msec.2010.03.008.
- [17] Javadi A, Srithep Y, Lee J, Pilla S, Clemons C, Gong S, et al. Processing and characterization of solid and microcellular PHBV/PBAT blend and its RWF/nanoclay composites. *Compos Part A Appl Sci Manuf* 2010;41:982–90. doi:10.1016/j.compositesa.2010.04.002.
- [18] Bénézet J-C, Stanojlovic-Davidovic A, Bergeret A, Ferry L, Crespy A. Mechanical and physical properties of expanded starch, reinforced by natural fibres. *Ind Crops Prod* 2012;37:435–40. doi:10.1016/j.indcrop.2011.07.001.
- [19] Guan J, Hanna MA. Functional properties of extruded foam composites of starch acetate and corn cob fiber. *Ind Crops Prod* 2004;19:255–69. doi:10.1016/j.indcrop.2003.10.007.
- [20] Bocz K, Tábi T, Vadas D, Sauceau M, Fages J, Marosi G. Characterisation of natural fibre reinforced PLA foams prepared by supercritical CO₂ assisted extrusion. *Express Polym Lett* 2016;10:771–9. doi:10.3144/expresspolymlett.2016.71.
- [21] Boissard CIR, Bourban P-E, Tingaut P, Zimmermann T, Manson JAE. Water of functionalized microfibrillated cellulose as foaming agent for the elaboration of poly(lactic acid) biocomposites. *J Reinf Plast Compos* 2011;30:709–19. doi:10.1177/0731684411407233.
- [22] Neagu RC, Cuenoud M, Berthold F, Bourban P-E, Gamstedt EK, Lindstrom M, et al. The potential of wood fibers as reinforcement in cellular biopolymers. *J Cell Plast* 2012;48:71–103. doi:10.1177/0021955X11431172.
- [23] Mooney DJ, Baldwin DF, Suh NP, Vacanti JP, Langer R. Novel approach to fabricate porous sponges of poly(D,L-lactic-co-glycolic acid) without the use of organic solvents. *Biomaterials* 1996;17:1417–22.
- [24] Srithep Y, Ellingham T, Peng J, Sabo R, Clemons C, Turng L-S, et al. Melt compounding of poly (3-hydroxybutyrate-co-3-hydroxyvalerate)/nanofibrillated cellulose nanocomposites. *Polym Degrad Stab* 2013;98:1439–49. doi:10.1016/j.polymdegradstab.2013.05.006.
- [25] Gibson LJ, Ashby MF. *Cellular Solids: Structure and properties*. 2nd ed. Cambridge: Cambridge University Press; 1999.
- [26] Saba N, Jawaid M, Allothman OY, Paridah MT. A review on dynamic mechanical properties of natural fibre reinforced polymer composites. *Constr Build Mater* 2016;106:149–59. doi:10.1016/j.conbuildmat.2015.12.075.
- [27] Manikandan NK, Thomas S, Groeninckx G. Thermal and dynamic mechanical analysis of polystyrene composites reinforced with short sisal fibres. *Compos Sci Technol* 2001;61:2519–29. doi:10.1016/S0266-3538(01)00170-1.
- [28] Sepe M. *Dynamic mechanical analysis for plastics engineering*. PDL handbook. Norwich, N.Y.: Plastics Design Library; 1998.
- [29] Rodriguez-Perez MA, Rodriguez-Llorente S, De Saja JA. Dynamic Mechanical Properties of Polyolefin Foams Studied by DMA Techniques. *Polym Eng Sci* 1997;37:959–65.
- [30] Ventura H, Ardanuy M, Capdevila X, Cano F, Tornero JA. Effects of needling parameters on some structural and physico-mechanical properties of needle-punched nonwovens. *J Text Inst* 2014;1–11. doi:10.1080/00405000.2013.874628.
- [31] Ventura H, Claramunt J, Navarro A, Rodriguez-Perez MA, Ardanuy M. Effects of Wet/Dry-Cycling and Plasma Treatments on the Properties of Flax Nonwovens Intended for Composite Reinforcing. *Materials (Basel)* 2016;9:93. doi:10.3390/ma9020093.
- [32] Madsen B, Lilholt H. Physical and mechanical properties of unidirectional plant fibre composites—an evaluation of the influence of porosity. *Compos Sci Technol* 2003;63:1265–72. doi:10.1016/S0266-3538(03)00097-6.

- [33] Summerscales J, Dissanayake N, Virk A, Hall W. A review of bast fibres and their composites. Part 2 – Composites. *Compos Part A Appl Sci Manuf* 2010;41:1336–44. doi:10.1016/j.compositesa.2010.05.020.
- [34] Madsen B, Thygesen A, Lillholt H. Plant fibre composites – porosity and stiffness. *Compos Sci Technol* 2009;69:1057–69. doi:10.1016/j.compscitech.2009.01.016.
- [35] Garkhail SK, Heijenrath RWH, Peijs T. Mechanical properties of natural-fibre-mat-reinforced thermoplastics based on flax fibres and polypropylene. *Appl Compos Mater* 2000;7:351–72. doi:10.1023/A:1026590124038.
- [36] Díez-Gutiérrez S, Rodríguez-Perez MA, De Saja JA, Velasco J. Dynamic mechanical analysis of injection-moulded discs of polypropylene and untreated and silane-treated talc-filled polypropylene composites. *Polymer (Guildf)* 1999;40:5345–53. doi:10.1016/S0032-3861(98)00754-X.
- [37] Istrate OM, Chen B. Relative modulus–relative density relationships in low density polymer–clay nanocomposite foams. *Soft Matter* 2011;7:1840. doi:10.1039/c0sm01052a.
- [38] Rodríguez-Perez MA, De Saja JA. Dynamic mechanical analysis applied to the characterisation of closed cell polyolefin foams. *Polym Test* 2000;19:831–48. doi:10.1016/S0142-9418(99)00054-9.
- [39] Gunaratne LMWK, Shanks RA, Amarasinghe G. Thermal history effects on crystallisation and melting of poly(3-hydroxybutyrate). *Thermochim Acta* 2004;423:127–35. doi:10.1016/j.tca.2004.05.003.
- [40] Ventura H, Laguna-Gutiérrez E, Rodríguez-Perez MA, Ardanuy M. Effect of chain extender and water-quenching on the properties of poly(3-hydroxybutyrate-co-4-hydroxybutyrate) foams for its production by extrusion foaming. *Eur Polym J* 2016;85:14–25. doi:10.1016/j.eurpolymj.2016.10.001.

CONCLUSIONS AND *FUTURE WORK*

General conclusions

The research work performed in this thesis had the final aim of developing lightweight composite materials based on biopolymers and natural cellulosic fibres by employing more sustainable techniques, and this was successfully achieved.

Regarding the objectives set at the beginning—see section *ii. Objectives*—:

- The surface modification of natural cellulosic fibres for increasing adhesion and stability in biopolymeric matrices was studied.
- The work allowed establishing conditions to obtain optimal textile structures for composite reinforcement.
- The feasibility of biopolymers—PHB in this case—to be used as foamed matrices in composite materials was reported.
- Lab-scale production of biopolymer/cellulosic fibres nonwoven-fabric composites was performed, and the conditions for such a production were set.
- The structures, morphologies and properties of the elaborated composites were characterised, thus leading to a better general knowledge of this kind of material.
- The effects in those properties derived from the foaming process were studied.

Specific conclusions

Regarding the treatment of the flax-nonwoven structures studied in Chapter III, the main conclusions are:

- The wet/dry cycling treatment was effective in achieving a greater stability against the water absorption of the flax fibres used in this thesis.
- The plasma treatments showed very different results, thus pointing to the possibility of tailoring the hydrophilicity/hydrophobicity of the samples according to the nature of the matrix.
- Argon gas plasma treatments showed the most satisfactory results in increasing the hydrophilic behaviour of the nonwovens, even helping to enhance the mechanical properties.
- The corona plasma treatments can also be considered for increasing the hydrophilic behaviour of the nonwovens, attending to the balance between cost-effectiveness and simplicity of the treatment can be achieved with fair properties.

- Ethylene-gas plasma treatment showed the increase in the hydrophobicity of the nonwoven flax fabrics, although a previous activating plasma treatment is recommended to improve the effectiveness.

For the evaluation of the mechanical performance and aging behaviour of PHB-based composites produced using selected treated flax-fabric reinforcements, hydrothermal aging and tensile and thermal tests were performed. From the results of water uptake, water absorption kinetics, tensile and thermal properties of the composites, which were studied in Chapter IV, the main conclusions extracted are:

- The incorporation of the flax reinforcements produced an increase in the water uptake with respect to the neat matrix, showing high sensitivity to small variations in the fibre contents.
- The different surface treatments applied to the NW fabrics did not influence the water uptake, and proved to be ineffective in preventing water absorption, not even those with the ethylene-gas plasma treatment.
- The water diffusion, with a pseudo-Fickian behaviour for the composites, increased with the aging temperature.
- In the unaged state all the composites presented higher stiffness and strength than the neat matrix, being the composite treated with wet-dry cycling and argon-gas plasma the one presenting the best overall mechanical improvement in the unaged state, thus pointing to better adhesion.
- Aging had severe effects in reducing the mechanical properties of most of the samples due to fibre debonding and matrix damage. In this sense, the SEM images showed a connection between the water uptake and the damage observed.
- However, the composite treated with the wet/dry cycling presented the best resistance to aging, with a lower loss of stiffness and strength. Therefore, wet/dry cycling was found to be an effective treatment for stabilisation and improvement for PHB/flax composites.

The evaluation of the foamability of the PHB matrix used in this study was performed in Chapter V. Given the intrinsic difficulties for foaming that presented the matrix, two strategies were evaluated for the improvement of its foaming: the use of chain extender additives and a fast cooling. The main conclusions obtained from this study are:

- The results revealed a very complex system given the intrinsic complexity of the PHB and opposing simultaneous processes that impoverished and enhanced the foam's properties at the same time.
- The addition of chain extender was the more effective strategy for enhancing the foamability, leading to lower densities without producing a negative effect on the mechanical properties. However, this addition led to lower viscosity and coarser cellular morphologies, but at the same time, prevented the polymer degradation by reducing the degradation rate, thus leading to slightly better properties.
- The water-cooling strategy enhanced the density reduction only when the chain extender was not used, and could not reach the effectiveness of the CE addition.
- No clear synergies were observed when combining both strategies.
- The mechanical properties were strongly affected by the density reduction, as expected, and were similar for all samples.
- Optimal results were obtained with the use of 1 wt.% of chain extender, 3–4 wt.% of the chemical blowing agent used—in masterbatch form—, and air cooling, according to the balance between the mechanical properties and the density reduction.

Finally, all the aforementioned knowledge was used to produce cellular PHB/flax fabric composites, which were further characterised. Due to the structure presented by the fibres—in the nonwoven fabric—, the processing techniques were limited and the gas-dissolution batch foaming route had to be explored. Therefore, the study regarding this production, presented in the first section of Chapter VI, lead to the following conclusions:

- CellFRC of PHB/flax nonwoven fabric could be successfully produced by CO₂ gas dissolution using the pressure quench method.
- The good regularity was found according to the homogeneity of the precursors. In this sense, the fibres presented a homogeneous distribution through the thickness and a fair fibre-matrix adhesion could be observed.
- The presence of the fibre-reinforcement enhanced the viscosity of the polymeric matrix, what favoured the foaming, although also limited the total expansion due to constriction effects attributed to the structural integrity of the reinforcement.
- Best results of density reduction were achieved expanding the samples between 120 °C and 140 °C, at pressures of 10 MPa and 20 MPa—conditions at which the CO₂ gas was in supercritical state—.

- Specimens expanded at 10 MPa and 20 MPa presented similar relative densities around 0.4-0.5 regardless the matrix or reinforcement, although some differences were revealed in their cellular structure.
- The increase in the expansion temperature led to cellular structures of fewer larger cells, and the increase of the expansion pressure led to higher cell densities.
- The CellFRC obtained presented a considerably amount of porous phase and fibre, what reduces the amount of biopolymer required, what could lower the cost of this biodegradable solution, increasing its competitiveness.

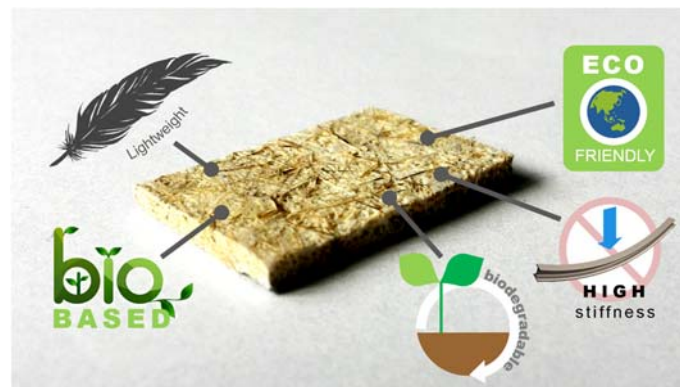
The cellular PHB/nonwoven flax fabric composites were characterised by means of dynamical mechanical analysis and differential scanning calorimetry. The effects of fibre addition, surface treatment of the reinforcement, use of chain extender additives and foaming condition, presented in the second section of Chapter VI lead to the following conclusions:

- The addition of the fibre reinforcement produced a significant increase in the flexural stiffness of the solid composites regardless the surface treatment applied, being the wet/dry cycling the one showing slightly higher fibre/matrix interaction.
- The fibre addition restricted the chain mobility increasing the glass transition temperature, and increased the crystallinity of the composites.
- The addition of chain extender improved the flexural stiffness of the matrix—and hence of the composites—, and decreased the crystallisation temperature.
- The dynamic mechanical thermal analysis revealed the contribution of the fibres to the elastic response, what increased the storage modulus. Moreover, the solid composites presented lower damping properties—lower $\tan \delta$ values—, while a progressive increase of the viscosity index was observed in samples with relative densities of 0.55 or lower, thus meaning better damping properties.
- The CellFRC—foamed samples—presented 140% higher flexural stiffness than unreinforced foams of the same density. In this sense, the flexural E values decreased with the reduction in the density, as expected, and hence the plots of relative stiffness against relative density followed the scaling law.
- Two macro-mechanical models—both considering the porosity fraction in their equations—presented reasonable fitting to the results obtained.

- The expansion conditions influenced the crystal formation during processing thus leading to the observation of some differences. The DSC analysis revealed the presence of unstable crystals with melting points around 147 °C in some of the CellFRC. In this sense, further analysis should be performed for a better understanding of the effects of processing in the crystal formation and final properties of the CellFRC achieved.

Concluding remarks

The milestone of the thesis, which was the development of lightweight composite materials based on biopolymers and natural cellulosic fibres by employing more sustainable techniques has been achieved.



The use of nonwoven flax fabrics for the reinforcement revealed to contribute to a homogeneous foaming behaviour, and cellular PHB/flax composites could be produced by means of quench-pressure method of gas-dissolution batch foaming.

Future work

From the results reached in this thesis, some interesting questions arise. These questions require more work and new research lines, to be developed.

- Further study of other green techniques to ensure an even better fibre matrix adhesion but, specially, a higher impermeability against water to enhance the aging properties would be of interest.
- The use of the acquired knowledge about the treatments applied to the fibres could be extended for the enhancement of natural-fibre reinforcements in composites of diverse nature. This has just been started regarding a parallel research line in cementitious composite materials.

- The interesting results observed in the effect of the fibres during the foaming process require further deepening in the knowledge about this topic. In this sense, studies concerning the gas sorption, crystallisation and degradative processes taking place during the process would be worthy to be carried out.
- The use of this novel approach in other polymers which present difficulties to be foamed should be studied, since the use of fibre-structures could set a new step towards the enhancement of foamability for some difficult-to-foam materials.
- Other characterisation techniques would be required to have a better understanding of the possibilities of this CellFRC. In this sense, impact tests could show improved impact resistance as expected from the results observed in the literature.
- The insulation properties of the material should also be studied, since the cellular structure and the presence of fibres point to a good thermal and/or acoustical insulating properties.
- Biodegradability studies could reveal interesting data, since shorter biodegradability times should be expected due to the porous structure and the presence of fibres.
- Moreover, the processing conditions should be evaluated in order to study the possibilities of scaling-up the production of this CellFRC.
- The search of industrial applications for the materials achieved is an important point to be addressed. In this sense, these materials show properties that could be interesting in sectors such as the automotive.
- The conformability of the solids and possibility of production of more complex shapes should be evaluated in order to determine possible applications for CellFRC.

List of Figures

INTRODUCTION

Figure 1. Biocomposites definition.	33
Figure 2. Difference between a conventional polymer and a biopolymer	34
Figure 3. “Global production capacities of bioplastics”	35
Figure 4. “Global production capacities of bioplastics in 2016 (by region)”	35
Figure 5. Classification of the fibre reinforced composites.	37
Figure 6. Summary of the chapters and scientific publications in the thesis.	44

CHAPTER I. STATE OF THE ART

Figure I.1. Interior carpeting of a car door made on PE/hemp fibres biocomposite	54
Figure I.2. Typical structures of fibre reinforcements	55
Figure I.3. Scheme for nonwoven production methods.	56
Figure I.4. Carding process showing the evolution of fibres during the process	57
Figure I.5. Needle-punching principle.	57
Figure I.6. Cellulose.	60
Figure I.7. Influence of the constituents on some of the properties of the plant fibres	61
Figure I.8. Stem cross-section of a flax plant.....	62
Figure I.9. Diagram of a stem configuration.....	63
Figure I.10. Flax structure from stem to cellulose crystals.....	64
Figure I.11. SEM images of flax bundles showing several fibres	64
Figure I.12. Schematic overview of bio-based polymers	68
Figure I.13. PHA-producer bacteria accumulating PHA granules.....	70
Figure I.14. General structure of PHAs and examples.....	72
Figure I.15. Molecular conformations of α and β forms, banded texture of a P3HB spherulite and schematic representation of spherulites and lamellar aggregates	75
Figure I.16. Schematic representation of the β -crystals formation in a P3HB.....	76
Figure I.17. Effect of fibre orientation on the tensile strength of a composite reinforced with uniaxial fibres	82
Figure I.18. Effect of water on fibre/matrix interface.....	85
Figure I.19. States of matter.....	86
Figure I.20. Surface etching in flax produced due to increasing exposure time to argon plasma.....	87
Figure I.21. Open cell foam and closed cell foam.....	90

Figure I.22. Comparative properties of dense and foamed materials	91
Figure I.23. Scheme regarding the cellular structure evolution of the foaming process	93
Figure I.24. Effects of coalescence and coarsening.....	94
Figure I.25. Schematic representation of the CO ₂ -foaming process.....	100
Figure I.26. Effect of batch foaming process variables on cell morphology	101
Figure I.27. Three dimensional structure of a cellular material.....	102
Figure I.28. Schematic compressive stress curves for an elastic-plastic foam	103
Figure I.29. Schematic tensile stress curves for an elastic-plastic foam.....	104

CHAPTER II. MATERIALS AND METHODS

Figure II.1. Scheme of fibre preparation for its characterisation.....	124
Figure II.2. Image of the needle-punching machine showing the processing units.	126
Figure II.3. Scheme of the wet/dry treatment, with detailed wetting cycle.	127
Figure II.4. General scheme of the low pressure plasma device.	128
Figure II.5. Hypothesized model of plasma-polymerized ethylene film and SEM image of the flax fibres after plasma polymerisation	129
Figure II.6. Plasma-induced fragmentation of the cellulose.....	129
Figure II.7. Ex-situ post-plasma oxidation reactions.	130
Figure II.8. Corona plasma scheme and equipment.....	130
Figure II.9. Melt compounding line.....	131
Figure II.10. Scheme of the film production with conditions.....	132
Figure II.11. Scheme of the film-stacking configuration and conditions.....	132
Figure II.12. Principle of extrusion foaming.....	133
Figure II.13. Scheme of the samples preparation for evaluation of the matrix foamability.....	134
Figure II.14. Foamed composites production by means of the pressure quench method.....	135
Figure II.15. General scheme of the composite samples production.	136
Figure II.16. SEM image of flax fibres' surface and of a NW structure.....	138
Figure II.17. Typical force-displacement curve of a NW sample	139
Figure II.18. Examples of stress-strain curves.....	140
Figure II.19. Typical compression curve of a foam.....	144
Figure II.20. Example of the DMTA curves obtained for the composites under study. ...	145
Figure II.21. Example of complex melting behaviour in DSC.	147
Figure II.22. Contact angle measurement.	148

CHAPTER III. TREATMENT OF FLAX-NONWOVEN FABRICS

Figure III.1. SEM images of untreated and wet/dry cycled flax bundles.....	167
Figure III.2. Effect on the surface roughness of the fibre due to increasing time in Ar-plasma treatment of samples.	168
Figure III.3. SEM image of the sample NW C-Ar30	168
Figure III.4. SEM image of surfaces of samples NW C-Cr1010 and NW C-Cr20.....	169
Figure III.5. SEM image of surfaces of samples NW C-Ar5-Et5; NW C-Ar5-Et10; NW C-Cr1010-Et10; and NW C-Et10	169
Figure III.6. Comparative SEM images of the surfaces of samples NW C-Ar5; NW C-Ar5-Et5; NW C-Ar5-Et10; NW C-Cr1010; and NW C-Cr1010-Et10.	170
Figure III.7. Deconvoluted curves of XPS C1s peaks of NW C-Cr1010; and NW C-Cr1010-Et10 samples	172
Figure III.8. Comparative of the C1s peaks found in the deconvolution curves for the C1, C2, C3 and C4 peaks of all samples.....	173
Figure III.9. Deconvoluted curves of XPS O1s peaks of NW C-Ar5; and NW C-Ar5-Et10.....	175
Figure III.10. TGA curves of selected samples.....	179
Figure III.11. X-ray diffraction patterns of some selected treated and the untreated samples.....	180
Figure III.12. Breaking force of the NW normalized by the sample weight.....	182

CHAPTER IV. MECHANICAL PERFORMANCE AND AGING OF PHB/FLAX FABRIC COMPOSITES

Figure IV.1. Water uptake curves for the aging at RT and at 65 °C	200
Figure IV.2. Saturation water uptake against average fibre content	201
Figure IV.3. Diffusion coefficient at RT and 65 °C against average fibre content	203
Figure IV.4. Stiffness and tensile strength values for unaged samples.....	205
Figure IV.5. Stiffness and tensile strength graphs comparing unaged and aged samples.....	207
Figure IV.6. Comparison of TGA curves for all unaged samples.	208
Figure IV.7. SEM images of the surfaces of unaged and aged samples.....	210

CHAPTER V. EVALUATION OF THE FOAMABILITY OF THE PHB MATRIX

Figure V.1. Complex viscosity against time.....	229
--	-----

Figure V.2. Density against CBA amount.	230
Figure V.3. SEM image of transversal (bias) fracture of specimen 5CBA-1CE/W.....	231
Figure V.4. SEM images showing the evolution of the cellular structure in the samples section when increasing CBA content.....	232
Figure V.5. Graphic summary of the cellular structure analysis.....	233
Figure V.6. χ_m percentages for the first and second heating cycle against relative density.....	235
Figure V.7. DSC first heating cycle-curves comparison for 0CBA samples and 1CE/A-series with increasing CBA contents from top to bottom.	236
Figure V.8. Compression curves for 1CE/A series	238
Figure V.9. Representation of relative compression properties	239
Figure V.10. Representation of relative tensile properties	240
Figure V.11. Impact toughness against density.	241

CHAPTER VI. CELLULAR PHB/FLAX COMPOSITES

Figure VI.1. Scheme for the samples preparation.	256
Figure VI.2. Definition of the temperature and pressure curves in the batch foaming process.....	258
Figure VI.3. Examples of the specimens from the preliminary tests.	260
Figure VI.4. Comparative of the Untreated/PHB composites before and after expansion... ..	261
Figure VI.5. Relative density values of the composite samples foamed on the exploratory tests	261
Figure VI.6. Steady state flow curves for the solid materials with and without fibres	263
Figure VI.7. Relative densities of the CellFRC obtained according to the variables of study.....	264
Figure VI.8. SEM images of the C-Ar20/PHB composite series.....	265
Figure VI.9. SEM images of the different cellular structures observed.....	266
Figure VI.10. Cell densities of the CellFRC	268
Figure VI.11. Evolution of the temperature and pressure curves in foaming process.	281
Figure VI.12. Criteria for the determination of the FWHM.....	284
Figure VI.13. Experimental flexural modulus against porosity fraction of the samples	287
Figure VI.14. Relative E-modulus against relative density plots.....	289
Figure VI.15. Values of $\tan \delta$ against relative density.	290
Figure VI.16. Representative E' curves for the PHB and CE-PHB series.	291

Figure VI.17. Representative $\tan \delta$ curves for the PHB and CE-PHB series.	293
Figure VI.18. Comparison of the DSC curves corresponding to first heating cycle of the C/PHB series expanded at 120 °C and 140 °C; and the C/CE-PHB series expanded at 140 °C.....	294

List of Tables

CHAPTER I. STATE OF THE ART

Table I.1. Chemical composition of selected natural fibres..	60
Table I.2. Properties of selected cellulosic fibres.....	61
Table I.3. Properties of some bio-based biodegradable polymers.....	69
Table I.4. Properties of some PHAs.....	73

CHAPTER II. MATERIALS AND METHODS

Table II.1. Properties of the flax fibres.....	123
Table II.2. Needling conditions.....	127
Table II.3. Characterisation techniques use, for chapters.....	151

CHAPTER III. TREATMENT OF FLAX-NONWOVEN FABRICS

Table III.1. Sample references and description of the treatment conditions applied..	164
Table III.2. Elemental composition percentage and O/C ratios for all the NW samples.....	171
Table III.3. Characterization results for NW.....	177
Table III.4. TGA) results for the NW.....	179

CHAPTER IV. MECHANICAL PERFORMANCE AND AGING OF PHB/FLAX FABRIC COMPOSITES

Table IV.1. Treatment conditions applied to the NW fabrics used as reinforcements.....	198
Table IV.2. Water uptake values.....	202
Table IV.3. Main parameters of the thermal characterisation.....	209

CHAPTER V. EVALUATION OF THE FOAMABILITY OF THE PHB MATRIX

Table V.1. Composition and reference of the samples prepared..	226
---	-----

CHAPTER VI. CELLULAR PHB/FLAX COMPOSITES

Table VI.1. Literature review regarding biopolymer/natural fibres CellFRC.....	255
Table VI.2. Cell size values, in μm	267

Table VI.3. Flexural modulus and $\tan \delta$ values for the matrix and the solid precursors..... 286

Table VI.4. Results extracted from the E' , E'' and $\tan \delta$ curves 292

Table VI.5. Comparative of flexural modulus (E) values for a foam without reinforcement and other CellFRC of similar characteristics 295

General Bibliography

- Abdelwahab, MA, A Flynn, B-S Chiou, S Imam, W Orts, and E Chiellini. 2012. "Thermal, Mechanical and Morphological Characterization of Plasticized PLA-PHB Blends." *Polymer Degradation and Stability* 97 (9). Elsevier Ltd: 1822–28. doi:10.1016/j.polymdegradstab.2012.05.036.
- Aguilar-Rios, A. 2014. "Improving the Bonding between Henequen Fibers and High Density Polyethylene Using Atmospheric Pressure Ethylene-Plasma Treatments." *Express Polymer Letters* 8 (7): 491–504. doi:10.3144/expresspolymlett.2014.53.
- Ahmad, F, HS Choi, and MK Park. 2015. "A Review: Natural Fiber Composites Selection in View of Mechanical, Light Weight, and Economic Properties." *Macromolecular Materials and Engineering* 300 (1): 10–24. doi:10.1002/mame.201400089.
- Albrecht, W, F Fuchs, and W Kittelmann. 2003. *Nonwoven Fabrics*. Weinheim: Wiley-VCH.
- Almanza, OA, MA Rodriguez-Perez, and JA De Saja. 2016. "The Thermal Conductivity of Polyethylene Foams Manufactured by a Nitrogen Solution Process." *Cellular Polymers* 18 (6). Rapra: 385–401. Accessed July 18. <http://cat.inist.fr/?aModele=afficheN&cpsidt=1316288>.
- Anandjiwala, R. D., and L. Boguslavsky. 2008. "Development of Needle-Punched Nonwoven Fabrics from Flax Fibers for Air Filtration Applications." *Textile Research Journal* 78 (7): 614–24.
- Araújo, JR, WR Waldman, and MA De Paoli. 2008. "Thermal Properties of High Density Polyethylene Composites with Natural Fibres: Coupling Agent Effect." *Polymer Degradation and Stability* 93 (10): 1770–75. doi:10.1016/j.polymdegradstab.2008.07.021.
- Ardanuy, M, J Claramunt, and R. D. Toledo Filho. 2015. "Cellulosic Fiber Reinforced Cement-Based Composites: A Review of Recent Research." *Construction and Building Materials* 79: 115–28. doi:10.1016/j.conbuildmat.2015.01.035.
- Ardanuy, M, J Claramunt, H Ventura, and AM Manich. 2015. "Effect of Water Treatment on the Fiber–Matrix Bonding and Durability of Cellulose Fiber Cement Composites." *Journal of Biobased Materials and Bioenergy* 9 (5): 486–92. doi:10.1166/jbmb.2015.1545.
- Arrakhiz, F Z, M El Achaby, M Malha, MO Bensalah, O.Fassi-Fehri, R Bouhfid, K Benmoussa, and A Qaiss. 2013. "Mechanical and Thermal Properties of Natural Fibers Reinforced Polymer Composites: Doum/low Density Polyethylene." *Materials & Design* 43. Elsevier Ltd: 200–205. doi:10.1016/j.matdes.2012.06.056.
- Avérous, L, and E Pollet. 2012. "Biodegradable Polymers." In *Environmental Silicate Nano-Biocomposites*, edited by Luc Avérous and Eric Pollet, 50:13–39. Springer London. doi:10.1007/978-1-4471-4108-2_2.
- Azwa, Z. N., B. F. Yousif, A. C. Manalo, and W. Karunasena. 2013. "A Review on the Degradability of Polymeric Composites Based on Natural Fibres." *Materials and Design* 47: 424–42. doi:10.1016/j.matdes.2012.11.025.
- Badia, JD, T Kittikorn, E Strömberg, L Santonja-Blasco, A Martínez-Felipe, A Ribes-Greus, M Ek, and S Karlsson. 2014. "Water Absorption and Hydrothermal Performance of PHBV/sisal Biocomposites." *Polymer Degradation and Stability* 108 (October): 166–74. doi:10.1016/j.polymdegradstab.2014.04.012.
- Bagherpour, S. 2012. "Fibre Reinforced Polyester Composites." In *Polyester*. InTech. doi:10.5772/48697.
- Barham, PJ, A Keller, EL Otun, and PA Holmes. 1984. "Crystallization and Morphology of a Bacterial Thermoplastic: Poly-3-Hydroxybutyrate." *Journal of Materials Science* 19 (9). 2-6 Boundary Row, London, Emglnd SE1 8HN: Chapman Hall LTD: 2781–94. doi:10.1007/BF01026954.

- Barkoula, NM, SK Garkhail, and T Peijs. 2010. "Biodegradable Composites Based on Flax/polyhydroxybutyrate and Its Copolymer with Hydroxyvalerate." *Industrial Crops and Products* 31 (1): 34–42. doi:10.1016/j.indcrop.2009.08.005.
- Beckermann, GW, and KL Pickering. 2008. "Engineering and Evaluation of Hemp Fibre Reinforced Polypropylene Composites: Fibre Treatment and Matrix Modification." *Composites Part A: Applied Science and Manufacturing* 39 (6): 979–88. doi:10.1016/j.compositesa.2008.03.010.
- Behravesh, AH, CB Park, LK Cheung, and RD Venter. 1996. "Extrusion of Polypropylene Foams with Hydrocerol and Isopentane." *Journal of Engineering and Applied Science* 2 (4): 1862–67. doi:10.1002/vnl.10153.
- Bénézet, J-C, A Stanojlovic-Davidovic, A Bergeret, L Ferry, and A Crespy. 2012. "Mechanical and Physical Properties of Expanded Starch, Reinforced by Natural Fibres." *Industrial Crops and Products* 37 (1). Elsevier B.V.: 435–40. doi:10.1016/j.indcrop.2011.07.001.
- Bertoniere, NR, and WD King. 1989. "Effect of Scouring / Bleaching, Caustic Mercerization, and Liquid Ammonia Treatment on the Pore Structure of Cotton Textile Fibers." *Textile Research Journal* 59: 114–21.
- Bhowmick, M, S Mukhopadhyay, and R Alagirusamy. 2012. "Mechanical Properties of Natural Fibre-Reinforced Composites." *Textile Progress* 44 (2): 85–140. doi:10.1080/00405167.2012.676800.
- Biagiotti, J, D Puglia, and JM Kenny. 2004. "A Review on Natural Fibre-Based Composites-Part I." *Journal of Natural Fibers* 1 (2): 37–68. doi:10.1300/J395v01n02_04.
- Bledzki, AK. 1999. "Composites Reinforced with Cellulose Based Fibres." *Progress in Polymer Science* 24 (2): 221–74. doi:10.1016/S0079-6700(98)00018-5.
- Bledzki, AK, and A Jaszkiwicz. 2010. "Mechanical Performance of Biocomposites Based on PLA and PHBV Reinforced with Natural Fibres – A Comparative Study to PP." *Composites Science and Technology* 70 (12). Elsevier Ltd: 1687–96. doi:10.1016/j.compscitech.2010.06.005.
- Bocz, K, T Tábi, D Vadas, M Sauceau, J Fages, and G Marosi. 2016. "Characterisation of Natural Fibre Reinforced PLA Foams Prepared by Supercritical CO₂ Assisted Extrusion." *Express Polymer Letters* 10 (9): 771–79. doi:10.3144/expresspolymlett.2016.71.
- Boissard, CIR, P-E Bourban, P Tingaut, T Zimmermann, and J-AE Manson. 2011. "Water of Functionalized Microfibrillated Cellulose as Foaming Agent for the Elaboration of Poly(lactic Acid) Biocomposites." *Journal of Reinforced Plastics and Composites* 30 (8): 709–19. doi:10.1177/0731684411407233.
- Bos, HL. 2004. "The Potential of Flax Fibres as Reinforcement for Composite Materials." Eindhoven University of Technology.
- Bozaci, E, K Sever, M Sarikanat, Y Seki, A Demir, E Ozdogan, and I Tavman. 2013. "Effects of the Atmospheric Plasma Treatments on Surface and Mechanical Properties of Flax Fiber and Adhesion between Fiber-Matrix for Composite Materials." *Composites Part B: Engineering* 45 (1). Elsevier Ltd: 565–72. doi:10.1016/j.compositesb.2012.09.042.
- Brancato, AA. 2008. "Effect of Progressive Recycling on Cellulose Fiber Surface Properties." Georgia Institute of Technology.
- Bugnicourt, E, P Cinelli, A Lazzeri, and V Alvarez. 2014. "Polyhydroxyalkanoate (PHA): Review of Synthesis, Characteristics, Processing and Potential Applications in Packaging." *Express Polymer Letters* 8 (11): 791–808. doi:10.3144/expresspolymlett.2014.82.
- Cabedo, L, D Plackett, E Giménez, and JM Lagarón. 2009. "Studying the Degradation of Polyhydroxybutyrate-Co-Valerate during Processing with Clay-Based Nanofillers." *Journal of Applied Polymer Science* 112 (6): 3669–76. doi:10.1002/app.29945.

- Campo-Arnáiz, RA, MA Rodríguez-Perez, B Calvo, and JA De Saja. 2005. "Extinction Coefficient of Polyolefin Foams." *Journal of Polymer Science Part B: Polymer Physics* 43 (13): 1608–17. doi:10.1002/polb.20435.
- Carus, M. 2013. "Production Capacities for Bio-Based Polymers in Europe: Status and Trends towards 2020." *Jec Composites Magazine*.
- Carus, M, and H Scheurer. 2011. "Directory for Innovative Renewable Materials and Bio-Based Products." *Nova-Institut GmbH*. Germany: nova-Institut GmbH.
- Castilho, LR, DA Mitchell, and DMG Freire. 2009. "Production of Polyhydroxyalkanoates (PHAs) from Waste Materials and by-Products by Submerged and Solid-State Fermentation." *Bioresource Technology* 100 (23): 5996–6009. doi:10.1016/j.biortech.2009.03.088.
- Chanprateep, S. 2010. "Current Trends in Biodegradable Polyhydroxyalkanoates." *Journal of Bioscience and Bioengineering* 110 (6). The Society for Biotechnology, Japan: 621–32. doi:10.1016/j.jbiosc.2010.07.014.
- Charlet, K, C Baley, C Morvan, JP Jernot, M Gomina, and J Bréard. 2007. "Characteristics of Hermès Flax Fibres as a Function of Their Location in the Stem and Properties of the Derived Unidirectional Composites." *Composites Part A: Applied Science and Manufacturing* 38 (8): 1912–21. doi:10.1016/j.compositesa.2007.03.006.
- Chen, G-Q. 2009. "A Microbial Polyhydroxyalkanoates (PHA) Based Bio- and Materials Industry." *Chemical Society Reviews* 38 (8): 2434–46. doi:10.1039/b812677c.
- Chodak, I. 2008. "Polyhydroxyalkanoates: Origin, Properties and Applications." In *Monomers, Polymers and Composites from Renewable Resources*, edited by Mohamed Naceur Belgacem and Alessandro Gandini, 451–77. Elsevier. doi:10.1016/B978-0-08-045316-3.00022-3.
- Chou, W, and F Ko. 1989. *Textile Structural Composites*. Edited by W. Chou and F. Ko. *Advanced Materials*. Elsevier S. Vol. 1. New York: Elsevier Science & Technology Books.
- Claramunt, J, M Ardanuy, and JA García-Hortal. 2010. "Effect of Drying and Rewetting Cycles on the Structure and Physicochemical Characteristics of Softwood Fibres for Reinforcement of Cementitious Composites." *Carbohydrate Polymers* 79 (1): 200–205. doi:10.1016/j.carbpol.2009.07.057.
- Claramunt, J, M Ardanuy, JA García-Hortal, and RD Tolêdo Filho. 2011. "The Hornification of Vegetable Fibers to Improve the Durability of Cement Mortar Composites." *Cement and Concrete Composites* 33 (5): 586–95. doi:10.1016/j.cemconcomp.2011.03.003.
- Claramunt, J, H Ventura, L Fernández-Carrasco, and M Ardanuy. 2017. "Tensile and Flexural Properties of Cement Composites Reinforced with Flax Nonwoven Fabrics." *Materials* 10 (3). Multidisciplinary Digital Publishing Institute: 215. doi:10.3390/ma10020215.
- Colton, JS. 1989. "The Nucleation of Microcellular Foams in Semi-Crystalline Thermoplastics." *Materials and Manufacturing Processes* 4 (2): 253–62. doi:10.1080/10426918908956288.
- Cox, HL. 1952. "The Elasticity and Strength of Paper and Other Fibrous Materials." *British Journal of Applied Physics* 3 (3): 72. <http://stacks.iop.org/0508-3443/3/i=3/a=302>.
- Crank, J. 1975. *The Mathematics of Diffusion*. 2nd ed. Clarendon Press.
- Crétois, R, N Follain, E Dargent, J Soulestin, S Bourbigot, S Marais, and L Lebrun. 2015. "Poly(3-Hydroxybutyrate-Co-4-Hydroxybutyrate) Based Nanocomposites: Influence of the Microstructure on the Barrier Properties." *Physical Chemistry Chemical Physics: PCCP* 17 (17). Royal Society of Chemistry: 11313–23. doi:10.1039/c4cp05524a.
- Dhakal, HN, ZY Zhang, and MOW Richardson. 2007. "Effect of Water Absorption on the Mechanical Properties of Hemp Fibre Reinforced Unsaturated Polyester Composites." *Composites Science and Technology* 67 (7–8): 1674–83. doi:10.1016/j.compscitech.2006.06.019.

- Dicker, MPM, PF Duckworth, AB Baker, G Francois, MK Hazzard, and PM Weaver. 2014. "Green Composites: A Review of Material Attributes and Complementary Applications." *Composites Part A: Applied Science and Manufacturing* 56: 280–89. doi:10.1016/j.compositesa.2013.10.014.
- Dittenber, DB, and HVS GangaRao. 2012. "Critical Review of Recent Publications on Use of Natural Composites in Infrastructure." *Composites Part A: Applied Science and Manufacturing* 43 (8): 1419–29. doi:10.1016/j.compositesa.2011.11.019.
- Díez-Gutiérrez, S, MA Rodríguez-Perez, JA De Saja, and JI Velasco. 1999. "Dynamic Mechanical Analysis of Injection-Moulded Discs of Polypropylene and Untreated and Silane-Treated Talc-Filled Polypropylene Composites." *Polymer* 40 (19): 5345–53. doi:10.1016/S0032-3861(98)00754-X.
- Duangphet, S, D Szegea, J Song, and K Tarverdi. 2013. "The Effect of Chain Extender on Poly(3-Hydroxybutyrate-Co-3-Hydroxyvalerate): Thermal Degradation, Crystallization, and Rheological Behaviours." *Journal of Polymers and the Environment* 22 (1): 1–8. doi:10.1007/s10924-012-0568-5.
- Eaves, D. 2004. *Handbook of Polymer Foams*. Edited by David Eaves. Rapra Technology Limited.
- Espert, A, F Vilaplana, and S Karlsson. 2004. "Comparison of Water Absorption in Natural Cellulosic Fibres from Wood and One-Year Crops in Polypropylene Composites and Its Influence on Their Mechanical Properties." *Composites Part A: Applied Science and Manufacturing* 35 (11): 1267–76. doi:10.1016/j.compositesa.2004.04.004.
- Esteves Magalhães, WL, and M Ferreira de Souza. 2002. "Solid Softwood Coated with Plasma-Polymer for Water Repellence." *Surface and Coatings Technology* 155 (1): 11–15. doi:10.1016/S0257-8972(02)00029-4.
- European Bioplastics. 2013. "Technology/Materials." <http://en.european-bioplastics.org>.
- Fan, M, and B Weclawski. 2017. "Long Natural Fibre Composites." In *Advanced High Strength Natural Fibre Composites in Construction*, 141–77. Elsevier. doi:10.1016/B978-0-08-100411-1.00006-6.
- Fang, L, and JM Catchmark. 2014. "Structure Characterization of Native Cellulose during Dehydration and Rehydration." *Cellulose* 21 (6): 3951–63. doi:10.1007/s10570-014-0435-8.
- Faruk, O, AK Bledzki, H-P Fink, and M Sain. 2012. "Biocomposites Reinforced with Natural Fibers: 2000–2010." *Progress in Polymer Science* 37 (11). Elsevier Ltd: 1552–96. doi:10.1016/j.progpolymsci.2012.04.003.
- Faruk, O, AK Bledzki, H-P Fink, and M Sain. 2014. "Progress Report on Natural Fiber Reinforced Composites." *Macromolecular Materials and Engineering* 299 (1): 9–26. doi:10.1002/mame.201300008.
- Fernandes, EG, M Pietrini, and E Chiellini. 2004. "Bio-Based Polymeric Composites Comprising Wood Flour as Filler." *Biomacromolecules* 5 (4): 1200–1205. doi:10.1021/bm034507o.
- Garkhail, SK, RWH Heijenrath, and T Peijs. 2000. "Mechanical Properties of Natural-Fibre-Mat-Reinforced Thermoplastics Based on Flax Fibres and Polypropylene." *Applied Composite Materials* 7 (5–6): 351–72. doi:10.1023/A:1026590124038.
- George, M, M Chae, and DC Bressler. 2016. "Composite Materials with Bast Fibres: Structural, Technical, and Environmental Properties." *Progress in Materials Science* 83 (October): 1–23. doi:10.1016/j.pmatsci.2016.04.002.
- Ghane, M, R Saghafi, M Zarrebini, and D Semnani. 2011. "Evaluation of Bending Modulus of Needle-Punched Fabrics Using Two Simply Supported Beam Method." *Fibres & Textiles in Eastern Europe* 19 (4): 89–93.
- Gibson, LJ, and MF Ashby. 1999. *Cellular Solids: Structure and Properties*. 2nd ed. Cambridge: Cambridge University Press.

- Gil-Castell, O, JD Badia, T Kittikorn, E Strömberg, A Martínez-Felipe, M Ek, S Karlsson, and A Ribes-Greus. 2014. "Hydrothermal Ageing of Polylactide/sisal Biocomposites. Studies of Water Absorption Behaviour and Physico-Chemical Performance." *Polymer Degradation and Stability* 108 (October): 212–22. doi:10.1016/j.polymdegradstab.2014.06.010.
- Gordeyev, S. A., and Y. P. Nekrasov. 1999. "Processing and Mechanical Properties of Oriented Poly (β -Hydroxybutyrate) Fibers." *Journal of Materials Science Letters* 18: 1691–92. <http://www.springerlink.com/index/gpp59t8636757673.pdf>.
- Graupner, N, and J Müssig. 2011. "A Comparison of the Mechanical Characteristics of Kenaf and Lyocell Fibre Reinforced Poly(lactic Acid) (PLA) and poly(3-Hydroxybutyrate) (PHB) Composites." *Composites Part A: Applied Science and Manufacturing* 42 (12). Elsevier Ltd: 2010–19. doi:10.1016/j.compositesa.2011.09.007.
- Guan, J., and M. A. Hanna. 2004. "Functional Properties of Extruded Foam Composites of Starch Acetate and Corn Cob Fiber." *Industrial Crops and Products* 19 (3): 255–69. doi:10.1016/j.indcrop.2003.10.007.
- Gunaratne, LMWK, RA Shanks, and G Amarasinghe. 2004. "Thermal History Effects on Crystallisation and Melting of poly(3-Hydroxybutyrate)." *Thermochimica Acta* 423: 127–35. doi:10.1016/j.tca.2004.05.003.
- Gurunathan, T, S Mohanty, and SK Nayak. 2015. "A Review of the Recent Developments in Biocomposites Based on Natural Fibres and Their Application Perspectives." *Composites Part A: Applied Science and Manufacturing* 77: 1–25. doi:10.1016/j.compositesa.2015.06.007.
- Ho, M-P, H Wang, J-H Lee, C-K Ho, K-T Lau, J Leng, and D Hui. 2012. "Critical Factors on Manufacturing Processes of Natural Fibre Composites." *Composites Part B: Engineering* 43 (8). Elsevier Ltd: 3549–62. doi:10.1016/j.compositesb.2011.10.001.
- Hu, R-H, M-Y Sun, and J-K Lim. 2010. "Moisture Absorption, Tensile Strength and Microstructure Evolution of Short Jute Fiber/polylactide Composite in Hygrothermal Environment." *Materials & Design* 31 (7): 3167–73. doi:10.1016/j.matdes.2010.02.030.
- Hua, ZQ, R Sitaru, F Denes, and RA Young. 1997. "Mechanisms of Oxygen- and Argon-RF-Plasma-Induced Surface Chemistry of Cellulose." *Plasmas and Polymers* 2 (3): 199–224. doi:10.1007/BF02766154.
- Inagaki, N. 1996. *Plasma Surface Modification and Plasma Polymerization*. Taylor & Francis. <https://books.google.it/books?id=SNOKJwHqTqwC>.
- Ishii, D, TH Ying, T Yamaoka, and T Iwata. 2009. "Characterization and Biocompatibility of Biopolyester Nanofibers." *Materials* 2 (4): 1520–46. doi:10.3390/ma2041520.
- Istrate, OM, and B Chen. 2011. "Relative Modulus–relative Density Relationships in Low Density Polymer–clay Nanocomposite Foams." *Soft Matter* 7: 1840. doi:10.1039/c0sm01052a.
- Jacobs, LJM, MF Kemmere, and JTF Keurentjes. 2008. "Sustainable Polymer Foaming Using High Pressure Carbon Dioxide: A Review on Fundamentals, Processes and Applications." *Green Chemistry* 10 (7): 731–38. doi:10.1039/B801895B.
- Javadi, A, Y Srithep, J Lee, S Pilla, C Clemons, S Gong, and L-S Turng. 2010. "Processing and Characterization of Solid and Microcellular PHBV/PBAT Blend and Its RWF/nanoclay Composites." *Composites Part A: Applied Science and Manufacturing* 41 (8). Elsevier Ltd: 982–90. doi:10.1016/j.compositesa.2010.04.002.
- Javadi, A, Y Srithep, S Pilla, J Lee, S Gong, and L-S Turng. 2010. "Processing and Characterization of Solid and Microcellular PHBV/coir Fiber Composites." *Materials Science and Engineering: C* 30 (5). Elsevier B.V.: 749–57. doi:10.1016/j.msec.2010.03.008.
- Jazbec, K, M Šala, M Mozetič, A Vesel, and M Gorjanc. 2015. "Functionalization of Cellulose Fibres with Oxygen Plasma and ZnO Nanoparticles for Achieving UV Protective Properties." *Journal*

- of *Nanomaterials* 2015: 1–9. doi:10.1155/2015/346739.
- Jelil, RA. 2015. *A Review of Low-Temperature Plasma Treatment of Textile Materials*. *Journal of Materials Science*. Vol. 50. Springer US. doi:10.1007/s10853-015-9152-4.
- Jeon, B, HK Kim, SW Cha, SJ Lee, M-S Han, and KS Lee. 2013. “Microcellular Foam Processing of Biodegradable Polymers — Review.” *International Journal of Precision Engineering and Manufacturing* 14 (4): 679–90. doi:10.1007/s12541-013-0092-0.
- Johansson, K. 2007. “Plasma Modification of Natural Cellulosic Fibres.” In *Plasma Technologies for Textiles*, edited by R Shishoo, 247–81. Cambridge: Woodhead Publishing Limited. <http://www.lavoisier.fr/livre/notice.asp?id=RSKWAXA6OL2OWR>.
- Johansson, L-S, JM Campbell, K Koljonen, and P Stenius. 1999. “Evaluation of Surface Lignin on Cellulose Fibers with XPS.” *Applied Surface Science* 144–145: 92–95.
- John, M, and S Thomas. 2008. “Biofibres and Biocomposites.” *Carbohydrate Polymers* 71 (3): 343–64. doi:10.1016/j.carbpol.2007.05.040.
- Joseph, PV, MS Rabello, LHC Mattoso, K Joseph, and S Thomas. 2002. “Environmental Effects on the Degradation Behaviour of Sisal Fibre Reinforced Polypropylene Composites.” *Composites Science and Technology* 62 (10–11): 1357–72. doi:10.1016/S0266-3538(02)00080-5.
- Kabir, MM, H Wang, KT Lau, and F Cardona. 2012. “Chemical Treatments on Plant-Based Natural Fibre Reinforced Polymer Composites: An Overview.” *Composites Part B: Engineering* 43 (7). Elsevier Ltd: 2883–92. doi:10.1016/j.compositesb.2012.04.053.
- Kaisangsri, N, O Kerdchoechuen, and N Laohakunjit. 2012. “Biodegradable Foam Tray from Cassava Starch Blended with Natural Fiber and Chitosan.” *Industrial Crops and Products* 37 (1). Elsevier B.V.: 542–46. doi:10.1016/j.indcrop.2011.07.034.
- Kalia, S, BS Kaith, and I Kaur. 2009. “Pretreatments of Natural Fibers and Their Application as Reinforcing Material in Polymer Composites-A Review.” *Polymer Engineering & Science* 49 (7): 1253–72. doi:10.1002/pen.21328.
- Kalia, S, K Thakur, A Celli, MA Kiechel, and CL Schauer. 2013. “Surface Modification of Plant Fibers Using Environment Friendly Methods for Their Application in Polymer Composites, Textile Industry and Antimicrobial Activities: A Review.” *Journal of Environmental Chemical Engineering* 1 (3). Elsevier B.V.: 97–112. doi:10.1016/j.jece.2013.04.009.
- Karimi, M. 2011. “Diffusion in Polymer Solids and Solutions.” In *Mass Transfer in Chemical Engineering Processes*. InTech. doi:10.5772/23436.
- Keller, A. 2003. “Compounding and Mechanical Properties of Biodegradable Hemp Fibre Composites.” *Composites Science and Technology* 63 (9): 1307–16. doi:10.1016/S0266-3538(03)00102-7.
- Keshavarz, T, and I Roy. 2010. “Polyhydroxyalkanoates: Bioplastics with a Green Agenda.” *Current Opinion in Microbiology* 13 (3): 321–26. doi:10.1016/j.mib.2010.02.006.
- Kongdee, A, T Bechtold, E Burtscher, and M Scheinecker. 2004. “The Influence of Wet/dry Treatment on Pore Structure-the Correlation of Pore Parameters, Water Retention and Moisture Regain Values.” *Carbohydrate Polymers* 57 (1): 39–44. doi:10.1016/j.carbpol.2004.03.025.
- Kozłowski, RM, M Mackiewicz-Talarczyk, and AM Allam. 2012. “Bast Fibres: Flax.” In *Handbook of Natural Fibres, Volume 1: Types, Properties and Factors Affecting Breeding and Cultivation*, edited by RM Kozłowski, 1st ed., 56–113. Woodhead Publishing Limited. doi:http://dx.doi.org/10.1533/9780857095503.1.56.
- Krenchel, H. 1964. *Fibre Reinforcement : Theoretical and Practical Investigations of the Elasticity and Strength of Fibre-Reinforced Materials*. Copenhagen : Akademisk Forlag. <http://lib.ugent.be/catalog/rug01:001280222>.

- Laguna-Gutiérrez, E. 2016. "Understanding the Foamability of Complex Polymeric Systems by Using Extensional Rheology" Universidad de Valladolid. <http://uvadoc.uva.es/handle/10324/16251>
- Larroché, E. 2003. *Materiales Compuestos*. Edited by A. Miravete, J. Cuartero, and Asociación Española de Materiales Compuestos. Barcelona: Reverte.
- Lawton, JW, RL Shogren, and KF Tiefenbacher. 2004. "Aspen Fiber Addition Improves the Mechanical Properties of Baked Cornstarch Foams." *Industrial Crops and Products* 19 (1): 41–48. doi:10.1016/S0926-6690(03)00079-7.
- Laycock, B, P Halley, S Pratt, A Werker, and P Lant. 2014. "The Chemomechanical Properties of Microbial Polyhydroxyalkanoates." *Progress in Polymer Science* 39 (2). Elsevier Ltd: 397–442. doi:10.1016/j.progpolymsci.2013.06.008.
- Le Duigou, A., A. Bourmaud, and C. Baley. 2015. "In-Situ Evaluation of Flax Fibre Degradation during Water Ageing." *Industrial Crops and Products* 70. Elsevier B.V.: 190–200. doi:10.1016/j.indcrop.2015.03.049.
- Le Moigne, N, M Sauceau, M Benyakhlef, R Jemai, J-C Benezet, E Rodier, J-M Lopez-Cuesta, and J Fages. 2014. "Foaming of poly(3-Hydroxybutyrate-Co-3-Hydroxyvalerate)/organo-Clays Nano-Biocomposites by a Continuous Supercritical CO₂ Assisted Extrusion Process." *European Polymer Journal* 61 (December): 157–71. doi:10.1016/j.eurpolymj.2014.10.008.
- Lee, SG, S-S Choi, WH Park, and D Cho. 2003. "Characterization of Surface Modified Flax Fibers and Their Biocomposites with PHB." *Macromolecular Symposia* 197 (1): 089–100. doi:10.1002/masy.200350709.
- Lei, Y, Q Wu, F Yao, and Y Xu. 2007. "Preparation and Properties of Recycled HDPE/natural Fiber Composites" *Composites Part A: Applied Science and Manufacturing*, July. doi:10.1016/j.compositesa.2007.02.001.
- Li, Y, H Ma, Y Shen, Q Li, and Z Zheng. 2015. "Effects of Resin inside Fiber Lumen on the Mechanical Properties of Sisal Fiber Reinforced Composites." *Composites Science and Technology* 108 (February): 32–40. doi:10.1016/j.compscitech.2015.01.003.
- Liao, Q, A Tsui, S Billington, and CW Frank. 2012. "Extruded Foams from Microbial poly(3-Hydroxybutyrate-Co-3-Hydroxyvalerate) and Its Blends with Cellulose Acetate Butyrate." *Polymer Engineering & Science* 52 (7): 1495–1508. doi:10.1002/pen.23087.
- Liao, R, WI Yu, and C Zhou. 2010. "Rheological Control in Foaming Polymeric Materials: I. Amorphous Polymers." *Polymer* 51 (2): 568–80. doi:10.1016/j.polymer.2009.11.063.
- Lin, Q, X Zhou, and G Dai. 2002. "Effect of Hydrothermal Environment on Moisture Absorption and Mechanical Properties of Wood Flour-Filled Polypropylene Composites." *Journal of Applied Polymer Science* 85 (14): 2824–32. doi:10.1002/app.10844.
- Lopez-Gil, A, F Silva-Bellucci, D Velasco, M Ardanuy, and MA Rodriguez-Perez. 2015. "Cellular Structure and Mechanical Properties of Starch-Based Foamed Blocks Reinforced with Natural Fibers and Produced by Microwave Heating." *Industrial Crops and Products* 66. Elsevier B.V.: 194–205. doi:10.1016/j.indcrop.2014.12.025.
- López-Manchado, MA, and M Arroyo. 2003. "Fibras naturales como refuerzos de matrices poliméricas." *Revista de plásticos modernos*. <http://cat.inist.fr/?aModele=afficheN&cpsidt=14912871>
- Luckachan, GE, and CKS Pillai. 2011. "Biodegradable Polymers- A Review on Recent Trends and Emerging Perspectives." *Journal of Polymers and the Environment* 19 (3): 637–76. doi:10.1007/s10924-011-0317-1.
- Ludwiczak, J, and M Kozłowski. 2015. "Foaming of Polylactide in the Presence of Chain Extender." *Journal of Polymers and the Environment* 23 (1): 137–42. doi:10.1007/s10924-014-0658-7.

- Luo, L, X Wei, and G-Q Chen. 2009. "Physical Properties and Biocompatibility of poly(3-Hydroxybutyrate-Co-3-Hydroxyhexanoate) Blended with poly(3-Hydroxybutyrate-Co-4-Hydroxybutyrate)." *Journal of Biomaterials Science. Polymer Edition* 20 (11): 1537–53. doi:10.1163/092050609X12464345023041.
- Luo, S, and AN Netravali. 1999. "Interfacial and Mechanical Properties of Environment-Friendly 'green' composites Made from Pineapple Fibers and Poly(hydroxybutyrate-Co-Valerate) Resin." *Journal of Materials Science* 34 (15): 3709–19. doi:10.1023/A:1004659507231.
- Madsen, B, and H Lilholt. 2003. "Physical and Mechanical Properties of Unidirectional Plant Fibre Composites—an Evaluation of the Influence of Porosity." *Composites Science and Technology* 63 (9): 1265–72. doi:10.1016/S0266-3538(03)00097-6.
- Madsen, B, A Thygesen, and H Lilholt. 2007. "Plant Fibre Composites – Porosity and Volumetric Interaction." *Composites Science and Technology* 67 (7): 1584–1600. doi:10.1016/j.compscitech.2006.07.009.
- Madsen, B, A Thygesen, and H Lilholt. 2009. "Plant Fibre Composites – Porosity and Stiffness." *Composites Science and Technology* 69 (7–8): 1057–69. doi:10.1016/j.compscitech.2009.01.016.
- Manikandan Nair, KC, S Thomas, and G Groeninckx. 2001. "Thermal and Dynamic Mechanical Analysis of Polystyrene Composites Reinforced with Short Sisal Fibres." *Composites Science and Technology* 61 (16): 2519–29. doi:10.1016/S0266-3538(01)00170-1.
- Martínez, V, C Herencias, E Jurkevitch, and MA Prieto. 2016. "Engineering a Predatory Bacterium as a Proficient Killer Agent for Intracellular Bio-Products Recovery: The Case of the Polyhydroxyalkanoates." *Scientific Reports* 6 (April). Nature Publishing Group: 24381. doi:10.1038/srep24381.
- Masani, MYA, G Kadir, A Parveez, AMD Izawati, CP Lan, and ASN Akmar. 2009. "Construction of PHB and PHBV Multiple-Gene Vectors Driven by an Oil Palm Leaf-Specific Promoter." *Plasmid* 62 (3). Elsevier Inc.: 191–200. doi:10.1016/j.plasmid.2009.08.002.
- Matuana, LM, O Faruk, and CA Diaz. 2009. "Cell Morphology of Extrusion Foamed Poly(lactic Acid) Using Endothermic Chemical Foaming Agent." *Bioresource Technology* 100 (23). Elsevier Ltd: 5947–54. doi:10.1016/j.biortech.2009.06.063.
- Mekonnen, T, P Mussone, H Khalil, and D Bressler. 2013. "Progress in Bio-Based Plastics and Plasticizing Modifications." *Journal of Materials Chemistry A* 1 (43): 13379. doi:10.1039/c3ta12555f.
- Meng, Q, M-C Heuzey, and PJ Carreau. 2012. "Control of Thermal Degradation of Poly(lactide)/ clay Nanocomposites during Melt Processing by Chain Extension Reaction." *Polymer Degradation and Stability* 97 (10). Elsevier Ltd: 2010–20. doi:10.1016/j.polymdegradstab.2012.01.030.
- Mitomo, H, and Y Doi. 1999. "Lamellar Thickening and Cocrystallization of Poly(hydroxy-alkanoate)s on Annealing." *International Journal of Biological Macromolecules* 25: 201–5. doi:10.1016/S0141-8130(99)00035-5.
- Mitomo, H, PJ Barham, and A Keller. 1987. "Crystallization and Morphology of Poly(β -Hydroxybutyrate) and Its Copolymer." *Polymer Journal* 19 (11). The Society of Polymer Science, Japan: 1241–53. doi:10.1295/polymj.19.1241.
- Mohammed, L, MNM Ansari, G Pua, M Jawaid, and MS Islam. 2015. "A Review on Natural Fiber Reinforced Polymer Composite and Its Applications." *International Journal of Polymer Science* 2015. doi:10.1155/2015/243947.
- Mohanty, AK, M Misra, and LT Drzal. 2005. *Natural Fibers, Biopolymers, and Biocomposites*. Edited by AK Mohanty, M Misra, and LT Drzal. CRC Press. doi:10.1201/9780203508206.
- Mokhothu, TH, and MJ John. 2015. "Review on Hygroscopic Aging of Cellulose Fibres and Their Biocomposites." *Carbohydrate Polymers* 131 (October): 337–54.

- doi:10.1016/j.carbpol.2015.06.027.
- Mooney, DJ, DF Baldwin, NP Suh, JP Vacanti, and R Langer. 1996. "Novel Approach to Fabricate Porous Sponges of poly(D,L-Lactic-Co-Glycolic Acid) without the Use of Organic Solvents." *Biomaterials* 17 (14): 1417–22. <http://www.ncbi.nlm.nih.gov/pubmed/8830969>.
- Morent, R, N De Geyter, J Verschuren, K De Clerck, P Kiekens, and C Leys. 2008. "Non-Thermal Plasma Treatment of Textiles." *Surface and Coatings Technology* 202 (14): 3427–49. doi:10.1016/j.surfcoat.2007.12.027.
- Morshed, MM, MM Alam, and SM Daniels. 2010. "Plasma Treatment of Natural Jute Fibre by RIE 80 plus Plasma Tool." *Plasma Science and Technology* 12 (3): 325–29. doi:10.1088/1009-0630/12/3/16.
- Najafi, N, MC Heuzey, PJ Carreau, and PM Wood-Adams. 2012. "Control of Thermal Degradation of Polylactide (PLA)-Clay Nanocomposites Using Chain Extenders." *Polymer Degradation and Stability* 97 (4): 554–65. doi:10.1016/j.polymdegradstab.2012.01.016.
- Neagu, RC, M Cuenoud, F Berthold, P-E Bourban, EK Gamstedt, M Lindstrom, and J-AE Manson. 2012. "The Potential of Wood Fibers as Reinforcement in Cellular Biopolymers." *Journal of Cellular Plastics* 48 (1): 71–103. doi:10.1177/0021955X11431172.
- Nechwatal, A, K-P Mieck, and T Reußmann. 2003. "Developments in the Characterization of Natural Fibre Properties and in the Use of Natural Fibres for Composites." *Composites Science and Technology* 63 (9): 1273–79. doi:10.1016/S0266-3538(03)00098-8.
- Niaounakis, M. 2014. *Biopolymers: Processing and Products*. Plastics D. William Andrew.
- Pan, P, and Y Inoue. 2009. "Polymorphism and Isomorphism in Biodegradable Polyesters." *Progress in Polymer Science (Oxford)* 34: 605–40. doi:10.1016/j.progpolymsci.2009.01.003.
- Peijs, T, S Garkhail, R Heijenrath, M Van Den Oever, and H Bos. 1998. "Thermoplastic Composites Based on Flax Fibres and Polypropylene: Influence of Fibre Length and Fibre Volume Fraction on Mechanical Properties." *Macromolecular Symposia* 127: 193–203. doi:10.1002/masy.19981270126.
- Peterson, S, K Jayaraman, and D Bhattacharyya. 2002. "Forming Performance and Biodegradability of woodfibre–BiopolTM Composites." *Composites Part A: Applied Science and Manufacturing* 33 (8): 1123–34. doi:10.1016/S1359-835X(02)00046-5.
- Pickering, KL, ed. 2008. *Properties and Performance of Natural-Fibre Composites*. First. Cambridge: Woodhead Publishing Limited.
- Pickering, KL, MG Aruan Efendy, and TM Le. 2016. "A Review of Recent Developments in Natural Fibre Composites and Their Mechanical Performance." *Composites Part A: Applied Science and Manufacturing* 83 (April): 98–112. doi:10.1016/j.compositesa.2015.08.038.
- Pilla, S, SG Kim, GK Auer, S Gong, and CB Park. 2009. "Microcellular Extrusion-Foaming of Polylactide with Chain-Extender." *Polymer Engineering and Science* 49: 1653–60. doi:10.1002/pen.21385.
- Pinto, J, E Solorzano, MA Rodriguez-Perez, and JA De Saja. 2013. "Characterization of the Cellular Structure Based on User-Interactive Image Analysis Procedures." *Journal of Cellular Plastics* 49 (7): 555–75. doi:10.1177/0021955X13503847.
- Pivec, T, Z Persin, M Kolar, T Maver, A Dobaj, A Vesel, U Maver, and K Stana-Kleinschek. 2014. "Modification of Cellulose Non-Woven Substrates for Preparation of Modern Wound Dressings." *Textile Research Journal* 84 (1): 96–112. doi:10.1177/0040517513483855.
- Poirier, Y, C Nawrath, and C Somerville. 1995. "Production of Polyhydroxyalkanoates, a Family of Biodegradable Plastics and Elastomers, in Bacteria and Plants." *Nat Biotech* 13 (2). Nature Publishing Company: 142–50. <http://dx.doi.org/10.1038/nbt0295-142>.

- Qiu, Y, W Xu, Y Wang, MA Zikry, and MH Mohamed. 2001. "Fabrication and Characterization of Three-Dimensional Cellular-Matrix Composites Reinforced with Woven Carbon Fabric." *Composites Science and Technology* 61 (16): 2425–35. doi:10.1016/S0266-3538(01)00164-6.
- Rastogi, V, and P Samyn. 2015. "Bio-Based Coatings for Paper Applications." *Coatings* 5 (4): 887–930. doi:10.3390/coatings5040887.
- Reddy, CSK, R Ghai, Rashmi, and VC Kalia. 2003. "Polyhydroxyalkanoates: An Overview." *Bioresource Technology*. doi:10.1016/S0960-8524(02)00212-2.
- Relvas, C, G Castro, S Rana, and R Figueiro. 2015. "Characterization of Physical, Mechanical and Chemical Properties of Quiscal Fibres: The Influence of Atmospheric DBD Plasma Treatment." *Plasma Chemistry and Plasma Processing*, May. doi:10.1007/s11090-015-9630-0.
- Rodriguez-Perez, M. A. 2005. "Crosslinked Polyolefin Foams: Production, Structure, Properties, and Applications." In *Crosslinking in Materials Science*, 184:97–126. Advances in Polymer Science. Berlin, Heidelberg: Springer Berlin Heidelberg. doi:10.1007/b136244.
- Rodriguez-Perez, M. A., S. Rodriguez-Llorente, and J. A. De Saja. 1997. "Dynamic Mechanical Properties of Polyolefin Foams Studied by DMA Techniques." *Polymer Engineering and Science* 37 (6): 959–65.
- Rodriguez-Perez, M. A, and J. A. De Saja. 2000. "Dynamic Mechanical Analysis Applied to the Characterisation of Closed Cell Polyolefin Foams." *Polymer Testing* 19 (7): 831–48. doi:10.1016/S0142-9418(99)00054-9.
- Russell, S. 2007. *Handbook of Nonwovens*. CRC Press, Woodhead Publishing.
- Saba, N, M Jawaid, OY Alothman, and MT Paridah. 2016. "A Review on Dynamic Mechanical Properties of Natural Fibre Reinforced Polymer Composites." *Construction and Building Materials* 106. Elsevier Ltd: 149–59. doi:10.1016/j.conbuildmat.2015.12.075.
- Sabharwal, HS, F Denes, L Nielsen, and RA Young. 1993. "Free-Radical Formation in Jute from Argon Plasma Treatment." *Journal of Agricultural and Food Chemistry* 41 (11): 2202–7. doi:10.1021/jf00035a072.
- Saheb, DN, and JP Jog. 1999. "Natural Fiber Polymer Composites: A Review." *Advances in Polymer Technology* 18 (4): 351–63. doi:10.1002/(SICI)1098-2329(199924)18:4<351::AID-ADV6>3.3.CO;2-O.
- Salim, YS, A Al-Ashraf Abdullah, CS Sipaut, M Nasri, and MNM Ibrahim. 2011. "Biosynthesis of poly(3-Hydroxybutyrate-Co-3-Hydroxyvalerate) and Characterisation of Its Blend with Oil Palm Empty Fruit Bunch Fibers." *Bioresource Technology* 102 (3). Elsevier Ltd: 3626–28. doi:10.1016/j.biortech.2010.11.020.
- Samanta, KK, M Jassal, and AK Agrawal. 2009. "Improvement in Water and Oil Absorbency of Textile Substrate by Atmospheric Pressure Cold Plasma Treatment." *Surface and Coatings Technology* 203 (10–11). Elsevier B.V.: 1336–42. doi:10.1016/j.surfcoat.2008.10.044.
- Satyanarayana, KG, GGC Arizaga, and F Wypych. 2009. "Biodegradable Composites Based on Lignocellulosic fibers—An Overview." *Progress in Polymer Science* 34 (9): 982–1021. doi:10.1016/j.progpolymsci.2008.12.002.
- Schmack, G, D Jehnichen, R Vogel, and B Tändler. 2000. "Biodegradable Fibers of Poly (3-Hydroxybutyrate) Produced by High-Speed Melt Spinning and Spin Drawing." *Journal of Polymer Science: Part B: Polymer Physics* 38: 2841–50. [http://onlinelibrary.wiley.com/doi/10.1002/1099-0488\(20001101\)38:21%3C2841::AID-POLB130%3E3.0.CO;2-%23/full](http://onlinelibrary.wiley.com/doi/10.1002/1099-0488(20001101)38:21%3C2841::AID-POLB130%3E3.0.CO;2-%23/full).
- Segal, L, JJ Creely, AE Martin, and CM Conrad. 1959. "An Empirical Method for Estimating the Degree of Crystallinity of Native Cellulose Using the X-Ray Diffractometer." *Textile Research Journal* 29 (10): 786–94. doi:10.1177/004051755902901003.

- Sepe, M. 1998. *Dynamic Mechanical Analysis for Plastics Engineering*. PDL handbo. Norwich, N.Y.: Plastics Design Library.
- Serafim, L. S., P. C. Lemos, M. G. E. Albuquerque, and M. A. M. Reis. 2008. "Strategies for PHA Production by Mixed Cultures and Renewable Waste Materials." *Applied Microbiology and Biotechnology* 81 (4): 615–28. doi:10.1007/s00253-008-1757-y.
- Shanks, RA, A Hodzic, and S Wong. 2004. "Thermoplastic Biopolyester Natural Fiber Composites." *Journal of Applied Polymer Science* 91 (4): 2114–21. doi:10.1002/app.13289.
- Shishoo, R. 2007. *Plasma Technologies for Textiles*. Woodhead Publishing Series in Textiles. Elsevier Science. <https://books.google.it/books?id=LI-kAgAAQBAJ>.
- Singh, S, and AK Mohanty. 2007. "Wood Fiber Reinforced Bacterial Bioplastic Composites: Fabrication and Performance Evaluation." *Composites Science and Technology* 67 (9): 1753–63. doi:10.1016/j.compscitech.2006.11.009.
- Singh, S, AK Mohanty, T Sugie, Y Takai, and H Hamada. 2008. "Renewable Resource Based Biocomposites from Natural Fiber and Polyhydroxybutyrate-Co-Valerate (PHBV) Bioplastic." *Composites Part A: Applied Science and Manufacturing* 39 (5): 875–86. doi:10.1016/j.compositesa.2008.01.004.
- Solorzano, E, and MA Rodriguez-Perez. 2013. "Cellular Materials." In *Structural Materials and Processes in Transportation*, edited by Dirk Lehmhus, Matthias Busse, Axel S. Herrmann, and Kambiz Kayvantash, 371–74. Weinheim, Germany: Wiley-VCH Verlag GmbH & Co. KGaA. doi:10.1002/9783527649846.
- Sorrentino, L, L Cafiero, M D'Auria, and S Iannace. 2014. "Cellular Thermoplastic Fibre Reinforced Composite (CellFRC): A New Class of Lightweight Material with High Impact Properties." *Composites Part A: Applied Science and Manufacturing* 64 (September): 223–27. doi:10.1016/j.compositesa.2014.05.016.
- Soykeabkaew, N, P Supaphol, and R Rujiravanit. 2004. "Preparation and Characterization of Jute- and Flax-Reinforced Starch-Based Composite Foams." *Carbohydrate Polymers* 58 (1): 53–63. doi:10.1016/j.carbpol.2004.06.037.
- Srithep, Y, T Ellingham, J Peng, R Sabo, C Clemons, L-S Turng, and S Pilla. 2013. "Melt Compounding of Poly (3-Hydroxybutyrate-Co-3-Hydroxyvalerate)/nanofibrillated Cellulose Nanocomposites." *Polymer Degradation and Stability* 98 (8). Elsevier Ltd: 1439–49. doi:10.1016/j.polymdegradstab.2013.05.006.
- Steinbüchel, A, and T Lütke-Eversloh. 2003. "Metabolic Engineering and Pathway Construction for Biotechnological Production of Relevant Polyhydroxyalkanoates in Microorganisms." *Biochemical Engineering Journal* 16 (2): 81–96. doi:10.1016/S1369-703X(03)00036-6.
- Sudesh, K, H Abe, and Y Doi. 2000. "Synthesis, Structure and Properties of Polyhydroxyalkanoates: Biological Polyesters." *Progress in Polymer Science* 25 (10): 1503–55. doi:10.1016/S0079-6700(00)00035-6.
- Sudesh, K, and H Abe. 2010. "Crystalline and Solid-State Structures of Polyhydroxy-alkanoates (PHA)." In *Practical Guide to Microbial Polyhydroxyalkanoates*. Smithers Rapra Technology.
- Summerscales, J, N Dissanayake, A Virk, and W Hall. 2010. "A Review of Bast Fibres and Their Composites. Part 2 – Composites." *Composites Part A: Applied Science and Manufacturing* 41 (10): 1336–44. doi:10.1016/j.compositesa.2010.05.020.
- Summerscales, J, A Virk, and W Hall. 2013. "A Review of Bast Fibres and Their Composites: Part 3 – Modelling." *Composites Part A: Applied Science and Manufacturing* 44 (January): 132–39. doi:10.1016/j.compositesa.2012.08.018.
- Suriyamongkol, P, R Weselake, S Narine, M Moloney, and S Shah. 2007. "Biotechnological Approaches for the Production of Polyhydroxyalkanoates in Microorganisms and Plants - a

- Review.” *Biotechnology Advances* 25 (2): 148–75. doi:10.1016/j.biotechadv.2006.11.007.
- Szegda, D, S Daungphet, J Song, and K Tarverdi. 2010. “Extrusion Foaming and Rheology of PHBV.” In *8th International Conference on Foam Materials & Technology (Foams)*, 6–11.
- Takahashi, S, JC Hassler, and E Kiran. 2012. “Melting Behavior of Biodegradable Polyesters in Carbon Dioxide at High Pressures.” *Journal of Supercritical Fluids* 72 (December): 278–87. doi:10.1016/j.supflu.2012.09.009.
- Thomas, S, and LA Pothan. 2009. *Natural Fibre Reinforced Polymer Composites. From Macro to Nanoscale*. Paris: Old City Publishing.
- Thomason, JL, and WM Groenewoud. 1996. “The Influence of Fibre Length and Concentration on the Properties of Glass Fibre Reinforced Polypropylene: 2. Thermal Properties.” *Composites Part A: Applied Science and Manufacturing* 27 (7 PART A). Elsevier: 555–65. doi:10.1016/1359-835X(96)00016-4.
- Thomason, JL, and MA Vlug. 1996. “Influence of Fibre Length and Concentration on the Properties of Glass Fibre-Reinforced Polypropylene: Part 1. Tensile and Flexural Modulus.” *Composites Part A: Applied Science and Manufacturing* 27 (7): 477–84. doi:10.1016/1359-835X(95)00065-8.
- Thomason, JL, MA Vlug, G Schipper, and HGLT Krikor. 1996. “Influence of Fibre Length and Concentration on the Properties of Glass Fibre-Reinforced Polypropylene: Part 3. Strength and Strain at Failure.” *Composites Part A: Applied Science and Manufacturing* 27 (11): 1075–84. doi:10.1016/1359-835X(96)00066-8.
- Thygesen, A. 2006. “Properties of Hemp Fibre Polymer Composites - An Optimisation of Fibre Properties Using Novel Defibration Methods and Fibre Characterisation Title.” Royal Veterinary and Agricultural University, Technical University of Denmark. doi:(Risø-PhD; No. 11(EN)).
- Tserki, V, NE Zafeiropoulos, F Simon, and C Panayiotou. 2005. “A Study of the Effect of Acetylation and Propionylation Surface Treatments on Natural Fibres.” *Composites Part A: Applied Science and Manufacturing* 36 (8): 1110–18. doi:10.1016/j.compositesa.2005.01.004.
- Tsuda, H. 2012. “Generation of Poly- β -Hydroxybutyrate from Externally Provided Acetate in Rice Root.” *Plant Physiology and Biochemistry: PPB / Société Française de Physiologie Végétale* 50 (1). Elsevier Masson SAS: 35–43. doi:10.1016/j.plaphy.2011.09.019.
- Tsui, A, Z Wright, and CW Frank. 2013. “Prediction of Gas Solubility in poly(3-Hydroxybutyrate-Co-3-Hydroxyvalerate) Melt to Inform Process Design and Resulting Foam Microstructure.” *Polymer Engineering & Science*, December, 1–13. doi:10.1002/pen.23822.
- Van Den Oever, MJA, HL Bos, and MJJM Van Kemenade. 2000. “Influence of the Physical Structure of Flax Fibres on the Mechanical Properties of Flax Fibre Reinforced Polypropylene Composites.” *Applied Composite Materials* 7 (5/6): 387–402. doi:10.1023/A:1026594324947.
- Verhoogt, H, BA Ramsay, BD Favis, and JA Ramsay. 1996. “The Influence of Thermal History on the Properties of poly(3-Hydroxybutyrate-Co-12%-3-Hydroxyvalerate).” *Journal of Applied Polymer Science* 61: 87–96. doi:10.1002/(SICI)1097-4628(19960705)61:1<87::AID-APP10>3.0.CO;2-X.
- Villalobos, M, A Awojulu, T Greeley, G Turco, and G Deeter. 2006. “Oligomeric Chain Extenders for Economic Reprocessing and Recycling of Condensation Plastics.” *Energy* 31: 3227–34. doi:10.1016/j.energy.2006.03.026.
- Vroman, I, and L Tighzert. 2009. “Biodegradable Polymers.” *Materials* 2 (2): 307–44. doi:10.3390/ma2020307.
- Wambua, P, J Ivens, and I Verpoest. 2003. “Natural Fibres: Can They Replace Glass in Fibre Reinforced Plastics?” *Composites Science and Technology* 63 (9): 1259–64.

- doi:10.1016/S0266-3538(03)00096-4.
- Wang, B, RR Sharma-Shivappa, JW Olson, and SA Khan. 2013. "Production of Polyhydroxybutyrate (PHB) by *Alcaligenes Latus* Using Sugarbeet Juice." *Industrial Crops and Products* 43 (May): 802–11. doi:10.1016/j.indcrop.2012.08.011.
- Wang, CX, and YP Qiu. 2007. "Two Sided Modification of Wool Fabrics by Atmospheric Pressure Plasma Jet: Influence of Processing Parameters on Plasma Penetration." *Surface and Coatings Technology* 201 (14): 6273–77. doi:10.1016/j.surfcoat.2006.11.028.
- Wang, C, and J-R Chen. 2007. "Studies on Surface Graft Polymerization of Acrylic Acid onto PTFE Film by Remote Argon Plasma Initiation." *Applied Surface Science* 253 (10): 4599–4606. doi:10.1016/j.apsusc.2006.10.014.
- Wang, J, W Zhu, H Zhang, and CB Park. 2012. "Continuous Processing of Low-Density, Microcellular Poly(lactic Acid) Foams with Controlled Cell Morphology and Crystallinity." *Chemical Engineering Science* 75. Elsevier: 390–99. doi:10.1016/j.ces.2012.02.051.
- Wang, S, W Chen, H Xiang, J Yang, Z Zhou, and M Zhu. 2016. "Modification and Potential Application of Short-Chain-Length Polyhydroxyalkanoate (SCL-PHA)." *Polymers* 8 (8). doi:10.3390/polym8080273.
- Wang, Y-W, W Mo, H Yao, Q Wu, J Chen, and G-Q Chen. 2004. "Biodegradation Studies of poly(3-Hydroxybutyrate-Co-3-Hydroxyhexanoate)." *Polymer Degradation and Stability* 85 (2): 815–21. doi:10.1016/j.polymdegradstab.2004.02.010.
- Wellen, RMR, MS Rabello, GJM Fechine, and EL Canedo. 2013. "The Melting Behaviour of poly(3-Hydroxybutyrate) by DSC. Reproducibility Study." *Polymer Testing* 32 (2). Elsevier Ltd: 215–20. doi:10.1016/j.polymertesting.2012.11.001.
- Wong, S, RA Shanks, and A Hodzic. 2007. "Effect of Additives on the Interfacial Strength of Poly(l-Lactic Acid) and poly(3-Hydroxy Butyric Acid)-Flax Fibre Composites." *Composites Science and Technology* 67 (11–12): 2478–84. doi:10.1016/j.compscitech.2006.12.016.
- Wright, ZC, and CW Frank. 2014. "Increasing Cell Homogeneity of Semicrystalline, Biodegradable Polymer Foams with a Narrow Processing Window via Rapid Quenching." *Polymer Engineering and Science* 54 (12): 2877–2886. doi:10.1002/pen.23847.
- Wróbel, M, J Zebrowski, and J Szopa. 2004. "Polyhydroxybutyrate Synthesis in Transgenic Flax." *Journal of Biotechnology* 107 (1): 41–54. doi:10.1016/j.jbiotec.2003.10.005.
- Xu, X, Y Wang, X Zhang, G Jing, D Yu, and S Wang. 2006. "Effects on Surface Properties of Natural Bamboo Fibers Treated with Atmospheric Pressure Argon Plasma." *Surface and Interface Analysis* 38 (8): 1211–17. doi:10.1002/sia.2378.
- Yamaguchi, M, and K Arakawa. 2006. "Effect of Thermal Degradation on Rheological Properties for poly(3-Hydroxybutyrate)." *European Polymer Journal* 42: 1479–86. doi:10.1016/j.eurpolymj.2006.01.022.
- Yamane, H, K Terao, S Hiki, and Y Kimura. 2001. "Mechanical Properties and Higher Order Structure of Bacterial Homo Poly (3-Hydroxybutyrate) Melt Spun Fibers." *Polymer* 42: 3241–48. <http://www.sciencedirect.com/science/article/pii/S003238610000598X>.
- Yan, L, N Chouw, and K Jayaraman. 2014. "Flax Fibre and Its Composites – A Review." *Composites Part B: Engineering* 56 (January). Elsevier Ltd: 296–317. doi:10.1016/j.compositesb.2013.08.014.
- Yuan, X, K Jayaraman, and D Bhattacharyya. 2004. "Effects of Plasma Treatment in Enhancing the Performance of Woodfibre-Polypropylene Composites." *Composites Part A: Applied Science and Manufacturing* 35 (12): 1363–74. doi:10.1016/j.compositesa.2004.06.023.
- Zafar, MT, N Zarrinbakhsh, AK Mohanty, M Misra, and AK Ghosh. 2016. "Biocomposites Based on poly(Lactic Acid)/willow-Fiber and Their Injection Moulded Microcellular Foams." *Express*

Polymer Letters 10 (2): 176–86. doi:10.3144/expresspolymlett.2016.16.

Zille, A, F Ribeiro Oliveira, and AP Souto. 2014. “Plasma Treatment in Textile Industry.” *Plasma Processes and Polymers*, no. iv: n/a-n/a. doi:10.1002/ppap.201400052.